BEHAVIOR OF REVERSE TOP-SEAT ANGLE CONNECTION AT AMBIENT AND ELEVATED TEMPERATURES

LEONG SIONG HEAN

THESIS SUBMITTED IN FULFILLMENT OF THE REQUIRMENTS FOR THE DEGREE OF DOCTOR OF PHILOSOPHY

FACULTY OF ENGINEERING
UNIVERSITY OF MALAYA
KUALA LUMPUR

2017

UNIVERSITI MALAYA

PERAKUAN KEASLIAN PENULISAN

Nama: LEONG SIONG HEAN

No. Pendaftaran/Matrik: KHA130126

Nama Ijazah: DOKTOR FALSAFAH

Tajuk Kertas Projek/Laporan Penyelidikan/Disertasi/Tesis ("Hasil Kerja ini"):

BEHAVIOR OF REVERSE TOP-SEAT ANGLE CONNECTION AT AMBIENT AND ELEVATED TEMPERATURES

Bidang Penyelidikan: STRUCTURAL ENGINEERING & MATERIALS

Saya dengan sesungguhnya dan sebenarnya mengaku bahawa:

(1) Saya adalah satu-satunya pengarang/penulis Hasil Kerja ini;
(2) Hasil Kerja ini adalah asli;
(3) Apa-apa penggunaan mana-mana hasil kerja yang mengandungi hakcipta telah dilakukan secara urusan yang wajar dan bagi maksud yang dibenarkan dan apa-apa petikan, ekstrak, rujukan atau pengeluaran semula daripada atau kepada mana-mana hasil kerja yang mengandungi hakcipta telah dinyatakan dengan sejelasnya dan secukupnya dan satu pengiktirafan tajuk hasil kerja tersebut dan pengarang/penulisnya telah dilakukan di dalam Hasil Kerja ini;
(4) Saya tidak mempunyai apa-apa pengetahuan sebenar atau patut semunasabahnya tahu bahawa penghasilan Hasil Kerja ini melanggar suatu hakcipta hasil kerja yang lain;
(5) Saya dengan ini menyerahkan kesemua dan tiap-tiap hak yang terkandung di dalam hakcipta Hasil Kerja ini kepada Universiti Malaya ("UM") yang seterusnya mula dari sekarang adalah tuan punya kepada hakcipta di dalam Hasil Kerja ini dan apa-apa pengeluaran semula atau penggunaan dalam apa jua bentuk atau dengan apa juga cara sekalipun adalah dilarang tanpa terlebih dahulu mendapat kebenaran bertulis dari UM;
(6) Saya sedar sepenuhnya sekiranya dalam masa penghasilan Hasil Kerja ini saya telah melanggar suatu hakcipta hasil kerja yang lain sama ada dengan niat atau sebaliknya, saya boleh dikenakan tindakan undang-undang atau apa-apa tindakan lain sebagaimana yang diputuskan oleh UM.

Tandatangan Calon

Tarikh
28 / 08 / 2017

Diperbuat dan sesungguhnya diakui di hadapan,

Tandatangan Saksi

Tarikh

Nama:
Jawatan:

UNIVERSITI MALAYA

ORIGINAL LITERARY WORK DECLARATION

Name of Candidate: LEONG SIONG HEAN

Registration/Matric No: KHA130126

Name of Degree: DOCTOR OF PHILOSOPHY

Title of Project Paper/Research Report/Dissertation/Thesis ("this Work"):

BEHAVIOR OF REVERSE TOP-SEAT ANGLE CONNECTION AT AMBIENT AND ELEVATED TEMPERATURES

Field of Study: STRUCTURAL ENGINEERING & MATERIALS

I do solemnly and sincerely declare that:

(1) I am the sole author/writer of this Work;
(2) This Work is original;
(3) Any use of any work in which copyright exists was done by way of fair dealing and for permitted purposes and any excerpt or extract from, or reference to or reproduction of any copyright work has been disclosed expressly and sufficiently and the title of the Work and its authorship have been acknowledged in this Work;
(4) I do not have any actual knowledge nor do I ought reasonably to know that the making of this work constitutes an infringement of any copyright work;
(5) I hereby assign all and every rights in the copyright to this Work to the University of Malaya ("UM"), who henceforth shall be owner of the copyright in this Work and that any reproduction or use in any form or by any means whatsoever is prohibited without the written consent of UM having been first had and obtained;
(6) I am fully aware that if in the course of making this Work I have infringed any copyright whether intentionally or otherwise, I may be subject to legal action or any other action as may be determined by UM.

Candidate's Signature

Date
28 / 08 / 2017

Subscribed and solemnly declared before,

Witness's Signature

Date

Name:
Designation:

ABSTRACT

Steel tubular column members have been widely adopted in construction industry due to its numerous advantages. However, the closed-section profile characteristics of tubular columns severely limit the connection possibilities. Welding method is acceptable but discouraged because of on-site issues. Bolted connections are preferable because of its simplicity, economical and easy assembly. A combination of both welding and bolting is the compromise between benefits and disadvantages. Therefore, a new bolted connection of open beam sections to tubular column that consists of welded angles and end plate, called reverse top-seat angle connection is proposed and investigated. This study focuses on experimental and numerical methods of examining the behavior of reverse top-seat angle connection at ambient and elevated temperature. Three specimens were tested at ambient temperature with monotonic loading while four specimens were tested at elevated temperature according to ISO834 heating curve under anisothermal conditions with static load. The results from tests in both conditions provide the validation data for finite element models developed in ABAQUS. Only half of the specimen is modelled and uses solid hexahedral brick elements. Contacts and pretension are included into the model for closer representation of the experimental tests while the temperatures are considered as static step in the model. For ambient models, the validated model was used in parametric studies on the geometrical details that may affect the connection behavior, including the angle thickness, plate thickness, leg length, stiffener and gauge length. Several parameters have been identified to provide a critical contribution to the connection behavior. Results from the elevated temperature tests show the difference in deformation of the connection due to the effects of higher temperature and the boundary conditions for both test conditions. In terms of connection performance under elevated temperatures, two configurations of the connections are discovered to remain ductile under the temperature of 700C while the other two specimens developed earlier failures. Effects of axial loadings, isothermal conditions and the effect of boundary conditions were studied as the variation under elevated temperatures. The results have shown that the connection is both practical and has comparable performance to other connection types to tubular columns with flexible modification options. The connection can be considered for future studies, considering the various additional components that could be added to the connection to increase the performance accordingly.

ABSTRAK

Tiang berongga besi semakin banyak digunakan di dalam bidang pembinaan kesan daripada beberapa manfaat yang diperolehi daripada pengunaannya. Namun begitu, keratan-rentas tiang besi berongga yang tertutup menimbulkan isu-isu kritikal yang berkaitan dengan sambungan rasuk kepada tiang berongga besi. Walaupun sambungan jenis kimpalan adalah satu jenis sambungan yang sesuai, namun, kimpalan tidak digalakkan atas sebab bahawa terhadap halangan tertentu di tapak pembinaan yang menhalangnya daripada digunakan. Sambungan yang menggunakan *bolt* besi adalah lebih mudah, berekonomi serta senang untuk dipasang. Kombinasi penggunaan kimpalam dan *bolt* adalah kompromasi antara manfaat serta keburukan kesan daripada pengunaan salah satu jenis. Dengan itu, sambungan jenis baru untuk rasuk besi kepada tiang berongga yang melibatkan bahagian berbentuk 'L' terbalik yang dikimpal ke tiang, dan rasuk disambung dengan plat besi ke bahagian 'L' tersebut adalah dicadangkan dan dikaji. Fokus kajian yang dijalankan adalah dalam keadaan suhu persekitaran serta keadaan suhu tinggi serta melalui analisis *finite-element*. Tiga spesimen dihasilkan dan diuji dalam keadaan suhu bilik dengan menggunakan beban statik serta empat spesimen yang diuji dengan mnggunakan lengkung suhu tinggi mengikut piawaian ISO834. Keputusan yang diperolehi daripada kedua-dua ujian digunakan sebagai data untuk mengesahkan model yang dihasilkan dengan menggunakan perisian *finite-element* ABAQUS. Hanya separuh daripada specimen dimodel dalam perisian tersebut serta menggunakan elemen *solid hexahedral brick* untuk analisis. Untuk kajian dalam suhu persekitaran, model yang telah disahkan digunakan untuk kajian tentang parameter yang mempengaruhi kelakuan sambungan termasuk ketebalan *plat*, panjang bahagian 'L', serta kesan daripada penambahan *plat* penguat. Beberapa parameter lain juga telah dikenal pasti sebagai penyumbang kepada

kelakuan sambungan. Keputusan yang diperolehi daripada ujian dalam keadaan suhu tinggi menunjukkan bahawa terdapat perbezaan ubah bentuk di antara sambungan dalam suhu persekitaran dan suhu tinggi. Didapati bahawa prestasi sambungan adalah masih tidak mencapai tahap kegagalan sambungan walaupun pada suhu 700 dan masih dalam keadaan mulur. Kesan daripada beban paksi, keadaan suhu tinggi tetap serta kesan daripada sokongan berbeza dikaji sebagai kajian perubahan yang memberi kesan kepada sambungan. Keputusan ujian menunjukkan bahawa sambugan yang telah dicadangkan boleh dikaji dengan lebih lanjut memandangkan kepelbagaian komponen yang boleh dipasang untuk meningkatkan prestasi sambungan.

ACKNOWLEDGEMENT

During this study, countless parties have assisted the author, whether in terms of moral support, financial or knowledge sharing. Firstly, to express gratitude to the supervisor for this study, Associate Professor Dr Norhafizah Ramli Bt. Sulong and Dr Jameel Mohammed. It is with their knowledge and expertise that I could complete this study successfully. With their guidance, this study is rendered practical and applicable to the current studies of the field. Their teachings are greatly appreciated and remembered.

Second, would like to express gratitude to all the colleagues during the course of this study especially: Faisal Javed, Yeo Shih Horng, Syamsul Bukhari. They have provided with all the information, knowledge and some, assisting in completing the minor tasks involved in the completion of this study. In addition, the heavy work required for the specimen testing and invaluable advice on testing procedures and technical advice.

Also to my parents who have supported my studies morally throughout these years. Their advice and support has given me the perseverance to complete the study all these years. Lastly, to all parties, especially towards the laboratory technicians who had also provided me with assistance through the duration of the study. For parties not mentioned here, I would like to also express my thanks.

TABLE OF CONTENTS

LIST OF TABLES

LIST OF FIGURES

LIST OF SYMBOLS

d	Beam-end displacement
d_b	Beam section depth
δ_t	Beam displacement at top flange (y-direction)
δ_b	Beam displacement at bottom flange (y-direction)
E	Elastic Modulus
$E_{a,\theta}$	Elastic Modulus of steel material at temperature θ
f_y	Yield strength of steel material
$f_{y,\theta}$	Yield strength at temperature θ
$f_{u,\theta}$	Ultimate strength at temperature θ
F_{Rd}	Resistance Force
k_i	Component for component method as per EC3: Part 1-8
$k_{y,\theta}$	Reduction factor for yield strength
$k_{u,\theta}$	Reduction factor for ultimate strength
L	Length of beam
t_a	Thickness of angle section
t_f	Thickness of T-stub considered
r_a	Root radius of angle section
θ	Rotattion of joint

CHAPTER 1

INTRODUCTION

1.1 Introduction

Steel tubular sections can be defined as members having cross section, which enclose outer perimeter with a finite value of thickness. Smaller size tubular sections such as 40mm section width or diameter are often used as members for trusses. However, the use of larger size tubular sections as columns is gaining popularity. Adoption of steel tubular sections as structural columns has several advantages. With a higher radius of gyration on the minor axis, tubular columns have higher compressive strength than a similar open section member does. Study show that, compared to standard open-section columns, the use of tubular section as columns results in reduction of steel by 14% to 24% for seismic load resisting moment frames (Kang et al., 2001).

In general, tubular columns in construction can be divided into bare steel tubes (BST) or concrete-filled tubes (CFT). The closed-profile concept of the hollow section works similarly to formwork, and the cavity is often filled with concrete to increase the strength and the load carrying capacity of the column (Cheng & Chung, 2003; Tizani et al., 2013). The addition of concrete provides an option for bolts to be effectively anchored into the column, thus increasing the tension resistance due to the combination from both concrete shear and the bolt tension capacity. Meanwhile the effect on the connection behavior is the shift in rotational axis towards the compression area of the beam, thus causing the connection to have high stiffness and moment capacity at the cost of low connection ductility (France et al., 1999) due to the increased stiffness at the column with in-filled concrete. It is common in construction to have concrete in-fill in reducing the effect of loads on to the steel column as a result from the increase in compressive resistance.

In terms of fire safety, structural steel has the risk of being exposed to high-temperature conditions. The requirement of performance-based design highlights the needs for evaluating the fire resistance of steel structures in terms of their structural and thermal responses for given set of loading and fire exposure conditions. Recent fire cases and full-scale fire tests show that joints may often be the weakest link in a structural frame in fire conditions. Extensive studies are available on structural members under fire, such as beams, columns, and connections for open section steel members, including studies conducted by Liu et al. (2002), Saedi Daryan and Yahyai (2009), Mao et al. (2009), Li et al. (2012) & M. Wang and Wang (2013). However, the number of studies conducted for steel connections in tubular column at elevated temperatures is relatively small. It is recommended that more studies should be conducted at elevated temperature conditions.

1.2 Problem Statement

When tubular sections function as structural columns, the connection of open section beams to these types of column requires further studies. In connecting open section steel beams to tubular columns, welded connection is considered as one of the acceptable solutions with good connection performance (Beutel et al., 2001; Torabian et al., 2012; Qin et al., 2014).

Welding may either involve direct connection on the tubular column face (Shin et al., 2004) or a through-beam method (Elremaily & Azizinamini, 2001). However, the welding method of the beam to tubular columns has several disadvantages. Direct welding of beam sections to tubular columns, have been shown in an earlier study (Alostaz & Schneider, 1996), leads to shear distortion in the tubular column and fracture of the column wall. Thin tubular column wall is critical against the effects of shear and bending loads. In addition, column size is partially governed by the beam width when direct welding is used as the connection method. With higher beam width, the column face must be equally wide to accommodate the beam. If larger sized column is to be used, advantage from the use of tubular columns is offset with the accommodation for the higher beam width. Additionally, in oil & gas industries, the use of welding to complete the connection is not preferred due to safety issues with existing volatile gases on-site. With the disadvantages highlighted, welding major connections are not a preferred method for connections to tubular columns, leading to the utilization of bolting.

Another viable connection method is the use of bolts. Shen and Astaneh (1999) described the advantages of bolted connections to open-section steel columns over welded connections. Energy dissipation under earthquake loadings are higher for bolted connections over welded connections. The advantages are also applicable for connections to tubular columns using bolts. While bolted connection has advantage over welded connection, a major consideration is the method to connect bolts from beams to tubular columns. As shown in Figure 1.1 for bolted end-plate connections to both open and tubular column types (Ghobarah et al., 1996; Adam & Hamburger, 2010), tubular columns limit the available options for a bolted connection. Conventional bolted connections are not feasible because of the limited access to the bolt nut, which hinders the tightening process and completion of the connection. Modifications on the bolted connection type by changing the bolt type and mechanism are needed to solve this problem.

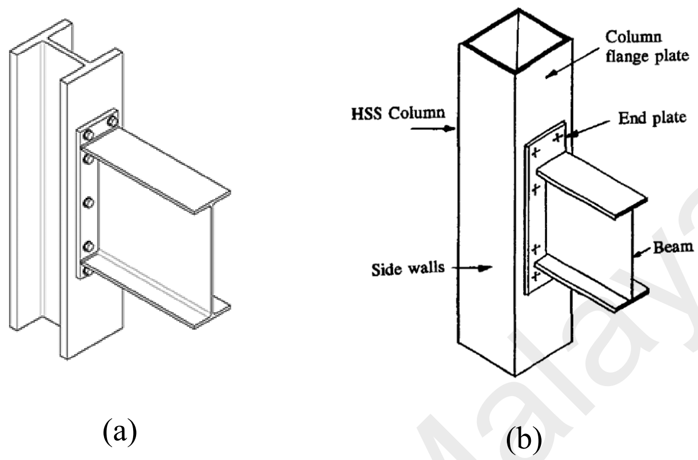

Figure 1.1 General end-plate connections to

(a) Open Section Column (Adam & Hamburger, 2010)

(b) Tubular Column (Ghobarah et al., 1996)

An alternative bolting method is having a one side tightening system where components are substituted for the bolt nut. The common term for this category of connection system is blind bolts. Blind bolts systems rely on two basic ideas, which is having a flare component that will expand when tightened and thus creating a nut substitute or creating bolt grooves on the member wall where the member wall acts as the nut, with examples as shown in Figure 1.2. Using the blind bolt system raises the question of the capability to hold the bolt in place while forces are being transferred through these bolts. However, current studies have not shown clearly the effect from these bolts and the structural capability. In addition, several studies have shown that the performance of the connection which uses these bolts to be highly dependent on the column thickness. The effect from the column thickness negates the cost saving advantage as described earlier.

A combination of welding with standard bolts within a single connection is then utilized to minimize the use of blind bolts. With the combination, certain parts of the connection can be welded to the column first and the connection to be completed at the site using standard bolts. A large number of different assemblies are available and considerable researches have been conducted (Málaga-Chuquitaype & Elghazouli, 2010; Bagheri Sabbagh et al., 2013; Y. C. Wang & Xue, 2013). Regardless of the connection configuration, the load transfer mechanism should be understood for each configuration.

The existing connection details with combination of welding and standard boltingare either classifiable as marginally pinned connections or having components which is dependent on the depth of the beam, such as the reverse-channel. These component details are highly dependent on the depth of connecting beam and unbeneficial for deep beams such as those higher than 500 mm. In addition, the center area of the beam is often under-utilized, which the connection can be further strengthened with additional connection components that contribute to connection capacity when necessary.

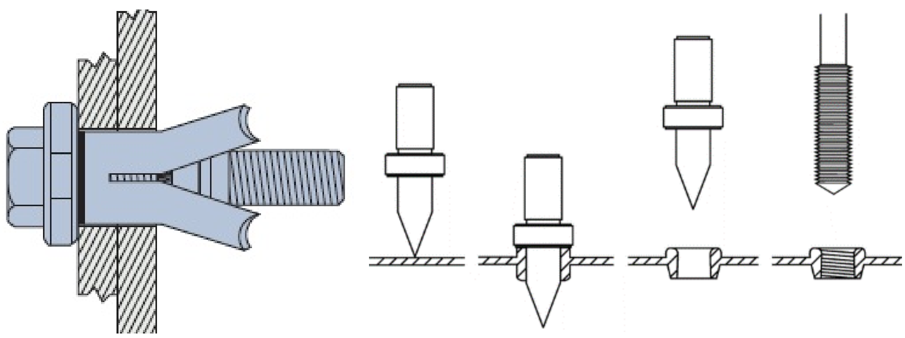

Figure 1.2 Flare systems and nut creation system in blind bolts.

In further consideration, fire poses a major critical effect to be considered for steel connections due to the relative rapid degradation of steel materials at high temperatures. Extensive studies have been conducted for steel beams and columns at elevated temperatures, however, studies have shown that there is still a considerable lack of research for joints at elevated temperatures. There are various types of connection possible with steel members due to flexibility of combination of bolts, plates and welding to form the connection to suit the purpose and site conditions. The best direction to cater for these gaps would be to conduct studies experimentally, as actual testing mirrors the actual behavior of the connection. However, the cost to conduct these tests are often the main issue and therefore, the alternative would be to make use of numerical methods to simulate previous tests and conduct further studies from the verified models.

Current studies have concluded that connection in elevated temperature conditions are expected to resist force changes in the connection due to elevated temperatures. The different changes include the compressive forces induced by the thermal expansion of steel components under high temperatures followed by internal tension forces under the cooling stage. Without the resistance to these force changes, progressive collapse of the structure has a higher possibility. Progressive collapse of a structure is should be avoided to have localized failures instead. With localized failure, the loading at the failed member is distributed among the other adjacent structural members and thus, additional capacity are necessary to retain the integrity of the structure as whole. Therefore, to reduce the possibility of a progressive collapse of a structure, each connection is to have a certain ductility before reaching the ultimate failure. Ductility can be achieved when beams are having a higher deflection beyond the yield failure of the beam, while for connections, is in terms of a high rotational capacity and the capability of resisting plastic deformations before the ultimate failure of the connection components. Therefore, high ductility is a greatly desired parameter for connections under elevated temperature conditions.

With the above reasoning, a new connection for open-section beams to tubular columns is proposed. The basic concept for the proposal is to avoid directly welding the beam on the column face and to use standard bolts as a component in the connection. A new connection called the reverse top-seat angle connection is proposed as shown in Figure 1.3, which is both simple and easy to fabricate while having a high yield moment to connection weight ratio. The available space between the plate and column face can be further utilized for other connection components such as additional fin-plate connection and further modifications to improve the connection performance or deformation behavior. Furthermore, the proposed connection details is not dependent on the beam depth as the focus is on moment resistance of the connection, which is largely influenced by the lever arm of the bolts from the edges of the beam. A balance between maximizing lever arm, connection detail requirements, fabrication difficulty and cost is considered for the proposed connection.

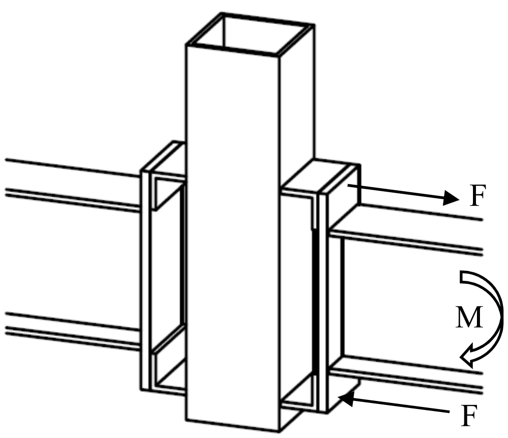

Figure 1.3 Proposed Reverse Top-Seat Angle Connection

1.3 Research Objectives

The main objective of research is to develop a new type of connection called the reverse top-seat angle connection for tubular columns and to study the behavior and performance of this connection at ambient and elevated temperature conditions. In addition, studies are also conducted to determine the strategies that improve the connection behavior by understanding the geometric variations that affects the connection performance, to assess the rigidity and fire resistance of the proposed connection. Specific objectives of the study are as follows: -

1. To develop a new semi-rigid connection for tubular columns and to conduct full-scale experimental tests at ambient and elevated temperatures.
2. To develop a finite-element model for predicting the behavior of reverse top-seat angle connections at ambient and elevated temperatures. The model will be validated with the experimental results.
3. To investigate the effect of various parameters on the connection behavior at ambient and elevated temperature conditions.
4. To compare efficiency and performance of the proposed connection with the existing connections.

1.4 Scope of Study

With the limitations surrounding the connection of open beam sections to tubular columns, where welding and blind bolt connections are considered less than favorable solution, a new type of connection is purposed. The study covers the experimental test, finite-element modelling and parametric studies of the reverse top-seat angle connection. The experimental tests consist of three specimens at ambient temperature and four specimens at elevated temperature conditions. The experimental test specimens at elevated temperature are different in terms of three parameters, while the specimens at ambient temperature vary by two parameters.

The evaluation of connection performance is normally conducted using monotonic loading. Elevated temperatures according to ISO834 fire curve is applied using an-isothermal method, where the temperature varies with time and initial static single value load. Meanwhile, the finite-element studies are performed using multi-purpose finite-element analysis software, ABAQUS. The mathematical model and some of the numerical studies are validated with existing results in literature as well as with the conducted experiments. The parametric studies examine the variations of geometric properties and its effect on the connection behavior. The model results are also used for performance comparison with existing connection types to tubular columns.

For elevated temperature conditions, the effect of loading type and boundary conditions are examined. Boundary condition studies include bolted connections to frame support and simple support. In addition, various levels of axial restraints and the effect of isothermal loading conditions are taken into consideration as another aspect of study. Although critical, the cooling stage at elevated temperature are not covered in this study as the measurements have to be earlier planned and warrants a different scope altogether. Progressive collapse of the structure is also another area under similar conditions and not studied in this research.

1.5 Significance of Study

The present research work provides an alternate connection for tubular columns, which is easy to fabricate and flexible in terms of modifications for the performance improvement. The connection has been shown to use less number of bolts, lower welding length requirements and significant improvement of connection performance with minimal changes to the connection overall weight. Ductility of the connection is affected by neither the increase in stiffness nor the increase in yield moment, which are commonly concluded for other connection configuration to tubular columns.

In terms of fire safety for structural steel, a review of the currently available literature shows that the experimental results for steel joints in elevated temperatures is currently lacking and therefore the current work provide experimental results which contributes in expanding the experimental database. For validation of design models, including for analytical, component-method and the finite-element method, the experimental outcome can be used to compare the accuracy of the proposed method. In addition, the behavior of the connection in fire also shows the distribution of temperatures and how each component interacts and the contribution in general to the connection overall behavior.

1.6 Layout of Thesis

Chapter One outlines purpose and general background of the study. It also includes the detail objectives of the research work. The contribution from the results of the study is also detailed. In addition, limitations of the present work are also highlighted.

Chapter Two discusses the previous studies that has been conducted and investigated on connection for tubular columns. It includes studies on blind-bolts, direct and indirect connections to tubular columns, and joints in elevated temperatures. Various approaches are available in literature; however, the focus of present work is on experimental and finite-element method. Significance and importance of the various studies in literature is also presented.

Chapter Three focuses on the description of methods and procedures used for the present work. In terms of experimental tests, it includes the test setup, loading arrangement, specimen details, instrumentation and data collection. Finite-element studies are divided into sections of ambient and elevated temperature conditions. Details of various parameters used in analysis such as temperature load application, type of element, appropriate material model, boundary condition, etc. are also mentioned.

Chapter Four presents the results and discussion of reverse top-seat angle connection at ambient and elevated temperature condition. Test results, behavior, deformation and failure modes observed in the experimental tests and finite-element studies are mentioned. Discussion on the structural behavior and deformation are also highlighted. Parametric studies such as effect of stiffeners, boundary conditions and other relevant parametric changes are also detailed in the respective chapters. Comparisons of the performance of the proposed connection with existing connections are also presented. In terms of elevated temperature condition, results from the test are presented with the deformation pattern examined. Elevated temperature models created in ABAQUS are developed and validated with the experimental results.

Plastic strain concentration is determined from the validated models for detailed investigation on the deformation of the connection under elevated temperature conditions. Further extension to the model is studies on the boundary conditions and effect of axial loadings towards the connection behavior. Finally, the ratio between the connection under elevated temperature and ambient temperature is proposed as a simpler method to cater for the combined effect of the various components of the connection because of the degradation of steel material at elevated temperatures.

A summary and conclusion of the study with main findings are discussed in Chapter Five. This includes the discussion on the factors that may have affected the results produced from testing and modeling, discussion on the various possibilities to improve the study, and recommendations for future investigations.

CHAPTER 2

LITERATURE REVIEW

2.1 Introduction

A joint is defined in Eurocode 3: Part 1-8 (2005) as the zone where two members interconnect. In the design process, the full value of shear, axial and moment forces is assumed to transfer between these members. In comparison to the term joints, steel connections refer to the assembly system of steel components that combines to provide the means to transfer loads accordingly. These steel components can be a combination of, but not limited to, steel plates, sections of members, welds and bolts. While the terms connection and joints are relatively different, the terms are considered interchangeable in the context of the current research work.

A variety of connection configurations currently exist, including those that were fabricated in-situ as a solution for case-to-case basis due to limitations encountered at the site, such as clashing with pipes, utilities and spacing issues. Some of the common steel connection configurations to open section columns are as shown in Figure 2.1. End plate connections can be divided into flush end-plates, extended end-plate, flexible end plates or partial depth end plates. In this connection type, a plate connected is welded to the beam end and bolted onto the supporting member in a column-beam case. Meanwhile, angle connections can be further divided into double angle web connections, top and seat angle connection and the top and seat with double web angle connection. In angle connections, angle members are cut into lengths and bolted to the column and members to complete the joint.

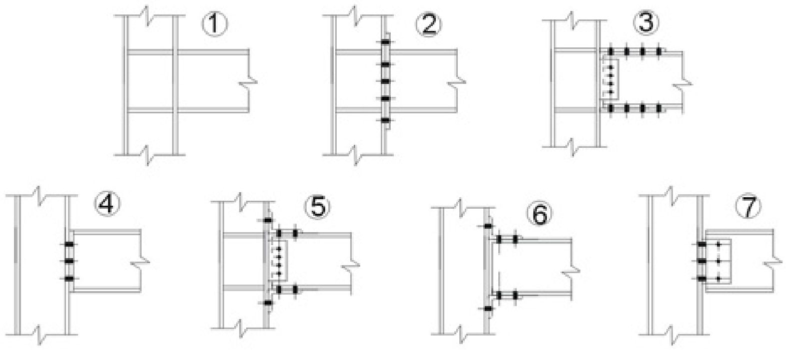

Key:- (1) – Welded Connections, (2) – Extended End-Plate. (3) – Top and Flange Splice (4) – Flush End Plate, (5) – Top, Seat and Double Web Angles, (6) – Top and Seat Angles, (7) – Double Web Angles

Figure 2.1 Common Steel Connection Configurations (Galambos, 1988)

Design of connection is based on support conditions determined for the supported beam design. The two common conditions assumed are rigid and pinned support. Moments are distributed to rigid supports due to the resistance capability that results in a smaller beam member section. It is common concept that moment loads are resisted by the beam for pinned supports, ending in a comparatively larger beam size. Therefore, the classification of the support is essential as it determines the forces and loads that have to be resisted by the connection components and the different structural checks required.

Concept of pinned connections allows for the rotation with minimal loads while rigid connections are expected to have minimal deformations until the design loads are achieved. The simplification of the connection to either rigid or pinned extremities has been included with the current concept of semi-rigid connections. As depicted in Figure 2.2, minimal loads are required to induce rotation in pinned connections while higher loads are required for rigid connections.

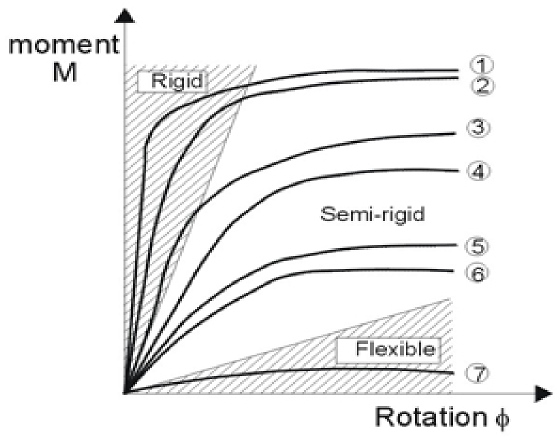

Figure 2.2 Typical moment-rotation curves for various connections type.
(Galambos, 1988)

In this chapter, the discussions are first on the joints definition in Eurocode 3: Part 1-8 (2005), followed by steel material behavior in both ambient and elevated temperatures. Subsequently, tubular columns are briefly described. With the studies on the connections to tubular columns, bolted and the combination of both bolting and welding connection configurations is focused. Therefore, blind bolt is considered a connection option and the studies are discussed. Subsequently, connections to tubular columns at ambient and elevated temperatures are outlined in separate sections respectively.

2.2 Joint Behavior to EC3: Part 1-8

In Eurocode 3: Part 1-8 (2005) rotation capacity is defined as the angle through which the joint deforms for a given resistance level without failing while rotation stiffness the moment that is required to produce a unit rotation in a joint. Moment bending forces are the result from load and eccentric distance that produces rotation in an axis. Behavior of connections is commonly represented as a moment-rotation graph as shown in Figure 2.3.

Major parameters includes the rotation stiffness $S_{j,ini}$, moment resistance of joint, $M_{j,Rd}$ and joint rotation, Φ. The moment-rotation curve can be obtained through actual experimental testing of the joint, empirical methods or computer based modeling.

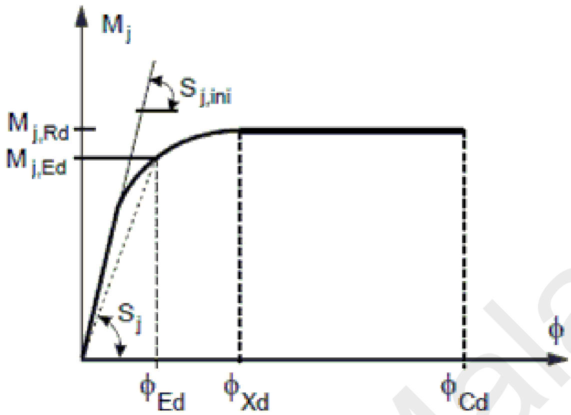

Figure 2.3 Simplified bi-linear graph of moment-rotation curves.
(EC3: Part 1-8, 2005)

Rotational stiffness of a joint is denoted by S_j, which can be determined numerically using Equation 2.1 as shown in EC3: Part 1-8 (2005). In the equation, E represents the Young's Modulus while *z* denotes the lever arm, *k* as the stiffness factor for the component involved. Parameter μ is the stiffness ratio that depends on the ratio between an applied moment and the maximum moment designed for the connection, where clause 6.3.1 (6) in EC3: Part 1-8 (2005) can be used to calculate the value of parameter μ. The equivalent stiffness, k_i can be determined using the multiple spring systems theory as according to Hooke's law, with the analogy that each component is a spring and have a limited stiffness value.

$$S_j = \frac{Ez^2}{\mu \sum_i \frac{1}{k_i}} \qquad \text{Equation 2.1}$$

The requirements to classify the connections are explained in EC3: Part 1-8 (2005) and shown in Equation 2.2 and Equation 2.3 for rigid and pinned connection, respectively. Connection is classified as semi-rigid if both conditions are not fulfilled. The classification is dependent on the beam second moment of area, I_b and the length of the beam, support-to-support, L_b.

$$S_{j,ini} \geq 25E\frac{I_b}{L_b} \quad \text{Equation 2.2}$$

$$S_{j,ini} \leq 0.5E\frac{I_b}{L_b} \quad \text{Equation 2.3}$$

2.3 Steel Material Behavior

2.3.1 General Steel Material

Steel material is usually uniform and therefore, little variation can be found due to the standardized process of producing steel sections. The common properties of steel in any analysis and design includes the yield stress, ultimate stress and the Modulus of Elasticity. The typical stress-strain graph is as shown in Figure 2.4 as documented by Cafer (2009). Strains of 0.002 in elongation length ratio are still considered to be in the elastic range while the ultimate stress lies between the 0.1 and 0.2 strain. Poisson ratio according to EC3: Part 1-1 (2005) is set as 0.3 for both elastic and plastic range although the standard specified the value for the elastic range.

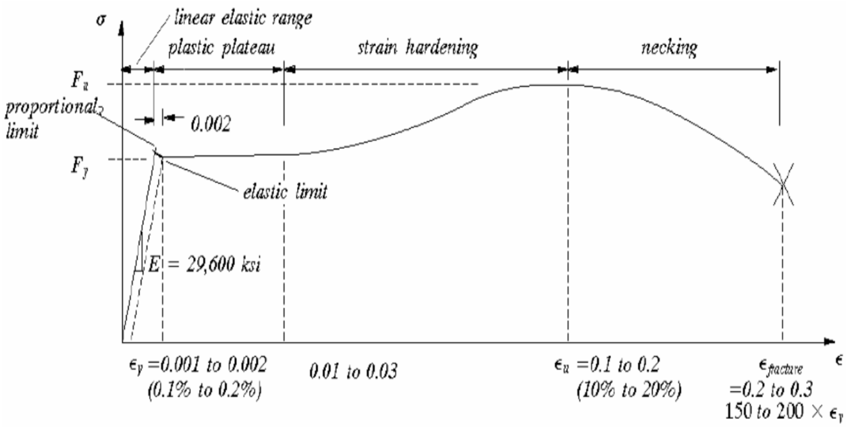

Figure 2.4 Typical Stress-strain behavior of steel material.

2.3.2 Elevated Temperature Steel Material

Steel materials behave differently at elevated temperature compared to at ambient condition. According to Eurocode 3: Part 1-2 (2005), the thermal elongation behavior of carbon steels can be established with the formulas as shown in formulae 2.7(a), (b) and (c) in EC3: Part 1-2 (2005). Figure 2.5 illustrates the summary resultant from the formulae 2.7 in EC3: Part 1-2 (2005) for the relative elongation of steel as a function of increasing temperature.

From the graph, it is shown that the elongations of steels between temperatures of 750°C to 850°C remains unchanged, which constitutes that in the range of temperatures, the steel connection does not suffer from an increase in stresses due the elongation of steels under temperatures. The basis for measurement is at 20°C, which would result in an elongation due to the local temperatures of anywhere between 30°C and 35°C as the basis of ambient temperatures, but the change as seen in Figure 2.5 is relatively minor and negligible.

Relatively, the change in length with respect to the temperature involved has a linear behavior. The effect of thermal elongation is not a complicated phenomenon to be considered in the analysis, however, the actual elongation of each of the components is not relatively known and therefore further calibration is needed. The current research work did not include the effect of thermal expansions for simplicity and reducing further considerations that complicates the behavior analysis.

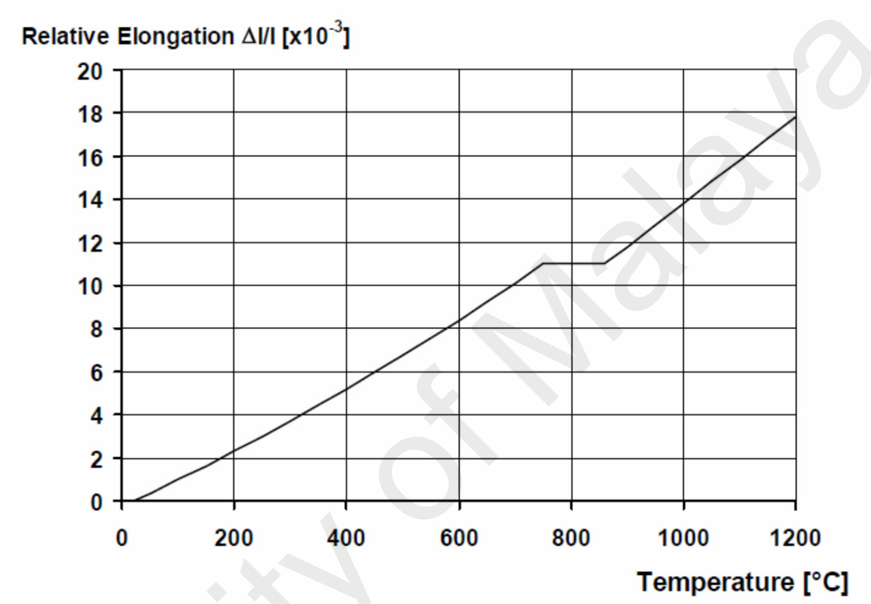

Figure 2.5 Relative Elongation of carbon steels as a function of temperatures.
(EC3: Part 1-2, 2005)

Meanwhile, thermal conductivity of carbon steel is governed by the graph shown in Figure 2.6. From the graph, thermal conductivity of steels decreases as temperatures increase and continues to remain constant after 800°C but no thermal conductivity is defined for temperatures after 1200°C, as the temperature results in a strength ratio approaching zero. Proposed analysis method for the thermal distributions in steel connections is covered in sections of 4.3.1 and 4.3.2 of EC3: Part 1-2 (2005). However, the thermal distributions in both connections and beams are affected by the heat transfers from convection and radiation. This is traced to the heat flux of both exposed and unexposed sides of the steel components where the heat transfer is affected by the temperatures of the gas and steel surface temperatures, which falls under the guidelines provided by EC1: Part 1-2 (2002). In addition, multiple nominal temperature-time curves is defined in the code, however, other than the external fire curve and hydrocarbon curve, the focus in the current research is the standard fire-curve, which collates to the ISO834 curve.

Generally, the consideration in analysis is the relevant thermal actions and variation of strength with temperature. A large number of studies have ignored this property in the analysis, with the assumption that the temperatures are uniform throughout the connection for simplifications. An example simplification is shown in the variation of the temperatures to be used at the joints which has been proposed as according to Table 2.1 as was studied by Simões da Silva et al. (2001), which is particularly useful for individual connection component studies. In most studies, such as those by Saedi and Yahyai (2009a) the thermal elongations are not considered and where in the case of Simões da Silva et al. (2001), it was not considered due to a lack in calibration of thermal elongations data.

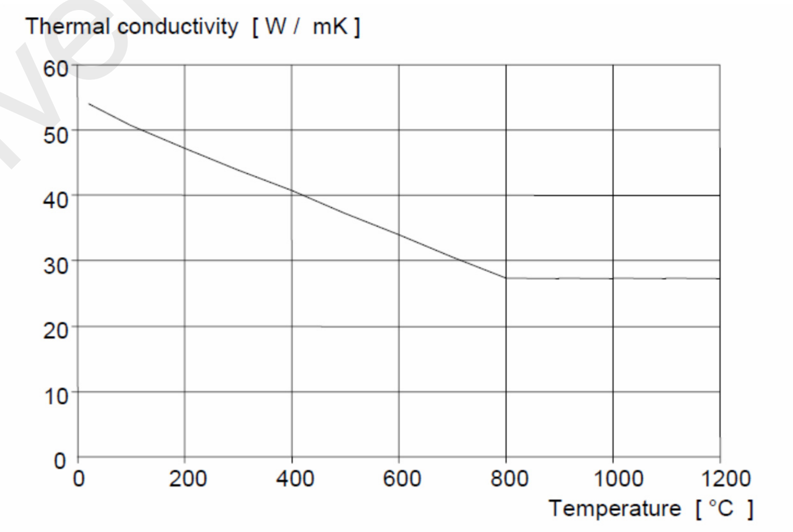

Figure 2.6 Thermal Conductivity of steels as a function of temperature.

(EC3: Part 1-2, 2005)

The major property of steel that is critical in the consideration for elevated-temperatures condition analysis is the reduction factors for the degradation of the strength, Young's modulus and the proportional limit of the material due to the temperatures. In EC3: Part 1-2 (2005), the material reduction factors of steel depending on the temperature are as shown in Table 2.2. For temperatures in between those specified, e.g at 550°C, the factors can be linearly interpolated accordingly. The factor was a result from the tensile tests done in isothermal conditions, where the specimens are heated to the specific temperature regardless of rate and subjected to tensile forces.

Eurocode 3: Part 1-2 (2005) has also provided the stress-strain curve for steel, defining the slope of the elastic area, the curve after the proportional limits and the limitation strain for the behavior under elevated temperature. Definition of the curves is as shown in Table 2.3 with Figure 2.7 showing the general stress-strain curves under temperature. In addition, as indicated in Annex A of EC3: Part 1-2, strain hardening can be applied for temperatures below 300°C, at a summarized value of 1.25 of yield stress. This proposed value is applied to the material in the current research.

Table 2.1 Temperature distribution ratio for components at elevated temperatures. (Simões da Silva et.al. 2001)

Element	Temperature Ratio
Beam Bottom	1.00
Beam Top	1.02
Beam Web	1.06
Bottom Bolt	1.01
Middle Bolt	1.03
Top Bolt	1.04
Column Web	1.14
Column Flange	1.03
End-Plate	1.03

Table 2.2 Reduction factors for steel at various temperatures.
(EC3: Part 1-2, 2005)

Temperature	Modulus of Elasticity	Proportional Limit	Yield Strength
20	1.00	1.000	1.000
100	1.00	1.000	1.000
200	1.00	0.807	0.900
300	1.00	0.613	0.800
400	1.00	0.420	0.700
500	0.78	0.360	0.600
600	0.47	0.180	0.310
700	0.23	0.075	0.130
800	0.11	0.050	0.090
900	0.06	0.0375	0.068
1000	0.04	0.025	0.045

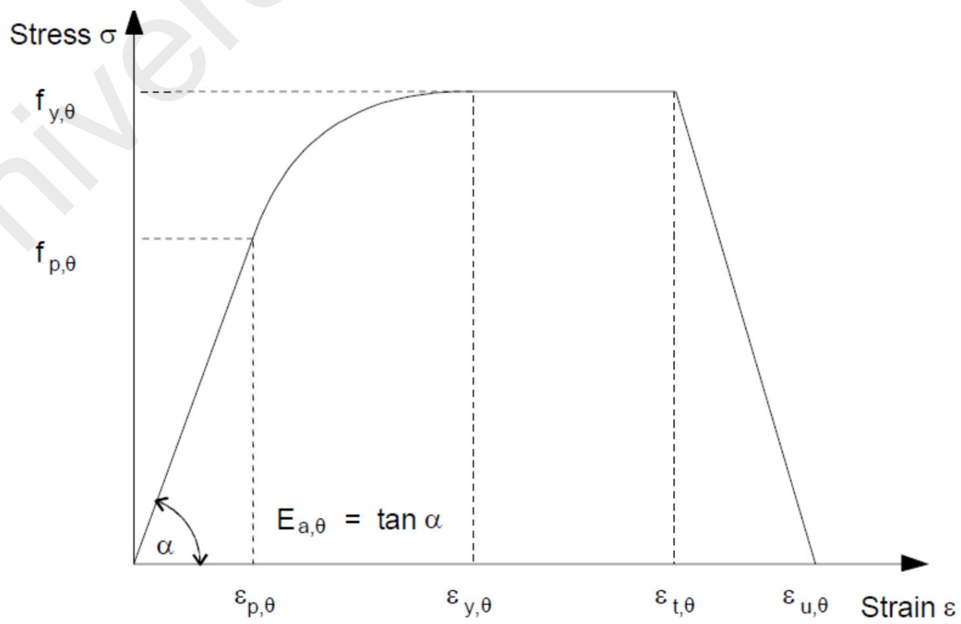

Figure 2.7 Stress-strain curve for steel at elevated temperatures

Table 2.3 Material curve definition formula (EC3: Part 1-2, 2005)

Strain range	Stress σ	Tangent modulus
$\varepsilon \leq \varepsilon_{p,\theta}$	$\varepsilon\, E_{a,\theta}$	$E_{a,\theta}$
$\varepsilon_{p,\theta} < \varepsilon < \varepsilon_{y,\theta}$	$f_{p,\theta} - c + (b/a)\left[a^2 - \left(\varepsilon_{y,\theta} - \varepsilon\right)^2\right]^{0.5}$	$\dfrac{b\left(\varepsilon_{y,\theta} - \varepsilon\right)}{a\left[a^2 - \left(\varepsilon_{y,\theta} - \varepsilon\right)^2\right]^{0.5}}$
$\varepsilon_{y,\theta} < \varepsilon < \varepsilon_{t,\theta}$	$f_{y,\theta}$	0
$\varepsilon_{t,\theta} < \varepsilon < \varepsilon_{u,\theta}$	$f_{y,\theta}\left[1 - \left(\varepsilon - \varepsilon_{t,\theta}\right)/\left(\varepsilon_{u,\theta} - \varepsilon_{t,\theta}\right)\right]$	-
$\varepsilon = \varepsilon_{u,\theta}$	0.0	-
Parameters	$\varepsilon_{p,\theta} = f_{p,\theta}/E_{a,\theta}$ $\quad \varepsilon_{y,\theta} = 0.02$ $\quad \varepsilon_{t,\theta} = 0.15$ $\quad \varepsilon_{u,\theta} = 0.2$	
Functions	$a^2 = \left(\varepsilon_{y,\theta} - \varepsilon_{p,\theta}\right)\left(\varepsilon_{y,\theta} - \varepsilon_{p,\theta} + c/E_{a,\theta}\right)$ $b^2 = c\left(\varepsilon_{y,\theta} - \varepsilon_{p,\theta}\right)E_{a,\theta} + c^2$ $c = \dfrac{\left(f_{y,\theta} - f_{p,\theta}\right)^2}{\left(\varepsilon_{y,\theta} - \varepsilon_{p,\theta}\right)E_{a,\theta} - 2\left(f_{y,\theta} - f_{p,\theta}\right)}$	

2.4 Tubular Sections

Common steel tubular sections can be categorized into two, i.e rectangular shaped and round, the latter commonly referred to as pipes, differences shown in Figure 2.8. Higher strength tubular sections are produced through the cold-rolled method and otherwise for hot-rolled sections. Cold rolled tubular sections are identified through a welding seam on either side face of the section, due to the procedure of shaping the steel sheet to section configuration and welding the connecting edges to close the shape.

Figure 2.8 Rectangular and round tubular sections

In structural terms, columns mainly resist the compression loads and therefore is susceptible to buckling, depending on the slenderness ratio. A higher slenderness ratio results in the column to have buckling failure at a certain load level. The critical minor axis is taken into consideration. To reduce the slenderness ratio, assuming similar lengths, the radius of gyration has to be increased. In comparison, the radius of gyration is lower for the tubular columns when compared to the open section columns for the minor axis, resulting in a smaller section column.

The use of tubular columns results in a total steel-weight-usage reduction between 14% and 24% for seismic loads resisting moment frames (Kang et al., 2001). The tubular column can be furthered improved as the closed-profile concept of the hollow section works similarly to formwork, and the cavity is often filled with concrete to increase the strength and the load carrying capacity of the column (Cheng & Chung, 2003; Tizani, Wang, et al., 2013)

2.5 Blind-Bolt Studies

In connections to tubular columns, modifications to the bolting system are necessary to preserve bolting major configurations. This involves in the use of blind bolts that require only one-sided tightening and access. A major concept is raised on the capability to hold the bolt in place while forces are being transferred through these bolts. Understanding the blind bolts system is necessary to determine the options available for connecting open section beams to tubular columns.

The currently available commercial brands (Tizani, Al-Mughairi, et al., 2013) include the following: Hollo-Bolts ("Lindapter,") which provide one-sided bolt-tightening through expansion of the sleeve; flow-drill bolts ("Flowdrill,") which create nut imitating grooves on member; Molabolts, HuckBolts which compress the sleeve; AJAX bolts ("Ajax Engineered Fasteners,") which have collapsible washers, which are shown in Figure 2.9.

Various studies of blind bolts connection to tubular columns have been conducted. This includes on the tension and shear behavior and capability to understand the behavior of blind bolts. Standard or blind bolts are usually loaded in either tension or shear for any connection configurations. Shear behavior of Hollo-Bolts in both single and double shear have been previously conducted (Liu et al., 2012a). Owing to the significantly larger holes required to fit Hollo-Bolts, the out-of-plane deformation is higher in Hollo-Bolts than in standard bolts (Elghazouli et al., 2009). The increased hole sizes also cause the initial stiffness of the connection to be lower than when a standard bolt is utilized. The pullout of the bolt from the column is a common failure because of the increased hole size. Size for the Hollo-Bolt holes are generally larger than standard bolt hole sizes to cater for the flare component that is larger than the bolt shank diameter. Hollo-Bolts deform by pullout through a large hole when subjected to tension loads.

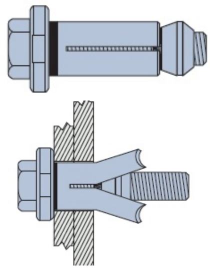

(a) Hollo-Bolts

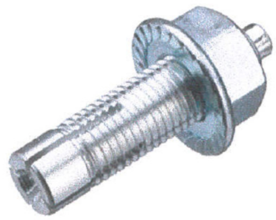

(b) Molabolts

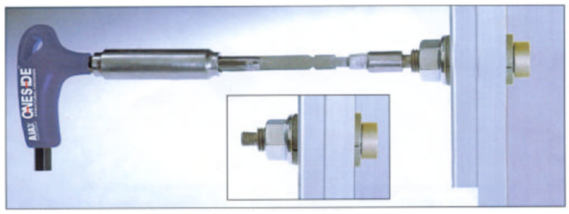

(c) AJAX-Bolts

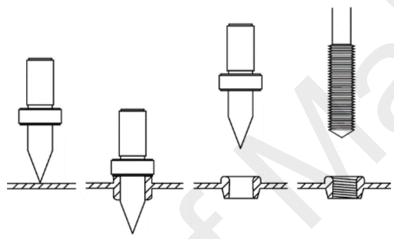

(d) Flowdrill-Bolts

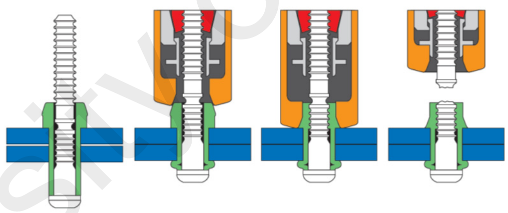

(e) Huck-Bolts: Blind Oversized Mechanical (BOM)

Figure 2.9 Different blind-bolts available.

In terms of blind bolt mechanism, the flare component of Hollo-Bolts has been found to have relatively low contribution to the overall bolt behavior (Wang et al., 2010). Compared to standard bolts in T-stub, the tension behavior of the blind bolts work in reverse. Thick members are advantageous to blind bolts while thin members work well for standard bolts. Comparison among threaded long bolts, standard blind bolt, and extended blind bolt has also been conducted (Pitrakkos & Tizani, 2013). In this study, the performance of extended blind bolt exceeds the performances of the other two variations under tensile tests. The increase in performance is a result of the higher shear area covered by the additional flare component at the end of the long thread.

Tizani and Ellis (2003) tested a Reverse Mechanism Hollo-Bolt (RMH) that was proposed by Barnett et al. (2000), as shown in Figure 2.10. Connections made with standard Hollo-Bolts lacks in clamping force and generally not considered as moment-resisting connections. The testing setup included an assembly of bolted together of two T-stubs, and the applicantion of axial tension loads. The other setup involved a thick T-stub connected to a tubular column, and tension loads were applied. The bending of the T-stub was eliminated because of the thickness. The test results show that RMH has higher ductility than standard bolts and that its stiffness has comparable properties to standard bolts. Any applied tension forces will be distributed as shear force on the flare component of RMH. Although this modified bolt has greater performance than Hollo-Bolts, this setup has not been used for other subsequent research.

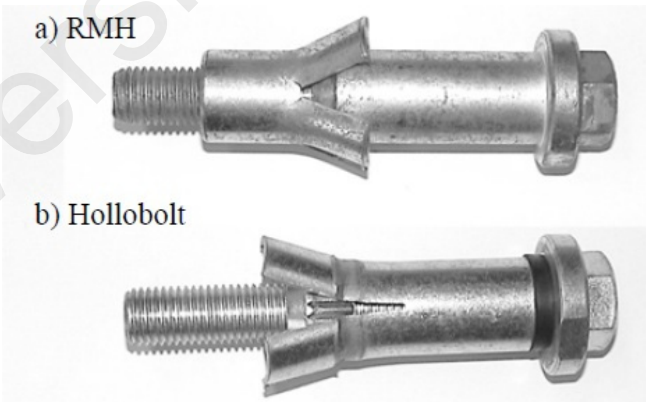

Figure 2.10 Difference between Reverse Mechanism Hollo-Bolt and Standard Hollo-Bolt (Tizani & Ridley-Ellis, 2003)

The performance of Huck-Bolts is comparable with that of standard A325 bolt performance, whereas mechanically oversized bolts has low levels of resistance (Korol et al., 1993). The resistance factors of Huck-Bolts and A325 bolts are 0.65 and 0.75, respectively. This insignificant difference in resistance factor shows that Huck-Bolts have a comparative behavior with standard structural bolts (Tabsh & Mourad, 1997). Other studies on connections by using flow-drill bolts (France, Buick Davison, et al., 1999b; France, Buick Davison, & Kirby, 1999) have shown that flow-drill bolts are as capable as standard bolts. The study has indicated that blind bolts are generally suitable for connections to tubular columns.

In terms of design for Hollo-Bolts and flow-drill bolts, the guidelines provided by the British Steel (Pipes, 1997) organization are applicable. In the guideline, shear and tension values for bolts are provided. The geometrical requirements to be used with these blind bolts are also shown. However, no studies have compared these bolts in terms of their effectiveness, cost, load transfer mechanism and structural performance. Comparison of blind bolt types will be useful for design considerations and different industrial applications. While blind bolts are comparable to standard structural bolts, the specialized nature of these bolts results in cost increase and these proprietary systems limits the usage globally. In addition, standard steel fabricators may not be competent to install the systems, relying on the sole distributors of the components in the respective regions of the world. As a result, blind bolts may not be economically viable until the blind-bolts can be mass-produced in any part of the world.

2.6 Previous Studies on Connection at Ambient Temperature

Investigations in ambient temperatures involve in static loads and cyclic loads and the focus of studies is on the behavior and deformation of the bare connection and column under loads. Without the effect of temperatures, this has eliminated the steel degradation factor and material property variation throughout the connection. Actual specimen testing contributes as a recommended method of study, as the behavior shown by the test results is reflective of practical usage under the boundary conditions specified. In previous years when the computational method is less advanced, specimen testing remains the method of choice. However, the consumption of resources results in a high wastage due to the various configurations and connection types available.

With the current advancement in computational power, an alternative is the representation of the studied subject as a computer model. It is able to simulate and produce results and deformation pattern similar to experimental results to a certain level of accuracy. With acceptable accuracy, the models are representative of the studied subject and thus parametric studies can be conducted with variation of the accepted model.

Where cases that the connection type has never existed, multiple model parameters would be easier to modify and evaluate as compared to having to fabricate a variety of new specimens for testing. Among the more common modeling techniques includes analytical models, finite-element models, component based models and empirical models. Reviews on previous studies on connections with different approaches are explained in the following sub-sections.

2.6.1 Experimental Studies

Significant numbers of studies are available for end-plate connections by using blind bolts (Wang & Chen, 2012; Wang et al., 2013). The proposed method by Maquoi et al. (1984) to weld threaded studs on to the column flange (Figure 2.11) in order to act as the bolts for the incoming end-plate connections has been discussed in various studies (Korol et al., 1993; Barnett et al., 2001). It was recognized that each stud must be protected from damage during the erection and assembly stage. The small welded area of the bolt is susceptible to failures due to the cantilever force acting on the bolt when the bolt clashes with other elements. Meanwhile, deformation of the column in the threaded stud connection is determined using the component method from EC3: Part 1-8 ("Eurocode 3: Design of steel structures," 2005) in a study conducted by Vandegans and Janss (1995).

To observe the actual shear deformation from blind bolts, a series of connections using angle connections is tested. The angle is subjected to shear load (Liu et al., 2012a). The resulting shear deformation is mostly contributed by the deformation of the angle section. In web angle connection, eccentricity exists because of the gap between the angle and column. Thick top angle sections transfer shear forces onto the blind bolts. Connection ductility is increased with the use of blind bolts. For thin top angles, the deformation of the top angle section occurs; thus, prying force develops in the bolt. Therefore, bolts are not fully loaded in terms of shear force only but are also affected by tension forces developed from the prying action. To avoid prying action, is it possible by having two row of bolts and position of bolt rows to be closer to root of the angle section.

Elghazouli et al. (2009) investigated a series of connections by using angle connections depicted in Figure 2.12. Ten specimens were tested under monotonic loadings. Variations in the tests included angle thickness, tubular column thickness, beam size, and changes in blind-bolt grade. For angle connections, the bolt gauge distance and the stiffness of the angle contributed to the resistance of the connection. In cases where the angle is sufficiently stiff, the bolts will be affected by the grade and size. From the tests, three deformation patterns were observed with bolted angle connections, namely, bending of angle, pulling out of the blind bolt, and column flange pullout. As one of the critical components, the column thickness governed the connection behavior. The connection width should be similar to the column width to avoid any local deformation on the column face.

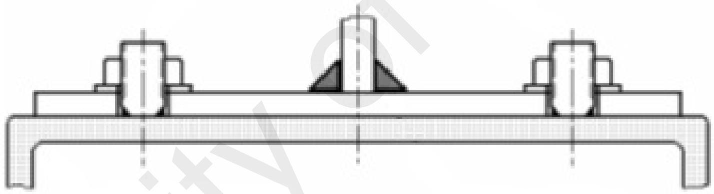

Figure 2.11 Welded threaded studs

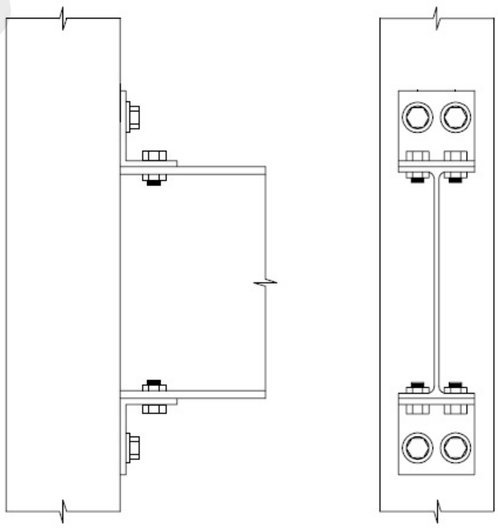

Figure 2.12 Angle Connections to Tubular Column
(Elghazouli et al., 2009)

By using AJAX bolts, standard bolts, and plates by Lee et al. (2010c) proposed a series of moment connections consisting of extended T-stub to BST tubular columns (Figure 2.13). The column and T-stub components were studied by connecting a T-stub to the column and subjected to axial loading. The column had a punching failure in tension, and crushing failure is observed in compression. The full connection was tested after the components were studied. Connection to the column sides was also proposed by using channels and plates (Lee et al., 2010b).

Further moment connection proposals were made (Lee, Goldsworthy, et al., 2011b, 2011a), concept was to shift away from the flexible face of the column and utilize the entire column section to resist the applied loadings. The extended T-stub and channel was concluded to be five times stiffer than the connection in the previous study. The connection was considered as rigid to EC3: Part 1-8 (2005) standards. However, the proposed connections were relatively complicated and required multiple fabrication works for only a single joint. Fabrication simplicity is often preferred to reduce construction time.

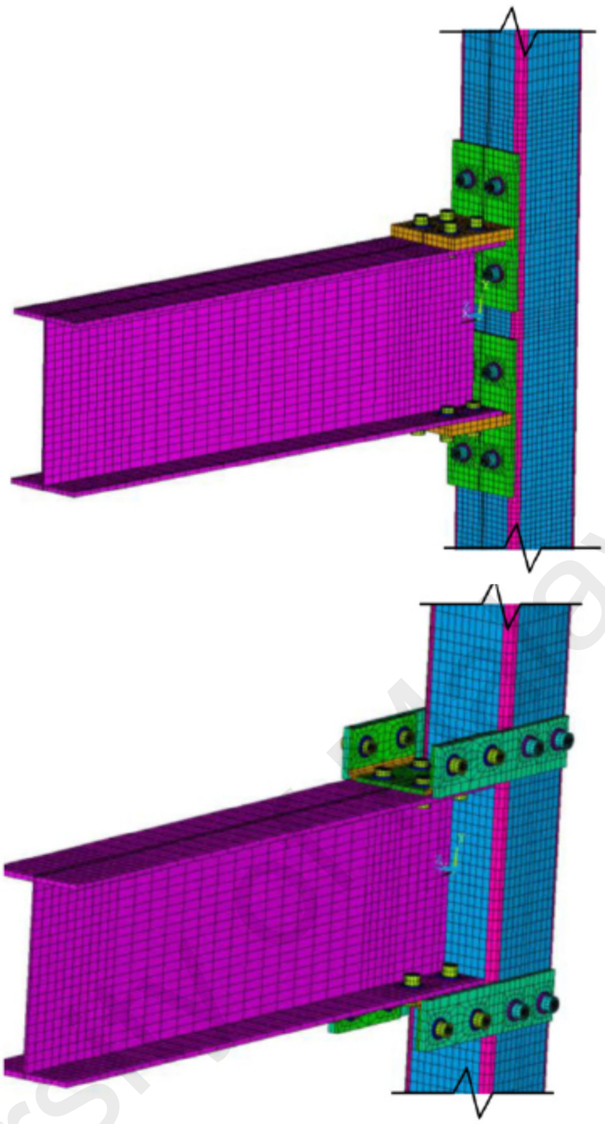

Figure 2.13 Extended T-stub and Channel Connection to Tubular Column
(Lee et al., 2010c; Lee, Goldsworthy, et al., 2011a)

Without using blind bolts, connection configurations are proposed with the combination of welding other steel parts to the tubular column and bolting the beam to the welded part. With this method, the welded components work as an extension from the column with space available for external bolting and thus standard bolts can be used. According to another test conducted at elevated temperatures (Ding & Wang, 2007), a reverse channel connection (Figure 2.14) has been shown to display advantageous behavior, which including high ductility measured through the rotation, ability to develop catenary action and moderate fabrication cost.

Compared with direct column connections, including end plate and fin-plate connections, reverse channel connection was adopted by Malaga and Elgazhouli (2010a) for further studies at ambient temperatures. A series of tests under monotonic loadings was conducted for top-seat angle connections with reverse channel. The effects of angle thickness, column thickness, and reverse channel thickness were studied. Similar to previous studies using angle connections, the affecting parameter included gauge distance, angle thickness, reverse channel thickness, and provision of web angles. Without the use of blind bolts, bolt pullout failure did not occur in this study. In thin-walled members, column flange pullout usually occurs in members when using bolted connection.

Reverse channel connections with end-plate connections are tested under monotonic loading to determine the moment-rotation behavior (Wang & Xue, 2013). Several specimens are fabricated. The end-plate thickness, reverse channel dimensions and thickness, column width, and the type of end-plate connection were studied. The main outcome is the deformation and failure of the reverse channel, and a column width that is similar to connected member width results in minimal column deformations. The critical point for this connection type is commonly at the heel of the reverse channel. When a thin end plate is used, bolt pullout failure may occur at the reverse channel web.

By using a concept similar to beam splicing, Bagheri Sabbagh et al. (2013) proposed new connections wherein the beam was bolted to an external diaphragm and a web fin plate. Among the three connections proposed, the connection shown in Figure 2.15 was selected for further experimental testing. By substituting a fin plate for a T-section, Al-Rodan (2004) proposed a connection with better performance than the fin-plate connection. The welds increased the moment of inertia and the flange bending capacity.

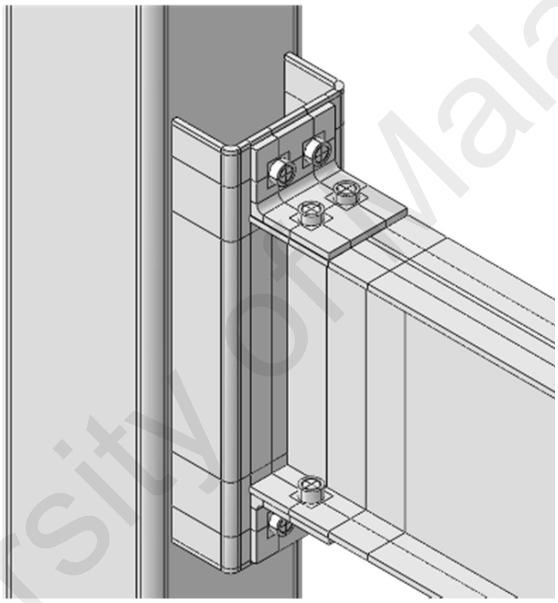

Figure 2.14 Reverse Channel Connection

Yao et al. (2008) used double T-sections bolted to circular hollow section (CHS) and square hollow section (SHS) columns at the top and bottom flanges of the beam. At the column, modified AJAX bolts with an additional perpendicular end were used, and the connection was shown to resist seismic loads. By realizing the issue with the welding of beams, Wu et al. (2005) proposed a connection wherein the bolts were connected through the depth of the CFT SHS column. Compared with other tests, the connection did not fail with an angular drift of 7%, whereas others reached up to 5%. The effect of the column width to thickness ratio was highlighted as the major contributing component to the dissipation of energy from the cyclic loads.

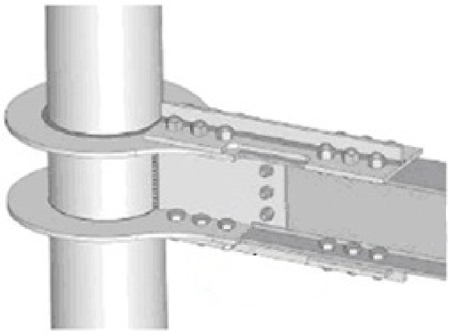

Figure 2.15 Connection to CHS with diaphragm.
(Bagheri Sabbagh et al., 2013)

A similar concept has been explored in a series of connections involving CHS (Sheet et al., 2013). A comparison between CHS and SHS shows that the connections perform similarly and that a minimal difference exists between the two profiles. Another connection with through beams without welding and bolting is also proposed. An angular drift of 5% is achieved with the proposed through connection. Although a through component may seem a viable option, a through bolt raises the issue of fabricator accuracy and construction viability.

On connections with through bolts, bolts can be inserted on one side and installed first; however, installing the other side will be difficult because of the existing stud from the bolts, thereby resulting in smaller clear distance for the beam. A probable scenario would be that the columns on the next gridline have to be pulled apart. If both beams will be installed together, multiple lifting equipment must be employed and the question of costs needs to be further considered.

For tubular beams connected to tubular columns, Satish Kumar and Prasada Rao (2006) proposed a connection involving a welded channel to the tubular column and bolted to the tubular beam. Considering the closed section of the tubular beam, square gaps were cut to the side of the beam, thereby enabling access to the bolting of the beam. With the large gap, the failure mode would occur near the thinner side of the cutout at the beam. However, the tested connection showed sufficient ductility and was suitable for seismic designed steel structures.

2.6.2 Empirical Models

Empirical is the study of connection behaviors based on observation without any form of postulations, or earlier knowledge of the behavior. Usually, this is applied in earlier studies of the connection. This is due to the limited knowledge available on a particular connection type and the feasibility of the connection.

Derivation of the empirical models require no previous knowledge of the analyzed problem and therefore, analysis are mostly based on the moment-rotation behavior graph where the empirical equations are developed to best reflect the shape of the graph produced from specimen testing by graph-fitting methods. From literature review, the more often used method is the regression analysis of the results. The common empirical model exists in a number of types: linear, polynomial, power and exponential models.

The earliest linear model was proposed by Rathburn (1936) from a ratio of rotation and moment representing Z, the semi-rigid connection factor. No doubt, that this can only be applied to the regression graph only due to the linear line involved.

From the linear models, improvements over the model has been made by introducing polynomial models as done by Sommer (1969) and referred to by Frye and Morris (1975). The polynomial model reflected closer to the actual graph when compared to the linear model as the actual curve has slight curve in the elastic-plastic zone. Equation for the model is as shown in Equation 2.1.

$$\theta = C_1(KM) + C_2(KM)^3 + C_3(KM)^5 \qquad \text{Equation 2.1}$$

Meanwhile, Ang and Morris (1984) used another improved model over Sommer's proposal. The Ramberg-Osgood model when compared with the study by Sommer shows that the model is fairly similar, but the format has changed into a ratio form as shown in Equation 2.2, where K is the standardization factor concerning with the geometry and connection configuration and *n* is the curve sharpness factor.

$$\frac{\theta}{\theta_o} = \frac{KM}{(KM)_o}\left[1 + \left(\frac{KM}{KM_o}\right)^{n-1}\right] \qquad \text{Equation 2.2}$$

This model is then modified by Liu and Chen (1986) to reflect the test results accurately, into Equation 2.3 by considering the cubic B-spline method by Jones (1981). This involves in the strain hardening connection stiffness, K_P. The model, although accurate, is limited by sharp curves on the moment rotation graph. Which then lead to the model above being improved by Kishi and Chen (1986) into Equation 2.4 for accommodating any sharp changes in the moment-rotation curve.

$$M = M_o + \sum_{j=1}^{n} C_j \left[1 - \exp\left(\frac{\theta}{-2j\alpha} \right) \right] + \sum_{k=1}^{n} D_k (\theta - \theta_k) H[\theta - \theta_k] \qquad \text{Equation 2.3}$$

$$M = M_o + \sum_{j=1}^{n} C_j \left[1 - \exp\left(\frac{\theta}{-2j\alpha} \right) \right] + M_o + R_{kf} \cdot \theta \qquad \text{Equation 2.4}$$

In studies done by Lee and Moon (2002), the proposed empirical model for defining the moment-rotation graph of a semi-rigid connection should be, where *n* and α is the shape parameters. The model does not consider on the stiffness, strength nor standardization factor, but relies on the *n* and α constants, derived from the results of 75 experimental data, with the inclusion of the initial stiffness (k_i) and plastic stiffness (k_p), which is as shown in Equation 2.5.

$$M = \alpha[\ln(n \cdot 1000 \cdot \theta + 1)]^n \qquad \text{Equation 2.5}$$

Without doubt, the empirical models have application in situations where the testing conditions and configurations are similar to the experimental studies done for the derivation of the models. Clearly, the use of empirical models as a generalized form of solution for obtaining the moment-rotation graph or any form of steel connection behavioral analysis is certainly not recommended as the models rarely consider the material properties or the variation of the steel connection configuration parameter accurately.

Non-linearity of steel connection behavior also is another factor pressing against the use of empirical methods. Although, the simplicity of the model although is agreed and achieves acceptable accuracy when compared to experimental results, it should not be used as the governing formula in analysis of steel connections. In terms of connections to tubular columns, the use of empirical method is not major subject.

2.6.3 Analytical Models

Analytical models are based models on analysis considering fixed equations. The equations, developed from empirical models as the basis, have fixed parameters in which, by using the relevant parameters and combined with suitable calculations would produce required results. This modeling technique generally considers a couple of fixed parameters of the connection and is much more reliable when compared to empirical models as the effects from material properties, structural factor and component behavior is catered for. In some cases, the derived analytical model is a result of logical and detailed application of structural theories and assumption, in which it is combined to form an analysis model to understand the connection better.

The analytical method focuses on the derivation of rotational stiffness and moment resistance of a joint based on the basic concepts of structural analysis. The derivation can also be used in the component method. Several well-known analytical models are available for connection in open-column section, as reviewed by Díaz et al. (2011), but are still limited for connections in tubular column. The total deformation of a connection to a blind-bolted end-plate tubular column is attributed to the deformation of the end plate and the column (Ghobarah et al., 1996).

Yang and Lee (2007) proposed on the initial stiffness and ultimate moment for double angle connections using analytical models. The proposed model analyses were compared to the models from Frye-Morris (1975), and Ang-Morris (1984). The comparison results show that the Wu-Chen model reflect closer to the actual behavior of the tested joint, with the condition that the initial stiffness and ultimate moment to be accurately predicted first. Derivation is made from the model and the final proposed model was found to be a more accurate than the Wu-Chen model, with error of less than 7.8%. The initial rotational stiffness of a double angle connection proposed is given by Equation 2.6.

$$K_{e,\,double} = 2 \cdot \left[\frac{bEt^3\left[b^2 + 2(1-v)a^2\right]\frac{1}{\eta}}{9\left(1-v^2\right)a^3} \right] \qquad \text{Equation 2.6}$$

Heidarpour and Bradford (2008) detailed on the failures of the T-stub component and each possibilities of failure. Derivation of the analytical equation for the first yield point and subsequent yield points involves in assumption that the deformation of the bolts is fully affected by the deformation of the end-plate or column flange only. The bolt has an infinitely stiff stratum although the bolts were assumed non-preloaded in the analysis. The resulting load displacement graph is observed to be having noticeable difference with the theoretical results that was attributed to strain hardening and post-yield strength that was not considered in the theoretical approach.

Analytical method focuses on the derivation and formulation of behavior for the simplifications of design. Derivation from this method can be used individually for component design or in the component method where the overall behavior can be analyzed with reasonable accuracy. The total deformation of a connection to a blind bolted end plate tubular column is attributed to the deformation of the end plate (Δ_{ep}), column flange opposite side of the beam (Δ_{cft}) and the column flange where direct tensional forces are acting (Δ_{cfc}) (Ghobarah et al., 1996) where the formula are shown in Equations 2.7, 2.8 and 2.9 respectively. P refers to the applied forces, I equal to the end plate moment of inertia, L as the length of the segment considered, A_s is the effective shear area and v as the Poisson ratio for steel. Value for the other coefficients to be referred to the figures provided in the study.

$$\Delta_{ep} = \frac{P}{R_{ep}} \text{, where} \qquad \text{Equation 2.7}$$

$$R_{ep} = \frac{12EI_{ep}}{b^3(1+r_2)}\left(2 - \frac{6}{b(1+r_2)} \times \frac{1}{\dfrac{12}{a(4+r_1)} + \dfrac{4+r_2}{b(1+r_2)}}\right)$$

$$\Delta_{cfts} = \frac{\gamma_s P(H_o - 2t_o)^2}{D_{cf}} \quad \text{for Bare Steel Tubes} \qquad \text{Equation 2.8}$$

$$\Delta_{cfts} = \frac{\gamma_f P(H_o - 2t_o)^2}{D_{cf}} \quad \text{for Concrete Filled Tubes}$$

$$\Delta_{cft} = 0.003\alpha_c P \qquad \text{Equation 2.9}$$

Post elastic stiffness has been determined to be approximately 5% and 9% of initial stiffness from experimental tests done (Korol et al., 1993; Tabsh & Mourad, 1997) and 7% was taken for the study. However, the value of 10% was taken by Málaga-Chuquitaype and Elghazouli (2010b). From observation of both studies, a value lower than 7% is expected to be able to increase the accuracy of the validation studies due the higher post-yielding stiffness of the models developed.

While other investigations focused on the behavior of end plate connections, Jones and Wang (2010) developed a method to determine the load-displacement for a fin plate connection to tubular columns. Depending on the ratio of the column thickness and width of the column connected side, the maximum displacement and yield point can be determined. Three failure mechanisms are defined including with membrane action only or a combination of membrane action and yield line with the contribution varying depending on the ratio described. Further studies on the behavior of the tubular column under shear and bending loads results in a simplified method to determine the capacity of the column when connected with fin plate (Jones & Wang, 2011) incorporating the yield line mechanism.

The analytical method, although it may seem to be a viable method, requires detailed understanding of each of the analytical methods, the derivation and a proper application of each of the required parameters. As with every other method, the model can be manipulated accordingly to suit the available parameters but lacking of important parameters would generally render the model being not applicable any further.

2.6.4 Component-based Method

The component-based method has been widely adopted to model the beam-to-column connection response. Different components have to be considered depending on the connection type, and the constitutive laws for each component are determined. A component method for connections to open-section columns is available and well established. The main difference for the tubular columns connection is the blind-bolt component and the behavior of the thin-wall tubular column flange. Other components can be assumed to behave according to the outline provided by EC3: Part 1-8 (2005).

For connections using blind bolts, the behavior of the blind bolt is currently characterized through the linearization of force–deformation data from experimental tests conducted previously (Wang et al., 2010). In terms of the component method, this study focuses on the initial stiffness and resistance of the connection. The angle section behavior plays a significant role; therefore, Madas (1993) and Lin and Sugimoto (2004) compared the behavior proposed in EC3: Part 1-8 ("Eurocode 3: Design of steel structures," 2005) to obtain accurate behavior. For end-plate connections, three failure modes have been proposed wherein effective gauge distances are altered accordingly for angle connections.

The proposed dimensions are based on the stiffness of the angle section in tension zone. Wang et al. (2010) proposed Hollo-Bolt stiffness for the deformation of the flaring sleeve, including parameters for the area of the flaring sleeve, thickness of the shell element, meridional length, flaring sleeve angle coordinate, and angle coefficient. This proposed stiffness was combined with the bolt stiffness outlined in EC3: Part 1-8 (2005) for the final stiffness.

In terms of the behavior for the column, Malaga and Elghazouli (2010b) proposed the stiffness of the tubular column face subjected to tension forces, which involved the column face width and column thickness. The resistance of a tubular column in tension was determined from the least resistance of the punching resistance and yielding (which depends on the number of bolts in tension, bolt hole diameter, bolt spacing and plastic moment capacity of the column face).

Meanwhile, in terms of the behavior of the column, stiffness of the tubular column face subjected to tensional forces can be expressed through equation 2.10 shown by Málaga-Chuquitaype and Elghazouli (2010b). In equation 2.11, the parameters are where C_t is valued at 0.18 from previous studies, b_c as column face width, E is the Young's Modulus, t_c is the column thickness, while v being the Poisson's ratio for steel valued at 0.3.

$$k_{bsl} = \frac{t_s A_{slp}}{\left[v s_1^2 C_3 - s_2^2 \left(C_1 - \frac{v}{2} C_2 \right) \right] \sin\alpha}, \qquad \text{(Equation 2.10)}$$

$$C_1 = \cos^2\alpha \cot\alpha, \quad C_2 = \cot\alpha$$

$$k_{cf} = \frac{\pi E t_c^3}{12(1-v^2) C_t \left(\frac{b_c - t_c}{2} \right)^2} \qquad \text{(Equation 2.11)}$$

Meanwhile, the resistance of a tubular column face towards tensional forces is determined from the least resistance of the punching resistance and local yielding (Elghazouli et al., 2009) which are expressed as equation 2.12 and equation 2.13 respectively. Due to the lack of data for hollo-bolts, the blind bolt component is expressed as force-displacement data as indicated in Table 2.4. The parameters N being the number of bolts subjected to tension, D_H the bolt hole diameter, F_y as yield stress depending on the column material and L to be the bolt spacing of the same row, and m_{plc} is the plastic moment capacity of the column face per unit length.

$$B_{y1} = \begin{pmatrix} \frac{N\pi D_H t_c F_y}{\sqrt{3}} & for \quad 2(L + 0.9D_H) \geq N\pi D_H \\ \frac{2(L + 0.9D_H) t_c F_y}{\sqrt{3}} & for \quad 2(L + 0.9D_H) \leq N\pi D_H \end{pmatrix} \qquad \text{(Equation 2.12)}$$

$$B_{y2} = f_k \gamma m_{plc} \qquad \text{(Equation 2.13)}$$

Table 2.4 Force displacement data for Hollo-bolts (Elghazouli et al., 2009)

Grade 8.8		Grade 10.9	
Force (kN)	Displacement (mm)	Force (kN)	Displacement (mm)
0	0.0	0	0
32	0.2	78	0.4
88	4.0	100	2.6
115	7.6	108	4.5

Considering that the moment capacity of the column face would involve the column thickness and width, these parameters were not explicitly specified for the resistance of the column in tension. Other parameters for angle connections have been documented in previous studies, including the prying action. New dimensions are proposed for flexible angles wherein prying may occur. Bolt slippage is also considered. Slippage occurs when the acting forces overcome the friction between the two surfaces. The major components that influence the connection behavior are the column face flexibility and the Hollo-Bolt grade.

Other studies are based on individual component, and the summary of the interaction stiffness between bolts and columns is improved from the works of Jaspart (Jaspart et al., 2004) because of the separation of each bolt row as a component instead of the treatment of the tension zone as a whole (Park & Wang, 2012). The contribution of the sidewall because of deformation has also been considered. However, it is assumed applicable to flow-drill bolts due to verification with test results in study by France (France, Buick Davison, et al., 1999a, 1999b; France, Buick Davison, & Kirby, 1999). The behavior of flow-drill bolts and that of the more commonly used Hollo-Bolt are significantly different because of the mechanism and fastening method of each system.

Liu et al. (2012b) suggested new component characteristics for column faces in tension/compression and angles in the tension/compression of Hollo-Bolted and combined channel/angle connection. The resistance of the channel in the tension and stiffness of the column was obtained from previous studies (Wang & Guo, 2012). Bolt stiffness and resistance in tension were set according to EN1993-1-8 (2005), including three modes of failures. In terms of the compression area for the channel, the angle and channel were combined as a unit. Two yielding mechanisms were considered, and the occurrence of either mechanism depended on the angle stiffness. They were applicable to both angle connections directly connected to the tubular column or to the channel. However, the model can obtain accurate predictions only up to the yield capacity and initial stiffness of the connection.

2.6.5 Finite-Element Method

The FE method is the closest simulation to the actual behavior if proper settings are used. The basic T-stub component for joint analysis is developed for the parametric study of blind bolts (Elghazouli et al., 2009). On the basis of the test results, end-plate connections are modeled and different parameters are explored, including steel strength, concrete strength, bolt diameter, and end-plate thickness and width (Wang & Spencer Jr, 2013). Connection behavior is affected by the end-plate thickness and type. Liu, et al. (2012b) modeled and analyzed the full geometry of Hollo-Bolts for comparison with actual test results. Similarly, Tizani et al. (2013) modeled the entire bolt with SOLID95 elements by using ANSYS, including the extension at the back of the bolt regarded as a single component.

By using shell elements for the main members and connector elements for bolts, Bagheri Sabbagh et al. (2013) developed a connection model by using ABAQUS. The connection was further selected for experimental testing by using the results from the model. Comparison between the FE model and experimental test results by Lee et al. (2010b) shows that the results match closely with the proposed FE model by using ANSYS. To accommodate snug tight bolts, 50 kN pretension is used in the model. The results from experimental testing (Lee, Goldsworthy, et al., 2011b) are used to validate the model of the proposed connection (Figure 2.16).

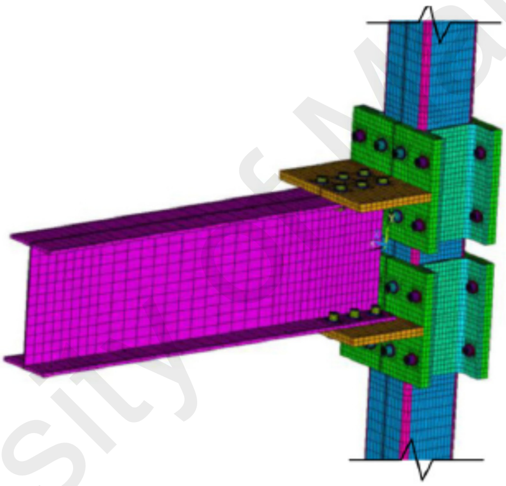

Figure 2.16 FEM Model of Channel with T-stub Connection
(Lee, Goldsworthy, et al., 2011b)

Coupled with the experimental test results, Lee et al. (2010a) showed that the connection to the sides of the tubular column is a concept that can be explored. Although no comparison was conducted with the connection to the column flange, deformation limits were set to 1% and 3% of the column width for serviceability and ultimate states, respectively. Assuming that the tension loads were uniform, each bolt resisted an approximately 100 kN shear force at the maximum deformation. When loaded at 175 kN, the deformation between the column and plate was 0.5 mm. With this minor deflection, this concept can be used for moment-resisting connections to tubular columns.

Following the experimental test results of an earlier study on reverse channel connection (Wang & Xue, 2013), FE model is proposed and validated in ABAQUS (AlHendi & Celikag, 2015b). Element C3D8R is used but no pretension is applied to the bolts. The validated model is used for further parametric studies to determine the parameters that affect connection behavior. A comparison is made with the moment-rotation behavior of the connections. Mesh sensitivity, friction effect, and load speed are explored prior to the actual study. The reverse channel is the critical component that affects the connection behavior with specific parameters such as the thickness, width ratio, and channel height. In terms of bolting, the use of large bolts and small gauge distances improves the connection behavior. To reduce the effects on the column face deformation, the channel height is recommended to have a ratio higher than 0.72.

In terms of yield line deformation, the reverse channel connection is further examined by using the ABAQUS FE software (Jafarian & Wang, 2015). Analytical formulas from previous study are then applied to determine the yield load, ultimate resistance, and deflection. The yield pattern of the reverse channel depends on the position of the bolts. The ultimate resistance is governed by the membrane action of the reverse channel, punching shear of the plate, and bolt failure. A comparison with the test behavior indicates that the proposed method can predict connection stiffness with reasonable accuracy, but the post yield remains significantly stiffer than the actual behavior.

Understanding that the reverse channel connection has limited access to the bolts, the connection configuration is modified and studied using ABAQUS (AlHendi & Celikag, 2015a). The reverse channel is split into two separate components, which is empty at the central area. Two short reverse channels are welded and bolted each to the beam. Model variation results show that the double reverse channel results in lower moment values but similar stiffness when compared to the standard reverse channel connection with the same channel profile.

2.7 Connection at Elevated Temperature Studies

In comparison to ambient temperature analysis, elevated temperature condition studies require additional consideration such as the degradation of materials with temperatures. For model or analytical based studies, validation with ambient temperature models are initially needed, followed by the validation with elevated temperatures, to reduce the considerations associated with ambient temperature study.

Under ambient temperature, the focus of the studies is on the connection deformation and performance in terms of moment-rotation. Meanwhile, under elevated temperatures conditions, researches have shown that a number of additional forces have developed in the connection. Due to the expansion of steel, compression forces may develop in the beam, and in addition to the vertical shear from the applied loading, the beam web may be susceptible to shear buckling. In comparison to the elevated temperature condition having a combined of shear, moment and compression axial forces, in the cooling phase, tension forces may develop as catenary loads in the beam due to the reduced temperatures from the cooling phase. The changes in the loading has been highlighted in various studies, including by Sun et al. (2015) and (Yu et al., 2008). The general forces are summarized into Figure 2.17 as illustrated by Mariati (2012).

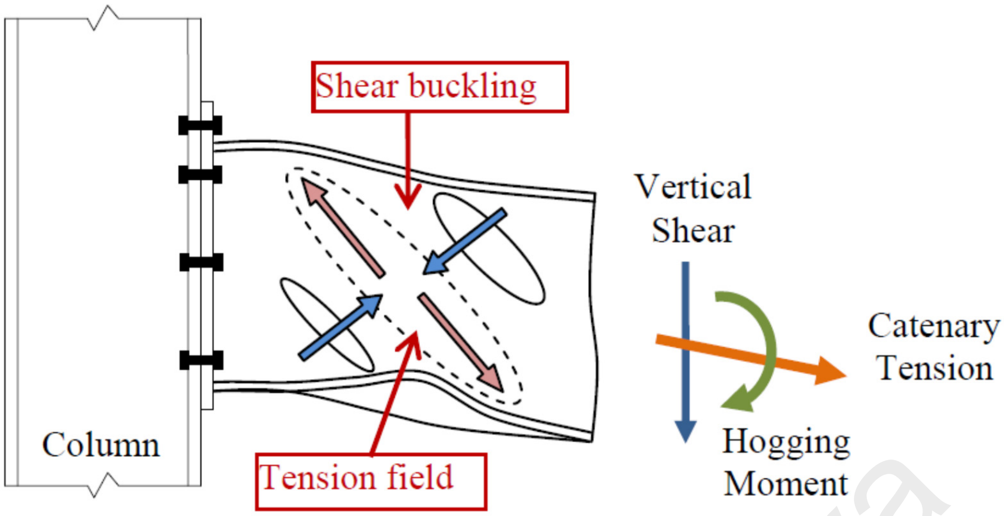

Figure 2.17 Developed forces in beam due to elevated temperature. (Mariati, 2012)

Another concept, which is categorized under the elevated temperature conditions in general, is the relationship between the ductility and progressive collapse. Due to high temperatures, columns may collapse under the decreased capacity and thus, the forces are further distributed to the beams followed by the connection. Under standard design circumstances, the ambient temperature limit is the yield point of any component in the connection while for the elevated temperature conditions, the combination of developing forces under the increase of temperature and post elevated temperature conditions result in additional designs checks. To resist the additional forces, the ductility of the connection is a critical factor.

It is observed that high deflections of the beam are a common deformation at elevated temperatures and therefore the connections must be able to have the rotational capacity without failing, possessing sufficient ductility to achieve the higher deflection and subsequently provide the catenary action to resist the additional forces. The additional forces are similar to the forces applied when progressive collapse is in view, for example when a column fails, showing that ductility of the connection is a critical parameter in the mitigation of progressive collapse. The use of ductility to mitigate the progressive collapse of a structure is further highlighted in the studies by Tschemmernegg and Humer (1988) and Burgess et al. (2012).

2.7.1 Experimental Studies at Elevated Temperature

An experimental study on the modeling of extended end-plate joints in fire using spring component has recently been undertaken by Wang et al. (2007). Reduction of steel properties in the context of elevated temperatures is according to Chinese Standard for steel plates. The components taken into consideration include: - column web in tension, flexure zone in column flange, flexure zone in end-plate, column web in compression and also the shear zone of the column web. Other components, such as the bolt in tension are not considered. ISO834 temperature curve was utilized to provide the elevated temperature condition but due to the small variation in temperature in which the difference is considered insignificant, the heating is considered uniform throughout the connection location.

With angle of loading, α of, 35°, 45° and 55°, shear forces and tying forces are the resulting loads from the distribution to the axis and thus, Yu et al. (2008) investigated four types of connections including web cleats, end plate connections and fin plate connection types. Results obtained from the study show that the web cleat connections have high rotational capacity. Behavior of fin plate connections on the other hand is governed by the capacity of bolt shear.

Experimental tests and studies on top and seat angle connections have been conducted by Saedi Daryan and Yahyai (2009a). Twelve configurations were utilized in the study and the results show the thermal strength of the connection relies heavily on the angle thickness and temperature restraint bolts. Increasing these values would generally lead to increase of thermal stiffness. Furthermore, angle connections will not be able to withstand elevated temperatures of more than 900ºC. At a temperature of 900ºC, the connection stiffness can almost be ignored. It is also emphasized that the bolts are one of the most important components in a bolted connection, as the premature failure of bolts would prevent the connection from achieving its maximum capacity.

Elevated temperature tests on various connections, including on the fin plate connection, web cleat connection, and end-plate connection types has been conducted by Wang et al. (2011). This study has revealed a multitude of possible connection failures, which are vital for further validation studies or design studies. Highlights of the study includes that connections with shallower depths has been found to be able to reach higher connection rotations which is different to the common conception that deeper connections would be able to resist more.

At fixed joints, the catenary effect of the beam would result in the failure of the connection, while the catenary effect on pinned connections, especially web cleat connections, show high resistance. Therefore, the web cleat connection is recommended for further studies.

Under high temperatures, steel material stiffness and strength degrade because of material degradation from external heat. The degradation of strength and stiffness is given in EC3: Part 1-2 (2005) Testing at elevated temperature conditions is expensive because of the additional cost of providing a furnace. Several limitations are also presented, including the time factor. Owing to the high heat generated, specialized data measurement equipment that is able to withstand and continue working under elevated temperature conditions is required.

Several connection types are studied under the effect of elevated temperatures, including T-stub, fin-plate, extended end plate, and reverse channel connections to CFT columns (Ding & Wang, 2007). Strain data are not measured because of the high cost of thermal strain gauges and their low performance at high temperatures. However, displacements and temperatures are measured by protecting the transducer with hollow ceramic tubes to minimize the effect of temperature on the transducers. Among the various connections tested, the reverse channel connection is considered one of the preferred connections because of its excellent ductility and performance under catenary action. It is measured that under the cooling phase, deformation continues to develop, signifying tension catenary forces acting on the connection and beam. However, in order for catenary action to develop in the beam, the span must be sufficiently long.

Eight tests have been conducted at ambient temperatures and at 550 °C for fin-plate and reverse channel connections to CFT columns (Huang et al., 2013). The parameters studied include the difference between the SHS and CHS as the column member, and the effects of temperature and the types of channel used on both the CHS and SHS section columns. Compared with other tests at elevated temperatures, video processing is used to measure the deformation of specimens. The connections are governed by either bolt head punching through the channel thickness at ambient temperature or by the tensile fracture of the bolts. The use of ductility as the basis is more effective than designing the connection to a higher strength for higher survivability in fire conditions.

Considering that the reverse channel critically governs the behavior of the connection type, the influence of different types of reverse channel is researched (Lopes et al., 2013). Standard channels and built-up sections and channels cut from hollow sections are tested in both compression and tension loads. Behavior at both ambient and elevated temperatures is compared together with the proposed stiffness of the reverse channels. At ambient temperature, failure by bolt pullout occurs, as well as shear failure near the sides of the channels. The constant thickness of the channel results in the continuous deformation found in channels cut from hollow sections, whereas the deformation stops at the sides of the channel for the built-up and standard channel sections. Deformations at elevated temperatures are observed to be an exaggerated form of the same deformation at ambient temperatures. The exaggeration is caused by the degradation of the steel material under heat. The use of channels cut from hollow sections is recommended because of the increased stiffness.

A similar method is applied, and connection parameters are studied at elevated temperature conditions (Jafarian & Wang, 2014). Variations include the channel thickness, channel width, leg length, and bolt row. Only ambient, 550 °C, and 750 °C temperatures are selected to test the effect of these parameters on the behavior of the reverse channel. The reverse channel is welded onto a thick plate at the top and bottom and subjected to tension load. The joint may increase in ductility at elevated temperatures, whereas the membrane action governs the behavior of the reverse channel. Behavior arising after the yield lines formed on the reverse channel has not been studied.

Wang and Davies (2003) studied the SHS as the column component in fire together with the connecting beam assembly. Two beams with end plates were bolted to a single column. Loads were applied axially on the column and on both beams, the configuration results in an either balanced or unbalance loads. Anisothermal temperature condition was used. The governing factor in the buckling of the SHS column was the column-to-plate thickness ratio. A value of 30.7 instead of 38 (as provided by EC4: Part 1-1 (2004) is proposed. Local buckling may occur near the beams when loads are balanced; otherwise, local buckling occurs on the column length. This phenomenon provides an outline to the column to be used when SHS is designed for fire conditions to avoid local buckling deformation.

Although testing of the entire connections provides understanding on the connection behavior and interaction between connection members, investigating on the individual components is necessary to provide a basis for the component-based method (López-Colina et al., 2010; López-Colina et al., 2011). Experimental tests were conducted, wherein 20 mm plates were used to apply compressive loads onto a BST column side and at different temperatures up to 642 °C. SHS100, SHS120, and SHS140 were the sizes selected for the tubular column.

2.7.2 Finite Element Studies for Elevated Temperature

Using the results in Saedi Daryan and Yahyai (2009a), Saedi Daryan and Yahyai (2009b) conducted modeling on angle connections at elevated temperatures, which includes top-seat angle connections, specimens S3 and S9. Main purpose of the study was to investigate on the failure mechanism in top-seat angle connections. The behavior of the models was compared to the experimental tests and the model results have shown that the model is in good agreement with the experimental tests. Degradation of the material has been according to the guides set out by EC3. One of the result models is as shown in Figure 2.18

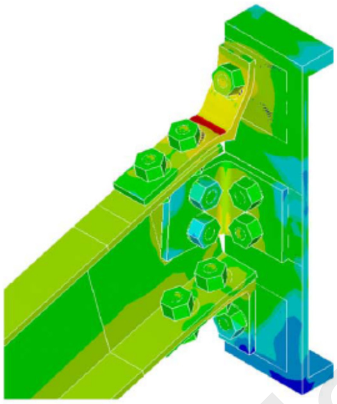

Figure 2.18 Analysis results of Finite Element Model (Saedi Daryan & Yahyai, 2009b)

Mao et al. (2009) studied on the response of steel beam-column connections, especially fin plate, under fire loads by conducting experimental tests and attempts to model the exact response in the finite element software, ANSYS, in which the validated methods is used to model for other connections of interest. In terms of the thermal loading, the an-isothermal and isothermal method is used. In the finite element model shown as the result, it is observed that the bolt row from the fin-plate at the beam web is not modeled in finite element.

Another of the latest finite-element model studies was conducted by Díaz et al. (2011) on end plate connections. Several effects of various loads / forces are studied with the finite element model, namely: effect of thermal expansion, effect of transverse load pattern of beam, effect of axial load on column, effect of applied moment of beam, of shear force of beam and of axial force of beam. Effects from the shear force of beam and of transverse load pattern of beam is minor.

Meanwhile, effect of axial force on beam towards the stiffness of the connection is only significant in the plastic region and minor in the elastic region, which is for cases where the temperature is constant while the load increases. When the load is constant and temperature increases, the axial force instead do not affect the connection stiffness. There was no doubt that the thermal expansion was necessary in determining the connection stiffness.

Strejček et al. (2011) has conducted a study on the column web component at elevated temperatures using the finite-element and analytical method. Based on the experimental investigation conducted, the end-plate connection was modeled and the result show good agreement after adjustments has been made to the model to ensure maximum column web effect. The material properties were defined according to EC3: Part 1-2 (2005).

In terms of axial restraints, major studies have been conducted on the effect of axial restraints towards the behavior of beams in elevated temperatures. These studies include those by Liu (1996) which has also conducted modeling of end-plate connections with the effect of axial restraints. From the results of the study, fire resistance of any structural beams is enhanced with fixed end moment connections. It also shows the possibility of using finite element to simulate elevated temperature condition models. The study by Heidarpour and Bradford (2009) focuses on the empirical modeling of the connection behavior and the results have shown that the proposed concept has higher accuracy in comparison to finite-element software analysis, which is recommended for future analysis connections in elevated temperature conditions.

Studies by Dai et al. (2010) have shown that the static analysis is sufficient for analysis of elevated temperature conditions. A number of proposals on increasing the fire performance of a shear plate or fin plate connection type, including to increase bolt grades, matching web thickness of the shear plate, additional plates on the web and utilizing larger bolts holes has been suggested by Selamet and Garlock (2010) from the results of the finite-element analysis of the fin plate connections.

From various studies, it is shown that the temperatures in the furnace are not necessarily the temperature of the component in the connection due to various factors such as the heat transmission, heat transfer and the phases of the gasses. Therefore, a finite-element model is produced with the software FD5 with validations of a test on a fully welded spliced connection at elevated temperatures by Lee, Chiou, et al. (2011). The FD5 software was able to simulate the heat transfers and accurately simulate the result of the connection components temperature and subsequently the failure mode of the connection. With the results from this study, it is expected that further studies would continue to use this method proposed to predict the connection temperatures and thus, assist in achieving greater model accuracy.

A finite element model has been developed for the flush end plate connections at elevated temperatures in a study done by Li et al. (2012). An experimental test was conducted for the basis of the finite-element model. Besides that, two models, at 352.5°C and 751.5°C was applied with axial loadings. Response of the connection, in comparison with experimental results show acceptable accuracy and the effect of axial restraints have lowered the moment capacity and stiffness of the connection. At the same time, the ductility of the model has also been reduced.

Pakala et al. (2012) has modeled the behavior of the fin plate connections at elevated temperatures by using the ANSYS Software. Validations of the model are with the studies by Yu et al. (2009). Various parameters have been studied such as the bolt hole diameter, beam web thickness and edge distance.

From the results of the parametric studies, several items have been suggested that affects performance of the fin plate connections at elevated temperatures including gaps, sizes of bolts holes, and web thickness. Although this, the addition of top-seat angles is presumed to be able to help with the connection performance due to the higher ductility but have been found that there are limited literature available on this topic.

For end-plate connections, the robustness of the connection at elevated temperature conditions can be increased by utilizing the spaced extended end-plate, channel bolted extended end plate or by the usage of a "dog-boned" shaped beam, as shown in Figure 2.19, in a study by Wang and Wang (2013). Robustness is determined by the higher rotational capacity that the connection would respond under loads. Bolt size increase has been determined to be ineffective in increasing the resisting temperature of the connection. Other end-plate connections under fire studies using finite element has also been conducted by Chen and Wang (2012).

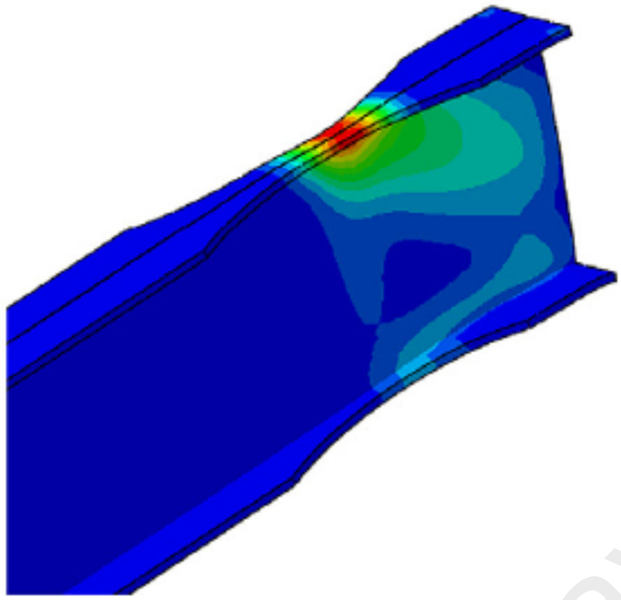

Figure 2.19 Dog-bone shaped beam deformation (Wang & Wang, 2013).

Following the test results in an earlier study (Ding & Wang, 2007), a FE model is developed in ABAQUS and verified (Elsawaf et al., 2011) for reverse channel connections to CFT columns, both SHS and CHS (Figure 2.20). Several sensitivity studies have been conducted, including those on mesh size, material mechanical property, contact parameters, effect of lateral restraint, and energy dissipation factor. Although lateral restraint has not been elucidated, the location is placed on the plate where loads are transferred to the beam; therefore, horizontal displacement restraint is assumed on the four-point edges of the plate. Temperature distribution is based on the actual measured value, and the behavior of the developed model is in good accuracy in comparison with test results.

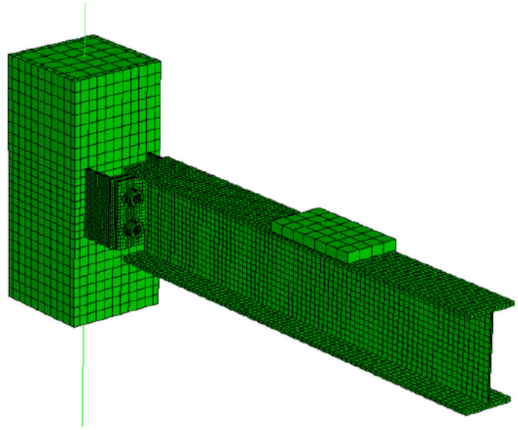

Figure 2.20 FEM Model for Reverse Channel Connection

A hybrid end-plate connection is proposed to increase the temperature resistance of the connection because of the increase in the connection ductility. Following the model verifications, parametric studies are conducted to determine the parameters that affect the connection before failure (Elsawaf & Wang, 2012). The parameters studied include the effects of reverse channel web thickness, effect of fire protection, bolt grade, and the application of fire resistant materials on the connection components. In addition to the study on the connection component, investigation on the effect toward connection survivability has also been connected. Loads on the column and the increase in material plastic strains lead to high survival temperature for the connections. However, the focus of this study is limited only to the reverse channel connection configuration.

A series of factors based on the current external temperatures is proposed for the different components in fin plate, end plate, and reverse channel connections (Ding & Wang, 2009). The proposed regions for each of the connection types and expected temperatures of these components are provided. The result of this proposal is an accurate model and simulation. However, temperatures in a joint are commonly assumed uniform for the simplicity of the analysis. A high temperature will result in a design with an increased safety factor.

Coupled with the experimental test results, the FE model is developed to simulate the behavior of the column component, including stiffness and resistance (López-Colina et al., 2010; López-Colina et al., 2011). The stiffness method is based on a four-point method from the plate edge, and the equilibrium of moments and buckling coefficient has been considered in this approach for the stiffness. For the resistance, the EC3: Part 1-8 (2005) guideline for resistance of column web is modified to adapt to hollow section members. By combining both studies, an analytical method that is able to predict the behavior of the compression component of the hollow section column is proposed (López-Colina et al., 2014). Moment rotation curves show good agreement with the test results from the component studies. Meanwhile, for a full joint validation, the proposed method is validated with available ambient and elevated temperature test results.

By using the tests results from Huang et. al. (2013), Lopes et. al. (2013), and Jafarian et. al. (2014), Heistermann et. al. (2013) verified the models for the reverse channel component and connections. The temperature at the connection models was applied as a predefined field and was uniform across the applied area. Reverse channel component in tension and compression was modeled with acceptable accuracy. Connection stiffness was also proposed.

Post-fire condition of the connection has also been examined in the literature (Elsawaf & Wang, 2013). Tensile forces caused by restrained shrinkage may be sufficiently large to cause tensile failure in the connection components. The proposed FE model is validated against the results of the study by Ding and Wang (2007). No experimental tests have been conducted on the cooling stage of the connection after exposure to fire. Similar conclusions have been drawn for the reverse channel connection, that is, to increase the web thickness of the channel. Limiting the design temperature to 50 °C of the beam maximum will increase survivability during the cooling stage. Further studies confirm that the connection may fail during the cooling stage (Song & Han, 2014).

The effect from axial loads on top-seat angle connections under elevated temperature conditions have also been covered in the study by Leong et al. (2016). Compressive axial loading increases the connection stiffness and yield moment while tension axial loading reduces both parameters. It is observed that the compressive axial loading reduces the effect towards the tension component while the tension axial loading increases the deformation of the connection. In addition, the 5% axial loading limit set by EC3: Part 1-8 (2005) requires further consideration as the effect from 1% axial loading is not negligible.

2.7.3 Analytical Studies

With the Ramberg-Osgood method, Al-Jabri et al. (2004) conducted studies to predict the degradation of the connection at elevated temperatures. With the connection response results for ambient temperature, the method proposed is able to predict with high accuracy on the non-linear behavior of end-plate connections. The moment capacity of the connection and the initial stiffness of the connection were taken as the major coefficient to be applied into the formula.

Producing column web stiffeners would result in additional costs towards construction and this would increase in material usage that is not recommended in this age of sustainable construction. Therefore, Spyrou et al. (2004a) has conducted a study to not only eliminate the usage of stiffeners, but also to increase understanding in the effects of transverse compressive forces on the column which may affect the capacity of a connection.

Failure modes of the column web are compared between the British Standard 5950 (BS 5950) code and EC3: Annex J. BS 5950 covers two failures, including crushing and buckling while EC3 covers an additional failure: web crippling. Guides by both codes are rejected by the author, that was claimed to be conservative and combined with the results of another study, it shows that the plotted graphs by both codes is too scattered. An experimental investigation is first carried out and a formula is derived for the ultimate compressive force of the column web with the effects of temperature.

The proposed equation given in Eqn. 2.7 shows better comparison to experimental results than of Eurocode 3 and BS 5950, where; ß = development width of the bearing zone, t_{wc} = column web thickness, E_{wc} = Young's Modulus of the column web, t_{fc} = flange thickness of the column, c = uniform distributed patch length, d_{wc} = depth of column between fillets.

$$P_u = t_{wc}^2 \sqrt{E_{wc}\sigma_{wc}} \sqrt{\frac{t_{fc}}{t_{wc}}} \left\{ 0.65 + \left[\left(\frac{1.6c}{d_{wc}} \right) \left(\frac{2\beta}{2\beta + c} \right) \right] \right\} \qquad \text{Equation 2.7}$$

Besides at the compression zone of the connection, Spyrou et al. (2004b) also studied on the tension zone of the connection. Focus of the study was on the T-stub component. T-stub component has been introduced by Zoetemeijer (1974) and implemented in Eurocode 3, and subsequently adopted by various researchers. T-stub is a method of modeling several components in tension zone of the connection, thus simplifying the modeling process and analysis of the connection. Three failure modes has been proposed and the analytical formulas, based on the concept of elastic, plastic flexure of flange of end plate / flange and the plastic elastic elongation of the bolts.

A semi-analytical model was proposed by Pirmoz et al. (2009). It is shown from previous study that the gage of the flange angle and thickness of the flange angle are among the most important factors that determine the moment-rotation performance of an angle connection. This study has provided a method in which the nonlinear stiffness of the connection can be determined.

In terms of stiffness, it is found that the stiffness of connections drops to almost 50% of the ambient stiffness at a temperature of 500°C and to a quarter at 650°C (Yang & Jeon, 2009). As fires may reach up to 2000°C, this study reveals that steel connection would probably not be able to maintain structural integrity in a fire and continue to resist loads. Undoubtedly, failure of a member may lead to a 'domino' effect and cause the failure of the whole structure.

Proposals on the stiffness of steel structural connections at elevated temperature conditions have been made by Mao et al. (2009) using ANSYS software. With the connection type being a fully welded beam to column connection, parameters such as the effect yield stress, column flange width, column thickness, plate thickness and beam parameters have been studied. Following the studies, a formula is presented to predict the stiffness of a connection under a four-sided heating. However, from the validations, the formula proposed has been found to be relatively conservative and therefore, further modifications are required with additional studies.

In terms of end-plate connections, 23 different experimental test results were used to validate the proposal by Huang (2011). With a 2 node model, the end-plate connection at elevated temperatures is studied and the result of this study have shown that at elevated temperature conditions, the axial restraint levels have significant effect over the moment capacity of the connection. While for axial restraints, the model proposed is able to predict with good accuracy. Values for axial tension resistances are still conservative with accordance to the EC3: Part 1-8 (2005) extension to elevated temperature conditions.

2.7.4 Component Method

The component method or the equivalent spring stiffness model has been used by Al-Jabri et al. (2004) for his studies on end-plate connections at elevated temperatures. Using the proposals from various sources, such as Agerskov (1976) for the bolts and Jaramillo (1950) for the column flange, the resulting connection response has shown good agreement with the experimental results. A tri-linear graph model has been defined, where the early initial stiffness of the model valued at k, has subsequent stiffness at the elasto-plastic region as $0.05k$ and the ultimate regions as $0.01k$. This method would generally be applied to analysis software due to its simplicity and effectiveness.

The force-deformation curve is a main point in the component models method. It is common practice determine the initial stiffness and ultimate load first for each component so that the proper spring with the relevant stiffness values can be used for analysis. For the behavior of steel joints at elevated temperatures, a component model has been developed by Simões da Silva et al. (2001) as shown in Figure 2.21. Ductility of the components are key to the component method and can be classified according to their ductility levels, either limited ductility, high ductility or brittle components and the force-deformation graph representing each ductility levels. Main parameters involved in the force deformation graph, where a general graph is as shown in Figure 2.22, would be the post-limit stiffness, K^{pl}; elastic stiffness, K^{e}; limit load, F^{y}; yield displacement, Δ^{y}; and limit displacement, Δ^{f}. Stress-strain diagrams for steel at elevated temperatures are also to be reduced according to the reduction factors developed.

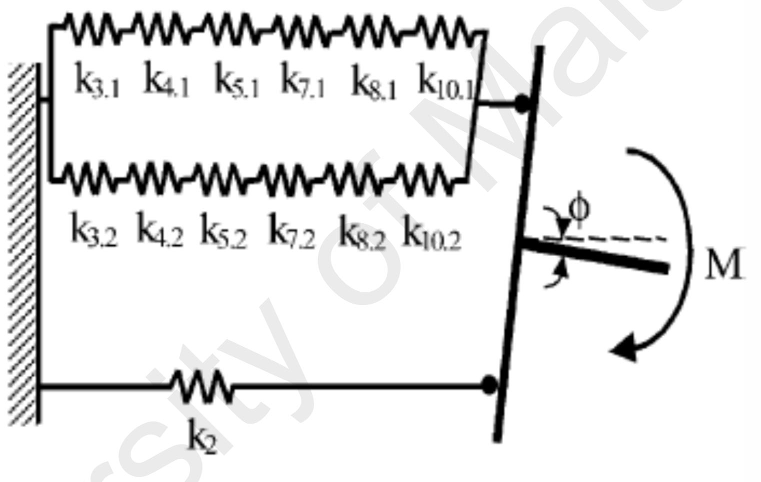

Figure 2.21: An example of component model (Simões da Silva et al., 2001)

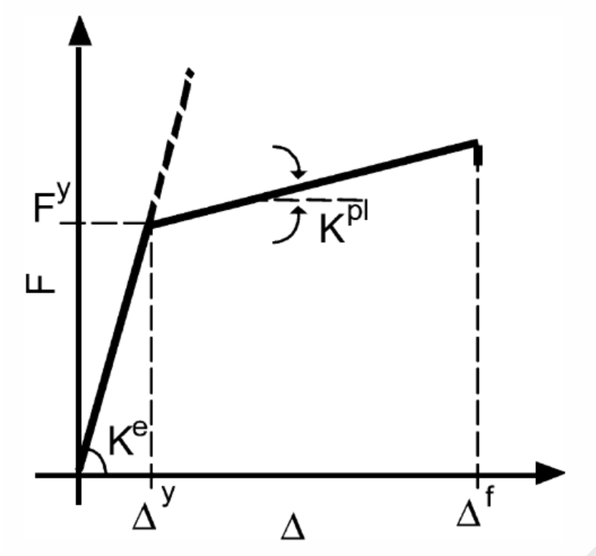

Fig 2.22: General force-deformation graph for connection components (Simões da Silva et al., 2001)

Developed by Izzudin (1991), the non-linear finite element analysis software ADAPTIC was used by Ramli-Sulong (2005) which developed a new model of connection using component-based approach. Validation works are carried on five connections types under monotonic and cyclic loading at ambient and elevated temperatures condition including angle connections, extended end plate connections and fin plate connections at elevated temperatures. Experimental testing validations for the component method utilized includes tests by Leston-Jones et al. (1997) and Al-Jabri (1999). For the top-seat angle connection validations, experimental tests by Davison et al. (1987) and Shen and Astaneh-Asl (1999) were used.

Studies on fin-plate connections have been done experimentally by Yu et al. (2009), although the main aim of the study is to develop a component based model for fin-plate connections. Fourteen specimens were used where twelve specimens utilized a single column of bolts at the beam web side, while another two has two columns of bolts. It is observed that at elevated temperatures, the bolts tend to be governed by shear alone and relatively less bearing deformation on the beam web even if the fin plate has a higher thickness compared to the beam web. At the points where the bolt with the bolt holes and when the beam flange with the column flange is in contact, the resistance of the connection increases. Components such as the plates in bearing and bolts in shear was being referred to the mathematical models by Marwan (2007).

According to Qian et al. (2009), there are two types of component modeling: modified rotational model and general connection element,. The modified model involves in axial thermal restraint that is applied indirectly while the other method is rather conventional, where the rotational stiffness is not specified and the components are free to deform accordingly to achieve the overall global rotational stiffness when assembled as a single connection element. The second method is more commonly used in the current studies. The first method was used by Qian et al. (2009) in the study. The study by Faella et al. (2000) has been taken as basis of the component model. Finite element models are also used for the analysis of the end plate connections. Two groups were tested, where the first group has thermal restraint while the other has none. Results are verified against experimental data collected by Qian et al. (2008). The results of either with or without thermal restraint show good correlations with the experimental data.

Meanwhile, for the effect of axial restraints on the connection, a study has been conducted by Pirmoz et al. (2011) in ambient temperatures for angle connections, showing that the axial tensional force with moment loads reduces connection moment capacity and initial stiffness in ambient temperatures. Meanwhile, Qian et al. (2009) studied the effect on end plate connections in elevated temperatures. A component model for the analysis is developed and the results show that the behavior of the model is in good agreement with the experimental results. From literature, no studies have been conducted on the effect of the axial restraints on the top seat angle connections at elevated temperature condition.

2.8 Concluding Remarks

Tubular columns have clear advantage over open section columns. However, the closed section profile has a limitation with the connection of beam to the column. The limited access for bolting process has led to the use of blind bolts to replicate bolted connections to tubular columns. Investigations have shown that blind bolts can function in a similar way to a standard structural bolt that is commonly used in connections to open-section columns. However, blind bolted connections are not classified as moment resisting connections due to the flexible deformation. Shear resistance is comparable to the standard bolting and therefore, to avoid the tension deformation, placement of the bolts are considered to allow for shear resistance only of the connection.

Limited studies have been found on tubular column connections at elevated temperatures compared with those at ambient temperatures. Different methods of obtaining the connection performance based on experimental, analytical, component, and FE approaches are reviewed. Experimental and FE models are expensive methods in terms of cost and computational effort. The component-based method has great potential, but the volume of work published in this method remains limited, particularly at elevated temperatures. In addition, the effects from axial forces are evident in elevated temperature studies, especially in boundary conditions reflected in actual construction works (bolted on both sides of the beam).

In terms of design for elevated temperature conditions, the current standard practice assumes that the temperatures are uniform across the connection (isothermal condition) and having degradation factored into the resistance design. However, as shown in various studies that the temperatures are often not uniform due to various material effects, including thermal conductivity, heating pattern and connection configuration. Due to the different thermal distribution, various components may fail before other expected components if isothermal condition is applied. While thermal analysis is accurate for temperature design, the complexity reduces the design efficiency and therefore, a new method is required for simplicity design in elevated temperature.

CHAPTER 3

METHODOLOGY

3.1 Introduction

This chapter addresses the experimental program and development of the finite-element model in examining the performance of reverse top-seat angle connections. For experimental studies at ambient temperature, the specimens are tested under static loadings with a hydraulic pressure compression machine. Deformations of the connection are observed and deflections of the beams are measured to determine the connection behavior. Meanwhile, at elevated temperature, tests are conducted in a large-scale industry furnace and a hydraulic jack providing the application of loading on the connection. Details of the tests, data collection method and instrumentations with the boundary conditions are presented in the following sections of this chapter.

In terms of finite-element models, the software used for the purpose is the multi-discipline finite-element analysis software, ABAQUS. The solid connection components of the finite-element model are meshed and produced in the software. These components are assembled and defined with the loading conditions and boundary conditions, which is subsequently analyzed for results. The different parameters that are involved in the model analysis, including the contact details, materials and load steps are outlined in this chapter. Units are generally not defined in the ABAQUS software; however, to obtain proper results, the units are decided beforehand and consistently used throughout the modelling procedure for the definition of parameter values and in the interpretation of the output results.

Under elevated temperature conditions, the application of temperature in the analysis as the major loading is a critical component for analysis. Method of application of temperature into the model is highlighted in this chapter. Comparatively, additional consideration of the material properties is required for the elevated temperature condition, in which the critical considerations are highlighted. In addition, with the complexity of non-linearity and material property degradation, several parameters or options are defined to increase convergence. All which are discussed in the following sections.

3.2 Proposal of a New Beam to Tubular Column Connection

A new connection called the reverse top-seat angle connection is proposed. In this connection, the angle sections are welded to the column face in reverse position when compared to the standard top-seat angle connection as shown in Figure 3.1. Welding of the angle sections are on a single leg, with the flat surface of the angle section perpendicular to beam length axis. Welding is reduced to locations where necessary to transfer the forces from the beam to the column through the whole width of the angle section. Forces are distributed across the column face, reducing concentration on the tubular column wall where the critical effect from the thickness is located. Next, the beam section is welded to an end plate and the assembly consists of bolting the end plate to the angle sections.

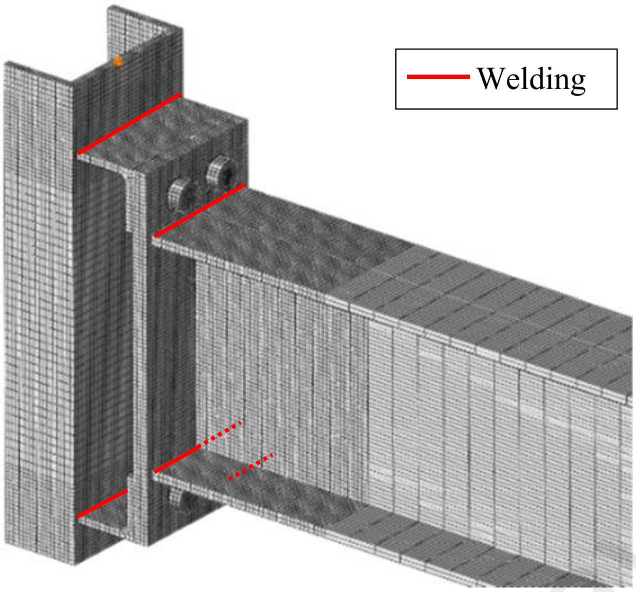

Figure 3.1 Reverse Top-Seat Angle Connection

The main concept for this connection configuration is the empty area of the mid area of the beam to enable future modifications of the connection. In addition, the increase in lever arm is expected to provide moment resistance necessary to classify the connection as a semi-rigid connection. In comparison specifically to reverse channel connections, mid-space of the beam is not considered to be wasted space in RTSA and these space can be added with additional other components to increase the load capacity of the RTSA connection. In terms of beams of greater depths, the components can be separated further enough to reduce wastage in steel sections that do not contribute to the structural capacity of the connection. The proposed connection requires less welding and bolts in comparison to other connections, thus providing the simplistic solution to low range loads.

In structural terms, the use of angle sections is expected to provide the ductility to resist the additional forces developing under elevated temperature conditions. It is also expected that the connection is able to develop the rotational capacity and necessary tensional capacity for catenary action.

3.3 Ambient Experimental Test

3.3.1 Specimen Description

Three specimens have been fabricated and the specimens generally consist of two UB 305x165x46 kg/m beams connected to a 600 mm SHS 200x200x10mm thick tubular column. Steel section size and detail differences are as indicated in Table 3.1. All welding is 6 mm leg size and is applied all-round, including from the angle to column, and the beam to the end plate. Parameters investigated through the experimental tests include the effect of angle thickness (AT1 with AT2) and the effect of stiffeners (AT2 with AT3).

Structural bolt M20 with Grade 8.8 is used for all specimens while the steel yield stress values for the material properties definition is as shown in Table 3.2. Washers are provided below the bolt head and nut. Material data for the members is provided by the supplier while the bolts are using the standard material values for Grade 8.8. Geometric dimension of the connection is presented in Figure 3.2. All bolts are hand-tightened and the bolt holes are 2 mm larger than the bolt shank diameter.

Table 3.1 Ambient temperature specimen geometrical details

Component \ Specimen	AT1	AT2	AT3
Beam		UB 305x165x46 kg/m	
End-Plate		20 mm thick	
Column		SHS 200x200x10	
Bolt		M20 Grade 8.8	
Angle	L80x80x10	L80x80x8	L80x80x8
Stiffener	-	-	6 mm

Table 3.2: Material Properties for test Specimens AT1, AT2 and AT3.

Component	Yield Stress (N/mm^2)
Beam	235
End-Plate	318
Column	388
Angle	275
Bolt	640
Elastic Modulus	2.0 x 10^5

In order to gauge the performance of the connection, comparison must be made with connections of similar nature, such as top-seat angle connections as studied by Málaga-Chuquitaype and Elghazouli (2010). In the study, the member used was UB 305x102x25 kg/m and therefore the beam section used in this study is UB 305x165x46 kg/m to have similar lever arm for any moment forces developed in the connection. Similarly, the angles used are of 8 mm thickness and the columns are of SHS 200x200x10 mm thick similar to the tests conducted in the previous study. As the beam flanges are located where the angle leg ends, to avoid the deformation of the end-plate, the end-plate thickness is increased to 20 mm. In addition, the shear resistance of the beam is resisted by the total shear capacity of the 20 mm grade 8.8 bolt, hence the size and grade being chosen.

3.3.2 Test Setup and Loading

Loading is applied on the central column using a hydraulic actuator, as shown in Figure 3.3 with a maximum total compressive force of 1000 kN. Loading applied on to the column can be applied with two options: - loading controlled or displacement controlled. With the load control method, the displacement cannot be controlled and the specimen may fail unexpectedly.

Even with knowledge of prior design, differences in fabrication compared to drawings could be a possible reason for lower connection resistance and therefore lead to earlier failures under lower load values. The specimen is simply supported, with one side being a pinned joint while the other is a roller joint as shown in Figure 3.4.

With displacement control, the deflection can be controlled, ensuring that the test can be stopped when the deflection achieves the required displacement value without sudden failure. For the experimental test in ambient temperatures, the 110 mm is set as the maximum displacement, which also corresponds to the maximum stroke of the hydraulic actuator. Displacement loading speed is set as 2.5 mm/minute.

3.3.3 Instrumentation and Data Collection

In terms of data collection, pressure loads that are applied are measured by monitoring the load cells that were incorporated within the actuator while the connection deformation is measured through displacement with the displacement transducers or the linear variable differential transformers (LVDT). All data are recorded with a data logger and measurement at every second for increased accuracy.

Behavior of the connection is measured as beam deflection on points located at 1000 mm and 500 mm from the column center with 100 mm and 200 mm capacity LVDT respectively on both side beams as shown in Figure 3.4 and Figure 3.5.

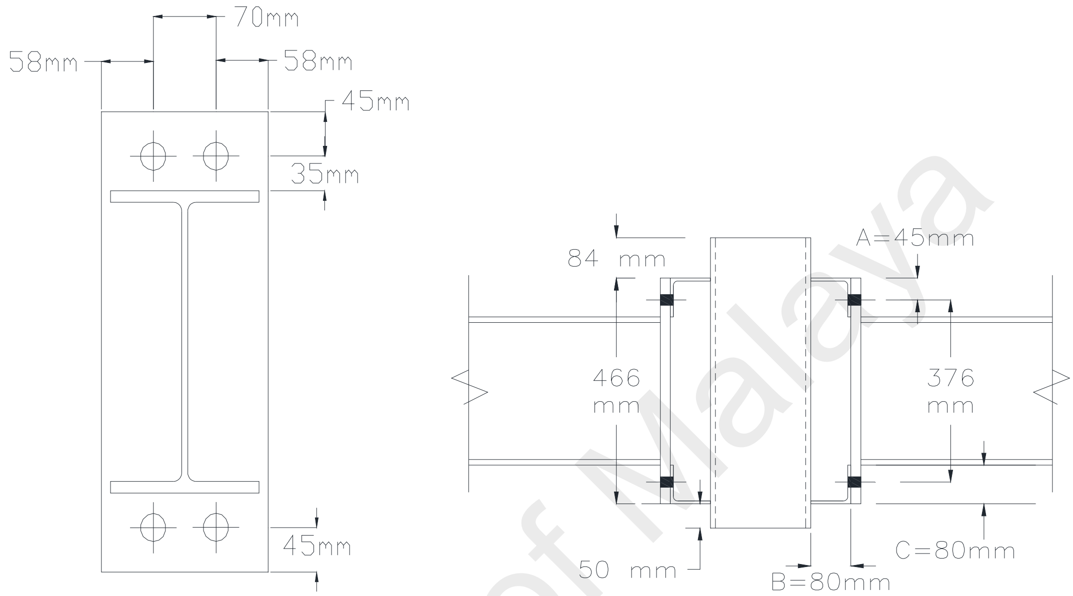

Figure 3.2 Geometrical dimensions for ambient specimens.

Figure 3.3 Hydraulic Actuator Used

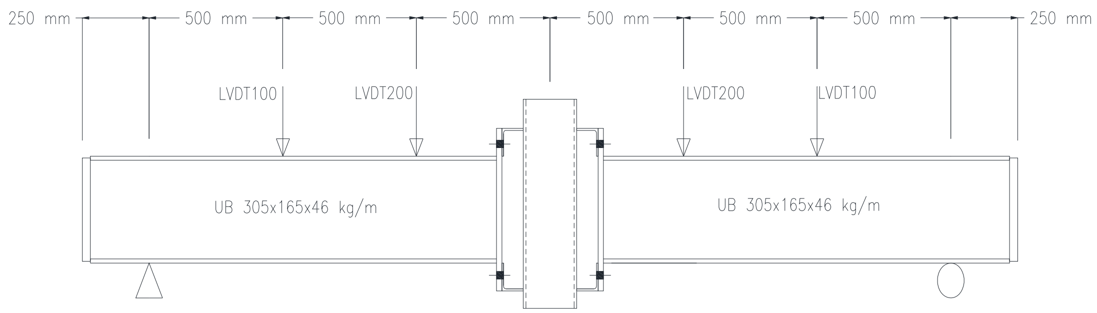

Figure 3.4 Instrumentation and ambient test setup

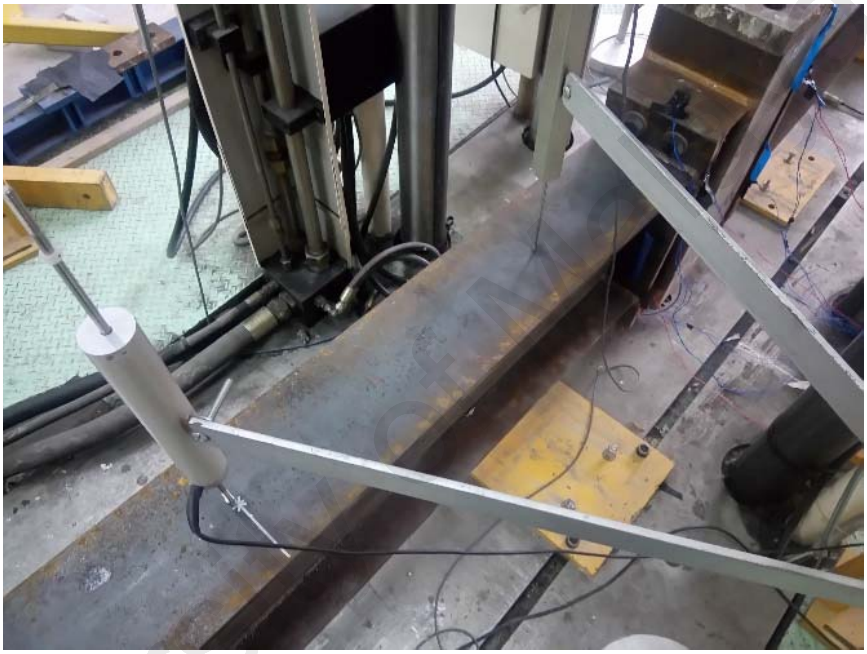

Figure 3.5 Location of LVDT Measurement

3.4 Elevated Temperature Test

3.4.1 Specimen Details

A column of 800 mm is connected with beam sections on two sides to form a cruciform specimen. Column section of SHS 200x200x9 mm thick is used for all specimens. Beam section is UB305x165x40 kg/m. Variations in the specimen is in terms of angle thickness, effect of stiffener plate and the effect of additional connection configuration at beam center. The overall specimen variation of details is as shown in

Table 3.3. Material properties of the steel sections measured from tensile coupon tests are shown in Table 3.4. The general arrangement of the specimen is as shown in Figure 3.6 with ET1, ET2 and ET3 having similar arrangement. The total length of the assembly consisting of two beams, the joints, two beam extensions and column is 3813 mm. In comparison to the other specimens, ET4 has additional connection elements at the central area of the beam, being a T-stub cut from the beam section, welded to the column and connected with 4M20 grade 8.8 bolts.

Table 3.3 Specimen Variation and Details for test in elevated temperature

Specimen / Parameter	ET1	ET2	ET3	ET4
Angle	L 80x80x8	L80x80x8	L80x80x12	L80x80x8
Column	SHS 200x200x10 mm thick			
Beam	UB305x165x40 kg/m			
Bolt	M20 Grade 8.8			
End Plate	20 mm thick			
Other Variation	None	Stiffener 10 mm between Angle Legs	None	Mid-Connection with "T" cut from UB305x46 and with 4M20 Bolts Grade 8.8

Table 3.4 Material Properties for Elevated Temperature Specimens.

Component	Designation	Yield Stress (N/mm^2)
Beam	UB 305 x 165 x 40	235
End-Plate	20 mm thick	350
Column	SHS 200 x 200 x 9	388
Angle	L 80 x 80 x 8 (Cut from L90x90x10)	316
Bolt	M20 Grade 8.8	640
Plates	10 mm thick	350

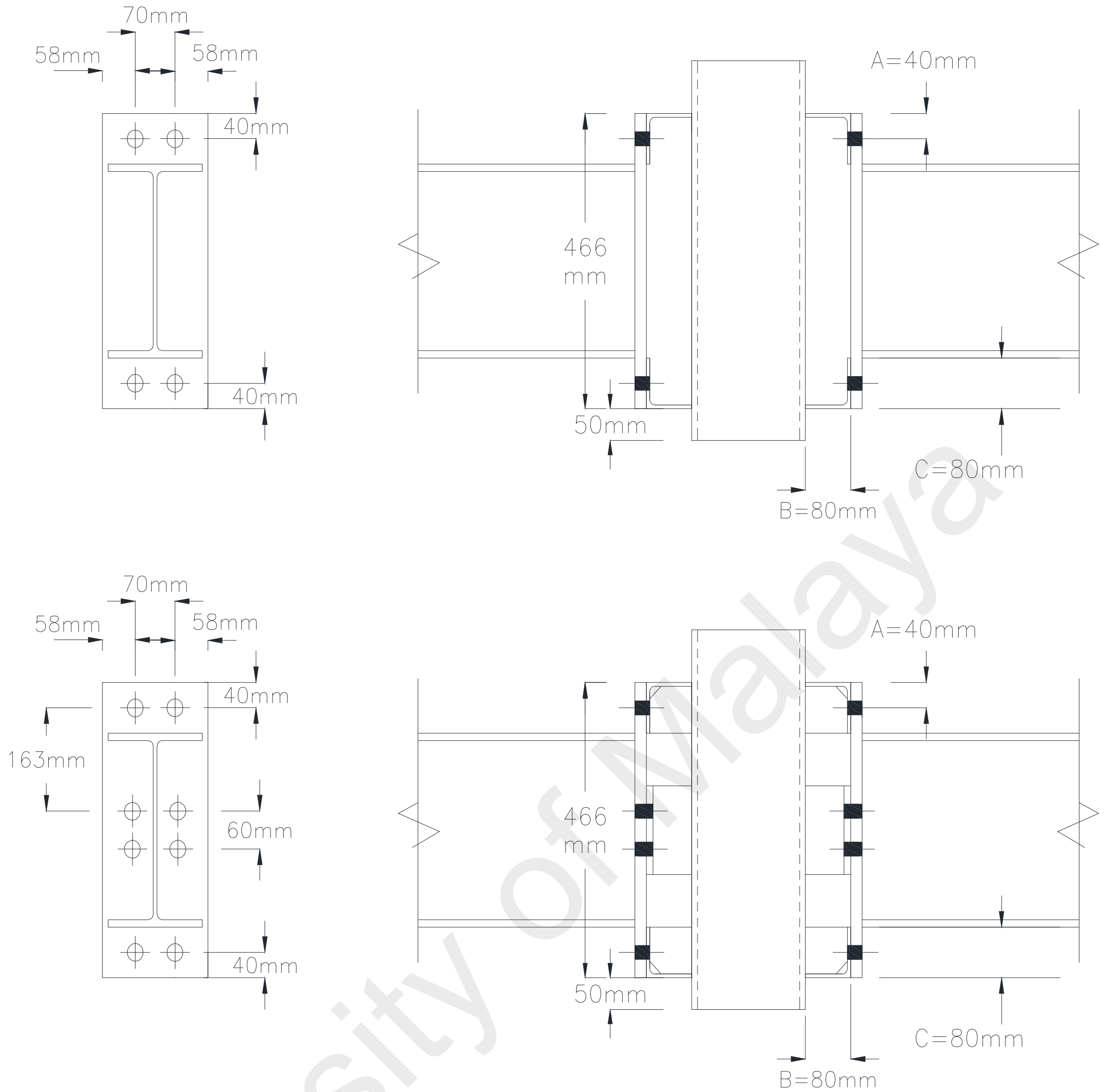

Figure. 3.6 Geometrical dimensions for elevated temperature specimens ET1 (Top) and ET4 (Bottom).

3.4.2 Heating and Thermal Regiment with Constant Load

Elevated temperature condition is provided by a large-scale furnace with internal chamber size of 2000 mm (L) x 1000 mm (W) x 1000 mm (H) powered with a 450A electrical source. An electronic controller divides the heating elements into zones, which deactivates certain zones if the furnace internal temperature of the particular zone is higher than the programmed temperature.

Loading of the specimen is provided through hydraulic actuator with a maximum of 150kN and transferred with a column stub, with size of UC203x203x46 as shown in Figure 3.7. Lower half of column stub is wrapped in thermal insulation to minimize transfer of heat to column stub and load cell. During experimental tests, the temperature of the column is monitored to ensure that the heat is not transmitted to the column stub. This is to ensure heating of the load cell does not occur. The area surrounding the opening for the column stub has also been covered with thermal insulation to reduce heat loss from this opening. However, the column stub is expected to displace vertically, and therefore, the thermal insulation is not packed tightly around the opening of the column stub as shown in Figure 3.8. By using a collapsible thermal insulation, heat loss is reduced while maintaining the ease of column stub displacement. As depicted in Figure 3.9, the thermal insulation is applied on both side openings of the specimen, preventing heat loss.

For the furnace, heating element arrangement and overall details are as shown in Figure 3.10 and Figure 3.11. The temperature on the specimen are limited to the length of the furnace internal length, 2000 mm. It should be noticed that the heating elements are located on the sides of the furnace. Heating pattern of the furnace is programmed accordingly to follow the temperatures outlined by the ISO834 fire curve, the temperature values can be defined using the general formula outlined by Equation 3.1, where t is indicated for the time in minutes, and T denotes the temperature value.

However, as the furnace is based on electrical source, the first 10 minutes of heating is a slow heating to achieve 350°C within the period. After this point, the temperatures are in accordance with the ISO834 fire curve. Comparison furnace temperature and ISO834 expected temperature is as shown in Figure 3.12, which shows a delay of 7 minutes, followed by a close relation of both curves.

Figure 3.7 Column stub and loading configuration

$$T = 20 + 345 * (log[8t + 1]) \qquad \text{(Eqn. 3.1)}$$

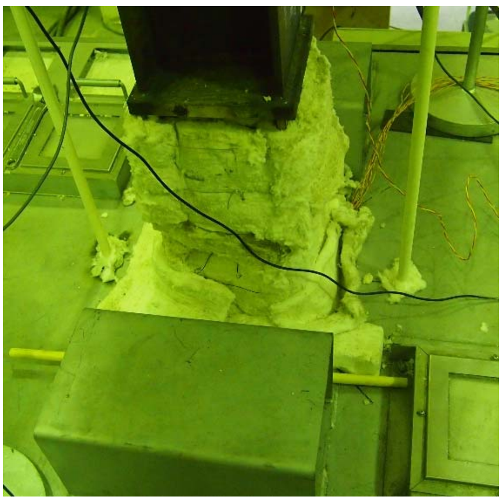

Figure 3.8 Thermal insulation surrounding column stub opening

Figure 3.9 Thermal Insulation of the specimen ends

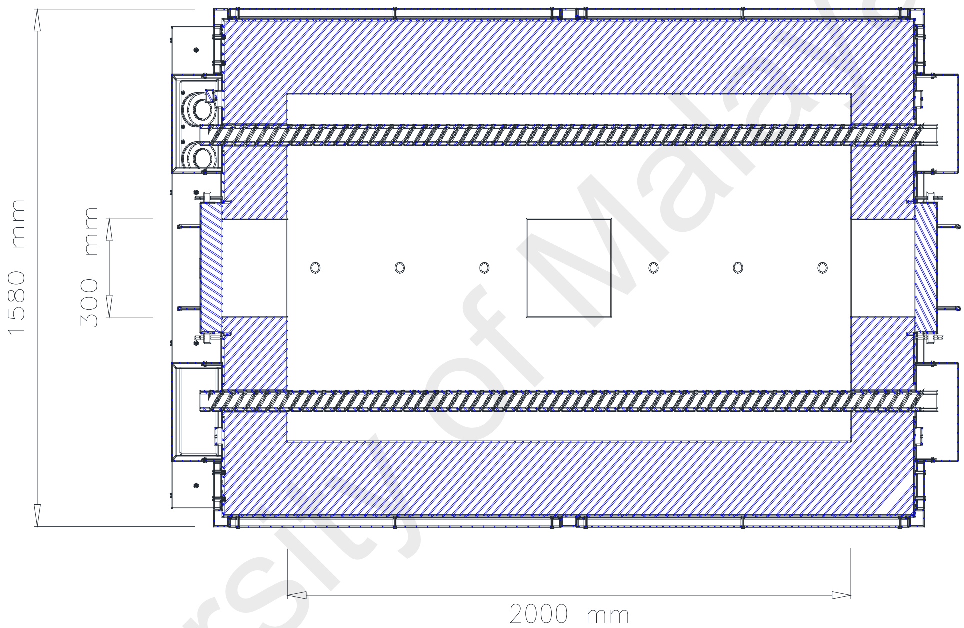

Figure 3.10 Plan View showing size and LVDT hole locations

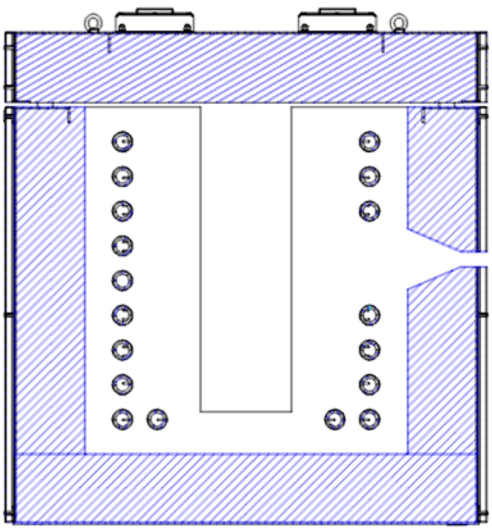

Figure 3.11 Front Internal View of Furnace showing heater arrangements

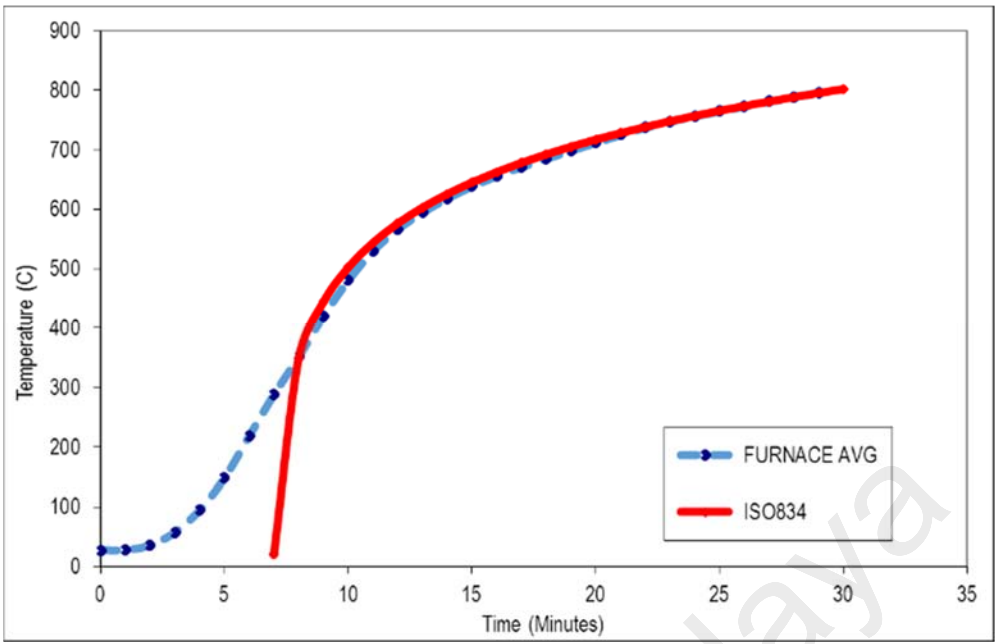

Figure 3.12 Temperature comparison between standard ISO834 curve and furnace temperature.

3.4.3 Boundary Conditions

The specimen is supported by two "A" frames as shown in the test setup of Figure 3.13 and Figure 3.14. These support frames have been designed to resist horizontal forces of up to 500 kN which is relatively more than the axial loads applied due to the heating and testing of members. Connection to the frames is by means of 4M30 Grade 8.8 Bolts as indicated by Figure 3.15. Meanwhile, the connecting plates at the end of the beam are 30 mm thick, which is designed so that it does not display any failure prior to specimen failure. The flush end plate creates a semi-fixed connection where the beam is still free to resist bending but unable to displace laterally.

3.4.4 Sensors & Measuring Equipment

Four LVDTs has been setup to measure the deformation and behavior of the joint. Two 200 mm capacity LVDT are used to measure the deflection of the hollow section column while the 100 mm LVDTs are used to measure the deflection near the beam, which is 300 mm from column center. To protect the LVDT, deflection reading of the beam is obtained by attaching the LVDT to 20 mm diameter ceramic rod extensions. Measurements of the 200 mm LVDT are on the column stub used to transfer the load to the connection column.

While the beam deforms, the ceramic rod drops corresponding to the deformation and the resulting measurement of this drop similar to direct measurements on the beam. LVDT setup points and ceramic rod is as indicated in Figure 3.16 and Figure 3.17. Several points are selected to measure the temperature using thermocouple wires type K that has been welded on to the beam, components and joints. Locations of the thermocouples on the specimen are as indicated in Figure 3.18 with the corresponding indicated point mark. Distances between the points on the beam are 500 mm apart.

Figure 3.13 Overall Experimental setup with A Frame Support on both sides

Figure 3.14 Furnace used for experimental tests

Figure 3.15 Beam bolted to support frame.

Figure 3.16 LVDT Arrangement & Ceramic Rod Extension

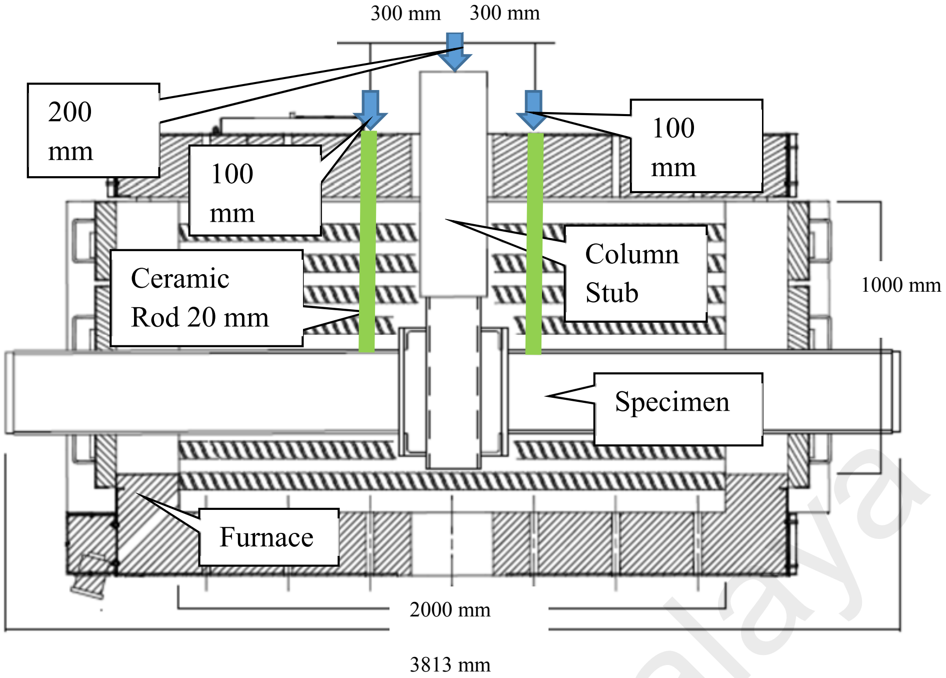

Figure 3.17 Overall Specimen placement and instrumentation

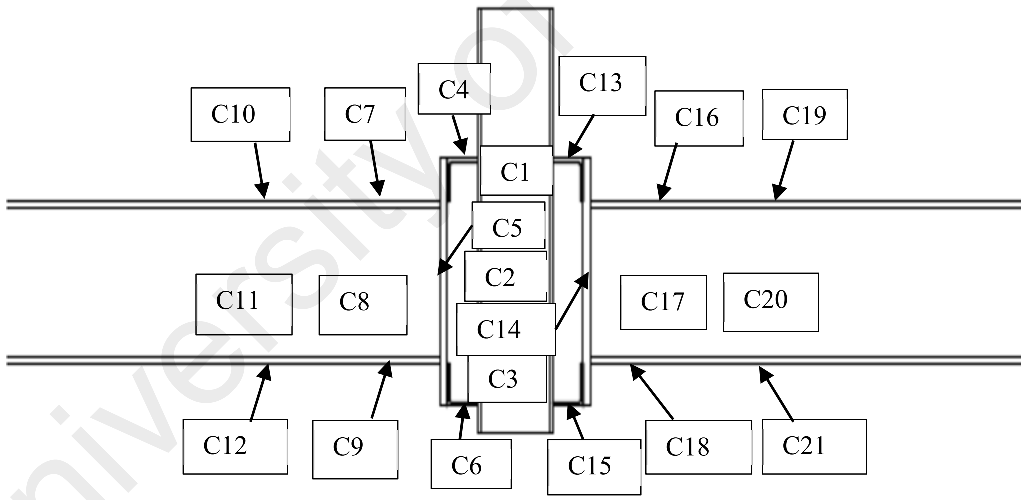

Figure 3.18 Thermocouple locations on the specimen

3.5 Finite-Element Modelling

3.5.1 Modelling of Component

Modelling of the components are based on two methods being used primarily in this research, depending on the components to be modeled. For general components, the solid extrusion method is used while for bolts, the revolution is used instead. In the solid extrusion method, the cross section of the component is created which is then extruded to the required length. Meanwhile the revolution method is on the creation of half-of the cross section and revolved around a fixed axis. Because the bolt head and nut is combined as one part to reduce complications, the extrusion method is not practical due to the various diameters of the bolt head, shank and nut.

3.5.2 Meshing of Components

One of the main procedures in producing hexahedral meshing would be the utilization of the *Partition* method to split the solid into smaller sections which can be sweep meshed. Undoubtedly, a few methods exist to partition the solid; however, the main concept is the definition of a cutting line that would serve to partition the whole component in the selected direction. Whole model is selected for partitioning to increase mesh uniformity. In terms of bolt partitioning, to create a uniform mesh, the diameter of the bolt shank is reflected onto the bolt head and nut where this created edge is used to partition down the bolt head.

Meanwhile, the mesh seed size is commonly defined as 5 mm size in general, in which the mesh is verified to check for unusual meshes, which may increase computational loads or result in analysis error. An example for the mesh procedure is as shown in the Figure 3.19 for bolts and 3.20 for the angle sections. It should be noted that a square frame is partitioned in the proximity of the bolt hole to limit the curvature meshing transition.

3.5.2.1 Element Types

Different elements used in analysis may provide different results, which is possible due to the different degrees of freedom provided. Solid elements for example are stiffer than line elements but solid elements are a closer simulation of actual experimental tests if model deformation and interaction are necessary to the study. In addition, the elements may not have the attached function relevant to the study, including temperature effects as with certain elements. Hexahedral shaped elements are commonly used in previous studies as shown in Table 3.5. For the present study, a standard 8-node element has been considered. The size of element is determined by performing mesh convergence study.

3.5.2.2 C3D8 Element

Element C3D8 is as represented in Figure 3.21, showing an 8-node solid brick element. The element can be used as a general-purpose element for all analysis types. However, under bending loads shear locking may occur. Shear locking occurs due to the linear nature of the element, where the element is unable to form a curvature, similar to actual materials under bending and thus causes shear to develop. Undoubtedly, this can be avoided with increased element numbers. One of the consequences of shear locking would result in a higher stiffness than expected.

Table 3.5 Elements used in previous studies

Author	Connection Type / Study	Element Used
Yang et al. (2000)	Web Angles, Welding at beam leg	C3D8, C3D20
Kishi et al. (2001)	Top-seat with web angles	C3D8
Hong et al. (2002)	Web Angles, Welding at beam leg	C3D8, C3D20
Pirmoz et al. (2008)	Top-seat with web angles	SOLID45, SOLID64
Cafer (2009)	Top-seat with web angles	SOLID186
Saedi Daryan and Yahyai (2009)	Top-seat angle	SOLID64

.

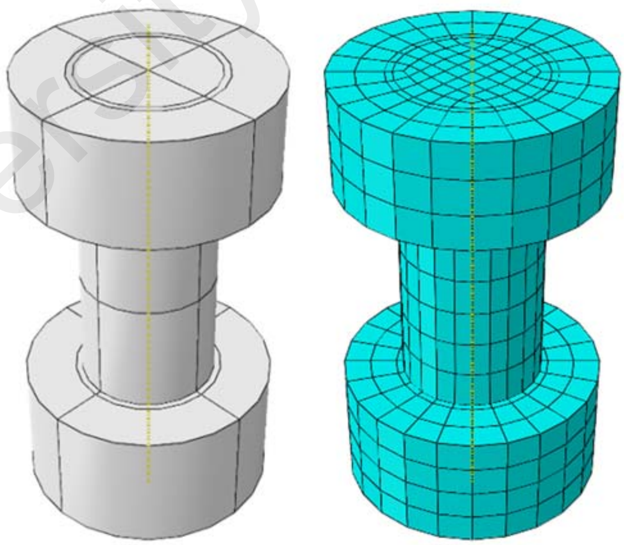

Figure 3.19 Meshing of Bolt Component

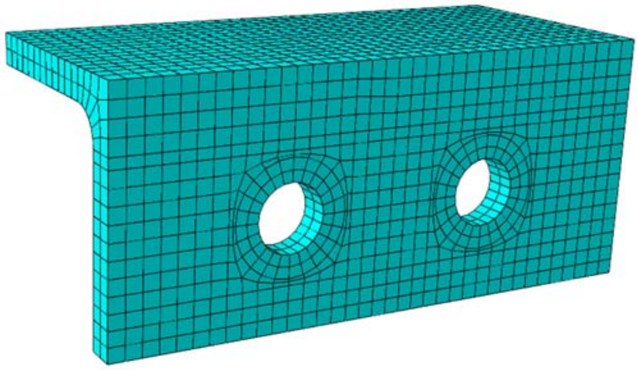

Figure 3.20 Meshing of Angle Component

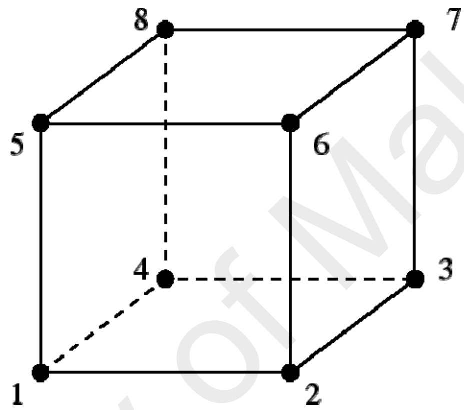

Figure 3.21 Representation of C3D8 element

3.5.2.3 C3D8I Element

Shear locking reduction is one of the main differences between the standard C3D8 and C3D8I. Without the shear locking in the C3D8I element, the bending stiffness can represented with increased accuracy. Computational effort is of minimal difference compared to the standard elements but higher than when C3D8R is used.

3.4.2.4 C3D8R Element

In comparison to the standard C3D8, the integration points in C3D8R elements is reduced to a single point at the center of the element as shown in Figure 3.22. With the single integration point, the element has the hour-glassing issue where the element may be skewed and deformed due to bending. This could result in the element to be unnecessarily flexible and meshing distortion to be excessive. However, the reduced integration points reduce the computational time and thus the element could be used for preliminary studies of the model to validate procedures.

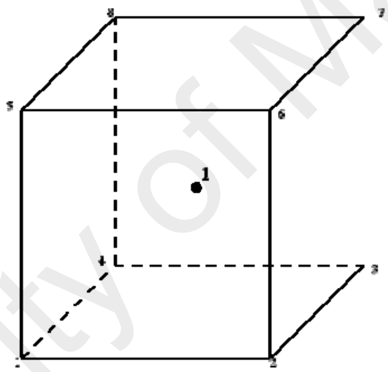

Figure 3.22 Representation of C3D8R element

3.5.3 Material Properties Considerations

Steel material is usually homogeneous and therefore, little variation can be found due to the standardized process of producing steel sections. The common properties of steel to be considered in design include the yield stress values, ultimate stress values and the Modulus of Elasticity. The typical stress-strain graph is as shown in Figure 3.23. Strains of 0.002 in elongation length ratio are still considered to be in the elastic range while the ultimate stress lies between the 0.1 and 0.2 elongation length ratio.

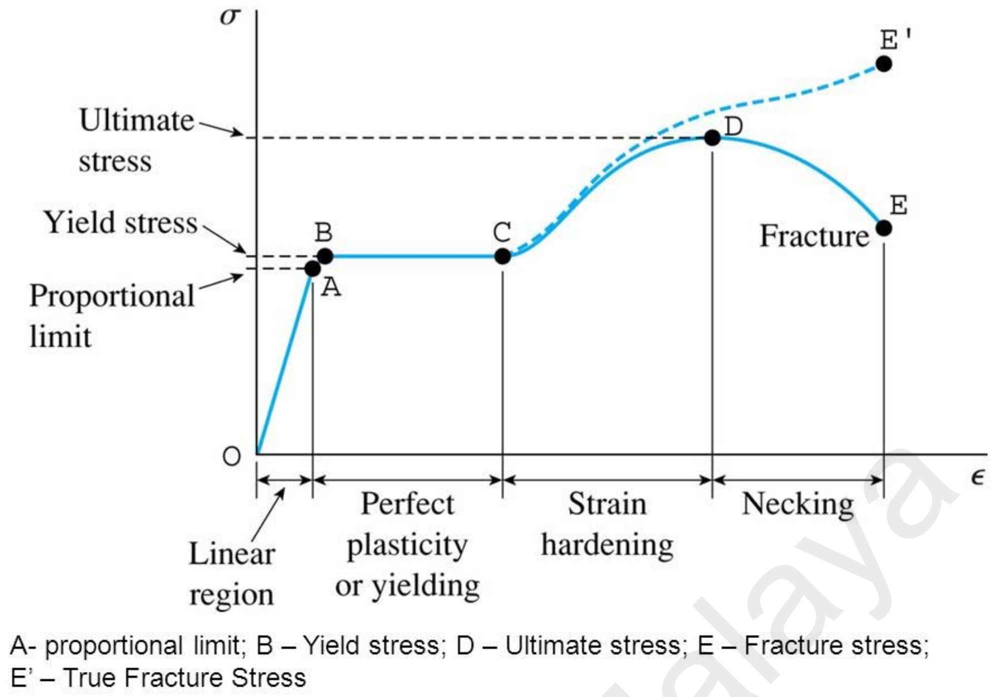

Figure 3.23 Typical Stress-strain behavior of steel material.

3.5.3.1 Ambient Temperature Materials

For consideration in a finite-element analysis, simplifications of the behavior have been considered in various studies, such as by Pirmoz et al. (2009) Kishi et al. (2001) and Saedi Daryan and Yahyai (2009). The results from the models have shown good agreement with the respective experimental results being simulated, where the material behavior is simplified to a bilinear graph, commonly encompassing the yield stress. An example of the simplification of the behavior by using bilinear material model is shown in Figure 3.24. This model is simplified from the material definition in EC3: Part 1-2 (2005) for 20C material model. Although the code generally describes the material model for elevated temperature materials, the definition of the materials are based on isothermal conditions, therefore, the details for 20C is applicable for constant ambient temperature steel material.

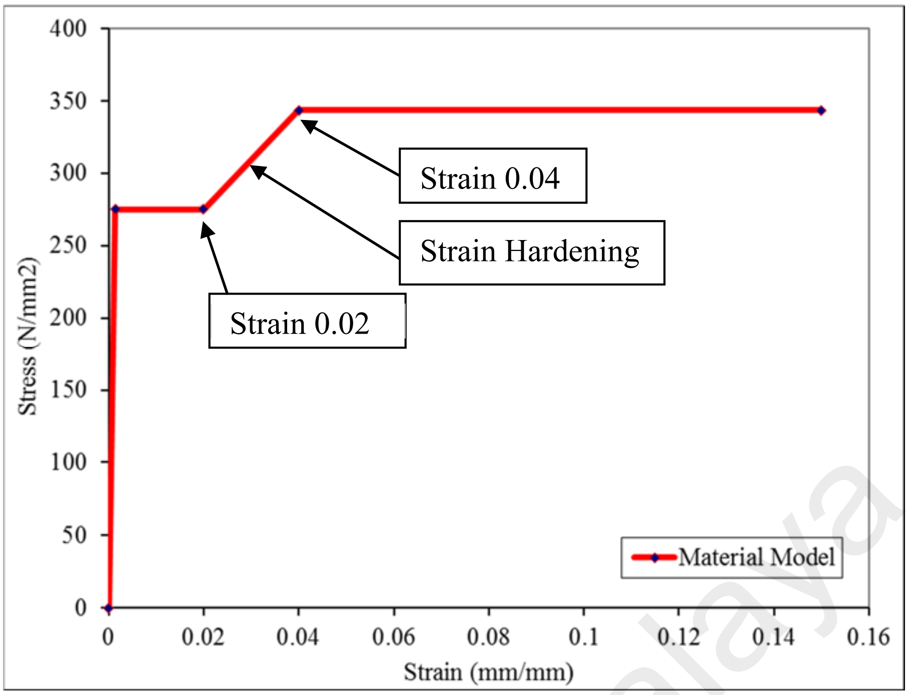

Figure 3.24 Bilinear Curve Adopted for Ambient Materials.

3.5.3.2 Elevated Temperature Materials

The typical stress-strain curve for steel at elevated temperature is as shown in Figure 3.25 as defined in EC3: Part 1-2. Both steel members and bolts used the same definition as have been outlined. The degradation factor detailed in EC3: Part 1-2 (2005) results from tensile tests done under isothermal conditions and therefore the degradation factors according to Outinen and Mäkeläinen (2002) as shown in Table 3.8 is used as the values were obtained from anisothermal heating tests.

Definition of the material models are as defined by EC3: Part 1-2 (2005) and the application into ABAQUS is simplified to a multi-linear material model, where the major points of the material model curve are at the starting point, the proportional limit point, two-curve fitting points, and yield stress at 0.02 strains and at 0.15 strains. For the two curve-fitting points, the first point is located at 0.006-0.007 strain ratio while the second point is at 0.014 strain.

A comparison is made between the proposed material model curve in EC3: Part 1-2 (2005) and the multi-linear model used for this study as shown in Figure 3.25. It should be noted that the material model does not allow for decrease in material properties, therefore, the material model in ABAQUS is defined up to the 0.15 strains level as beyond 0.15, the strain level will increase while the stress levels decrease, leading to material failure.

Table 3.6 Reduction factors for steel at various temperatures.
(EC3: Part 1-2, 2005)

Temperature	Modulus of Elasticity	Proportional Limit	Yield Stress
20	1.00	1.000	1.000
100	1.00	1.000	1.000
200	1.00	0.807	0.900
300	1.00	0.613	0.800
400	1.00	0.420	0.700
500	0.78	0.360	0.600
600	0.47	0.180	0.310
700	0.23	0.075	0.130
800	0.11	0.050	0.090
900	0.06	0.0375	0.068
1000	0.04	0.025	0.045

Table 3.8 Reduction factors for steel at elevated temperature

(Outinen & Mäkeläinen, 2002)

Temperature	Modulus of Elasticity	Proportional Limit	Yield Stress
20	1.00	1.000	1.000
100	1.00	0.970	0.970
200	0.90	0.807	0.932
300	0.80	0.613	0.895
400	0.70	0.420	0.857
500	0.60	0.360	0.619
600	0.31	0.180	0.381
700	0.13	0.075	0.143
800	0.09	0.050	0.105

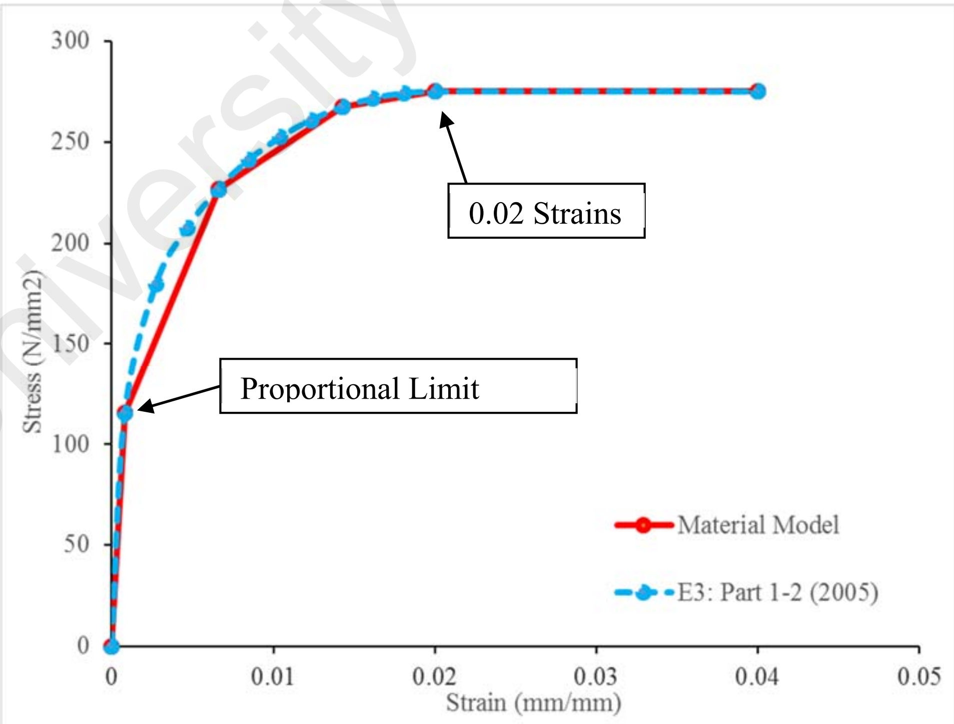

Figure 3.26 Comparison of EC3: Part 1-2 and material model of this study

3.5.3.3 Application of Material Model in ABAQUS

Results obtained from tensile tests of materials are classified as engineering stress-strain curves and to be applied into ABAQUS, must be converted to true stress strain curves for increased accuracy. In tensile tests for steel material, application of tensile forces reduces the specimen cross-section area and increases length as the tensile force is increased. Calculation of the engineering stress-strain material curves is with the assumption of a fixed specimen cross-section area and length and does not accurately indicate the material true behavior. Therefore, the conversion of the material from engineering to true materials is by using the formula indicated by Equations (3.2) to (3.3), with σ_{tru} being the true stress, σ_{nom} is the engineering stress while ε_{nom} is the engineering strain and ε_{tru} is the true strain values.

In addition, elastic material definition in ABAQUS is with the Young's Modulus value and Poisson's Ratio while the plasticity requires the definition to start from the onset of plastic behavior, which can be calculated through equation 3.4, where ε_{pl} is the true plastic strain values to the corresponding true stress values.

$$\sigma_{tru} = \sigma_{nom}(1 + \epsilon_{nom}) \qquad \text{(Equation 3.2)}$$

$$\epsilon_{tru} = ln(1 + \epsilon_{nom}) \qquad \text{(Equation 3.3)}$$

$$\epsilon_{pl} = \epsilon_{tru} - \frac{\sigma_{tru}}{E} \qquad \text{(Equation 3.4)}$$

3.5.4 Contact Definition

For both ambient and elevated temperatures, several parameters continue to remain unchanged, as these parameters are not affected by the variation in temperature. Among the parameters under this category are the density of steel, coefficient of friction, and the parameters set for the contact interactions. The contact definition or interaction is defined between any two surfaces of two different components, which share the same plane of location. Without the definition of contact, the components do not transfer any forces in between and bypass each solid with minimal restrictions.

3.5.4.1 Coefficient of Friction

Coefficient of friction is the dimensionless Coulomb friction value between two surfaces, which can be described as the ratio of tangential force and the force normal to the surface. In other studies, such as those by Kishi et al. (2001) the value of 0.1 has been considered. Guidelines provided by AISC (Manual for Steel Construction) mentions that the value of 0.33 should be used for class 'A' surfaces, where class 'A' refers to clean mill surfaces. However, the friction coefficient value of 0.25 has been considered in the study by Saedi Daryan and Yahyai (2009) where sensitivity studies conducted have shown that it has better agreement with experimental results. Value of 0.25 is then considered for all models in this study.

3.5.4.2 Contact Settings

Two contact types are specified, one for the tangential behavior while the other is the normal behavior. In terms of tangential behavior, while the contact between surfaces has been defined as friction, the resolution of the friction is defined with the Penalty method instead of the Lagrange Multiplier method. The penalty method allows for small relative movement between surfaces while the Lagrange method allows movement only when the shear stress value is achieved. It can be justified from this that the usage of Lagrange method would increase the computational method and therefore the Penalty method is used. In addition, the Lagrange method allows for small movement with relatively less conditions, which is expected in the connection behavior.

In the normal direction, it is defined as “Hard” contact with the option to allow separation after contact is established. Other interaction parameters includes, finite sliding for the formulation. Master and slave definition is also included where the members, which are expected to penetrate other components, are defined as the Master component and the opposite side to be the Slave component. An example is the area under the bolt head is defined as the slave while the bolt contact surface on the steel member is defined as the Master component as the bolt is expected to have a minor penetration on the steel member during the pretension stage.

3.5.4.3 Tie Contact

In structural steel structures, the often-encountered jointing element is welding of the steel components. The method of modelling the weld geometry is one of the methods to achieve proper representation of the connection. However, the computational effort to analyze the model may increase depending on a number of factors such as non-linearity, material property and geometry. For model simplification, the cross-section of the component is selected to 'tie' to the attaching surface, thus preventing the component detaching from the attachment surface, effectively creating a welded condition.

3.5.5 Loading Application in Model

The study on a connection, involves in the connection behavior under various loads. These loads are transferred from the floor to the beams and to the connections, causing deformations and failures of components. In experimental studies, the loads are commonly applied using a load-cell and hydraulic loader while in finite-element analysis; the loads are simulated by pure forces acting in the direction specified or moment loads about an axis. In elevated temperature analysis, the other form of load to be applied would be from the temperatures due the fire condition.

3.5.5.1 Direct Loads

Direct loading of the models involves two methods, either through pressure loads or through using the displacement method. In the actual experiment test, the direct loads are often applied on the column through spreader plates or column stub, however, in the model the pressure loads are applied directly on the component geometry. For the direct load, the load is divided across the applied area with uniform value while for the displacement method; it is assumed that the whole area has identical displacement values.

3.5.5.2 Applying Pretension Loads

It is common practice in bolted connections for the bolt to be tightened sufficiently and pretension loads are generated internally in the bolts. To apply pretension in the model, the pretension load is applied as the first step load, which value is determined by how much the bolt has been tightened. The selected area is the surface area in the bolt shank, which is automatically created in ABAQUS as shown in Figure 3.27. Subsequently, the bolt axis is selected to define the pretension-acting axis. The value for the pretension is defined in Newton-force units, which is negative in value for the pretension load to be applied correctly on the bolt, which results in the tightening of bolt.

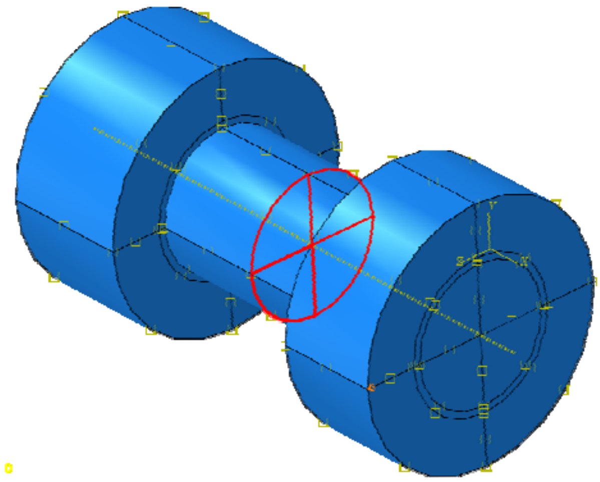

Figure 3.27 Pretension load application area

3.5.5.3 Temperature Loads

In comparison to the pretension loads or the direct forces, temperature loads are applied on the bodies as a whole by definitions of temperatures. Temperature loadings that are defined do not follow any standard fire curves with the concept that the behavior is not dependent on time factor. At constant moment load levels, the response of the connection at a particular temperature would not be affected by the amount of time that has passed but instead on the temperature of the component on the particular time. Therefore, at elevated temperature conditions, this justifies the use of the static structural systems, as it is not a dynamic behavior where dynamic analysis is dependent on the time factor. With similar concept, for isothermal analysis, the temperatures are defined as a constant value across the load steps but with variation in the load values.

As a model simplifications procedure, the temperatures are defined as a uniform temperature throughout the solid and do not consider the variation of temperature which would require further thermal analysis and consideration to thermal conductivity and the specific heat values of steel. In ABAQUS, thermal loads are applied by selecting the target solids and defining the relevant temperatures in the load steps in the "Predefined Field" section.

Temperature values are applied to individual components of the connection at a particular time, which means that different components may have higher or lower temperature values at a particular time. Values are taken from the recorded temperature values during the experimental test. Thermal loading can also be categorized into anisothermal and isothermal conditions, depending on the applied temperatures on the model

3.5.5.3a Anisothermal Temperature Loading

In anisothermal loading conditions, the temperatures are according to the ISO834 curve and the temperatures of each component is dependent a number of factors including the location of the heat source, material thermal radiation, and thermal conductivity. It is expected that the temperatures for each component will be different. Due to the variation in temperature in components, loadings with static values are commonly applied to reduce the effect from different load levels and focus on the differences in material properties. With consideration to both material and loading factors, no meaningful conclusion can be obtained without a comparison as control.

3.5.5.3b Isothermal Temperature Loading

In isothermal thermal conditions, the temperatures of the components are uniform with little to no variations. Loadings in this case can be of increasing or varied levels as the consideration of the variation in material properties is reduced. The isothermal condition is achieved by heating the furnace to the required temperature level until all the components achieve the required temperature.

3.5.6 Boundary Conditions

In any structural analysis, the three common supports are pinned, roller and fixed supports. These supports are essential for any finite element analysis and therefore can be defined in ABAQUS using the default supports options or individually defined. Figure 3.28 shows the supports available in ABAQUS. For general use supports, including pinned and fixed supports, the default settings are available. Fixed supports are labeled as “Encastre” in ABAQUS. In the default section, other than the pinned support, the other definitions also include rotation as part of the definition, which is applicable for symmetry areas of the model.

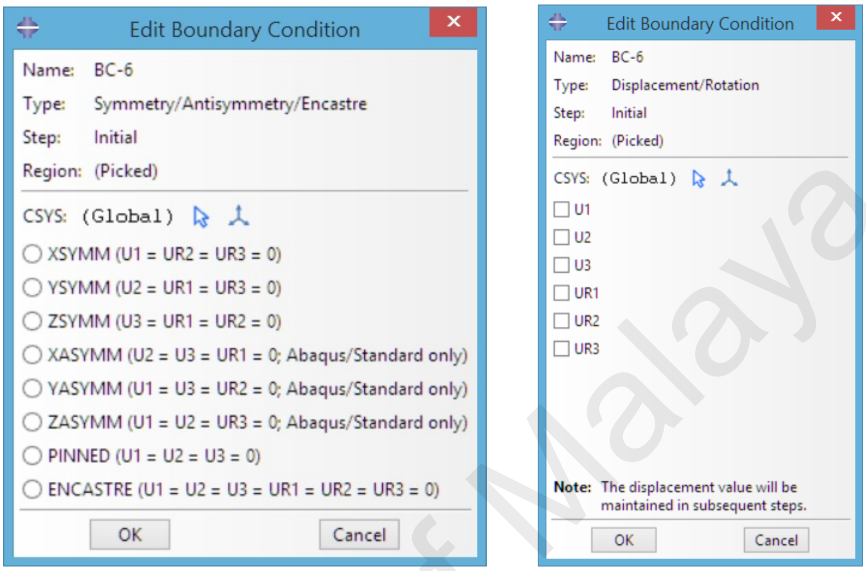

Figure 3.28 Default Abaqus Support options

The displacement support option can be used to define pinned supports due to concept of pinned supports where one horizontal and one vertical reactions at the support and able to rotate in the remaining of the three main 3D axis, by defining the displacement in the required axis as zero value. This therefore can be simulated depending on the selected geometrical component type; e.g for edges, both axes should be fixed in place while the other, using the surface, should only be fixed on one axis while in the other axis it is free to deform. The supports can be removed and redefined in steps where necessary. In static analysis for ABAQUS, it is necessary to define support at points to “hold” the model for the initial step, when the contact initializes, which can be removed from the next onwards. Without the definition of these temporary supports, the analysis may encounter singularity point error.

3.5.6.1 Temporary Boundary Conditions

In ABAQUS analysis, the temporary boundary conditions are necessary, as the software is unable to determine the relationship between the parts. Therefore, temporary supports are introduced where edge points of the parts are supported in several axis where there is no expected deformation occurring, in the first step as the contact initiation. This procedure would allow the parts to be held in position in the 3d-axis space, resulting in contact resolution between the components. In subsequent load steps, the temporary boundary conditions are removed by deactivating these definitions.

3.5.7 Model Simplifications

Models used for finite-element analysis usually undergo modifications to reduce analysis time and computational effort. Often for connection studies, the geometrical model is simplified using the concept that if the connection can be modeled as a mirror, only one half of the connection is modeled and in ABAQUS to be set as the Symmetrical option as shown in Figure 3.29 for the simplification of the model. Curvature areas are not modelled in the research to reduce analysis and meshing complications that may increase computational loads. Curve areas for angle section fillet and bolts are maintained to follow the behavior in actual specimens. It is known that the fillet for angle sections affects the deformation behavior of the section. Meanwhile the bolts are assumed circular, similar to the washers, instead of the hexagonal shape common in actual bolt head or nuts. In addition, welds are not covered in the study and therefore not modelled, assuming full strength bonding, with the contact properties as described earlier.

(a) Actual Specimen Configuration

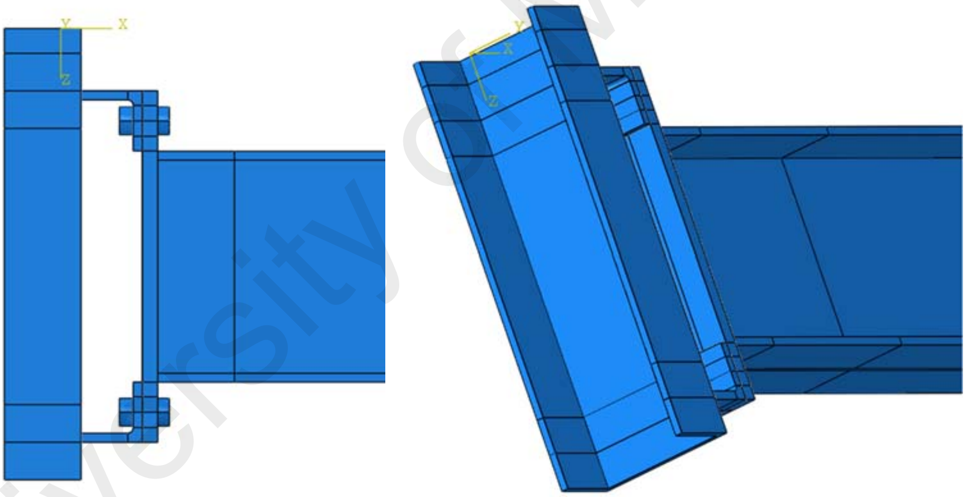

(b) Symmetry definition to half-model

Figure 3.29 Model symmetry applications

3.5.8 Finite Element Post Processing

After the analysis has been completed, the results are extracted from the software in forms of reaction forces or displacement values. For where displacement values are applied as the controlling load for the model, the reaction forces are taken as the result. This is done by querying the values of the reaction forces for the nodes at the area where displacement has been applied. Each node on the applied area results in a different reaction force value and thus the queried value to be totaled to obtain the actual reaction force value. Meanwhile, displacement values are extracted accordingly. Whether in terms of stress or plastic deformation patterns, no other post-processing is done and taken as is shown.

3.5.9 Load Steps Details

Analysis in ABAQUS involves the use of steps, which can be configured to achieve analysis convergence. However, the second load step is commonly reserved to initiate the contacts, while the first load step 'Initial' cannot be modified in any way but only where the supports and boundaries can be defined. For the study, instead of loadings, pretension of bolts is established and computed in the second load step while the loadings are applied in the third and subsequent load step. Meanwhile for elevated temperature condition analysis, the thermal loadings are applied in the fourth and subsequent load steps, considering that the static loads have to be solved to eliminate double uncertainties condition.

Non-linearity of an analysis may involve large strains and the end-deformation could be of different shape when compared to the original reference model. In that condition, the NGLEOM option is necessary to capture the deformations due to non-linear analysis and plasticity in the material model. Besides the non-linearity, the storage matrix is set as 'unsymmetric'. For elevated temperature analysis, due to the complexity from the material non-linearity and the continuous change in material property from the effects of temperatures, the automatic stabilization option is utilized to increase convergence.

3.6 Methodology Conclusion

In this study, a new connection for open section beams to tubular column is proposed. The new connection involves in welding angle sections to the column face and bolting a combination of end-plate and beam to the angle sections. Experimental tests and FE analysis are conducted to determine the behavior of the connection and deformation pattern. Three specimens are prepared for ambient temperature tests with simple supports and displacement based loading, while four specimens are prepared for elevated temperature tests under ISO 834 based temperature variation with constant loading. Elevated temperature tests are conducted with a large-scale furnace. Variations in the specimens include having different angle thickness and effect of stiffeners.

Results from the experimental tests are then used as a validation basis for FE models, using ABAQUS. In FE, the developed model is a solid element based model and reflects the actual state of the model, instead of using 2d elements. It is determined that temperature loading in the model shall not be time dependent as previous studies have shown that temperature and material degradation (based on EC3: Part 1-2, 2005) is sufficient to determine the resulting deformation and behavior. The validated model is then modified for further use in the parametric studies to determine the effect of various geometrical properties. Results from the parametric studies are critical to understanding the changes and components that contributes to the capacity of the connection. In addition, the models are also used to compare the performance with existing studies and determine the weaknesses of the connection proposed.

CHAPTER 4

RESULTS AND DISCUSSION

4.1 Introduction

Results and discussions from studies conducted at ambient and elevated temperature on reverse top-seat angle connections are presented in this chapter. Ambient temperature studies are presented in the first main section followed by elevated temperature studies. For ambient temperature, the experimental test results are presented first. Resulting connection performance is represented in the form of a moment-rotation curve that provides the connection behavior comparison between the different parameters in test specimens.

To further study the connection behavior, finite-element models are developed. First, the finite-element model procedures are validated with those of currently available test results of connections to tubular column. Next, similar procedures are then applied to develop a validation model for the current experimental test. Several parameters are modified for the validated models including material property values, boundary conditions and dimensions.

With the validation completed, the developed model is applied to simulate the behavior of the connection. Different geometric parameters that affect the behavior of the reverse top-seat angle connection are documented in the following sections and finally the comparison of the performance with tubular connection of other configurations is presented with relevant discussion.

Results from studies conducted at elevated temperature conditions are presented next. As temperatures are the major parameter that affects the connection behavior, the subsequent section focuses on the resulting temperature distribution of the specimen. Then deformation of the connection and behavior comparison is discussed in the next section. The validation of the finite-element model at elevated temperature with the experimental tests is outlined next, followed by the parametric studies. Parameters including the behavior of the connection in isothermal conditions, the boundary conditions of the connections and axial restraints are studied and thoroughly discussed in the last section.

4.2 Findings on Connection at Ambient Temperature

4.2.1 Experimental Test Results

Deformation of the connections at 110 mm column deflection is as indicated in Figure 4.1 while the moment-rotation curve of the connections is as shown in Figure 4.2. There is no major difference in the deformation from the left or right side beam in the experimental test, indicating close to equal load distributions on both connection sides.

Moment values are the product of the applied force and the distance from support to the column face while rotation is the deflection of the beam over the distance to the supports. Both calculations are represented by Equations 4.1 and 4.2, where M is the applied moment force, θ is the rotation and δ is the deflection. In addition, F being the applied load for each connection side L is the distance between the column face and support (which is calculated to be 1.4m) and l is the distance of the deflection transducer (LVDT) to the support. The applied force is assumed equal for both sides of the connection. It is observed from the deformation of connection AT1 and AT2 that the connection is governed by the bending of the angle, for both tension and compressive loads and the bending of the end-plate at the compressive zone. Tension forces developing due to the applied loads is less than the bending capacity of the 20 mm thick steel end-plate, however is greater than the 10 mm angle section bending capacity, thus the angle section governs the deformation in the tension zone. No visible deformations on the column face are detected due to the uniform distribution of load across the column face.

$$M = F.L \tag{Eqn. 4.1}$$

$$\theta = \frac{\delta}{l} \tag{Eqn. 4.2}$$

Meanwhile for specimen AT3, the stiffener plate reduced the bending deformation of the angle. T-stub prying similar to open section columns governs the deformation of the connection in tension zone. In the compression zone, deformation is similar to AT1 and AT2 with the exception of additional resistance due to the compression of the stiffener plate on the column face. There is no significant deformation or visible damage on the bolt shanks. With the stiffener, connection stiffness has negligible difference while the yield moment value is increased. With the addition of a stiffener, as seen in AT3, the column face deforms in reaction to the tension and compression forces distributed from the applied moment loads to the column face. The column face behaves as a beam under tension load, with the column corners acting as the supports.

(a) AT1 Deformation

(b) AT2 Deformation

(c) AT3 Deformation

Figure 4.1 Deformation pattern of the reverse top-seat angle experimental test specimens.

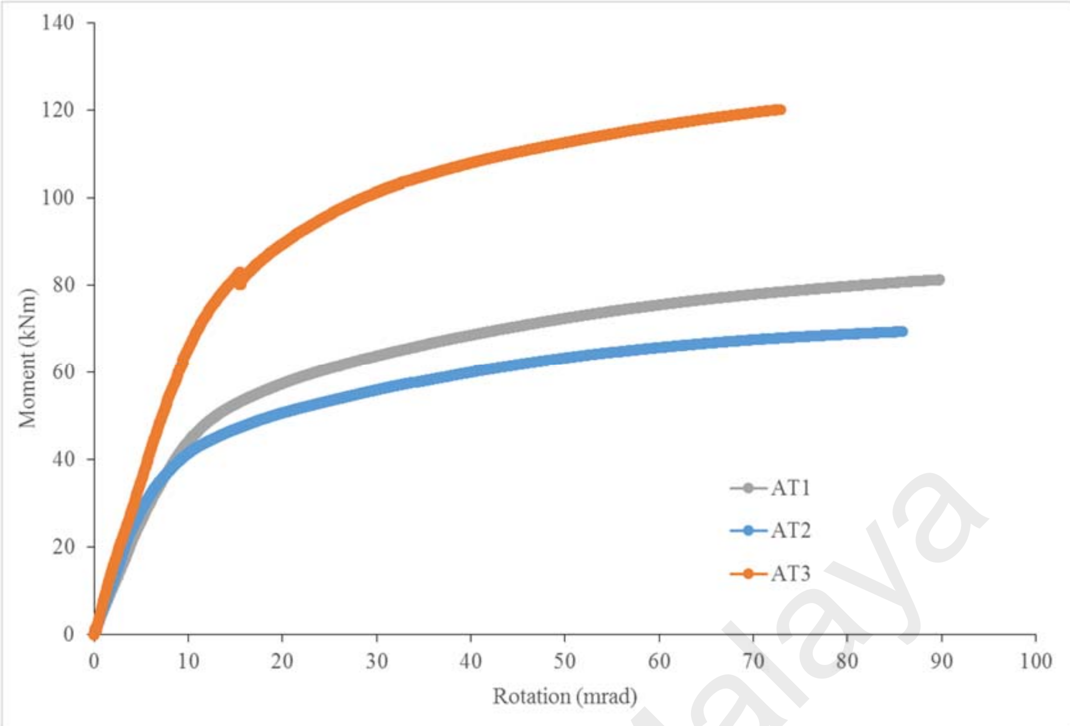

Figure 4.2 Deformation behavior of reverse top-seat angle connection.

4.2.2 Validation of FE Method

The main references for the verification are the studies on the reverse channel connection done by Elghazouli and Malaga (2010) and Wang and Xue (2013). While both studies cover the reverse channel connections, the focus of the former research is on the angle connection bolted to a reverse channel while the latter has focused on the end-plate connection bolted to the reverse channel configuration. Validating both studies provides a base accuracy of the proposed FE models, modelling method, and parametric assumption and values. In addition, the validations are able to eliminate uncertainties, which may be encountered during the validation for the experimental tests of the current study.

4.2.2.1 Validation of Reverse-Channel and Top-Seat Angle Connection

For model validation purpose, the work by Elghazouli and Malaga (2010), specimens T6.3-A8-d40-M and T10-A8-d65-M are selected and marked as specimen T1 and T2 in this research work respectively. Details of the steel section and material properties are detailed in Table 4.1 while the connection dimensions are indicated by the coupled Figure 4.3 and Table 4.2. The comparative behavior between the FE model and the experimental test results is as presented in Figure 4.4. As the experimental tests involve a one-sided cantilever connection configuration, the whole column section and the connection is modelled. However, the column is not modelled to full length and is assumed only to the extent of the connection.

Table 4.1: Section and material properties of specimen T1 and T2

	Column	Beam	Bolts	Channel	Top-Seat Angle
T1 T2	SHS 200x200x10	UB 305x102x25	8M16 Grade 10.9	CH 150x75x6.3 CH 150x75x10	L 100x75x8
Yield (N/mm^2)	511	329	900	400 (T1) 385 (T2)	312

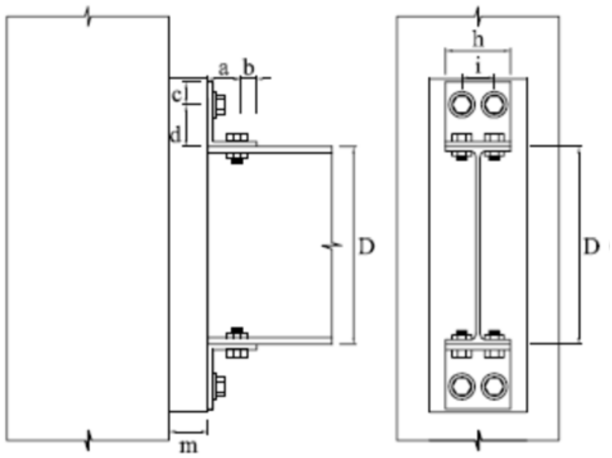

Figure 4.3: Reverse channel and top-seat angle connection configuration

Table 4.2: Dimension details of Specimen T1 and T2

Mark \ Parameter	a	b	c	d	m	h	i
T1	50	50	35	40	75	100	45
T2	45	30	35	65	75	100	45

Early stiffness and yield behavior of the model is reasonably accurate while the post-yield behavior is slightly different for specimen T1. Meanwhile, stiffness, yield and post-yield behavior are relatively accurate for the behavior of specimen T2 in general. The FE modesl shows similar deformations to those presented in the test results and thus verify that the deformation behavior of the model corresponds to the actual experimental test results as shown in Figure 4.5 and Figure 4.6. With thinner channel, the deformation is focused on the channel web while thicker channels result in the angle section becoming the critical component.

4.2.2.2 Validation of Reverse-Channel and End-Plate Connection

In the study done by Wang and Xue (2013), 8 specimens were tested but only 2 specimens are selected as the validation reference, which are Test 1 and Test 3 due to the deformation focus on the reverse channel component. In this validation, the two tests are modelled and labelled as WX1 and WX3. Steel section and material details are as according to Table 4.3 while the geometry dimensions are according to Figure 4.7 and Table 4.4. The connection deformation for WX1 matches actual experimental results, with double pullout behavior of the bolt rows as indicated in Figure 4.8. Meanwhile, for the end-plate connection with reverse channel the behavior of the model matches with the experimental results as shown in Figure 4.9. With the FE models showing acceptable accuracy with experimental test results, the procedures are repeated for the validation of the experimental results in the current study, however with minor modifications in terms of material properties, dimensions and boundary conditions relevant to the tests.

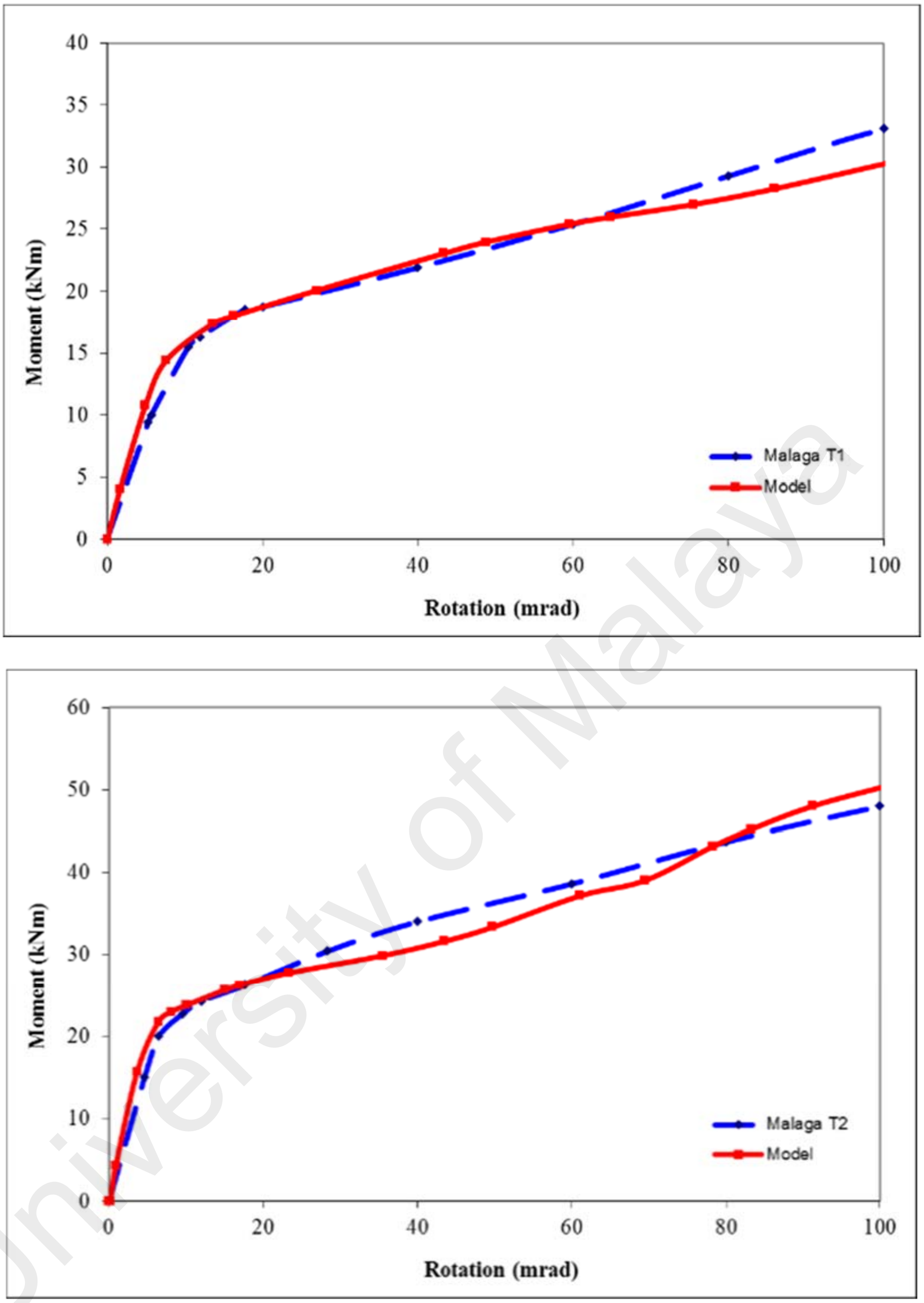

Figure 4.4. Comparison behavior of Model with Test T1 & Test T2 (Málaga-Chuquitaype & Elghazouli, 2010)

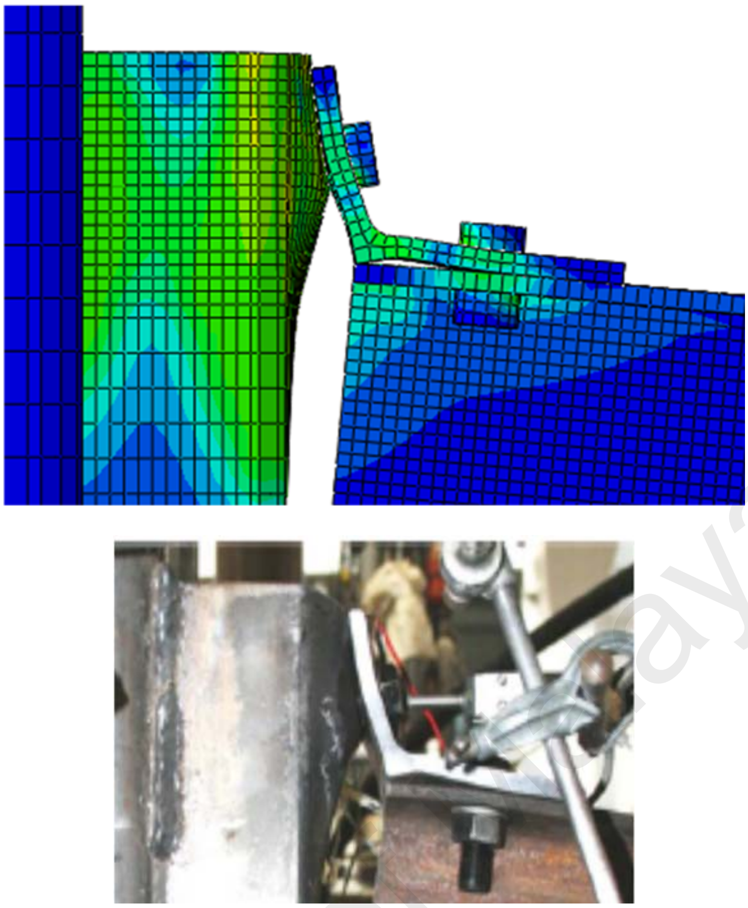

Figure 4.5: Comparative deformation between model and experimental for specimen T1. (Málaga-Chuquitaype & Elghazouli, 2010)

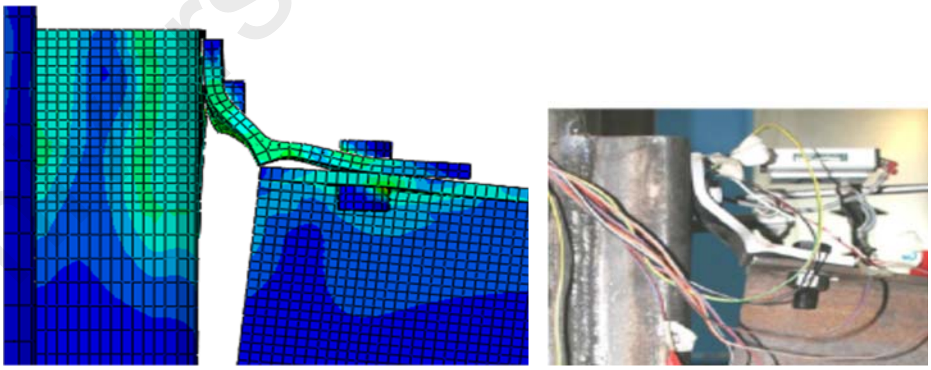

Figure 4.6 Comparative deformation between model and experimental for specimen T2. (Málaga-Chuquitaype & Elghazouli, 2010)

Table 4.3: Section and material properties of specimen T1 and T2

	Column	Beam	Bolts	Channel	End-Plate
WX1	RHS	UB	6M20 Grade 8.8 Ex-In	CH 180x90x26	10 mm thick
WX3	400x200x10	406x178x74		CH 180x75x20	end-plate
Yield (N/mm^2)	511	329	900	400 (WX1) 385 (WX3)	312

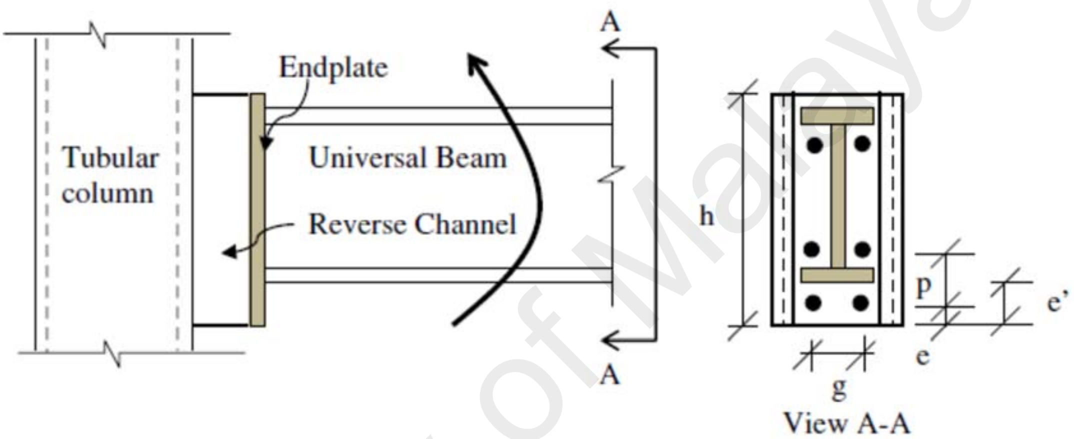

Figure 4.7 Reverse channel and end-plate connection configuration

Table 4.4 Dimension details of Specimens WX1, WX3 and WX4

Mark \ Items	e	e'	G	h	p
WX1	40	70	90	500	90
WX3	40	70	90	500	90
WX4	40	70	70	500	90

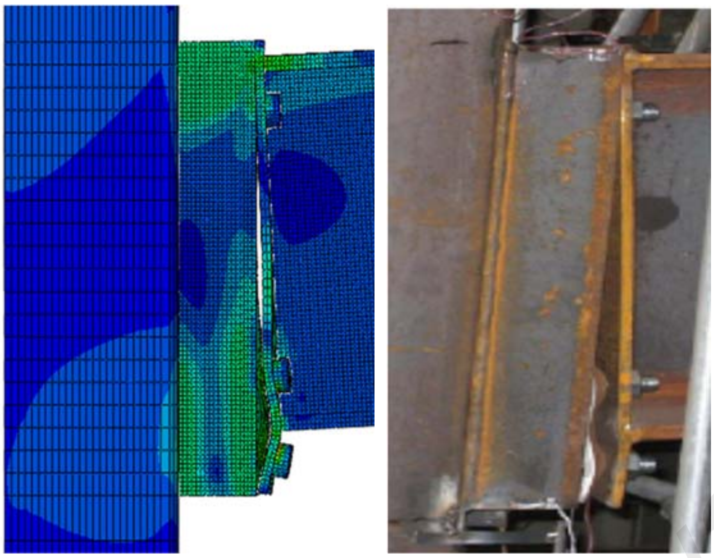

Figure 4.8 Comparative deformation for WSX1 (Wang & Xue, 2013)

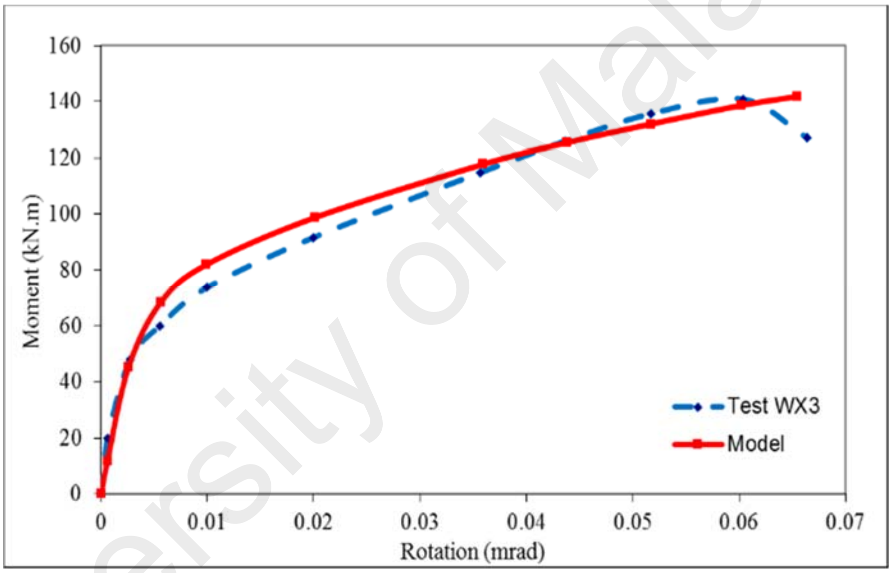

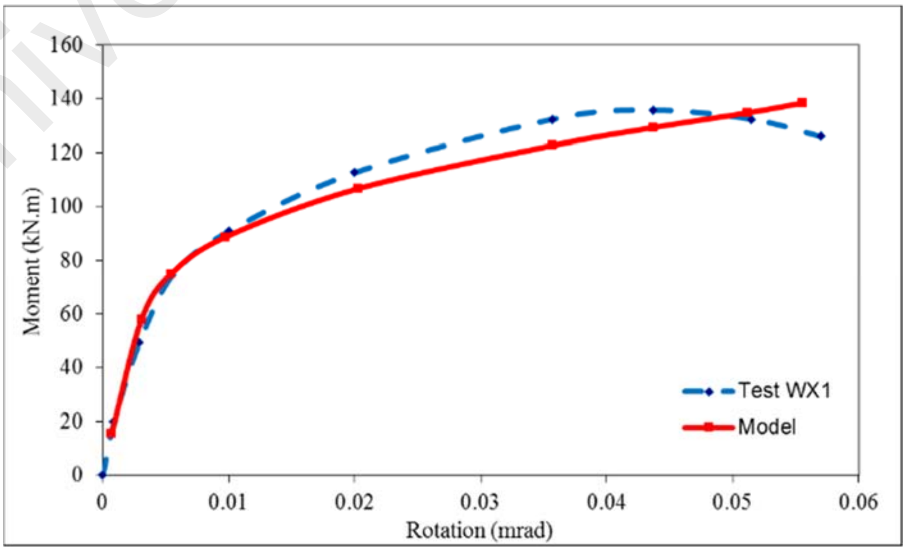

Figure 4.9. Comparison of Model with Test WSX1 and Test WSX3

(Wang & Xue, 2013)

4.2.2.3 Validation with Test Results of the Proposed Connection

Following the validation of model with previous studies, FE models are developed in ABAQUS according to the parameters and details described in an earlier section. Meshing of the model components such as bolt, angle and plate is as shown in Figure 4.10. Only half of the test specimen is developed for the analysis model. Similar to experimental test conditions, the column is displacement controlled to 110 mm by applying displacement load on the column top surface. The overall model detail including the boundary conditions and displacement location is as shown in Figure 4.11.

Moment is calculated from the reaction force resulting from the displacement load provided by the software as a total force. The beam is allowed to displace in the horizontal direction, similar to the roller support in the experimental test. Limited pretension is applied on to the bolts as the bolts were hand-tightened. Due to the major bending behavior governing the connection, element C3D8i is used. Welded portions are modeled as “tie” to the connecting surface.

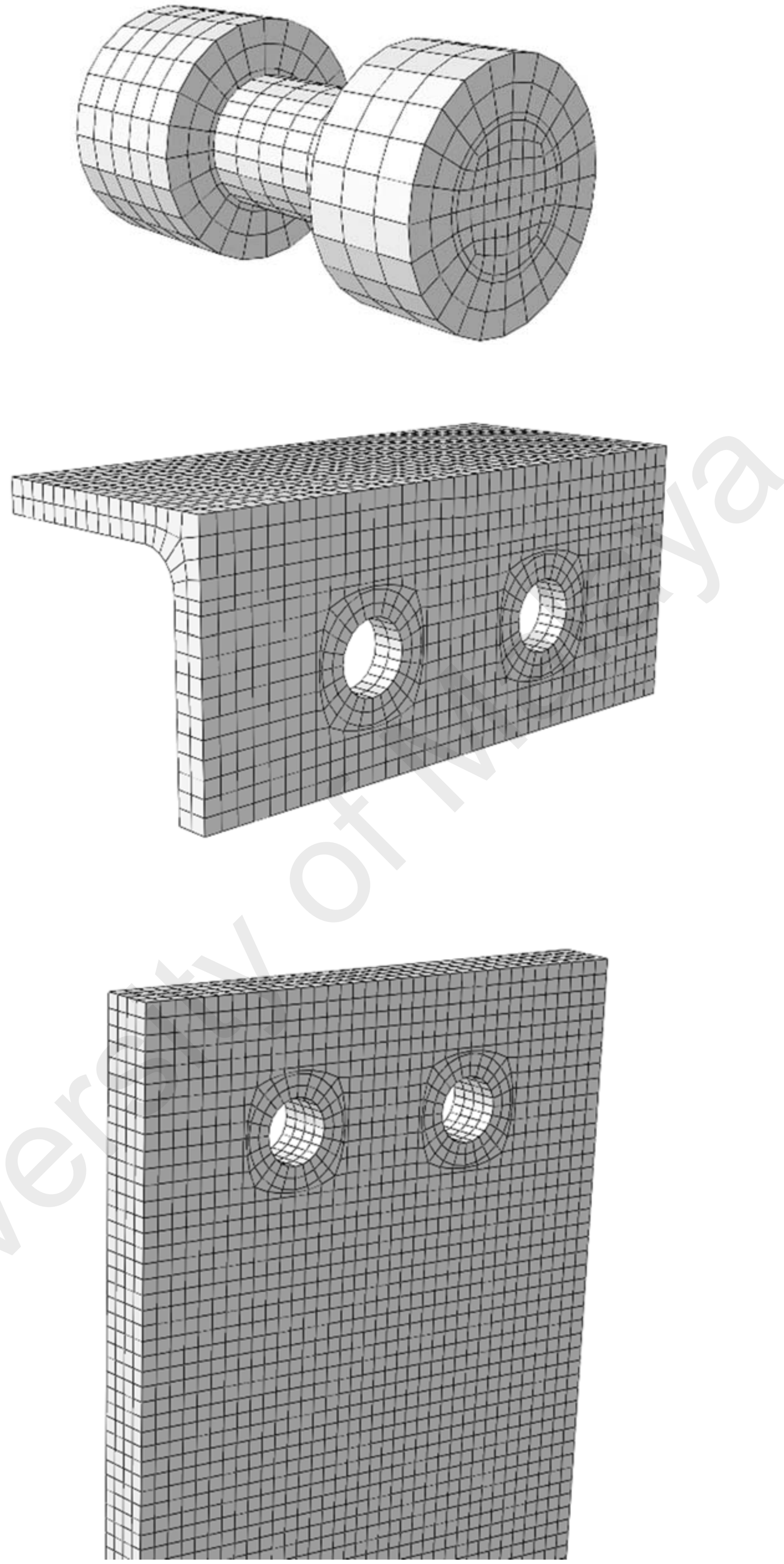

Figure 4.10. Meshing of model for validation of Proposed FE Model

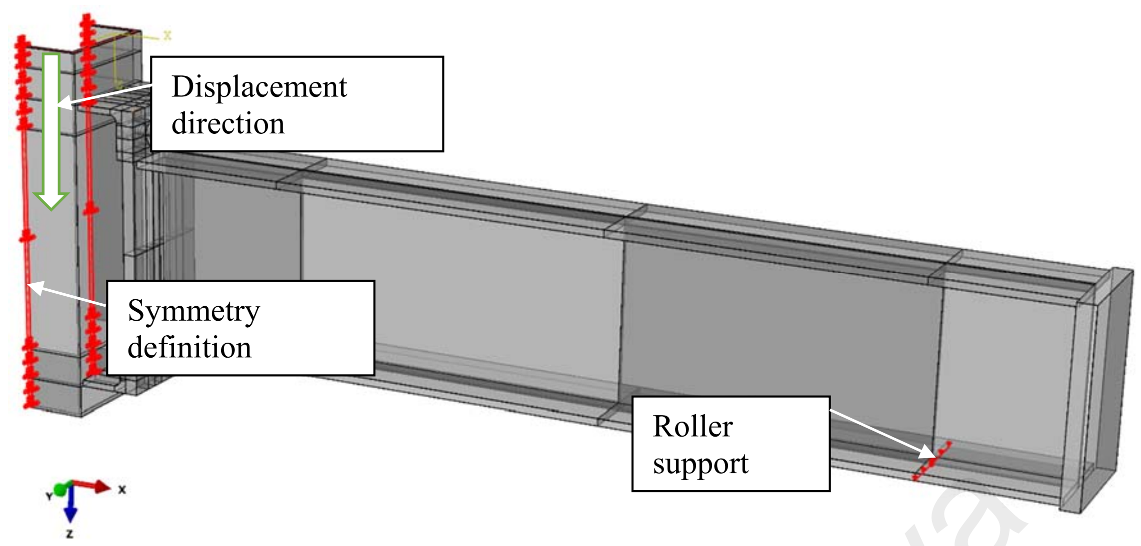

Figure 4.11 Boundary Conditions for Ambient Temperature Model

From the comparison indicated by Figure 4.12, the stiffness and post-yield behavior of the model is in good accuracy with the actual behavior. Similarly, for AT2 and AT3, the behavior of the model corresponds with the experimental results as shown in Figures 4.13 and 4.14 respectively. Other than the end-behavior showing minor divergence from actual results, the overall stiffness and yield show good accuracy. Plastic deformation starts at the tension angle near the heel, followed by the end-plate bending area due to the compression of the beam from the loading. It is understood that the load transfer mechanism for this connection configuration starts with the bending of the angle in tension, followed by the bending of the end-plate. In addition, the bolts on the tension side are in plastic state due to the bending resistance when load is applied.

Deformation comparison of the model and experimental test results are as shown in Figure 4.15 to Figure 4.17. The corresponding deformation of the end-plate is reflected in the models for AT1 and AT2 while the T-stub deformation of the angle is shown in the model for AT3. Although the exact component deformations are not measured, the deformation pattern shown is reflective for both model and actual specimen. With the accuracy shown in the comparison moment-behavior curves between the experimental results and model, and similar deformation patterns, the models can be considered as representative of the reverse top-seat angle connection.

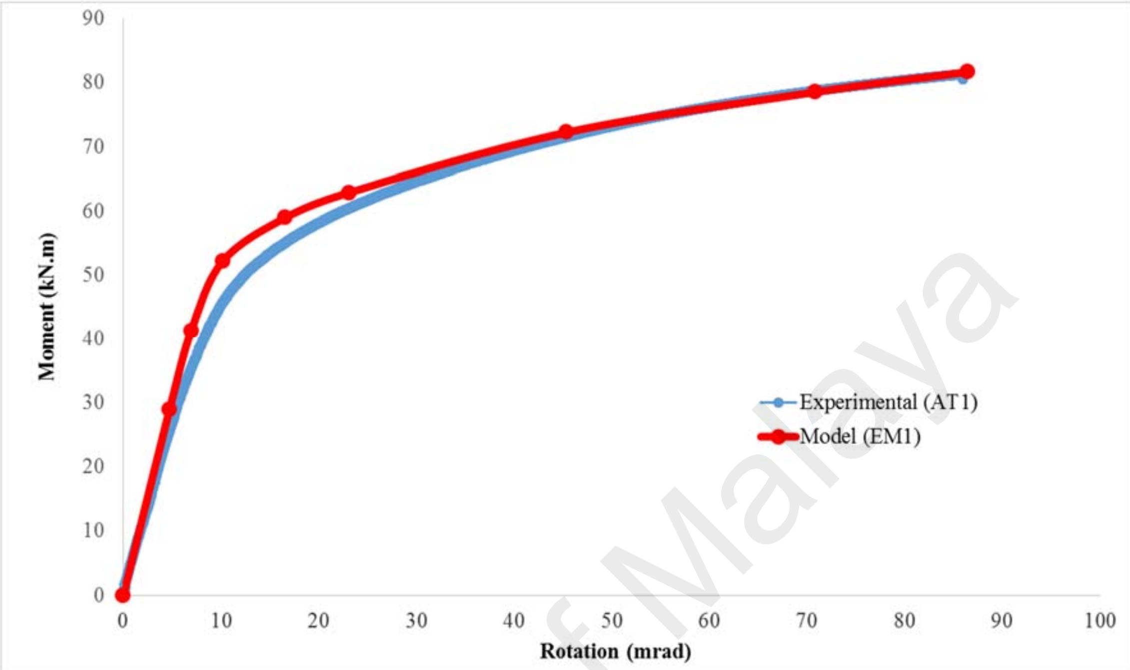

Figure 4.12. Comparison of AT1 and FE model EM1.

In terms of failure modes, the description can be categorized into the end-plate, angle, column and bolts. While stress can be an indicative for the onset of deformation at a particular location, however, the stress may still be in the elastic range, and therefore, plastic strain represents the near-failure locations of the component from the post-elastic strain values. Plastic strain distribution for the angle section is distributed along the heel of the tension angle in EM1. For EM3, the plastic strain is higher around the contact between the angle and the stiffener at the beam leg for the tension angle as indicated by Figure 4.18 (a), and Figure 4.18 (c) respectively due to the resistance of the stiffener from the tension forces applied to it. Plastic distributions for EM1 and EM2 are similar due the configuration of the connection. The 2 mm difference in the angle thickness did not affect the plastic strain concentration.

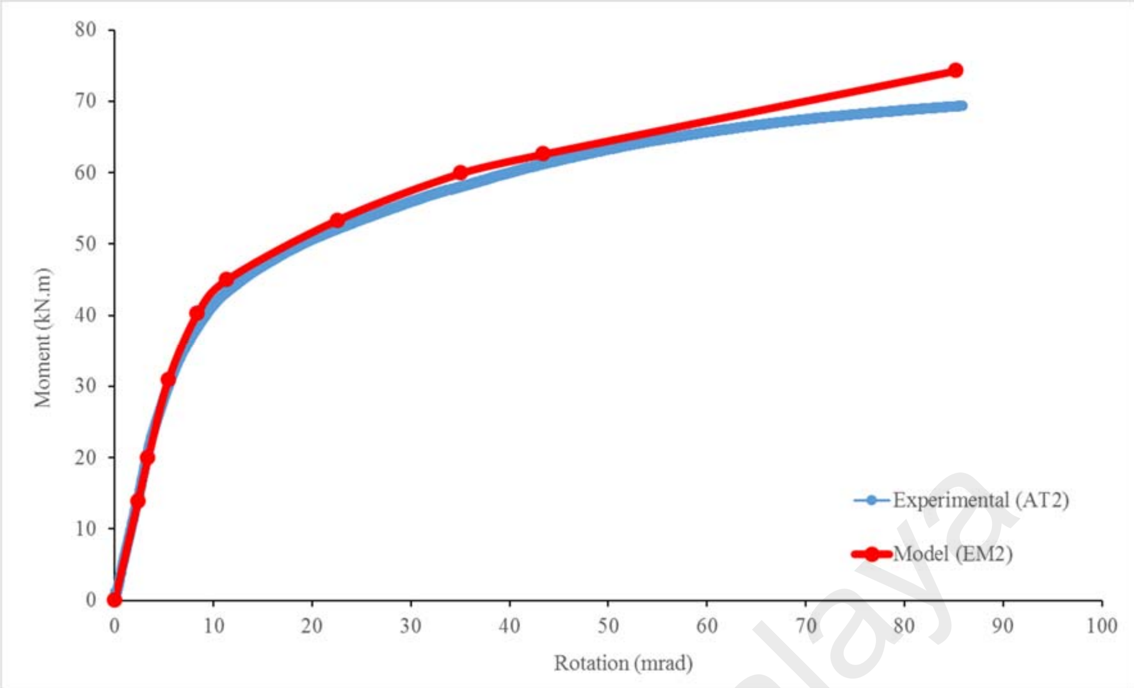

Figure 4.13 Comparison of AT2 and FE model EM2.

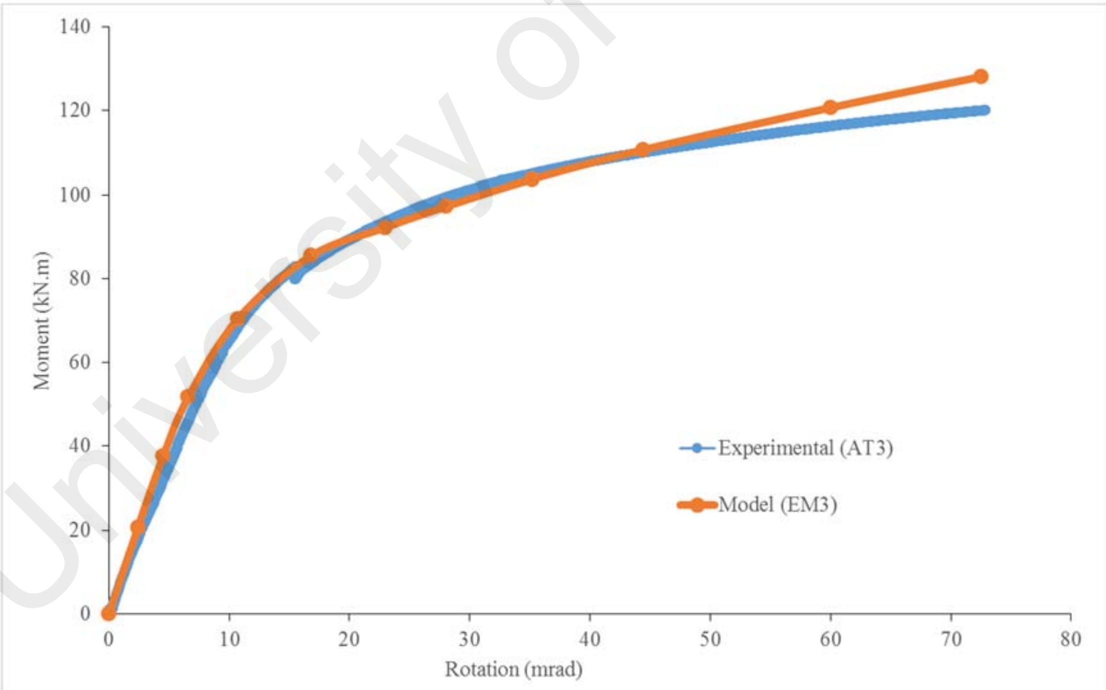

Figure 4.14 Comparison of AT3 and FE model EM3.

As a design check, for AT2 with assumption of a 3000 mm simply supported beam and considering self-weights of the column and connection components, the equivalent moment is approximate to be 2.8kN.m. The resulting central deflection is less than 1 mm while the maximum allowable deflection for a 3000 mm simply supported beam is L/200 is 15 mm. Under the self-weight of the system, deflections are still under permissible levels.

In the compression angle, the plastic strain is concentrated at an approximate distance of 10 mm from the heel of the angle for EM1 and EM2, shown in Figure 4.18(b). Comparing with the plastic zone of the tension angle, the whole cross-section is in the plastic range for EM1, showing the location of the bending of the compression zone angle. However, due to the stiffener in EM3, plastic strain is localized to the point where the stiffener edge contacts with the angle section. In addition, due to the compressive bending of the angle, the stiffener point on the beam leg shows plastic deformation from the compression on the stiffener as shown in Figure 4.18(d). Meanwhile, the end-plate deformation for all three models is concentrated in the area directly located behind the beam flanges, for both compression and tension zones.

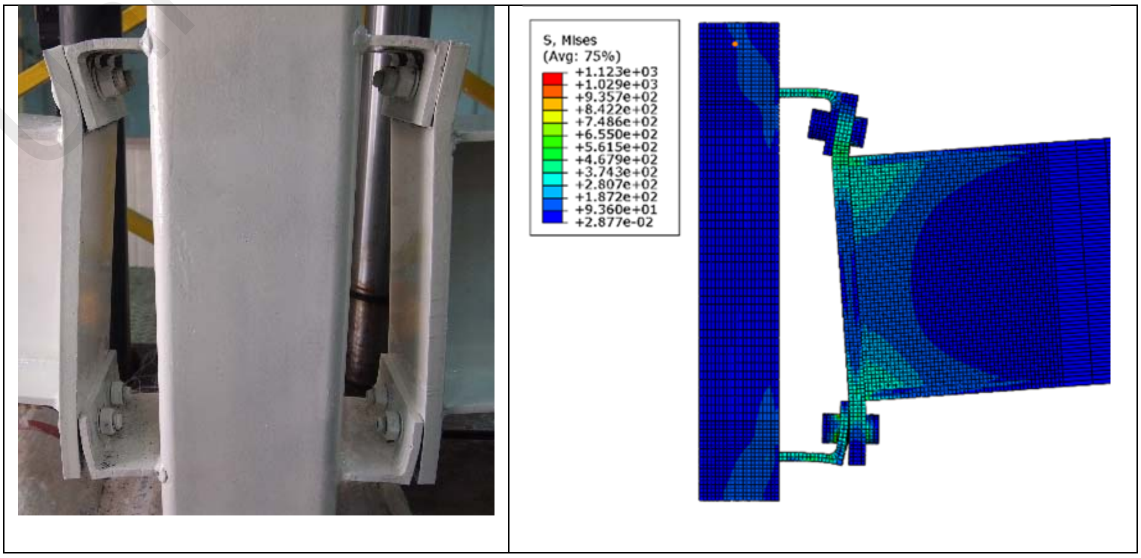

Figure 4.15 Deformation comparison between AT1 and EM1

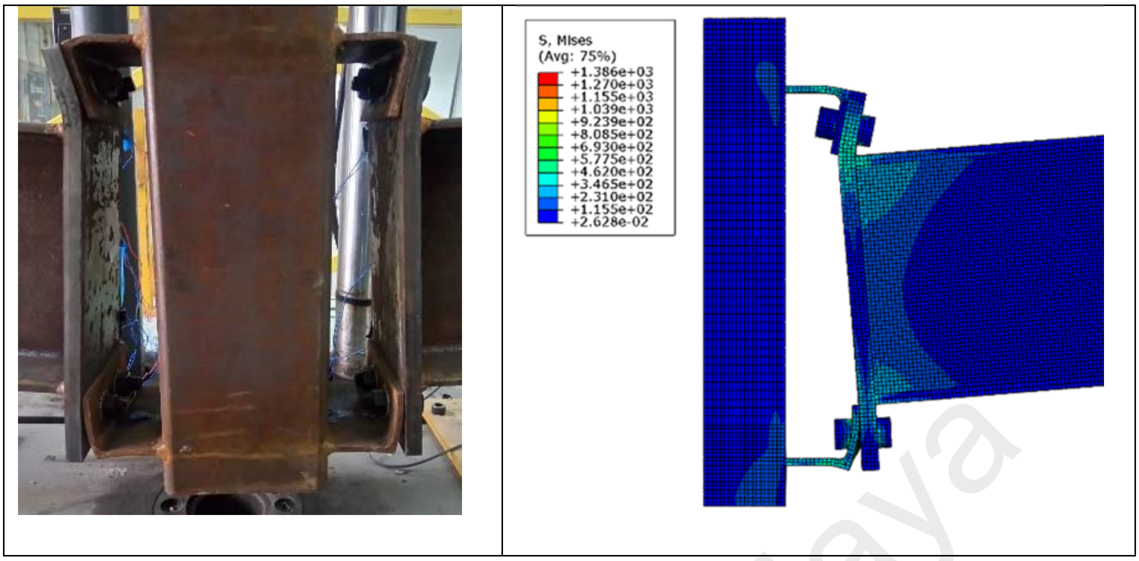

Figure 4.16 Deformation comparison between AT2 and EM2

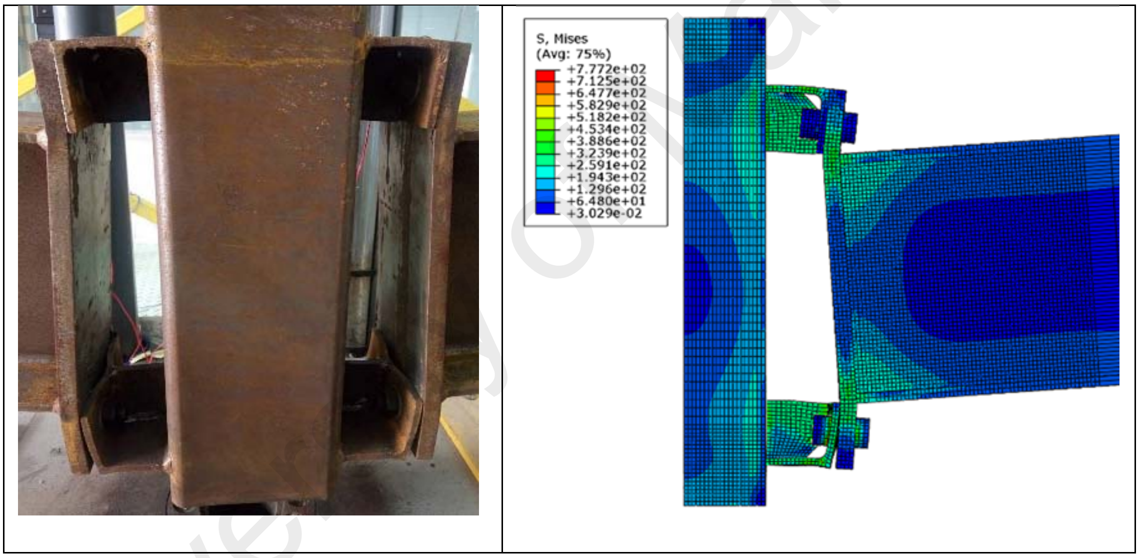

Figure 4.17 Deformation comparison between AT3 and EM3

In terms of the column component, minor or negligible plastic strains are noticeable on the column for EM1 and EM2 while the compression of the stiffener has resulted in a localized plastic deformation on the column face for EM3. Meanwhile, only tension bolts have plastic deformation on the shanks from the prying of the angles and end-plate, causing the bolts to have bending behavior.

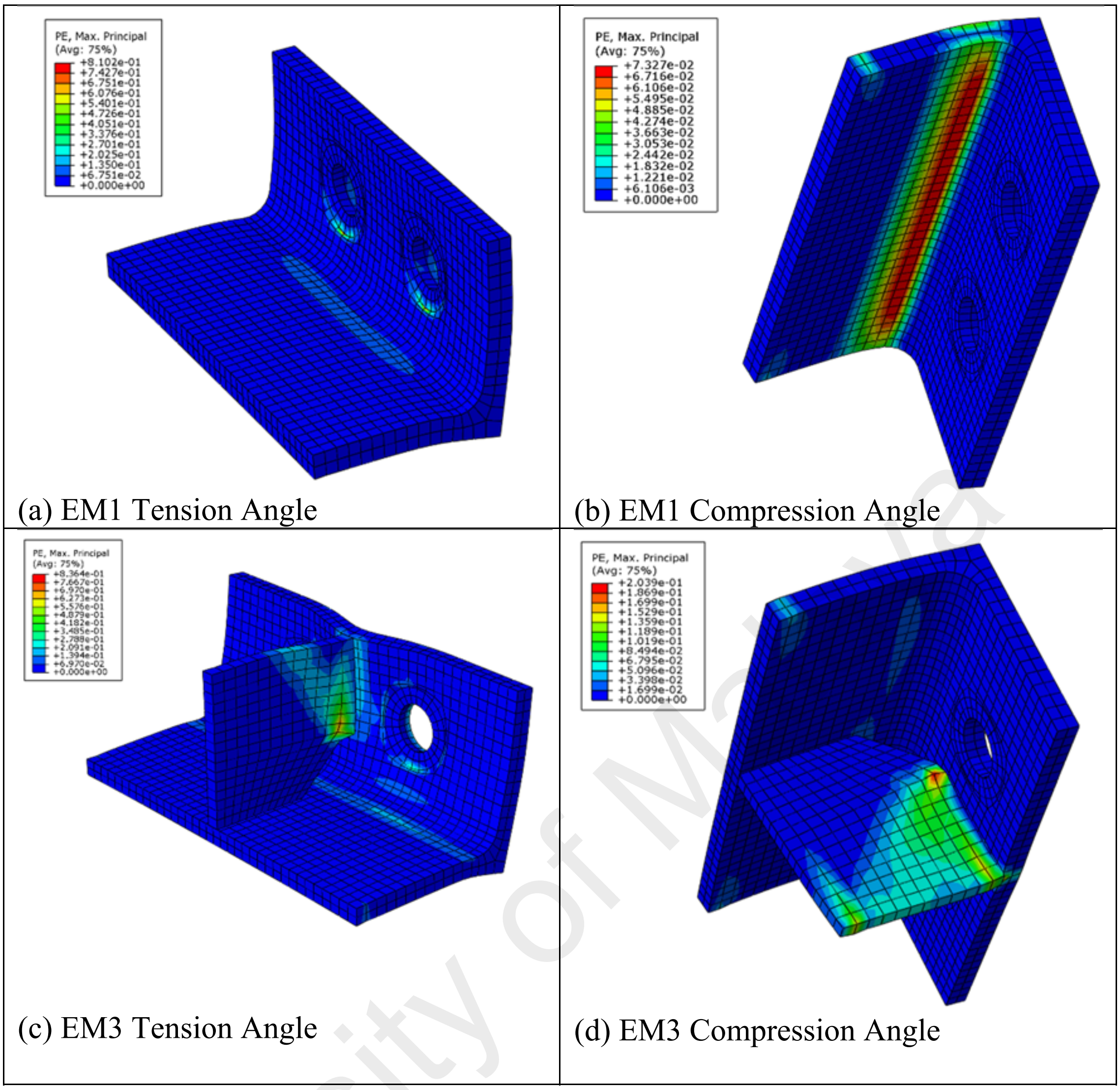

Figure 4.18 Plastic Strain of Angles in EM1 and EM3

Compared to EM1, EM2 has plastic deformation over a smaller area of the bolt shank and this is less severe, due to the lower deformation of the end-plate, as a result of the lower angle thickness. EM1 on the other hand, has higher end-plate deformation from the increased angle section stiffness due to the increased steel angle thickness. For EM1 and EM2, the bending is about the y-axis, which is similar to the bending axis of the beam, while the deformation of bolt for EM3 is due to the T-stub behavior modified by the addition of stiffeners in Figure 4.19. Plastic deformation of the EM3 tension bolts is not the result of flexural bending but from the prying force resulting from the cantilever angle sections.

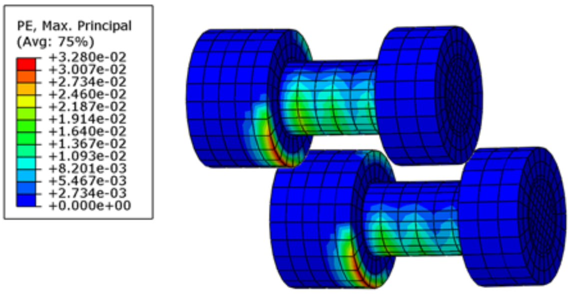

(a) EM1

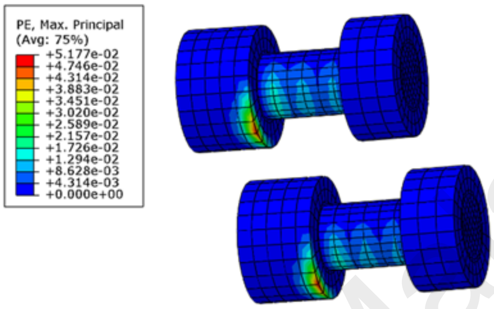

(b) EM2

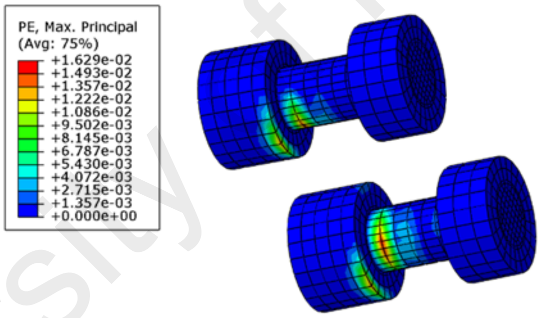

(c) EM3

Figure 4.19 Tension bolt plastic strain for EM1, EM2 and EM3

4.2.3 Parametric Studies for Ambient Temperature

To determine which component of the connection critically affects the behavior, several geometrical properties are studied using the validated FE Model from the previous section. The parameters include the effects of end plate thickness, angle thickness, angle leg length, gauge length and stiffener plate. The stiffener plates are added at the middle of the top and seat angle between the column and beam side leg. From these studies, further capacity optimization can be achieved for the connection with reinforcement at the proper locations. A summary of the parameters studied and the related model indications are as indicated in Table 4.5.

Table 4.5 Connection configuration summary

Mark	Angle	Plate	Note
EM1	L 80x80x10	20 mm	Reference Model Without Stiffener
EM3	L 80x80x8	20 mm	Reference Model with Stiffener, 6mm Thick
MT1	L 80x80x6	20 mm	Effect of Angle Thickness
MT1a	L 80x80x8	20 mm	Effect of Angle Thickness
MT1b	L 80x80x12	20 mm	Effect of Angle Thickness
MT2	L 80x80x10	10 mm	Effect of End-Plate Thickness
MT2a	L 80x80x10	12mm	Effect of End-Plate Thickness
MT2b	L 80x80x10	16mm	Effect of End-Plate Thickness
MT3	L 80x40x6**	20 mm	Reduced Angle Column Side Length, B to 40 mm
MT4	L 80x50x6**	20 mm	Reduced Angle Column Side Length, B to 50 mm
MT5	L 80x60x6**	20 mm	Reduced Angle Column Side Length, B to 60 mm
MT6	L 80x80x6	20 mm	Reduced Gauge Length, A to 40 mm from 45 mm
MT6a	L 80x80x6	20 mm	Increased Gauge Length A to 50 mm from 45 mm
MT7	L 120x80x10	20 mm	Increased Angle Leg Length – Beam Leg, C
MT8	L 80x80x8	20 mm	Increased Stiffener Thickness to 8mm
MT9	L 80x80x8	20 mm	Increased Stiffener Thickness to 10 mm
MT10	L 80x80x8	20 mm	Increased Stiffener Thickness to 12 mm
MT11	L 80x80x10	20 mm	Semi-flush Plate Effect
MT12	L 80x80x10	20 mm	Flush Plate Effect
MT13	L 80x80x10	20 mm	Boundary Condition Change

Note: **Members to be cut from L 80x80x6 as the section not common in market.

4.2.3.1 Effect of Angle Thickness

The comparison of the effect of angle thickness can be made with EM1 for 10 mm thick angles and with MT1, MT1a and MT1b for angle thicknesses of 6mm, 8mm and 12mm respectively. Decreasing the thickness from 10 mm to 6mm not only decreases the yield moment, but also decreases the connection stiffness as shown in Figure 4.20. By decreasing the angle thickness to 6mm, the plastic area for the angle is spread over the length of the angle resulting in a more severe deformation and subsequently achieving the strain hardening point of steel material that occurs starting from 2% strain. From the material behavior curve, the strain hardening results in an increased material stress resistance which explains the higher moment value than expected towards the 70mrad point when comparing between 6mm and 10 mm thick angle sections. Meanwhile, plastic area for the end-plate remains directly behind the beam flange, at the tension zone bending area. It is also observed that the angle thickness affects the slenderness of the angle, thus reducing the capacity of the angle section in bending for the elastic portion of the behavior.

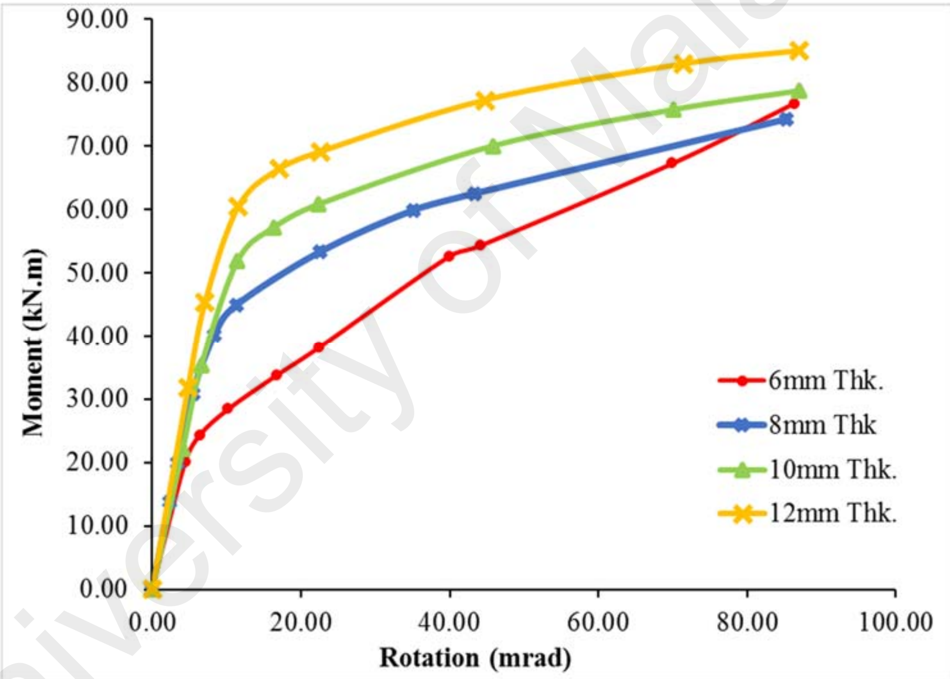

Figure 4.20 Effect of Angle Thickness on RTSA Behavior

4.2.3.2 Effect of End-Plate Thickness

Comparing EM1 and MT2, with a reduction of the plate thickness by 50% to 10 mm, the difference in deformation pattern of the connections is evident in the tension zone of the connection. With 20 mm thickness, the end plate was sufficiently stiff and therefore created a small gap between the tension angle and the end plate at the end deformation. Meanwhile for the other plate thicknesses of 10 mm, 12mm and 16mm, lower stiffness causes the plate to deform together with the tension angle and subsequently no gap is formed. In addition, the bending of the tension angle is not noticeable. Comparison of the deformations for model EM1 with 20 mm thick end-plate and MT2b with 16 mm thick end-plate is as shown in Figure 4.21.

In terms of connection behavior, with reference to Figure 4.22 reduction in stiffness results with the reduction in thickness for the end-plate. Consistent with the reduction, the overall capacity has also decreased where both end and yield moment is significantly decreased. Instead of having stress focused on certain areas as seen with the validated model, stress is distributed evenly along the whole length of the angle leg. This shows that instead of being in tension, both angles are resisting the applied loads by compression. Analysis result shows that the end-plate thickness plays a critical contribution to the connection behavior and capacity.

The tension loads developing in the connection has a higher value than the bending capacity of the angle and 16mm thickness plate, resulting in a flexural bending of the plate as seen in MT2. The similar tension force however is less than the flexural capacity of 20 mm plate, resulting in the difference in the deformation pattern seen between EM1 and MT2. MT2 deformation is applicable to all models with end-plate less than 20mm thick. In the compression zone of the connection however, compression force result in the deformation to be similar, resulting from the fact that the rotation point of bending is located at the compression flange. To avoid the end-plate from deforming at the tension zone, the recommended thickness should at least be double the thickness of the angle section in tension.

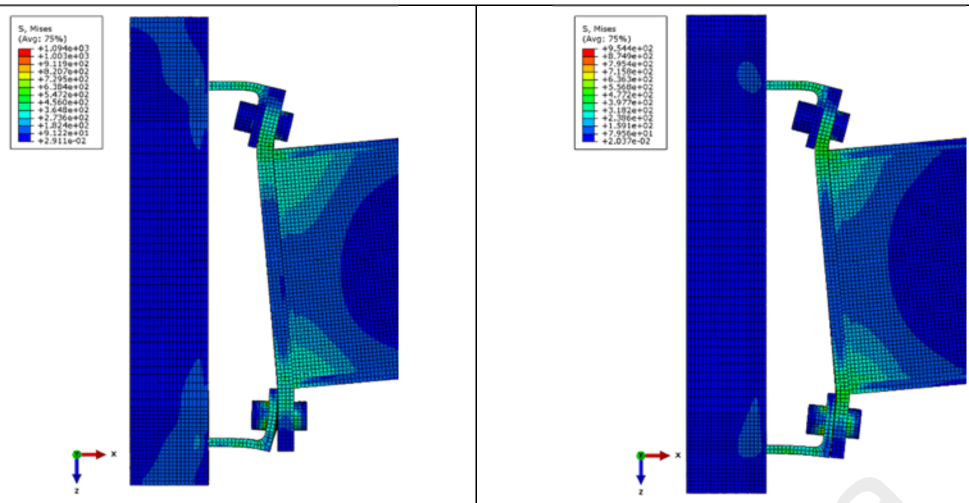

(a) EM1

(b) MT2

Figure 4.21 Effect of end-plate thickness on RTSA deformation pattern

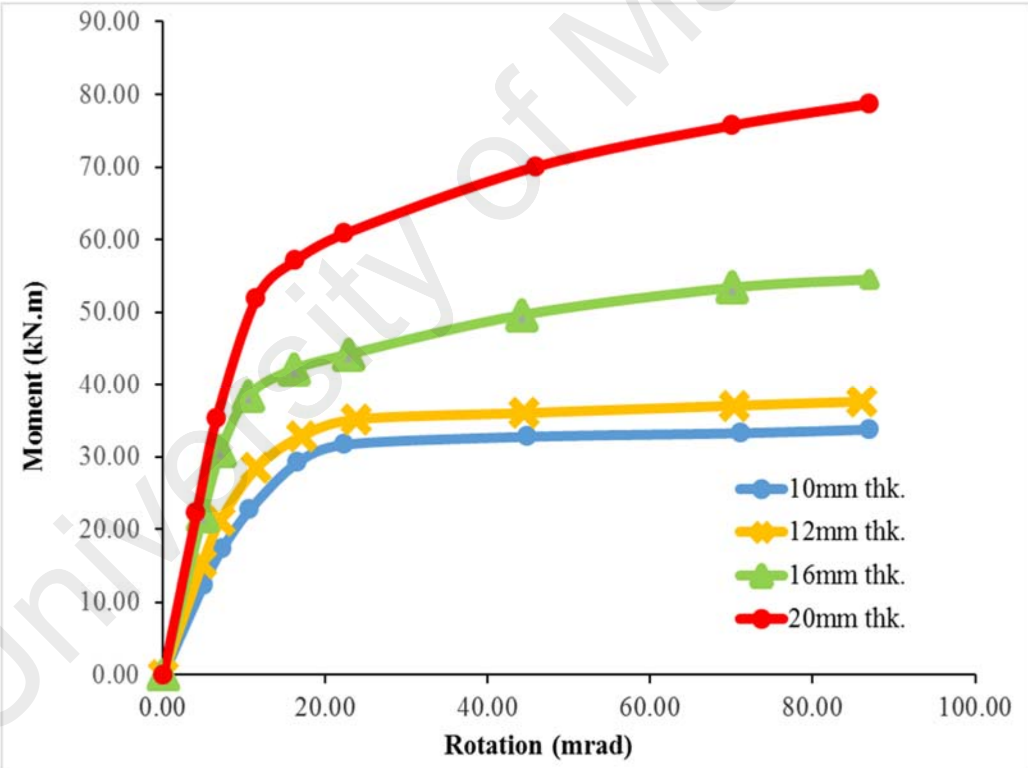

Figure 4.22 Effect of End-plate Thickness on RTSA Behavior

4.2.3.3 Effect of Angle Leg Length at Column Side

Angle leg length at the column side, as represented by dimension ‘B’ in Figure 3.2 of the previous section, results in a reduction in the eccentricity. The model involves in MT1, MT3, MT4 and MT5 where the leg length is 80 mm, 40 mm, 50 mm and 60 mm respectively. Instead of comparison with EM1, MT1 is used, as the control as current market available sizes for L80x40 is only available with 6mm thickness. The 40 mm decrease in leg length, seen in MT3 (40 mm) by comparison with MT1 (80 mm), affects the end moment as shown in Figure 4.23, slightly increasing the capacity.

The decrease in angle leg length at the column side reduced the end capacity as shown by the behavior of the 60 mm angle length, which was decreased by 20 mm from the experimental test of 80 mm length. Meanwhile, the effect on the end moment is observed to be decreasing in parallel to the angle leg length. At angle length of less than 80 mm (MT4 and MT5), the end-moment is observed to be almost fixed at approximately 68 kN.m. This is coupled with the increase in the yield moment.

Further reduction in angle (column side) leg length will result in an increase in moment capacity but lower end moment. It is expected that the decrease in angle length will reduce the slenderness of the angle, and thus increase the capacity at an earlier stage. End moment is contributed by the allowance of the angle to have double bending, near the welded area and near the heel of the angle, thus increasing the final moment value. Angle bending points are compared in Figure 4.24, as indicated for both 80 mm leg length and 40 mm leg length. This is further evident with the plastic area formed on the bottom angle, where the 80 mm leg length has a major plastic area at two points while the 40 mm has only one point.

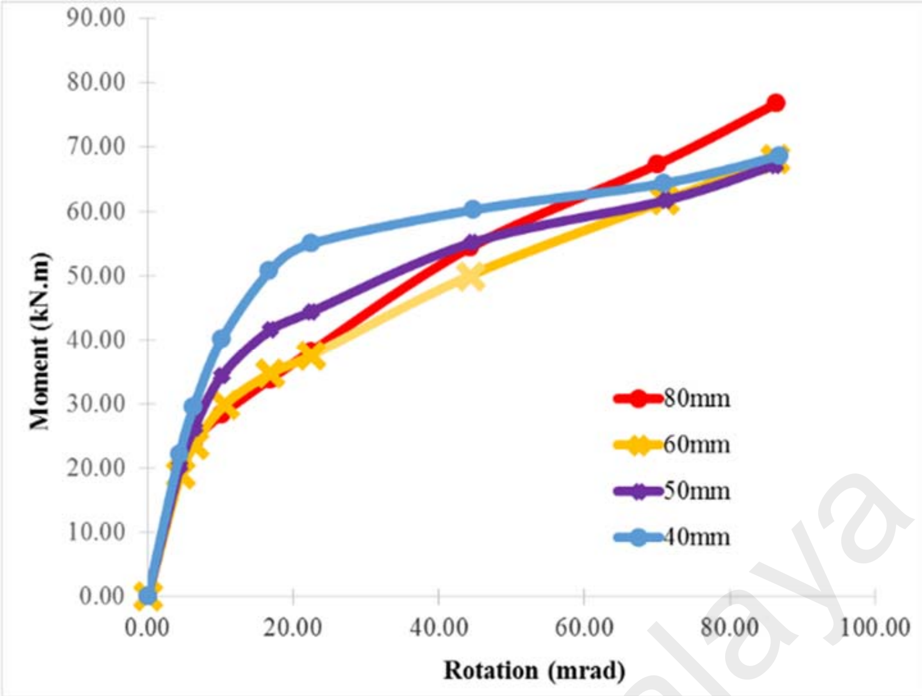

Figure 4.23 Effect of Angle Leg Length (B) on RTSA Behavior

It is concluded that the length of the angle, not only contributes to the slenderness of the angle, thus affecting the early capacity, but also the end-moment capacity by increasing the bending points. The lowered angle length serves as an offset to the lowered angle thickness. The results of the 40 mm angle length are comparable to the results of the control model, albeit with slightly lower stiffness.

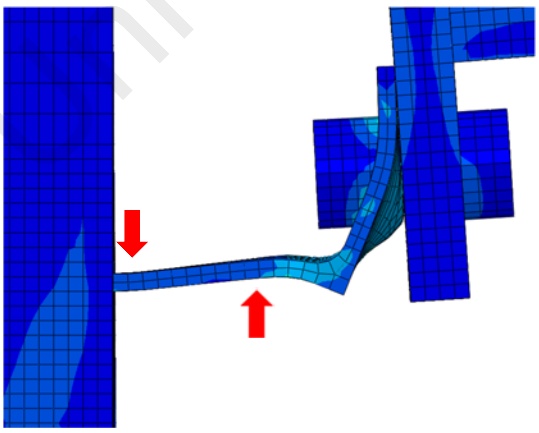

(a) 80 mm length (MT1)

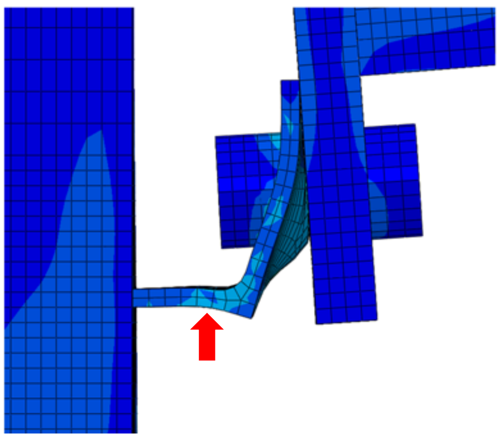

(b) 40 mm length (MT3)

Figure 4.24 Angle bending points due angle leg length

4.2.3.4 Effect of Angle Gauge Length

According to several researchers, the angle gauge length has significant effect on the behavior of connections involving angle components. Gauge length for an angle section is the distance from the bolt hole to the root of angle section. However, for simplicity, the study on the effect of the gauge length is substituted with modification of the distance from the flat surface of the angle section to the bolt hole, as indicated by dimension ‘A’ in Figure 3.2. Subsequently, a comparison is made between models by decreasing the gauge length from the 45mm value for MT1 to 40 mm and 50 mm, with MT6 and MT6a respectively (Figure 4.25). The comparison can only be made with the 6mm thick angles as reduction of gauge angles with 10 mm thick angles will have the bolts clash with the angle root due to the close proximity when the gauge value is reduced to 40 mm.

Although the stiffness did not vary, however, the decrease in 5mm has increased the yield moment slightly by 17% due to higher resistance of angle in bending in the tension zone. In addition, the post-yield moment is increased significantly by 13.9%. With an increase in the gauge length to 50 mm, as in the case for model MT6a, reduces stiffness by a significant margin of 17.3%, and yield moments value decreases by 21.5%. As shown in EC3:Part 1-8 (2005) , the increase in gauge length, results in parameter ‘m’ reducing the design resistance for T-stub deformation resulting in lower yield and stiffness.

The connection deformation also shows that the lower gauge length results in the compression angle buckling near the heel of the angle section. At the same displacement value, the plastic region only occurs on the tension angle near the heel, however, the plate is not in plastic state when the gauge length is reduced to 40 mm. With this result, it is possible to reduce the permanent deformation effect on the plate by reduction of the gauge length for the bolts. In general, the gauge length has an effect over the connection post-yield behavior.

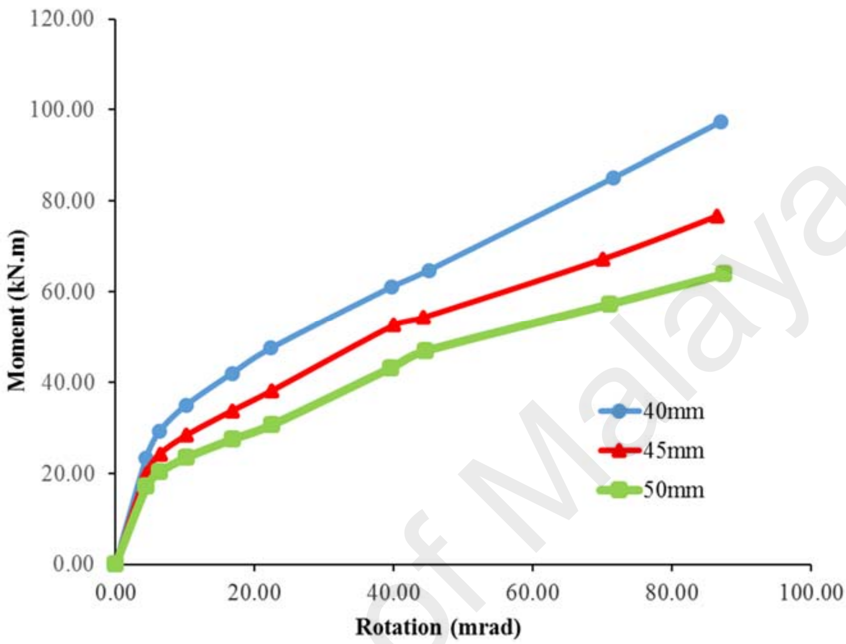

Figure 4.25 Effect of bolt gauge length (A) on RTSA Behavior

4.2.3.5 Effect of Angle Length on Beam Side

The moment rotation curve shown in Figure 4.26 is obtained by increasing the angle leg length on the beam side. It was expected that the additional leg length would cross on the beam flange and provide additional load resistance for the bending of the end-plate. However, as indicated in Figure 4.26, the additional 40 mm leg length is only affecting the end moment, slightly increasing the capacity with minimal differences in the stiffness or the yield moment values.

The result is due to the additional length is not secured onto the plate thus allowing a gap to form between the plate and angle. Without the bonding, the angle cantilever edge is allowed to deform freely. However, the additional length that extended beyond the beam flange still acts as a unit beyond the bolt row, at the length where the angle gauge length is measured, providing increased thickness. The additional length provides space for the stiffener to be fitted onto the angle and in comparison to the previous section on the effect of stiffener, the current stiffener configuration is not only reinforcing the angle section, but also behind the plate and beam flange, thus reinforcing the bending of the plate.

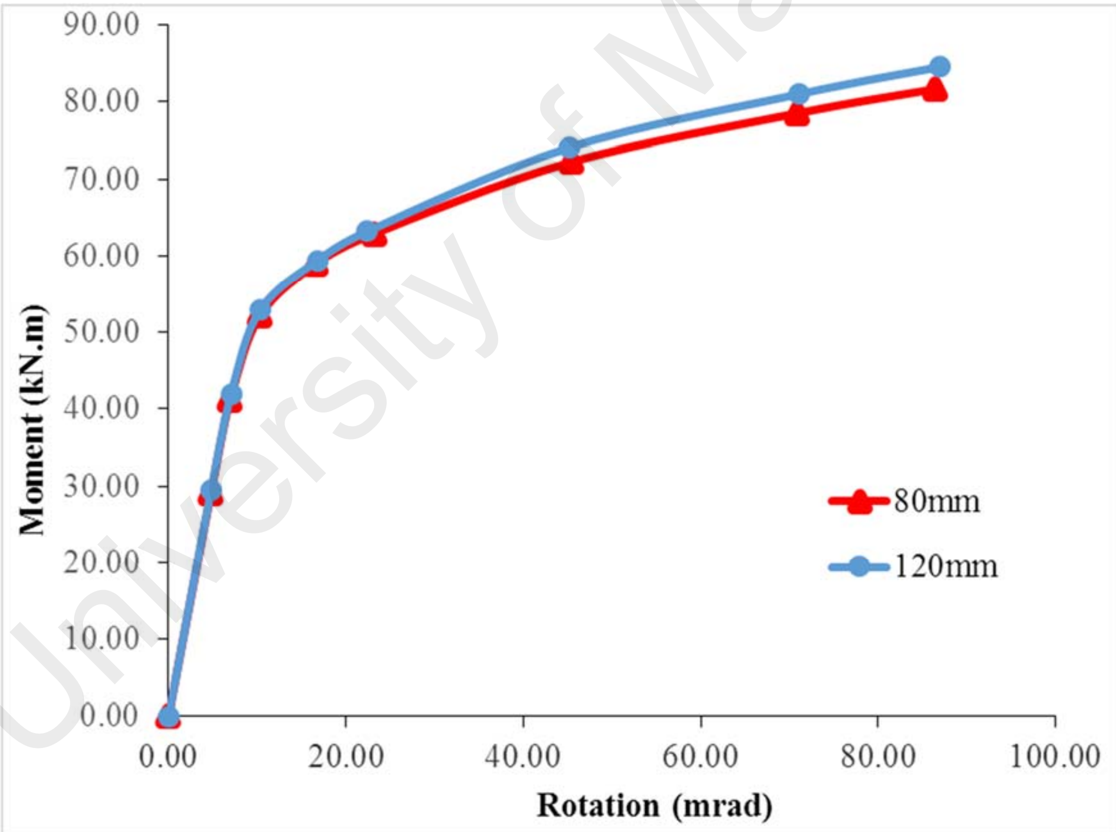

Figure 4.26 Effect of beam-side leg length (C) on RTSA Behavior

4.2.3.6 Effect of stiffener thickness

As seen from experimental test results, the connection configuration with attached stiffeners has deformation similar to the T-stub deformation commonly seen on connections to open section columns. The T-stub deformation is formed due to the addition of support at the center of angle face, thus reducing the cantilever behavior of the angle in bending.

In Eurocode 3: Part 1-8 (2005), T-stub deformation design involves two connecting elements, the vertical plate element and a horizontal element connected to the middle of the vertical element. Determination of T-stub capacity involving the parameter '*m*' which can be defined as the distance from the bolt to the root between the connecting elements. It is determined that the thickness of the horizontal element, which in the case of this study is the thickness of the stiffener, would reduce the value of *m* and thus increase the capacity value of T-stub modes 1 and 2.

The resulting connection behavior from the modifications of the stiffener thickness, from 6mm to 12mm, is as shown in Figure 4.27. Comparison with EM3, with 6mm thick stiffeners, shows minimal differences in the yield moment value. However, post-elastic moment at 72mrad is notably divergent. The increase of moment for stiffener thickness of 8mm begins from the 22mrad rotation point, while 10 mm and 12mm stiffener thickness diverge at 35mrad and 43mrad respectively. With the increasing stiffener thickness, connection stiffness and the connection yield capacity is not affected. However, the loads and forces required to deform the connection in the plastic zone is increased due to the reduction in the cantilever distance.

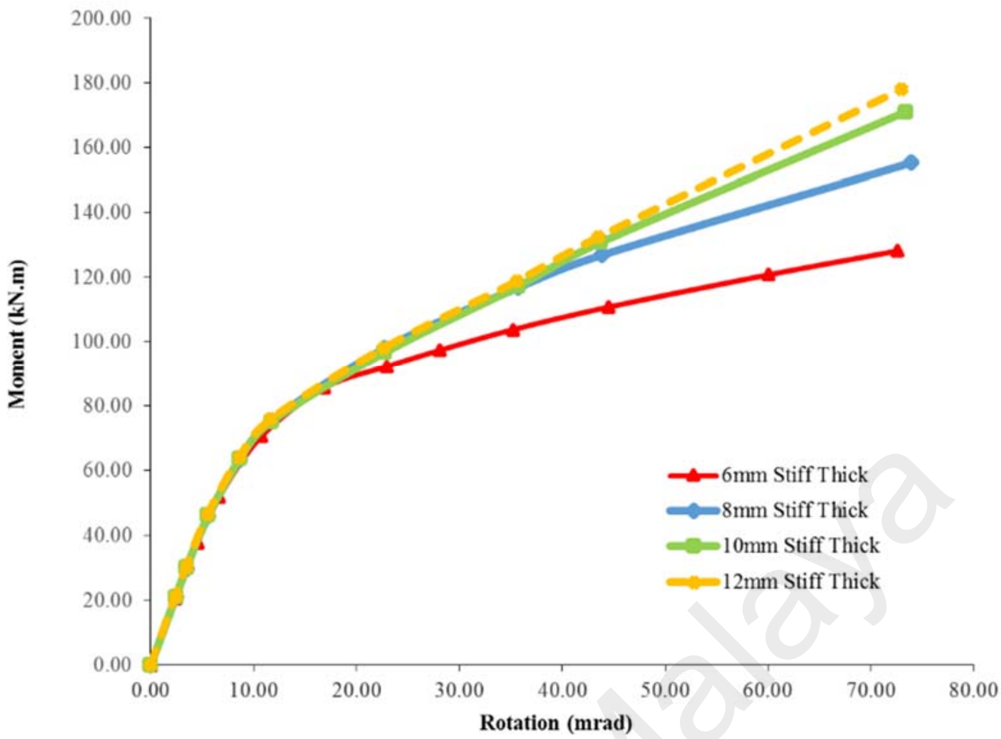

Figure 4.27 Effect of stiffener thickness on RTSA Behavior

4.2.3.7 Effect of Semi Flush Plate & Flush Plate

With reference to the models studied previously, one of the major deformations of the connection is the bending of end-plate in the compression zone, behind the compression beam flange. The simple method is to reinforce the plate area behind the beam compression flange and reduce the bending deformation. Considering that the compression angle of the standard configuration for reverse top-seat angle connection (Example:- EM1) has minimal contribution towards the behavior of the connection, the compression zone angle is modified to support the beam compression flange.

To study the effect of the reinforcement of the compression zone end-plate, the compression angle is shifted to the location where the edge of the angle section 'flat' area is level with the top of the beam compression flange surface. One configuration focuses on the effect from reinforcing the beam compression flange while the other configuration studies supporting the beam tension flange. Both configuration models are as shown in Figure 4.28. It should be noted that the lever arm has been reduced by 35mm for MT11 and by 70 mm for MT12.

Results from the analysis, as compared with EM1, shows that the modification of the compression angle compression has minimal effect on the stiffness of the connection in Figure 4.29 with MT11. However, the yield moment value is slightly reduced while the post-yield behavior results in a higher value compared to EM1, as expected with the reduction in lever arm distance which resulted in the reduced yield moment. Contribution of the reinforced compression zone end-plate is as indicated by the 23mrad rotational mark.

As indicated in Figure 4.29, the comparison of EM1 with MT12 shows a decrease in the yield moment value and an increase in post-yield behavior. However, the slight increase in connection stiffness is due to removal of the eccentricity with the flush plate configuration. Comparing the behavior of MT11 and MT12 in Figure 4.29 shows a 10% decrease in yield moment values but higher moment values at 87mrad, indicating higher ductility. Figure 4.30 shows the deformation of the connections at 110 mm column deflection. Instead of deforming under local bending for the compression angle, both MT11 and MT12 models show compressive plastic strain located at the heel of the angle section, where EM1 shows plastic strain at a distance of 10 mm from the angle heel. The compression angle is bowing under the forces exerted on the angle from the moment forces distribution.

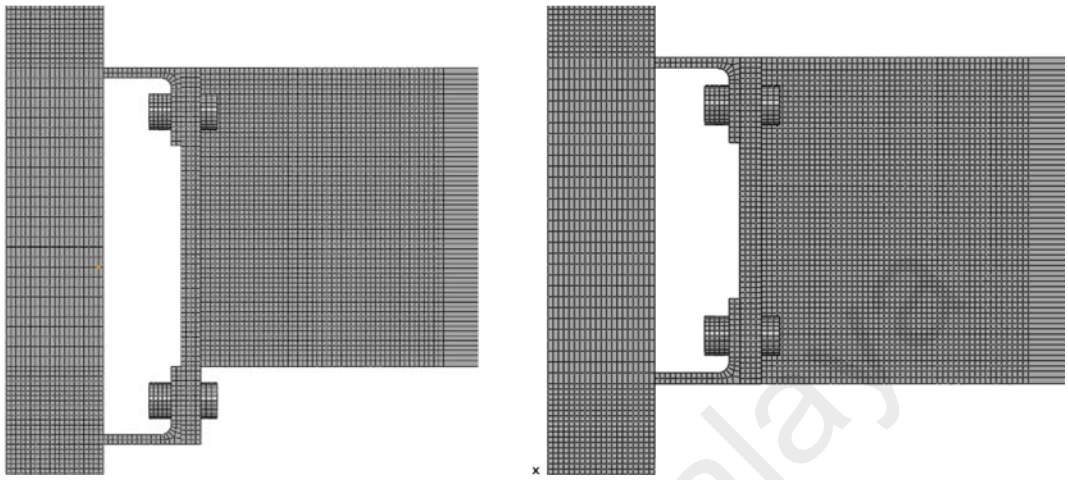

(a) Semi-Flush Plate (b) Flush Plate

Figure 4.28 Connection configurations for MT11 and MT12

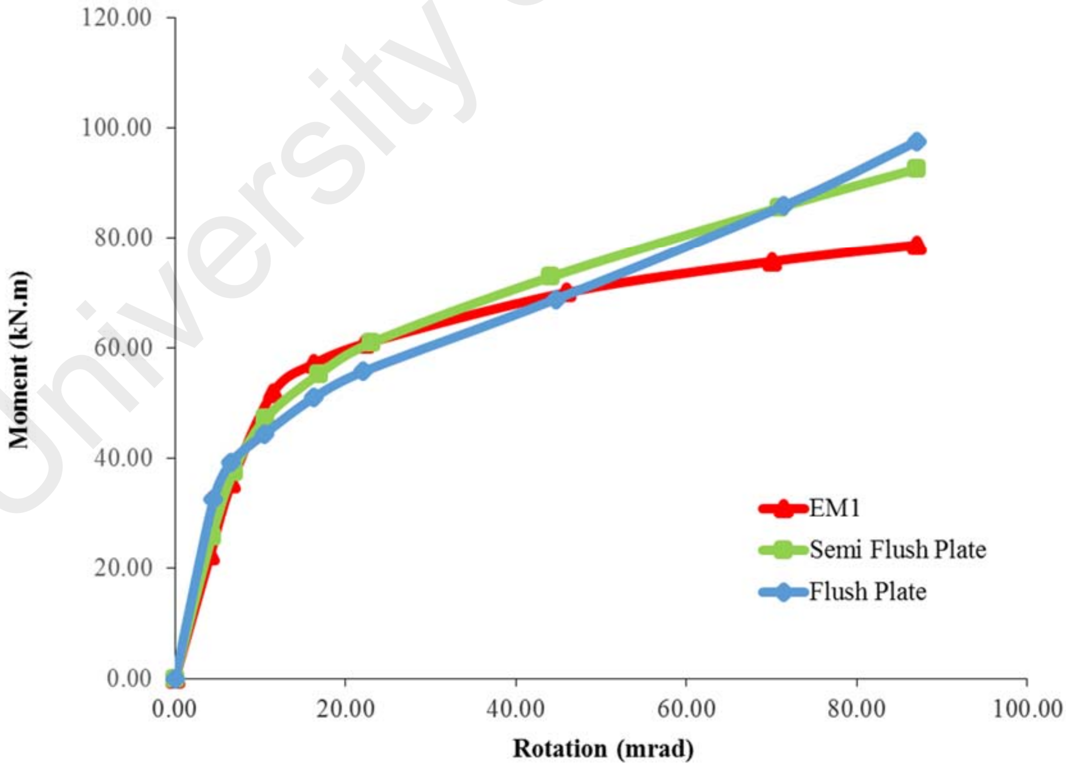

Figure 4.29 Behavior comparison of EM1 and RTSA Semi-Flush Model

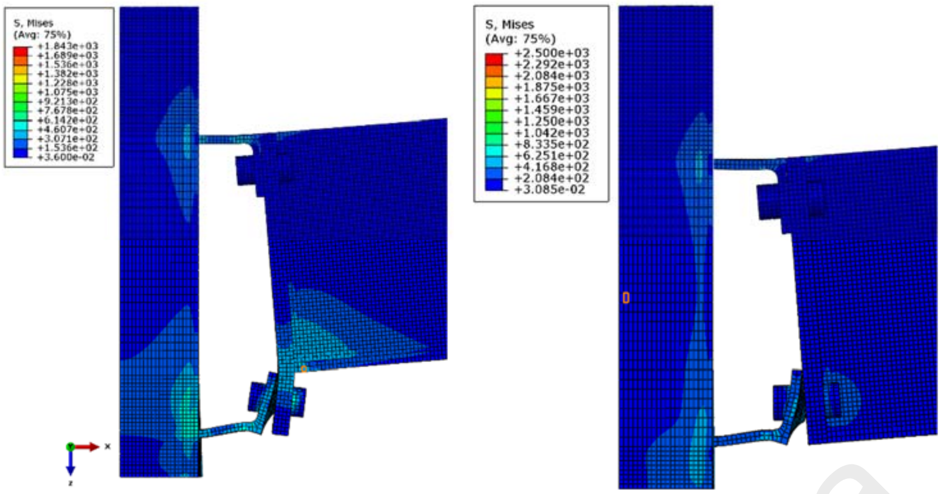

Figure 4.30 Deformation of Semi-flush and flush model

4.2.3.8 Effect of Boundary Conditions

Experimental tests for connection studies are commonly conducted under pin-and-roller support or cantilever-based loading, where one side of the beam is left free to deflect and deform. On the other hand, the actual condition of the connection at the construction site would be connected on both sides of the beam to columns. At both column ends, the connection prevents the beam from displacing horizontally by, reducing the degrees of freedom. With the reduced degrees of freedom at the beam end, the effect of the rotation of the beam is reduced and subsequently deformation of the connection is expected to increase.

Model EM1 is used as the basis of the study at the beam end-plate end defined as 'pinned', preventing displacement in all x-y-z directions, as shown in Figure 4.31. Displacement loads, pretension and material properties remains similar to those previously defined. In comparison to model EM1, the support distance is from the end of plate to the column face. The resulting behavior of the connection in terms of moment-rotation is as compared in Figure 4.32.

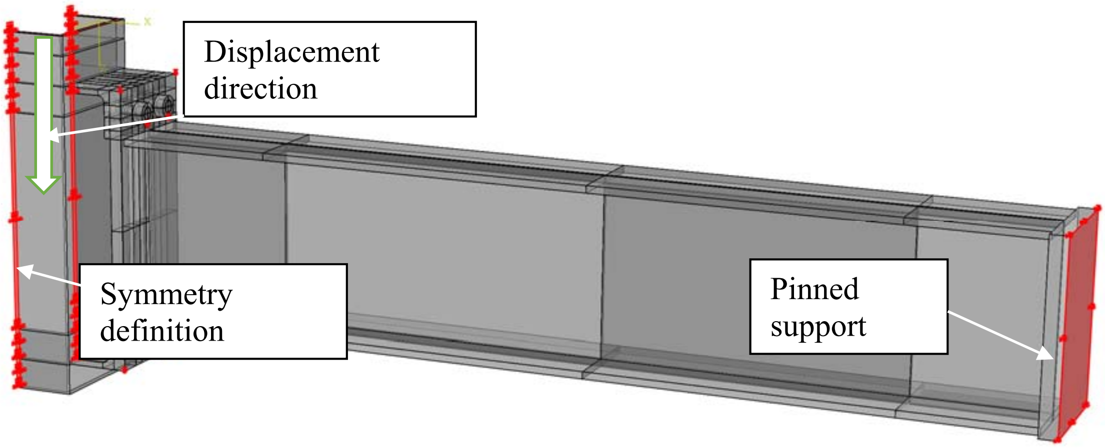

Figure 4.31 Boundary conditions for the study on boundary effect

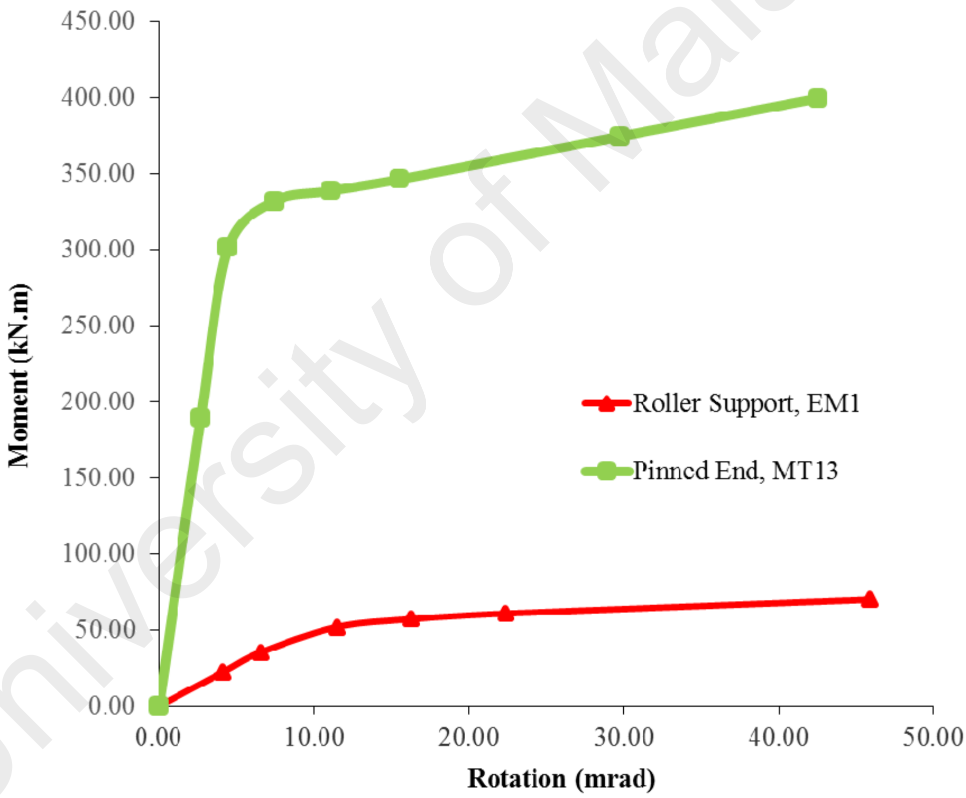

Figure 4.32 Effect of boundary condition on RTSA Behavior

Due to the decreased degrees of freedom, the stiffness and yield moment value of the connection has increased by 1200% and 525% respectively. In terms of deformation, there is little or minor deformation of the end-plate in AT13. The tension zone angle section is, at lower rotation levels, governed by the angle in bending followed by the tension capacity of the angle section at higher rotation levels.

Meanwhile, the compression zone angle is under flexure at two hinge points, being near the angle heel and near the welding area to the column as shown in Figure 4.33. In addition, from the tension forces applied to the connection due to the distribution of moment loads, the column face is being pulled out, which forms a curved shape, similar to flexural resistance result of the column face. The tension bolts are expected to fail under shear considering the plastic strain on the bolts at a diagonal slope on the shank, from the bolt nut to the bolt head as shown in Figure 4.34.

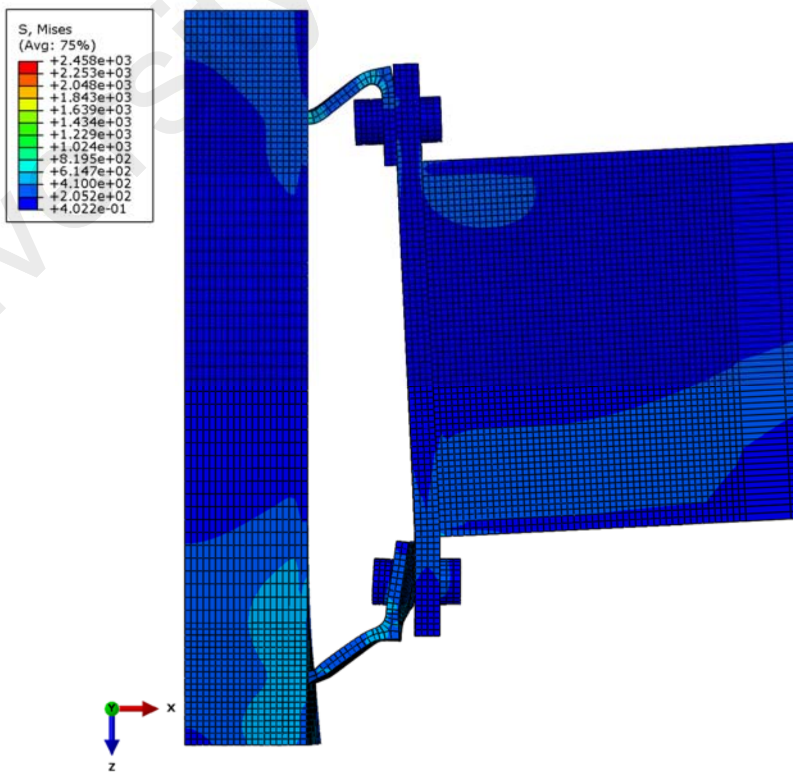

Figure 4.33 RTSA deformation due to fixed boundary condition

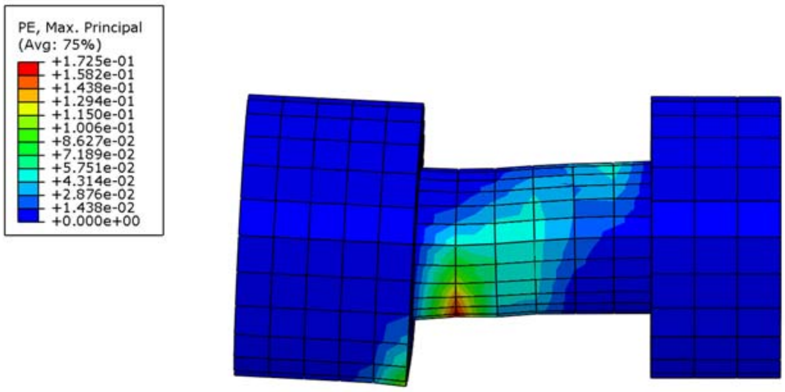

Figure 4.34 Tension bolt plastic strain under fixed boundary condition

In comparison to the simple supports utilized in the ambient temperature experimental tests, shear forces is the controlling force in the connection, as evident by the double hinge points described earlier. It is also observed that the end-plate compression zone did not have the flexural bending from the compression force. Under the full pinned support condition, the flexural capacity of the angle section is the critical parameter and thus, angle thickness is predicted to provide the contribution to the connection capacity, while it is expected that a thinner end-plate may provide similar resistances. Under shear major loads, which is the controlling load in general, cases, the possible solution is the addition of stiffeners as shown in an earlier section of this study.

4.2.3.9 Classification of Joint

Considering that the experimental results has a cantilever boundary type, FEM analysis results with the pinned support type is used as the gauge for the classification of the proposed joint. As shown from literature review, classification of joints are either with strength or stiffness comparison. According to clause 5.2.2.5 in Eurocode 3(2005): 1-8, to be considered as a rigid joint, the initial stiffness value must be at least equivalent to the second area of moment of the beam section to the supported length, as shown in equation 4.3. and equation 4.4 for the nominally pinned criteria. In the equation, E denotes the elastic modulus, I_b is the second moment of area for the beam, and L_b is the column-to-column distance.

$$S_{j,ini} \geq \frac{k_b E I_b}{L_b} \quad \text{(Eqn. 4.3)}$$

$$S_{j,ini} \leq \frac{0.5 E I_b}{L_b} \quad \text{(Eqn. 4.4)}$$

Assuming that L_b is equivalent to 1500mm, and I_b is 8503 cm^4 then $S_{j,ini}$ results in a value of 59881343284 N.mm/rad which is less than the resulting value of equation 4.3 but more than equation 4.4. Fulfilling conditions set out in clause 5.2.2.5 in EC3; the proposed connection is then classified as a semi-rigid connection. It is observed however, that in actual conditions, both side of the beam are to have similar joints for the length to be considered as the boundary conditions affects the initial stiffness.

4.2.3.10 Summary of Parametric Studies

The behavior of the connections in the parametric studies is summarized in Table 4.6 and general behavior of the parametric study is shown in Figure 4.35. The effect of the end plate thickness is clearly a major contributor to the load resistance of the connection. The performance of MT2 is the lowest among all other connections, where an almost 50% decrease in stiffness and yield moment from a 50% decrease in plate thickness. The decrease in plate thickness has a linear effect on the connection behavior.

With the reduced eccentricity, reducing the leg length on the column side increases the yield moment as displayed by models MT3 and MT1. In addition to the eccentricity, the slenderness ratio of the angle section also contributes to the behavior. However, a section with a higher slenderness ratio increases the ductility of the connection from the development of double hinges joints as shown for MT1. It should be noticed that the slenderness ratio at which the double hinges occur has not been fully investigated. Meanwhile the increase in beam-side angle length has minor contribution to increasing the connection plastic moments. However, possibility of reducing the end-plate bending deformation due to compression is shown with the semi-flush plate configuration displayed by model MT11.

Angle thickness contribution to the connection behavior is shown by the reduction in both yield moment and stiffness from the reduction in angle thickness. The angle component behaves in bending in both the compression and tension zones, and the increased flexural resistance due to the thickness is a major factor. However, the angle section used can be divided into slender and short sections. Slender sections show reduced stiffness and yield but an increased moment and ductility in high-deformation conditions due to the material properties with strain-hardening post 2% strain.

At higher connection deformation, the lower gauge length may provide additional load resistance through the tension capacity of the angle section, as seen in the behavior of MT6 that is higher than MT1. Hence, the behavior results emphasizes further that the gauge length has an effect, not only on the top-seat angle connection alone, but that it can be applied to any connection that involves bolted angle sections.

The major effect from the addition of a stiffener can be clearly seen with the increase in stiffness by 34% and yield moment by approximately 90% in a comparison between EM1 and EM3. This shows that the reverse top-seat angle connection can be structurally improved further with additional plates or beam central connection, as there are still areas where further components can be attached.

Table 4.6 Parametric Study Summary

Mark	Initial Stiffness (kN.m/rad)	Moment at yield (kN.m)	Moment at 40 mrad (kN.m) rotation	Comparison Remark
AT1	5650	49.1	68.5	Current study experimental
AT2	5464	54.5	60.1	Current study experimental
AT3	6294	102.5	107.83	Current study experimental
EM1	5935	52.2	70.4	Validation Model – Reference
MT1	4509	24.3	52.6	6mm thick angle
MT1a	5333	53.0	57.0	8mm thick angle
MT1b	6619	69.0	74.5	12mm thick angle
MT2	2509	29.3	32.6	10 mm thick end-plate
MT2a	3179	35.0	35.0	12mm thick end-plate
MT2b	4528	43.0	46.0	16mm thick end-plate
MT3	5047	50.7	59.8	Reduced Angle Leg, B to 40 mm
MT4	4581	41.5	53.5	Reduced Angle Leg, B to 50 mm
MT5	4240	29.9	47.9	Reduced Angle Leg , B to 60 mm
MT6	5273	29.3	61.1	Reduced Gauge Length, A to 40 mm
MT6a	3843	20.5	43.2	Increased Gauge Length A to 50 mm

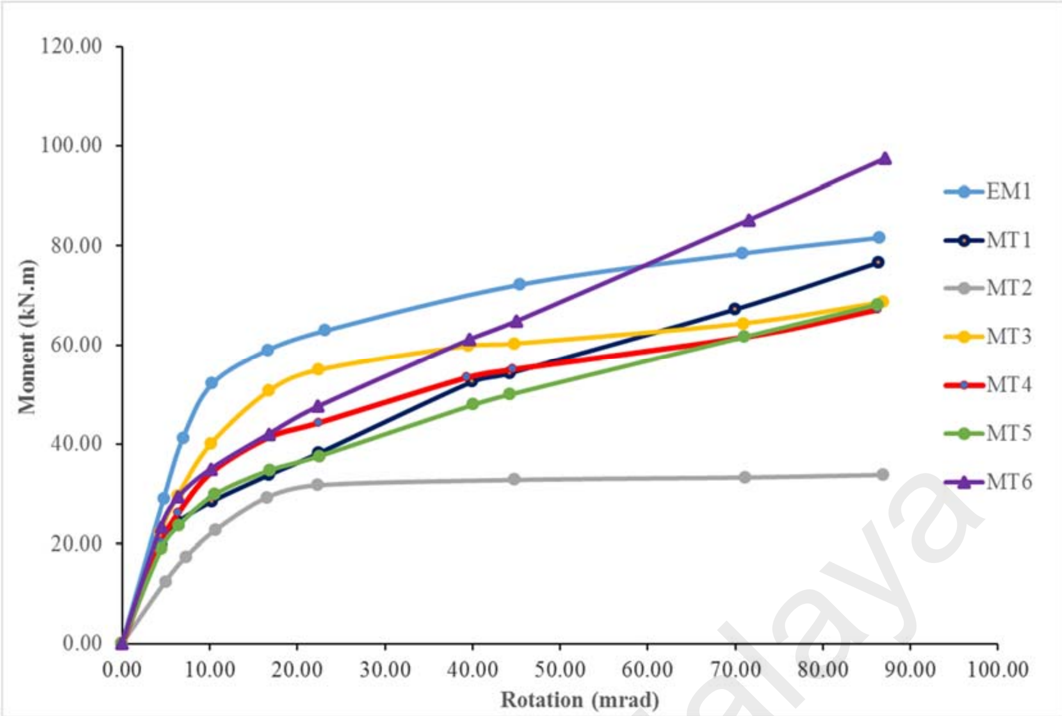

Figure 4.35 General behavior comparison of parametric study models

4.2.4 Load Transfer Mechanism

In the reverse angle connection, the angle sections and the end-plate component are considered as the basis of the contribution to the connection behavior under loads. The connection is divided into the tension zone and the compression zone. Behavior in the tension zone is governed by the angle section while the end-plate is critical in the compression zone. As loads are applied onto the beam, the moment is transferred as flexural, with the hinge located parallel to the beam flange for the compression zone. In the tension zone, the column angle leg behaves similar to bolted plates under shear force, with the fixed point at the root of the angle section. For angles with high slenderness ratio, plastic hinges develop at the points of high connection rotation, which increases the load capacity of the connection, higher than angle sections with low slenderness ratio. On the plate leg of the same angle section, the bending resistance deforms the angle under tension force.

However, plates with lower thickness deform together with the angle as a unit. In general, the tension zone system works similar to where the end-plate is fixed and the column side leg resist both bending and shear. Meanwhile for the compressive zone, as the current configuration does not provide supports directly at the beam flange, causing the end-plate to resist the compressive forces and deform by bending. As the angle is bolted to the end-plate, the prying deformation occurs as a result of the bending force of the plate. Subsequently, the compression angle has flexural deformation with the hinge on the column leg. Behavior of the connection is similar at the compression zone with the stiffener plate attached, as the column face functions as a supporting plate. An increase in column thickness is expected to provide higher resistance and thus increased load capacity.

4.2.5 Comparison with Existing Tubular Column Connection

To gauge the performance of the reverse top seat angle composed with existing connection, a comparative study is made with the experimental test results of reverse channel angle connection (RCA) investigated by Malaga & Elghazouli (Málaga-Chuquitaype & Elghazouli, 2010), labeled as CT1 and CT2. In addition, the reverse channel end-plate connection (RCE) by Wang & Xue (Wang & Xue, 2013), labeled as WX1, WX2 and WX4, is also compared in terms of stiffness, strength and ductility. The component differences for the comparison are as listed in Table 4.7, while the general connection configuration differences are shown in Figure 4.36, and dimensions are as highlighted by Table 4.8.

4.2.5.1 Comparison with Reverse Channel with Top-Seat Angle Connections

The study by Málaga-Chuquitaype and Elghazouli (2010) involves both cyclic and monotonic loading, only specimens using UB305x165x40 kg/m under monotonic loading is compared, as the beam size in the current study is UB305x165x46 kg/m. The increase in beam depth affects the bending moment value through the increase in lever arm. Thus, the connection behavior is no longer affected by the connection components but due to the beam depth, and therefore similar beam depths must be used for comparison. As reference, CT1 and CT2 refers to the specimen T6.3-A15-d40-M and W10-A8-d40-M respectively.

As shown in Figure 4.37, the reverse top-seat angle connection has shown a comparable performance with the reverse channel connection results shown by Malaga and Elghazouli (2010). The test specimen and validated model has higher stiffness and yield moment than the reverse channel connection, CT2. It should be noted that CT2 has web angle component. The central component has been determined to provide additional resistance to the capacity of the connection.

The behavior of the reverse channel connection and combined with a central connection, CT2 is comparable to MT1 as indicated in Figure 4.39, where the angle thickness is reduced by 40% to 6mm thickness. Both stiffness and yield moment are approximately 50% higher in EM1 when compared to CT1. Meanwhile, the addition of the central connection component has reduced the difference to 14.6% and 44% in terms of stiffness and yield moment respectively, with EM1 having the higher values. When the 40 mm gauge length is taken into consideration as shown using the comparison with model MT6, connection behavior of RTSA still has higher yield and stiffness values when compared to RCA. It should be noticed that the angle used is L80x80x6 for MT6. With comparison to the basic reverse top-seat angle connection, it is expected that the difference will be higher with the addition of beam central component for the RTSA connection, similar with the central web angle applied in specimen CT2. In addition, bolt in the tension zone of RCA are susceptible to prying due to the deformation of the angle section; therefore, the reduction of bolt to Grade 8.8 to follow EM1 may result in a CT2 connection with lower load resistance.

4.2.5.2 Comparison with Reverse Channel with End-Plate Connections

In terms of end-plate connection type, the investigation by Wang and Xue (2013) is used as the reference point, particularly specimens ST1, ST3 and ST4 due to the fact that the beam used is a UB406x178x74 and that a beam with higher depth causes the moment resistance to increase from the increase in lever arm value. Model M1 is modified from EM1 by changing the beam size from UB305 to the UB406 used in the study by Wang and Xue (2013). The resulting behavior is as shown in in Figure 4.38. On further inspection, the material yield values are different and therefore, modified according to model M2. Model M3 determines the improvement effect from the addition of 10 mm stiffener plates on model M2.

Specimens ST1, ST3 and ST4 have higher yield moments than M1 and M2, while model M3 has the comparatively highest yield moment values. In terms of initial stiffness, the compared RCE connection has among the highest stiffness, with up to 200% higher stiffness compared to the reverse top-seat angle connections AT1. Using similar beams in the model to provide similar lever arm, the difference is reduced to 50% higher than RTSA, between WX3 and M1. With the stiffener, it is calculated that the difference in stiffness is only higher by 32.9%. Meanwhile in terms of, yield moment values, only WX4 has higher values with 13.7% comparing to M1. M3 however shows higher yield moment values of at least 57.6%.

However, the connection stiffness does not translate to connection ductility, in which the general failure for reverse channel connections occurs between 40mrad to 60mrad rotation. Reverse top-seat angle connections have not shown any signs of ultimate failure at the 60mrad point where tearing failures have occurred with several of the RCE specimens, showing higher connection ductility.

In the comparison to RTSA connections, RCE beam flange is directly supported by two rows of bolts to the reverse channel. The two bolt row system increases the length of the reverse channel affected and modifies the hinge location when compared to the same connection with only the external bolt row. Having two bolt rows prevented the end-plate from deforming and increasing the stiffness, therefore reducing the effect from end-plate other than the failure mode. This has also increased the load resistance by reducing the support-to-support distance, which in RTSA angles act as a cantilever member under tension. Until connection failure, the end-plate and reverse channel deforms as a unit. Rotation hinge for the RCE connection is located at the beam flange for the compression zone and therefore the lever arm compared to RTSA is of close relation.

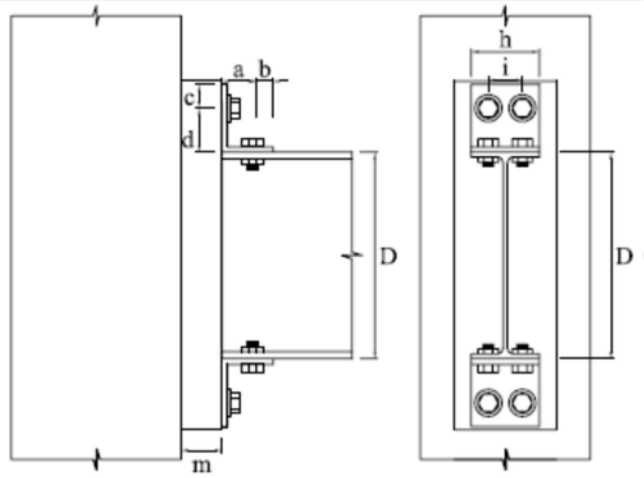

(a) Malaga and Elghazouli, CT series (Málaga-Chuquitaype & Elghazouli, 2010)

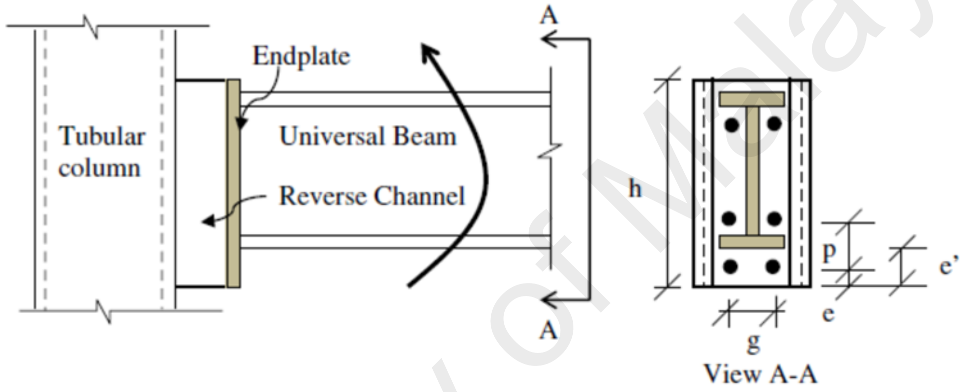

(Right) Wang and Xue, Model WX series.(Wang & Xue, 2013).

Figure 4.36. Geometrical Properties of experimental tests for comparison.

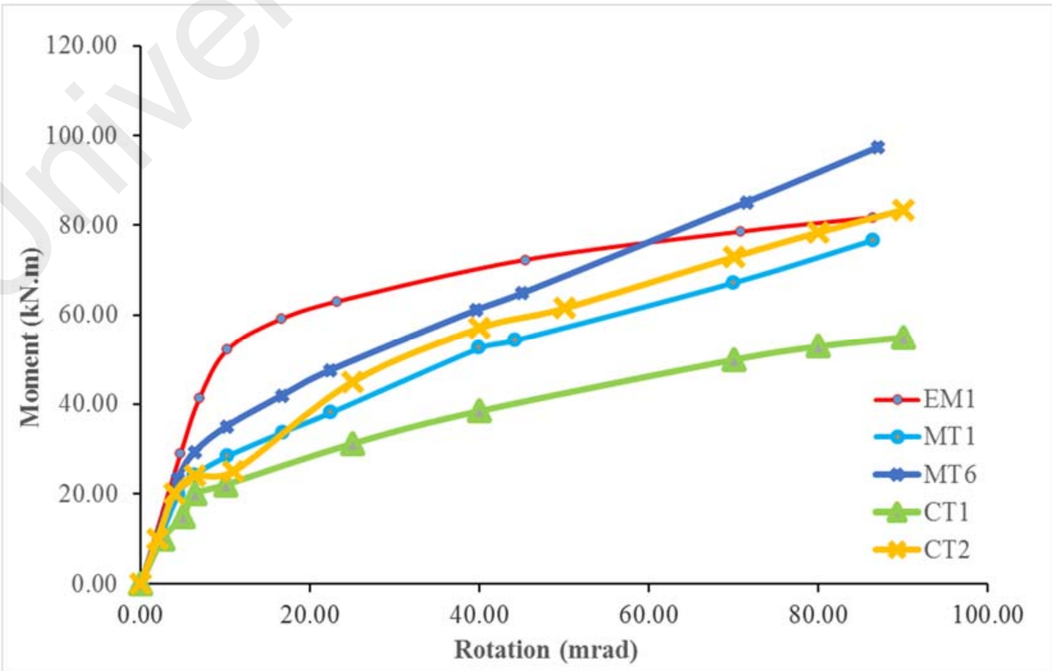

Figure 4.37 Behavior comparison with existing experimental results

Table 4.7 Comparison connection configuration summary

Mark	Column	Beam	Bolts	Component 1	Component 2
AT1 EM1 MT1 MT6	SHS 200x200x10	UB 305x165x46	4M20 Grade 8.8 External	L 80x80x10 L 80x80x6	20 mm End-Plate
M1		UB 406x178x74		L 80x80x10	
M2 M3		UB 406x178x74		L 80x80x10 MAT > M3 w/ Stiffener	
CT1 CT2		UB 305x165x40	8M16 Grade 10.9	CH 150x75x6.3 CH 150x75x10	L 150x80x15 L 100x75x8MD
WX1 WX3 WX4	RHS 400x200x10	UB 406x178x74	6M20 Grade 8.8 Ex-In	CH 180x90x26 CH 180x75x20 CH 150x90x24	10 mm End-Plate

Table 4.8 Connection dimensions for comparison

Mark \ Items	a	b	c	d	m	h	i
CT1	50	50	35	40	75	100	45
CT2	50	50	35	40	75	100	45
Mark \ Items	**e**	**e'**	**g**	**h**	**p**		
WX1	40	70	90	500	90		
WX3	40	70	90	500	90		
WX4	40	70	70	500	90		

Note:- (Malaga and Elghazouli, 2009)	(Wang & Xue, 2013)
a – distance from channel to horizontal bolt	e – edge distance
b – edge distance	e' – edge distance to beam flange
c – edge distance	g – bolt-bolt distance
d – distance from channel to vertical bolt	h – channel section height
m – channel depth	p – bolt row to bolt row distance
h – angle section width	
i – bolt-bolt distance	

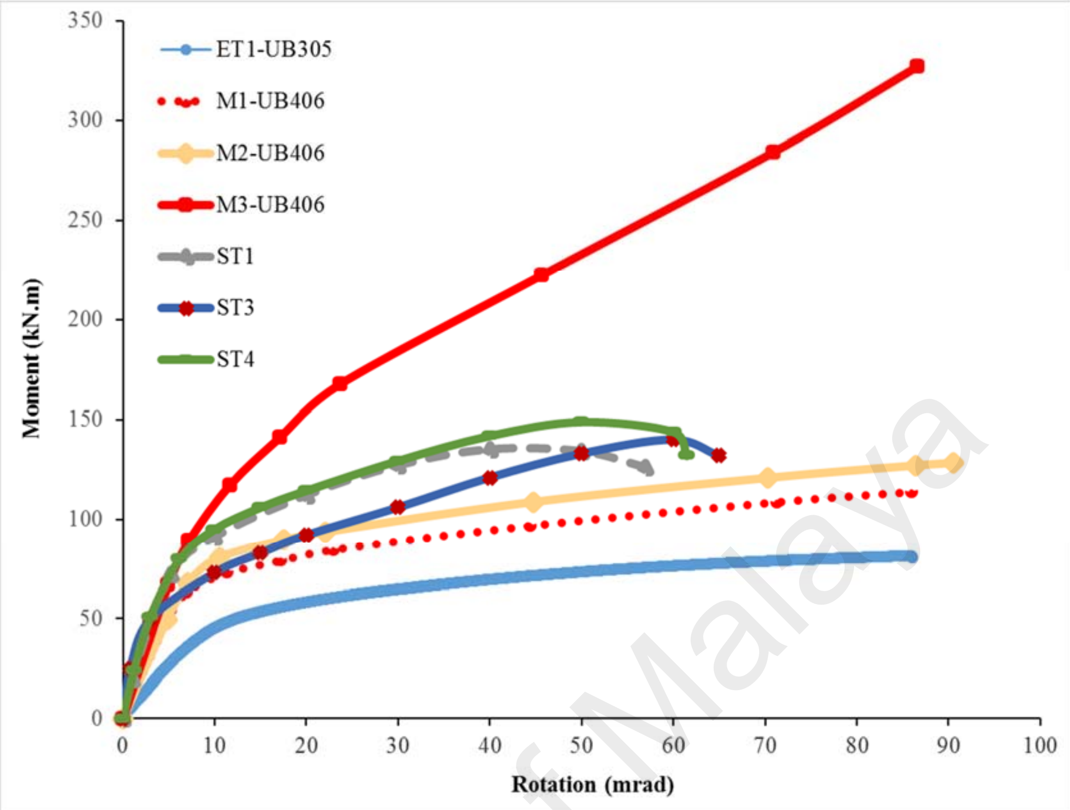

Figure 4.38 Behavior comparison with existing experimental results

4.3 Findings on Connection at Elevated Temperature

From test results of the connection in ambient temperature, the yield moment is calculated to be 54.5 kN.m, for AT2, corresponding to similar angle section thickness of ET1 therefore, similar loadings would be applied to the connection under elevated temperature without reaching the plastic state. Considering that both ends are pinned connections at the A-frame supports, with length of 3.6 m without the column width, a constant loading of 60 kN is applied to the column to induce moment forces in the connections. It is assumed that moment forces are equal for both sides of the column for each connection.

4.3.1 Experimental Test Results

4.3.1.1 Temperature Distribution

As shown in Figure 4.39, the temperature distribution for specimen ET1 is generally uniform throughout the connection with differences ranging between 18°Cto 150°Cacross the joint. Similar to specimen ET1, the temperature distribution for specimen ET2 has minor differences as shown in Figure 4.40. The total number of points has been reduced for the beam considering that the temperature distribution is generally uniform throughout the beam. Meanwhile, the temperature distribution of specimen ET3 and ET4 is as shown in Figure 4.41 and Figure 4.42 respectively. Highest temperatures are located at the beam web while the lowest temperatures are located on the compression angles (top angles). The largest difference in temperature is a maximum of 150°C.

Temperature distribution is also commonly represented in terms of temperature ratios for further studies, including the implementation into the component methods and analytical method as has been conducted by Silva et. al. (2001). Although a number of possible ways exist to define the temperature ratio, the current research work focuses on having the furnace temperature as the comparison basis. As with real-world applications, although steel material is a good heat conductor, the temperatures are not instantaneous. Temperatures of the connection components at any time is dependent on the thermal conductivity and specific heat values. Temperature ratio of the components in the connection for the individual specimen is as detailed in Table 4.9 to Table 4.12.

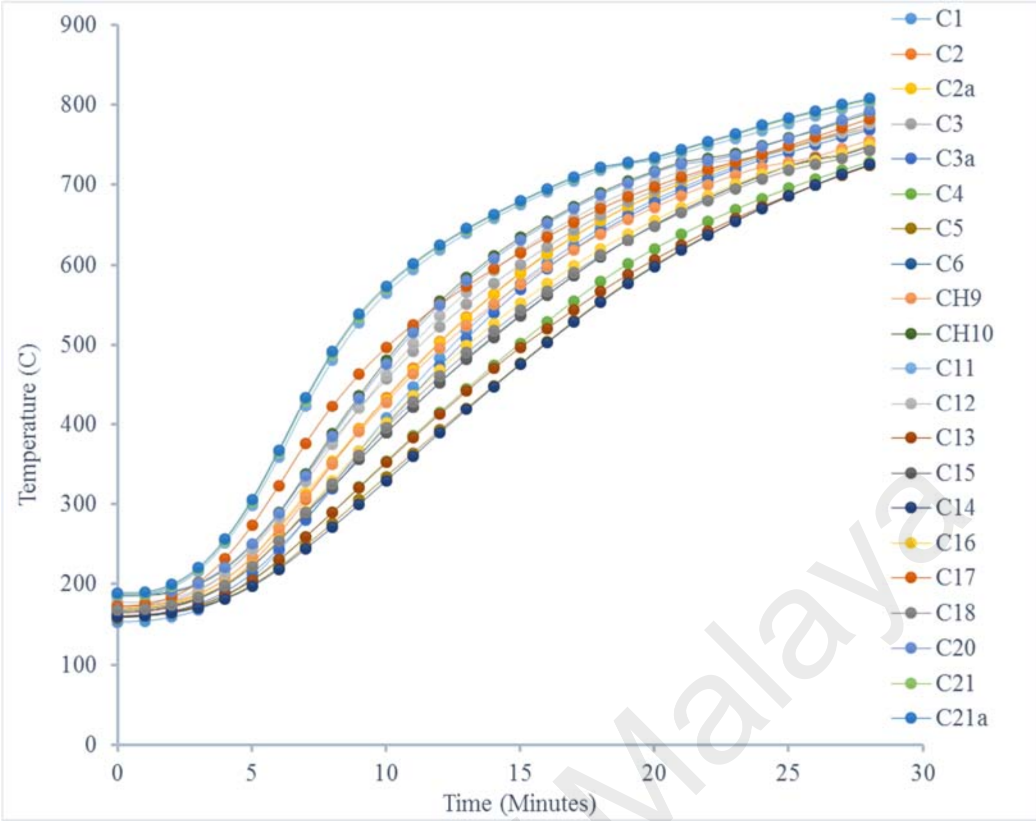

Figure 4.39 Temperature distribution for ET1

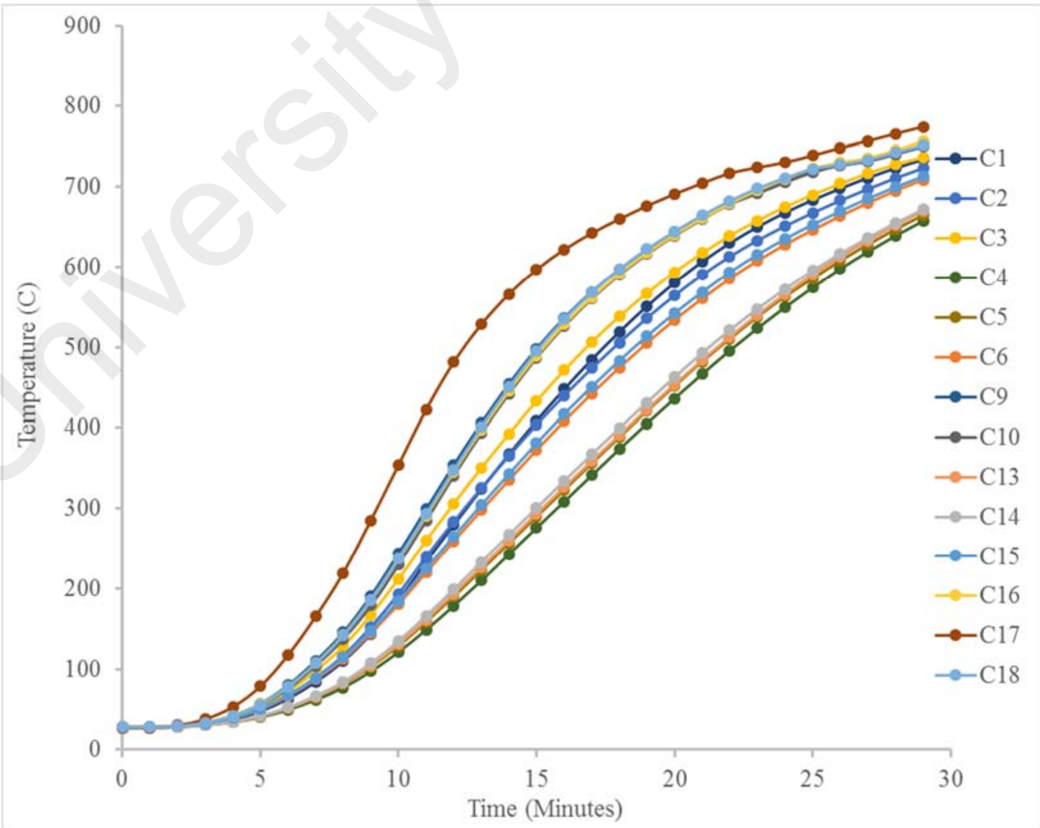

Figure 4.40 Temperature distribution for ET2

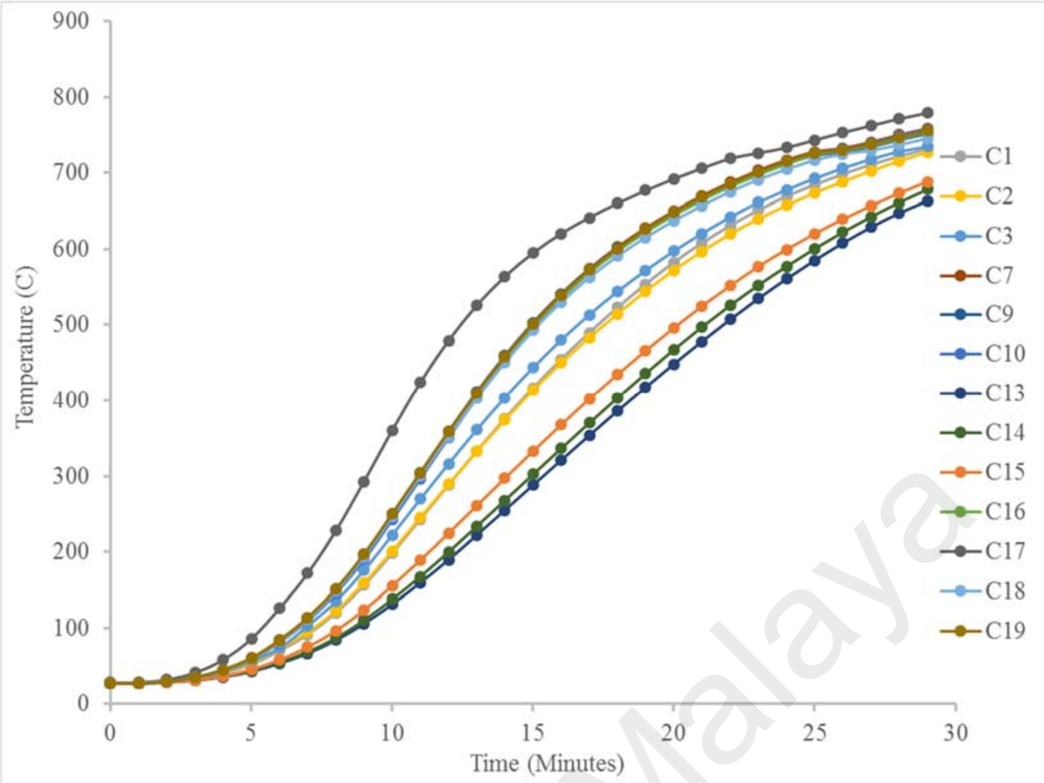

Figure 4.41 Temperature distribution for ET3

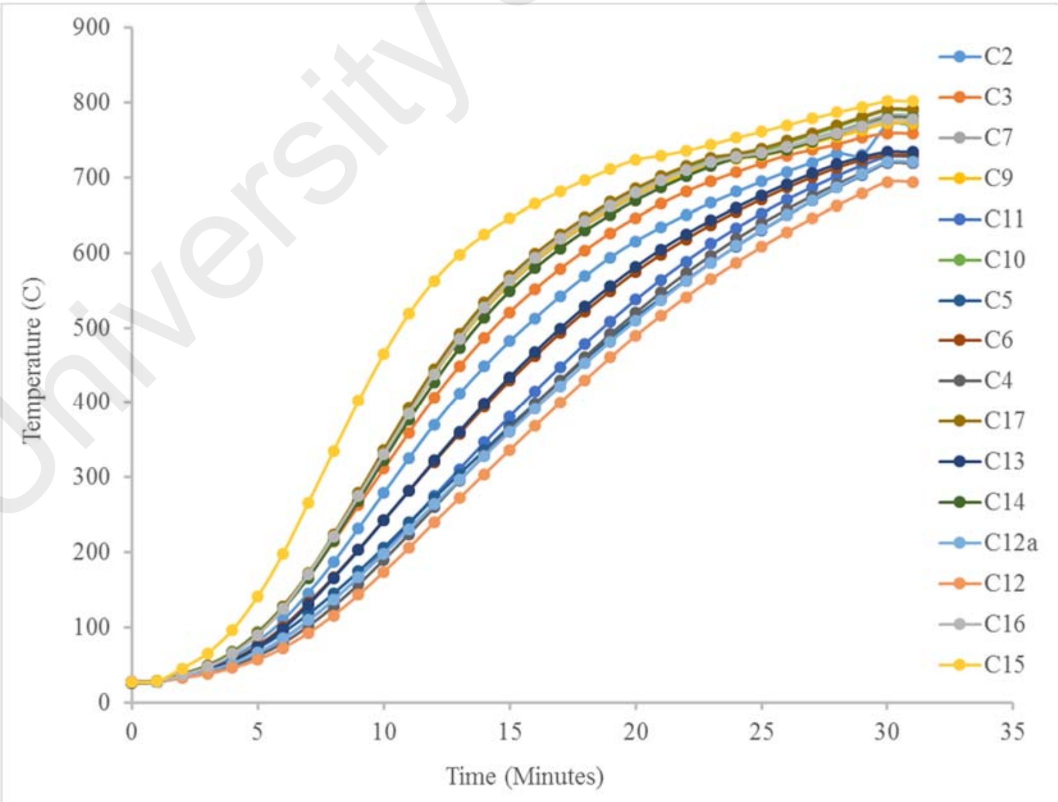

Figure 4.42 Temperature distribution for ET4

Table 4.9 Temperature ratio for connection ET1

Furnace Temperature	Column	Top Angle	Bottom Angle	End-Plate	Beam Top	Beam Web	Beam Bottom
197.23	0.84	0.81	0.85	0.81	0.92	0.94	0.88
326.77	0.61	0.57	0.61	0.56	0.65	0.76	0.63
401.40	0.56	0.51	0.55	0.49	0.60	0.74	0.58
536.57	0.56	0.48	0.54	0.46	0.60	0.77	0.58
603.50	0.64	0.53	0.59	0.50	0.68	0.85	0.65
704.73	0.83	0.71	0.76	0.68	0.86	0.94	0.82
751.07	0.89	0.79	0.84	0.77	0.91	0.95	0.88
759.07	0.90	0.81	0.86	0.79	0.92	0.95	0.89
790.93	0.93	0.86	0.90	0.85	0.93	0.96	0.91
798.00	0.93	0.87	0.91	0.86	0.94	0.97	0.92

Table 4.10 Temperature ratio for connection ET2

Furnace Temperature	Column	Top Angle	Bottom Angle	End-Plate	Beam Top	Beam Web	Beam Bottom
27.43	1.01	1.02	1.01	1.00	1.02	1.01	1.02
95.03	0.41	0.36	0.41	0.37	0.44	0.56	0.44
218.83	0.31	0.23	0.31	0.24	0.35	0.54	0.36
288.73	0.31	0.22	0.31	0.23	0.37	0.57	0.38
421.20	0.37	0.24	0.35	0.25	0.43	0.68	0.45
481.07	0.41	0.26	0.38	0.27	0.49	0.74	0.50
595.07	0.56	0.37	0.51	0.38	0.66	0.89	0.68
698.97	0.79	0.59	0.73	0.61	0.88	0.97	0.89
748.00	0.86	0.71	0.82	0.73	0.93	0.97	0.93
773.43	0.90	0.78	0.86	0.79	0.94	0.97	0.94
788.83	0.91	0.82	0.88	0.83	0.94	0.97	0.94
796.37	0.92	0.83	0.89	0.84	0.95	0.97	0.94

Table 4.11 Temperature ratio for connection ET3

Furnace Temperature	Column	Top Angle	Bottom Angle	End-Plate	Beam Top	Beam Web	Beam Bottom
27.03	1.01	0.98	1.01	1.03	1.01	1.02	1.01
107.73	0.38	0.33	0.34	0.34	0.41	0.54	0.40
236.80	0.30	0.23	0.25	0.23	0.35	0.53	0.34
301.27	0.32	0.22	0.25	0.23	0.37	0.57	0.37
436.23	0.37	0.24	0.28	0.25	0.45	0.67	0.44
494.70	0.42	0.27	0.31	0.28	0.50	0.73	0.50
599.27	0.57	0.37	0.44	0.39	0.68	0.88	0.68
701.27	0.79	0.60	0.66	0.62	0.89	0.97	0.88
750.60	0.87	0.71	0.77	0.74	0.93	0.97	0.93
768.00	0.89	0.76	0.81	0.78	0.95	0.97	0.94
784.63	0.91	0.80	0.84	0.82	0.94	0.97	0.93

Table 4.12 Temperature ratio for connection ET4

Furnace Temperature	Column	Top Angle	Bottom Angle	End-Plate	Beam Top	Beam Web	Beam Bottom	Mid-Connect
26.77	1.01	1.03	0.99	1.02	1.02	1.01	1.02	1.01
77.27	0.61	0.52	0.56	0.49	0.61	0.85	0.62	0.56
181.17	0.48	0.35	0.41	0.32	0.48	0.78	0.50	0.38
327.70	0.48	0.32	0.40	0.28	0.48	0.81	0.52	0.35
402.97	0.50	0.33	0.41	0.29	0.50	0.83	0.55	0.35
518.40	0.57	0.38	0.47	0.34	0.58	0.90	0.64	0.39
613.70	0.70	0.49	0.59	0.44	0.72	0.97	0.79	0.49
695.63	0.84	0.68	0.76	0.62	0.86	1.00	0.92	0.65
735.17	0.88	0.76	0.82	0.70	0.90	0.99	0.94	0.73
769.57	0.92	0.84	0.88	0.79	0.93	0.99	0.95	0.82
792.60	0.93	0.88	0.90	0.84	0.95	0.99	0.95	0.87

It is observed that at higher temperatures, the ratio between the specimen and furnace temperatures increases due to exposure time at high temperatures. At temperatures reaching approximately 800°C, the ratio is an average of 0.9 of the furnace temperature. There is a large jump in the part temperature ratios between 600°Cto 700°C. Below 500°C, the temperatures on the specimen are at an average of 0.5 of the furnace temperature. Before the heating regime is started, the specimen temperature is relatively higher than the furnace temperature is expected to be due to the enclosed space of the furnace and heat conducting properties of the steel material. However, the effect is relatively minor.

4.3.1.2 Connection Deformation

In terms of specimen deformation, as indicated by Figure. 4.43, compression causes the bottom angle to bend at the welded points between the angle and the end plate. As a result, the compression area component behaves in a flexural bending manner and collapses into the column. In terms of tension zone, the applied axial loading similar to shear force, results in the angle to bend at the welded area and finally being pulled apart from a "L" shape to an almost straight diagonal plate. Both occurrences are expected to increase the connection capacity before ultimate failure. It is also observed that the beams developed shear buckling in the beam web on both sides of the connections. The web shear buckling is caused by the combination of both shear force and axial loads due to the support system at both ends of the specimen. In comparison to the other tests, the LVDT measurement for this test focuses on the central column and not on the beam.

Figure 4.43 Specimen ET1 Deformation

Due to the existence of the central angle stiffener, the angles for the tension zone deform by prying forces in specimen ET2 as recorded in Figure 4.44. Although not visible, the column in both the compression and tension zones is affected by the additional stiffener, being compressed inwards for the compression zone and slightly pulled out at the tension zone. In the compression zone, the angle and stiffener work together as a block with the hinge location at the column face.

In specimen ET3's behavior, the increase in angle thickness has transferred the forces to the column, causing fractures and tearing on the column flange as depicted in Figure. 4.45. In comparison to ET1, the compression angle for specimen ET3 does not display the bending deformation and instead bends at the weld joints.

Figure 4.44 Visual deformation of specimen ET2

With the availability of the central connection, it is expected that the connection will be stiffer and provide increased load resistance. In terms of deformation, besides the prying on the T-stub at the tension angle, similar to specimen ET2 due the contribution of the stiffener, the tension angle appears to have failed at the welding area as shown in Figure 4.46 for ET4. At the same time, the flange of the column, which is considered as the area connecting the beam, is pulled out due to rotation and tension forces resisted by the central connection. Connection force transfer at the tension zone occurs from the column face and subsequently moving towards the beam web axis, which is as indicated by the failure modes shown in specimen ET4.

Figure 4.45 Deformation of tension zone for specimen ET3

Figure 4.46 Deformation of ET4 post elevated temperature test

4.3.1.3 Behavior of RTSA in Elevated Temperature

The resulting behavior of the specimens is compared in Figure. 4.47 (a-d) for the data recorded from the 200 mm LVDT while the data recorded from the 100 mm capacity LVDT is detailed in Figure 4.48. The results are based on the furnace temperature when the particular specimen is tested, plotted against the central column deflection readings from the LVDT average values. No data for the 100 mm has been recorded for ET1. The flat portion of the behavior at the end of the graph resulted from the LVDT having reached the maximum LVDT capacity. Stiffness of the specimens have been found to have minimal differences when compared to each other. Due to this, the possible comparable parameter is the yield value and the plastic behavior. Specimen ET1 has the lowest yield value, followed by ET4 and ET3. Meanwhile, specimen ET2 has yield values comparable to ET3.

In terms of beam deflection as reflected by the data recorded from the 100 mm LVDT, beam deformations for both ET2 and ET3 are similar while ET4 is showing flexibility due to the weld tear that could have occurred early into the test. The weld tear had little effect on the connection behavior at the early stage when temperatures were lower than 700°C, due to the amplified effect from material behavior at 700°C. Both ET2 and ET3 have similar deformation, which is followed by an increase in beam deflection for ET3 due to the tearing in the column failure of ET3, thus reducing the stiffness of the post-elastic behavior of the connection.

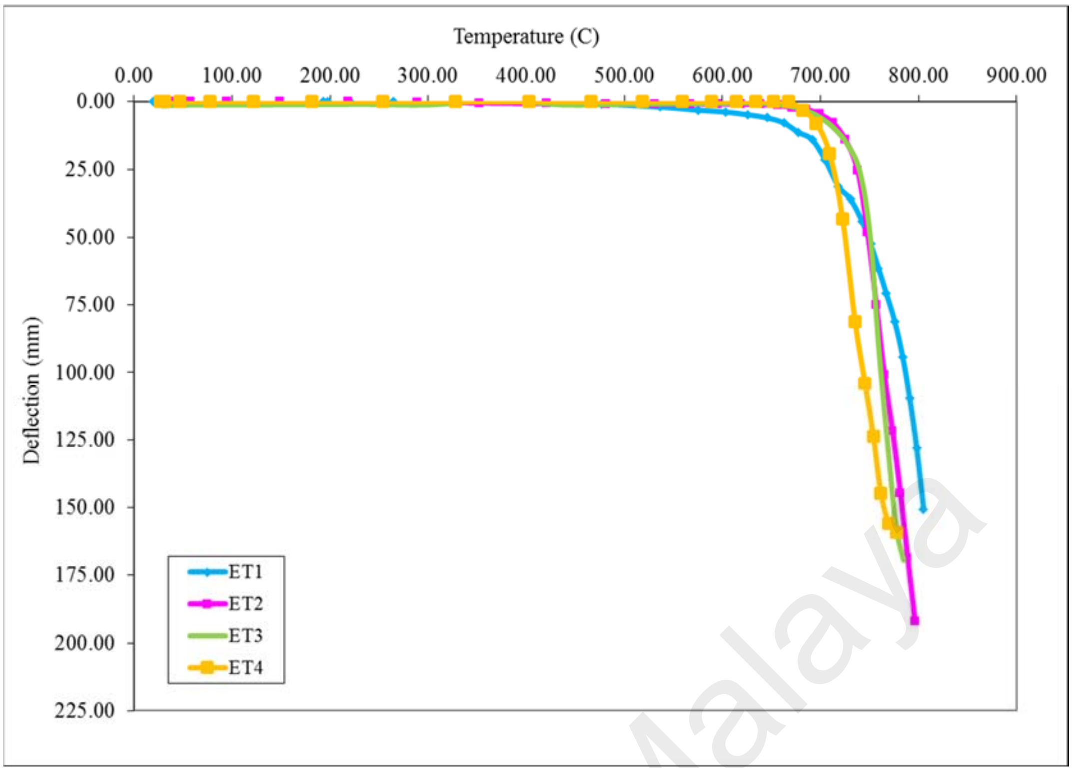

(a) General Behavior comparison

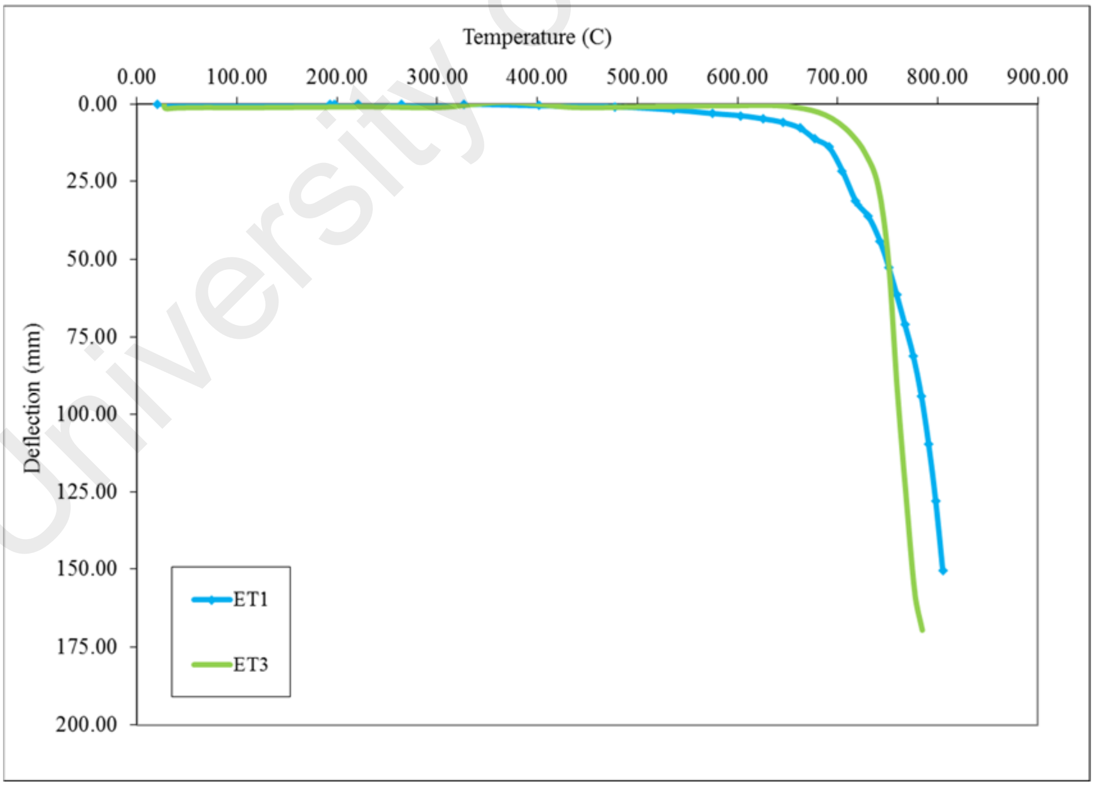

(b) Effect of angle thickness ET1-ET3

Figure 4.47 (a-d). Comparative effect on Reverse Top-Seat angle connections in elevated temperature conditions.

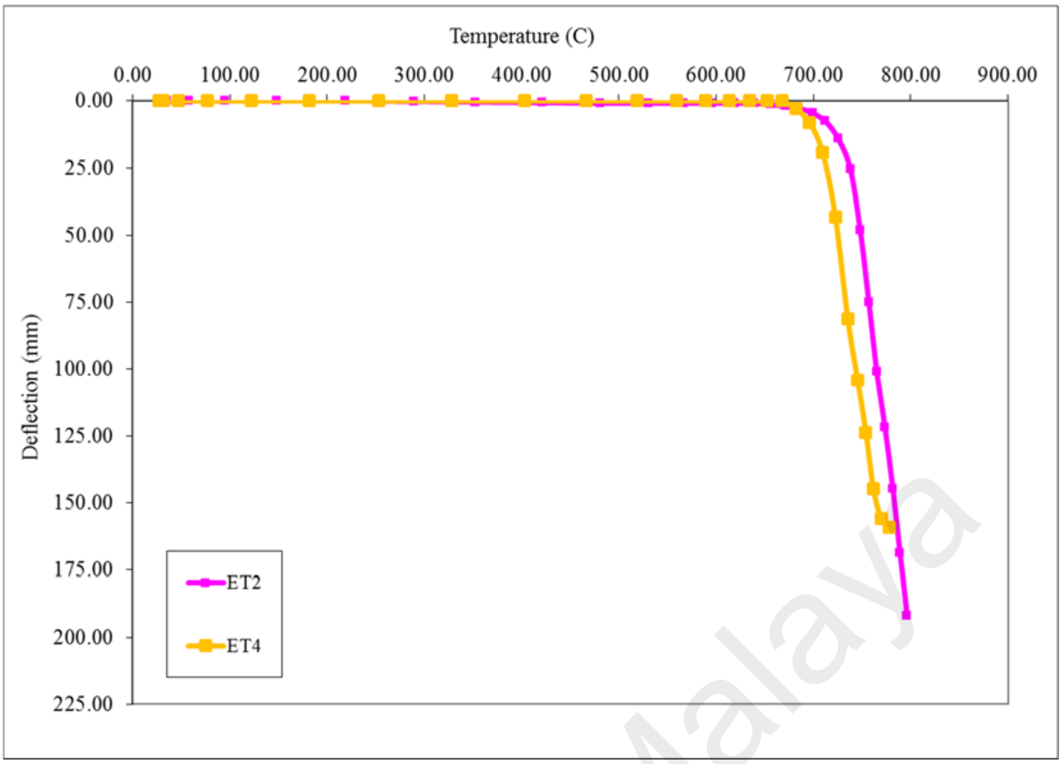

(c) Effect of Mid-Connection ET2-ET4

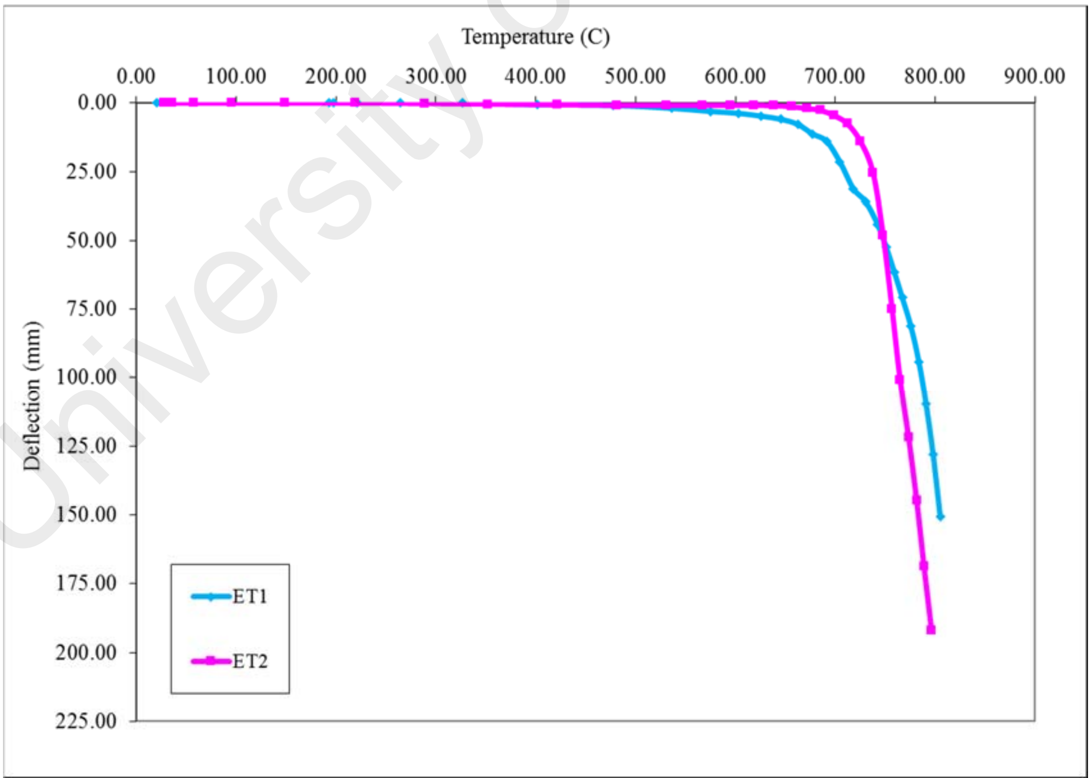

(d) Effect of Stiffener ET1-ET2

Figure 4.47 (a-d). Comparative effect on Reverse Top-Seat angle connections in elevated temperature conditions.

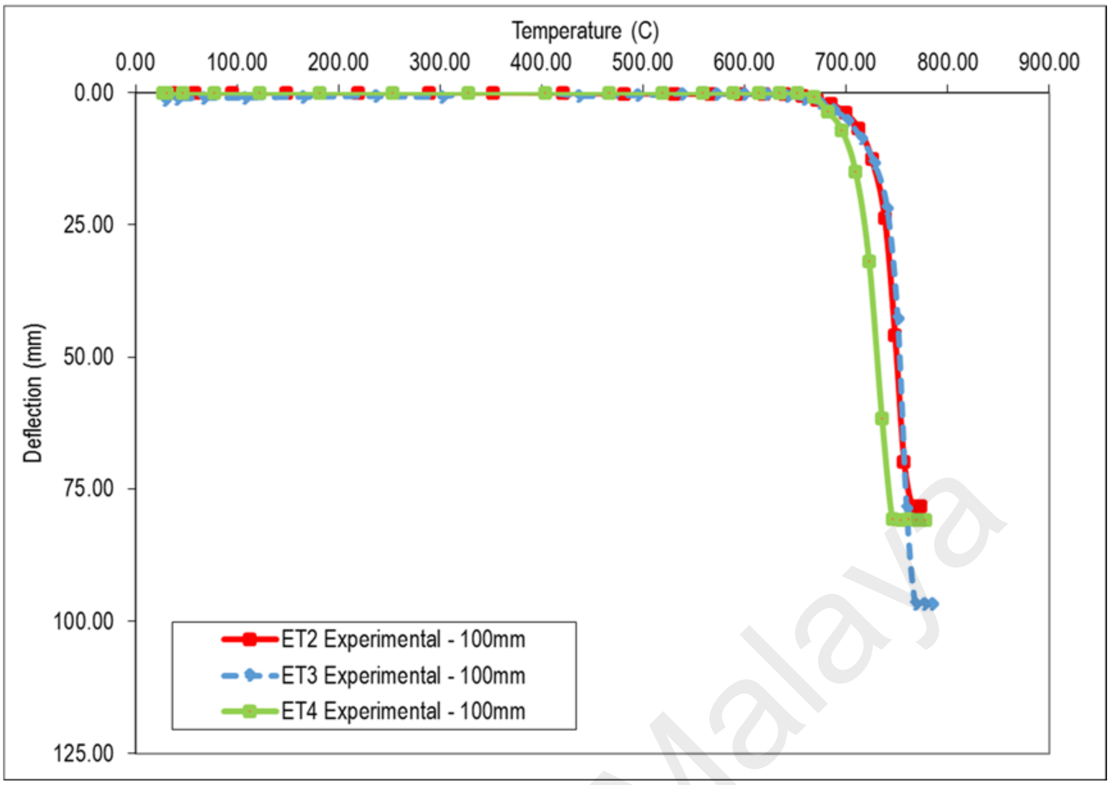

Figure 4.48 Deflection of beams under elevated temperature for 100 mm LVDT

4.3.2 RTSA Connection Comparison

4.3.2.1 Effect of angle thickness

From the results of previous study at ambient temperature on reverse top-seat angle connection, it was concluded that the angle thickness has a critical role in providing the load resistance for this connection configuration. Specimen ET3 when compared with specimen ET1, has higher thickness, subsequently it is expected that the stiffness is higher than specimen ET1 is. This is due to the deformation of the angle in bending under loads, both at the tension or compressive zone. However, as shown in Figure 4.47(b), the behavior in elevated temperature conditions are not as expected as the increase in angle thickness from 8mm to 12mm decreased the plastic behavior instead when compared.

By scrutinizing the deformation and failure of the connections, the increase in angle thickness in ET3 has caused the angle to have tension failure at the tension zone of the column flange that did not occur with specimen ET1. The deformation on the compressive zone angle section of ET3 is not as severe as the angle in specimen ET1. However, the decreased deformation in the angle may have reflected on the column, resulting in the tearing at the tension zone of the column as shown in Figure 4.45.

4.3.2.2 Effect of Stiffener

The comparison of the effect from the addition of stiffeners is as shown in Figure 4.47 (d), with specimen ET1 and ET2. Due to the boundary conditions in this study, the loads applied on to the connection is shear-centric. Until the beam begins to deform at higher temperatures, the loads are transferred through the shear resistance of the connection. It is from this reason that the connection is not able to utilize the increased capacity by the stiffener to resist the applied loads, therefore displaying similar stiffness with ET1. While the elastic-plastic behavior of ET2 is slightly higher, this is expected due to the stiffener. However, the column deformation capacity soon governs as the temperature increases, leading to reduced plastic resistance.

In ET1, the weaker angle deforms first, diverting all the forces away from damaging the column, while in ET2, the column instead becomes the weak point from the combination of angle and stiffener. From this, it is clear that the column is the second weakest component after the angle, depending on the geometry of the angle, especially the thickness of the angle.

In addition, the column is being deformed by tension forces for ET2. With the tension failure, this resulted in less load resistance in the column, relying only on the bending pullout of the 9mm thick column face that subsequently leads to the reduced post-yield behavior. Moreover, the tension angle in specimen ET1 is also deformed to a stage where the tension capacity of the angle governs the behavior, rather than the bending of the angle in the elastic phase. The tension resistance couple with the deformation of the column has resulted in a higher post-yield behavior for ET1. In terms of stiffness, the plates have reduced the bending of the angles that result in lower deformation and higher yield values.

4.3.2.3 Effect of Mid-Connection

The addition of bolts using a t-stub at the center of the beam with 4M20 Grade 8.8 results in lower post-yield behavior when compared as indicated in Figure 4.47 (c) for ET2 and ET4. In theory, the T-stub limits the rotation of the end-plate at earlier stages of the connection deformation, therefore providing increased resistance due to the additional shear resistance of the increased number of bolts. However, the welding failure at the tension angle on ET4 due to the bowing deformation of the column shape has contributed to the decreased load resistance of the connection. Subsequently, the plastic behavior is lower than the connection ET2 without the central connection component. Without the welding failure, the connection is expected to achieve lower deflection at the same rate of temperatures but further tests are necessary to validate this behavior.

4.3.3 FE Model Development in Elevated Temperature

4.3.3.1 Loading Application

In the tests, 30 kN is applied on each connection but due to the use of the stub to transfer loads to the connection, the weight of the connection and the stub is also considered within the total load applied on the model. Loads are converted to 8.2 Mpa pressure and applied on to column top surface in the –z direction.

4.3.3.2 Boundary Conditions

The specimen is supported by two "A" frames as shown in the test setup. Only half of the specimen is modelled to decrease computational time and load, while the column acts as the symmetry axis. At the area where the symmetry is defined, the column is not allowed to deform in the –x and –y direction and no rotation about the –z axis. Deflection is measured on the –z direction. Flanges of the beam are defined to have no deformation in the –y direction, as a result from the test shows that there was no deformation of the beam flange in the out-of-plane direction.

Despite this, the beam web is not restrained, allowing it to buckle accordingly. Pretension is defined at the bolt shaft mid surface and axis using load values of 75 kN due to the hand-tightening process. The resulting length is then maintained over the next load step. Moment is calculated from the resulting force multiplied by the lever arm. Rotation expressed in radians is the result by dividing with the deflection divided with the distance to support. Material degradation factor under elevated temperature conditions are as indicated in Table 4.13.

4.3.3.3 FEM Model Behavior

The comparison between the deflection of the central column in the experimental test and model results is as shown in Figure 4.49 to Figure 4.52. For specimen ET1 and ET2, the model corresponds closely to the behavior of the experimental test results, however, for specimen ET3 and ET4, the model is considerably more flexible in terms pf plastic behavior. The behavior is due to the failure of the column in specimen ET3 and welding failure occurring in specimen ET4. A separate model is created and analyzed for both ET3 and ET4 where the failure of column in ET3 and the welding failure in ET4 are incorporated into the model by removing the “tie” contact that exists between the angle section and column, leaving only the central area fully connection for the whole duration of the analysis.

Table 4.13 Reduction factors for steel material at elevated temperatures. (Outinen & Mäkeläinen, 2002)

Temperature	Modulus of Elasticity	Proportional Limit	Yield Strength
20	1.00	1.000	1.000
100	1.00	0.970	0.970
200	0.90	0.807	0.932
300	0.80	0.613	0.895
400	0.70	0.420	0.857
500	0.60	0.360	0.619
600	0.31	0.180	0.381
700	0.13	0.075	0.143
800	0.09	0.050	0.105

However, the area left in contact is different for ET3 and ET4 due to the severity of the damage. In ET3 this is limited only to the sides, approximately 40 mm from the sides of the angle section, while for ET4, the central 70 mm is left to tie with the column face throughout the analysis. The resulting behavior is as compared in Figure. 4.53 and Figure 4.54 and the modified model is shown to correspond well to the behavior of the experimental test recorded deflection. From these results of the modified model, it is concluded that the model behavior without the failures is a possible outcome and relevant for further comparison or parametric studies.

Behavior of the beam deflection, with data from the 100 mm capacity LVDT is as shown in Figure 4.55 to Figure 4.57 for ET2, ET3 and ET4 respectively. As indicated by an earlier section, no 100 mm LVDT data was recorded for specimen ET1. In addition, for ET3 and ET4, the tearing concept, using the method to allow separation between the surfaces has been included into the model. Behavior of the model corresponds well with the data, Results from the model includes the deflection at which the LVDT was not able to record due to limitations of the LVDT. In general, the deflection of the beam at 300 mm from the column central axis are lower than the deflection of the column, for same temperature levels. Accuracy of the models are further validated for both 200 mm and 100 mm recorded behavior.

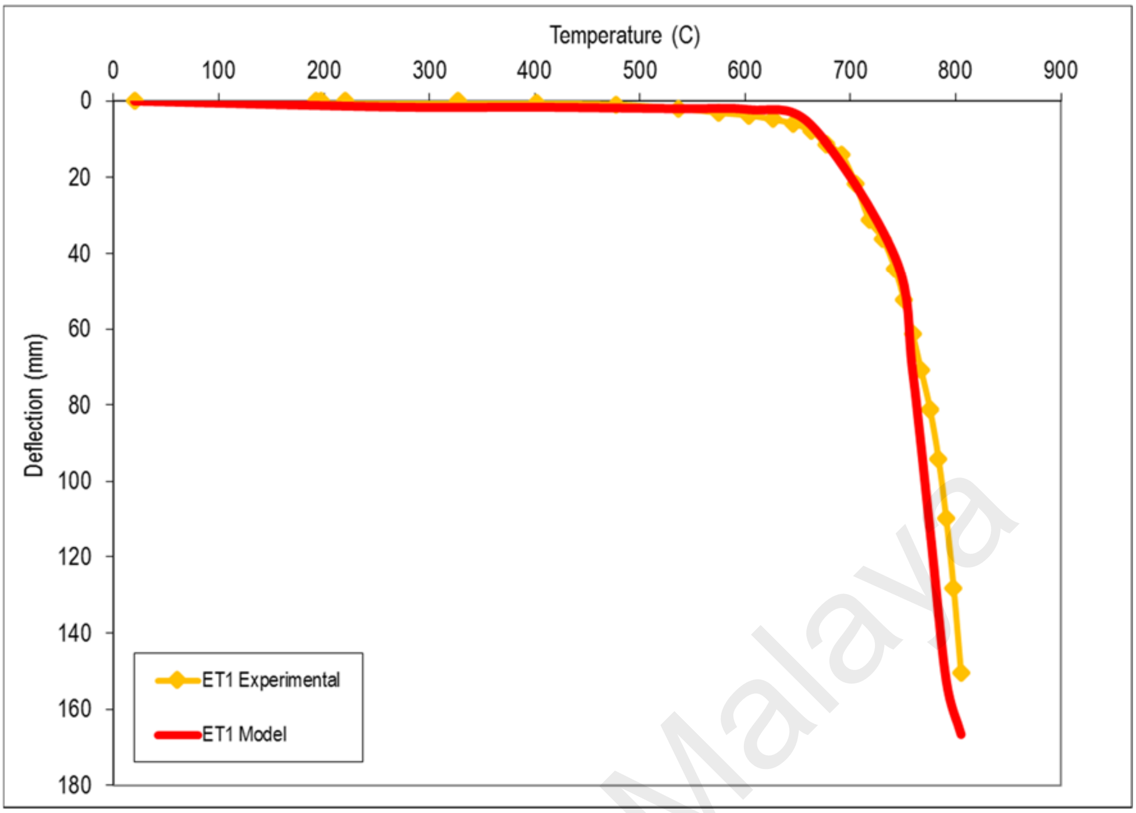

Figure 4.49 Comparison of ET1 and model for column deflection

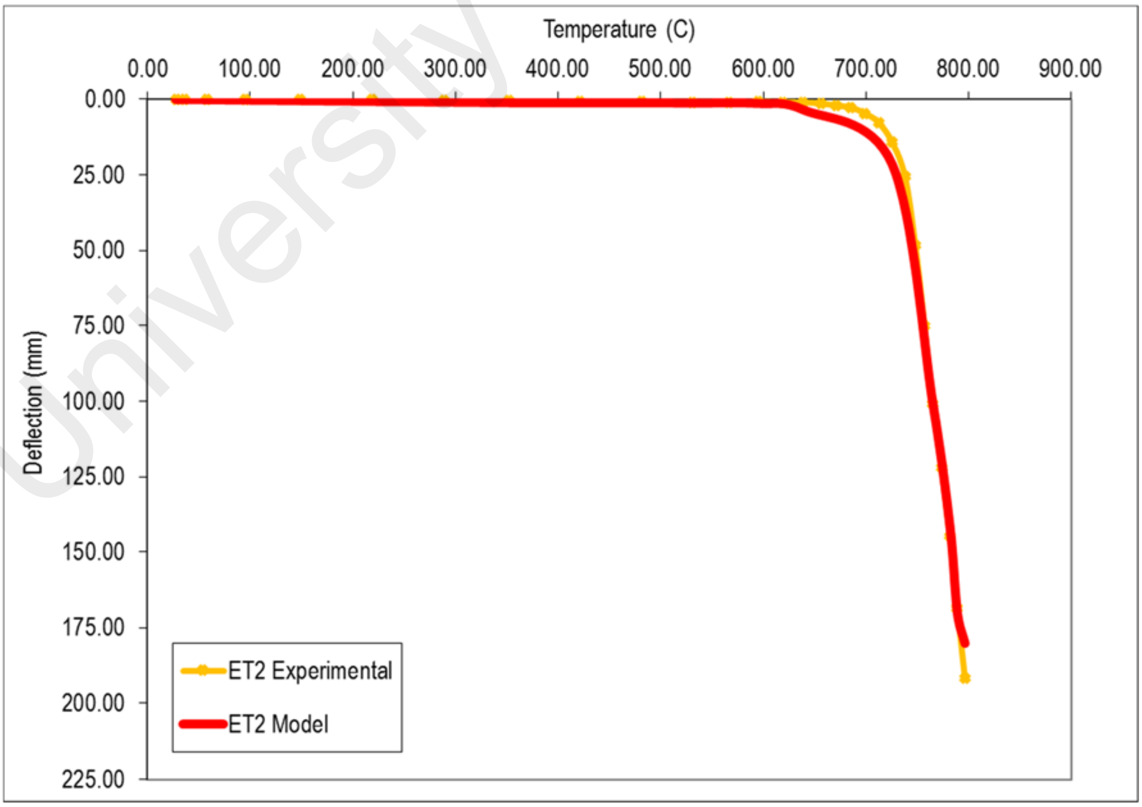

Figure 4.50 Comparison of ET2 and model for column deflection

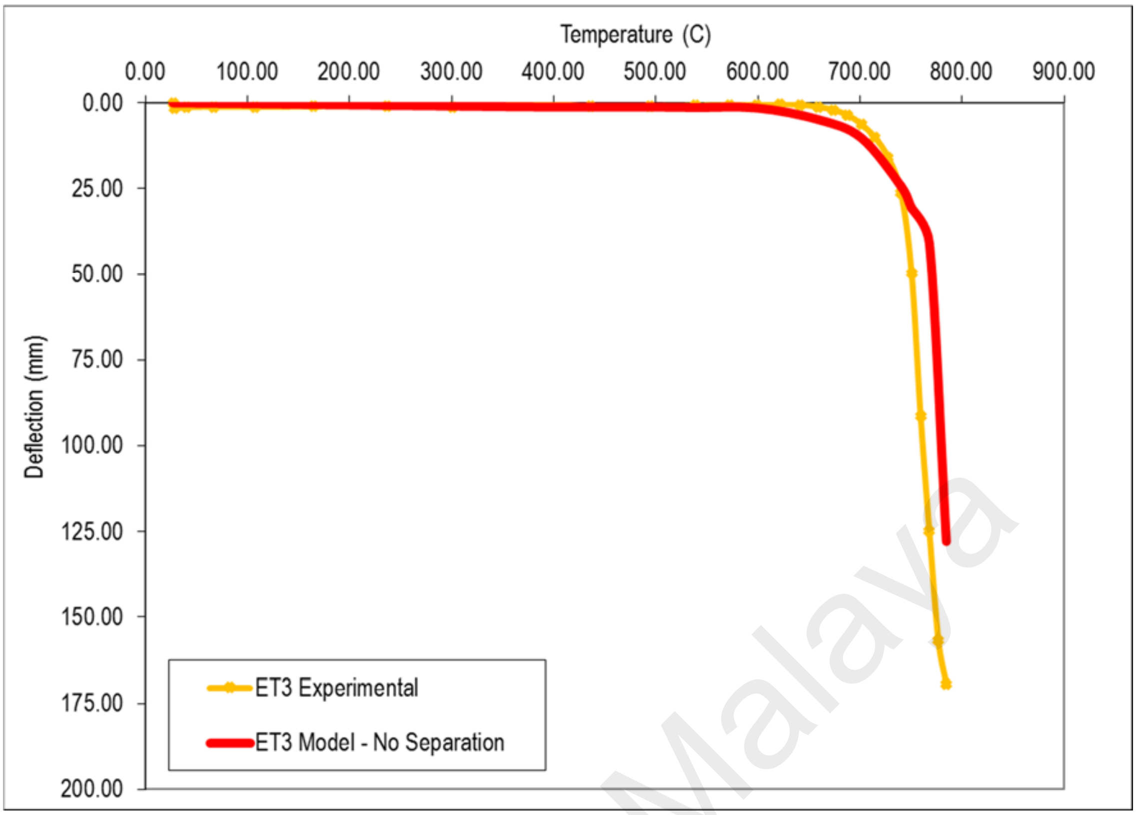

Figure 4.51 Comparison of ET3 and model for column deflection

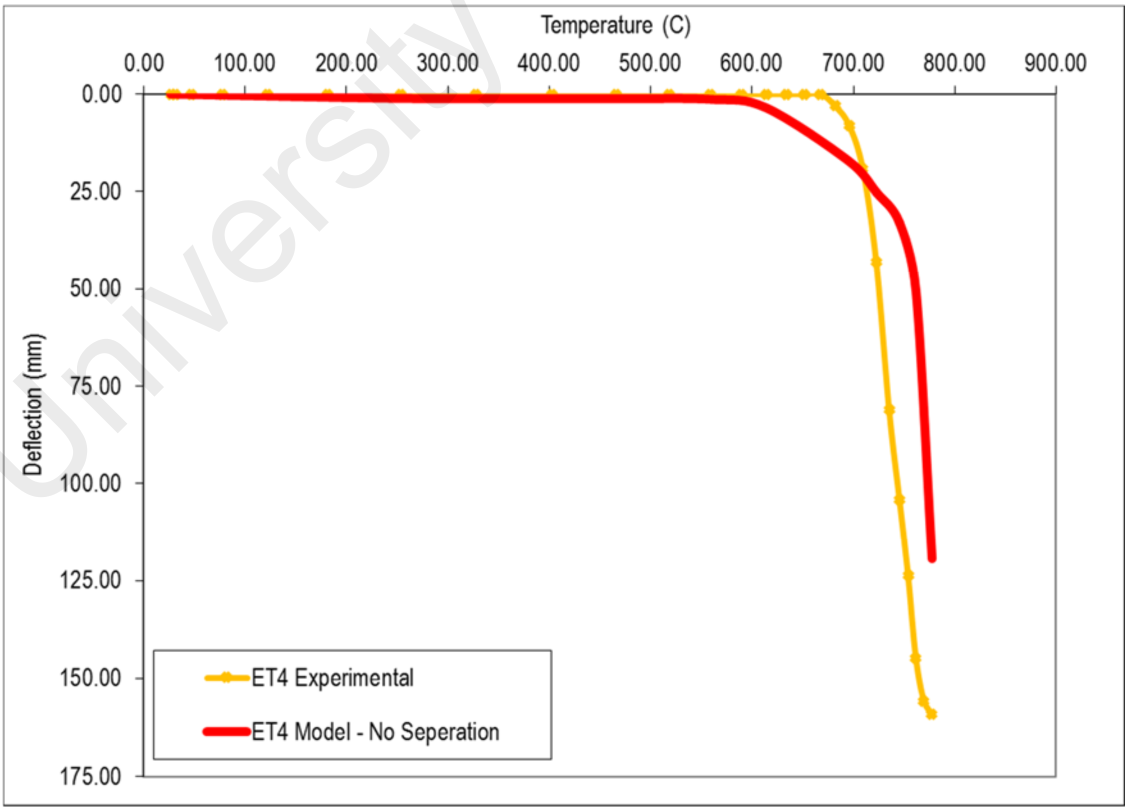

Figure 4.52 Comparison of ET4 and model for column deflection

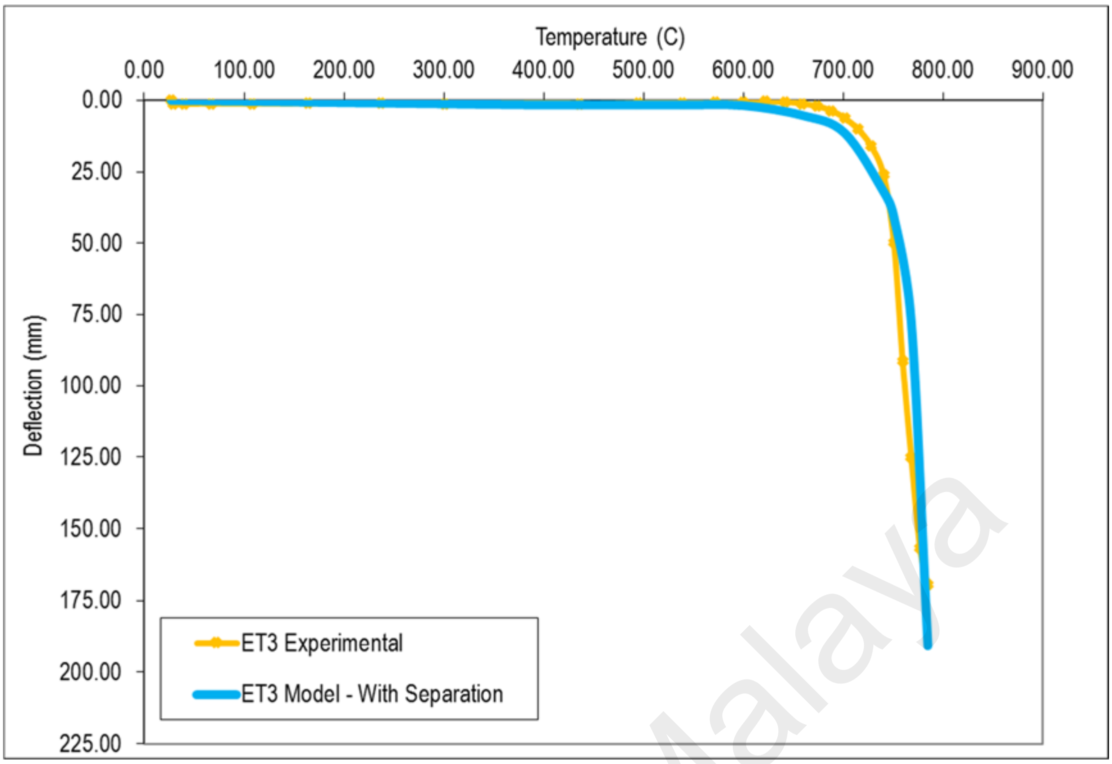

Figure 4.53 Comparison of ET3 and tear model for column deflection

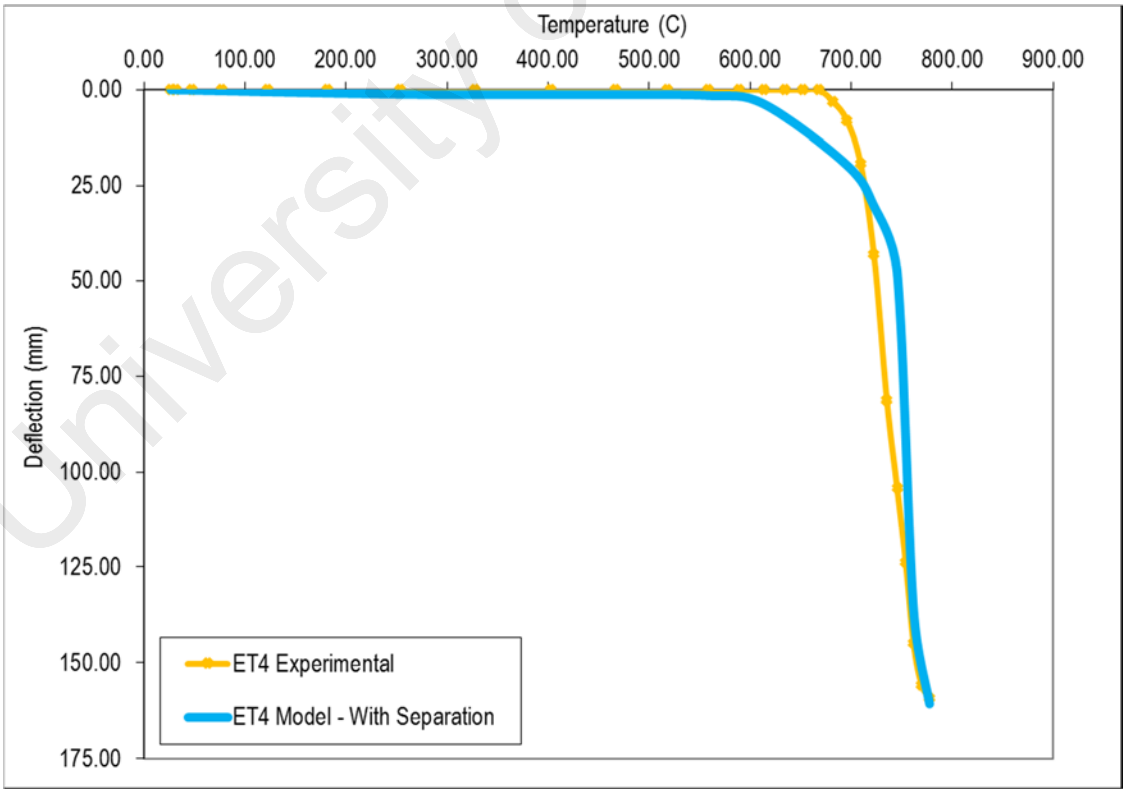

Figure 4.54 Comparison of ET4 and tear model for column deflection

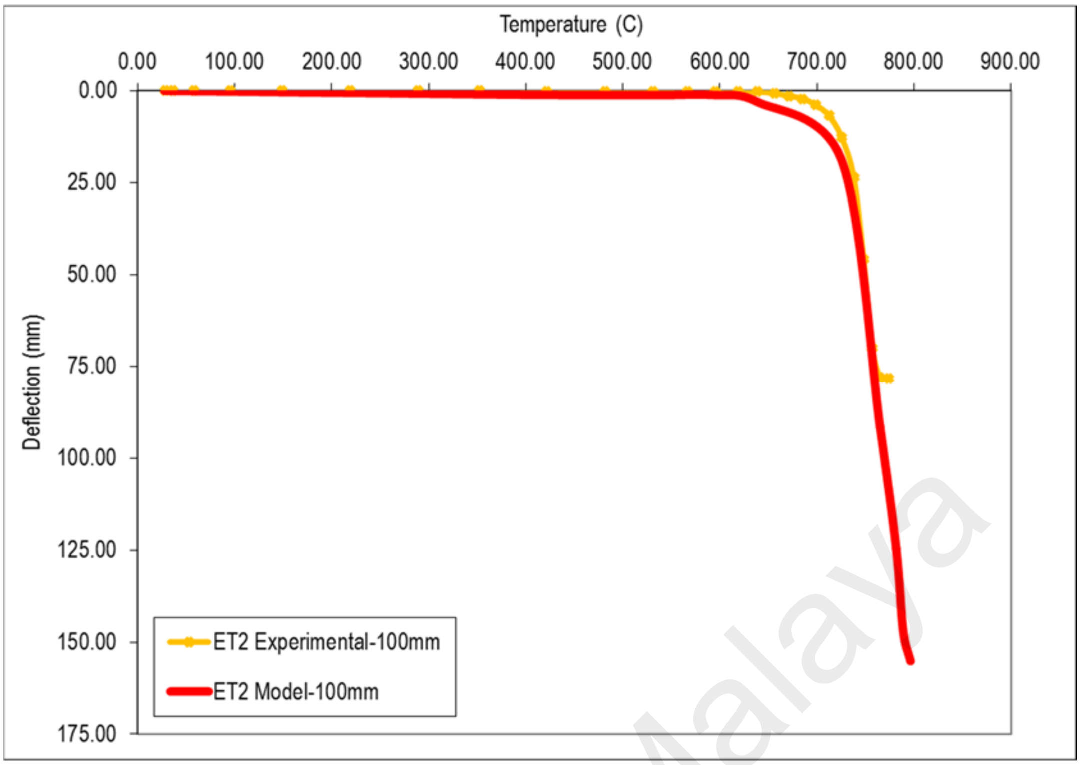

Figure 4.55 Comparison of ET2 and model for beam deflection

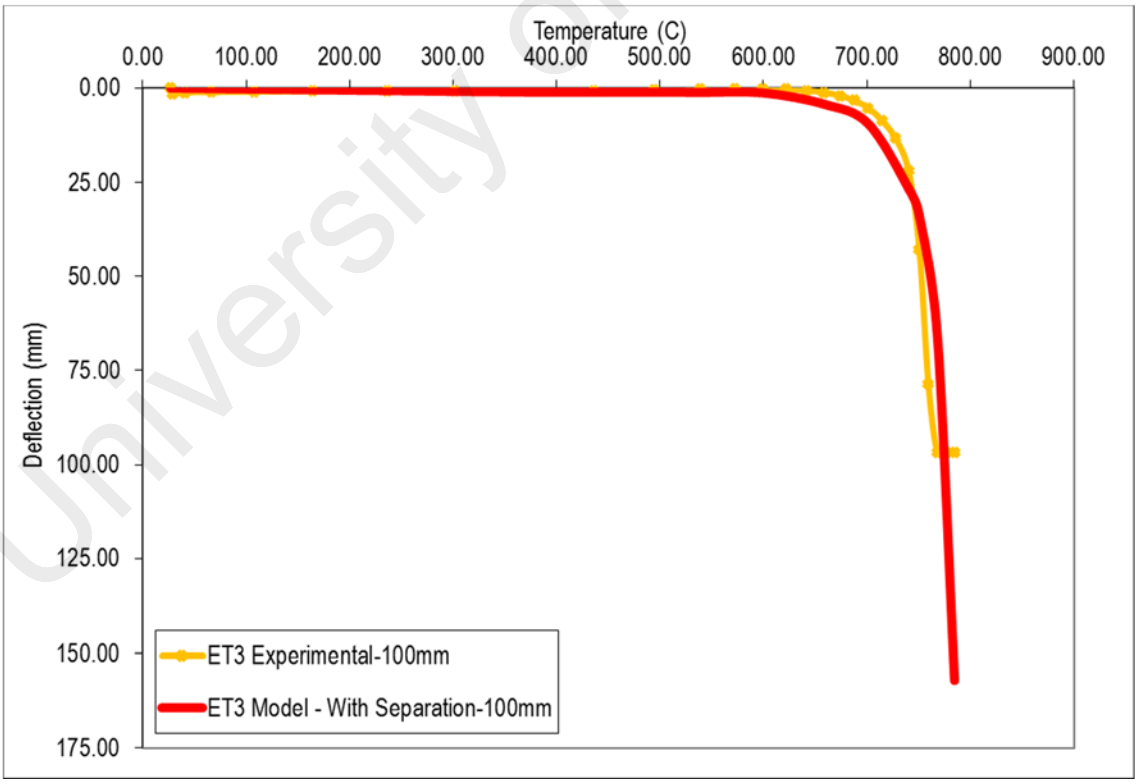

Figure 4.56 Comparison of ET3 and model for beam deflection

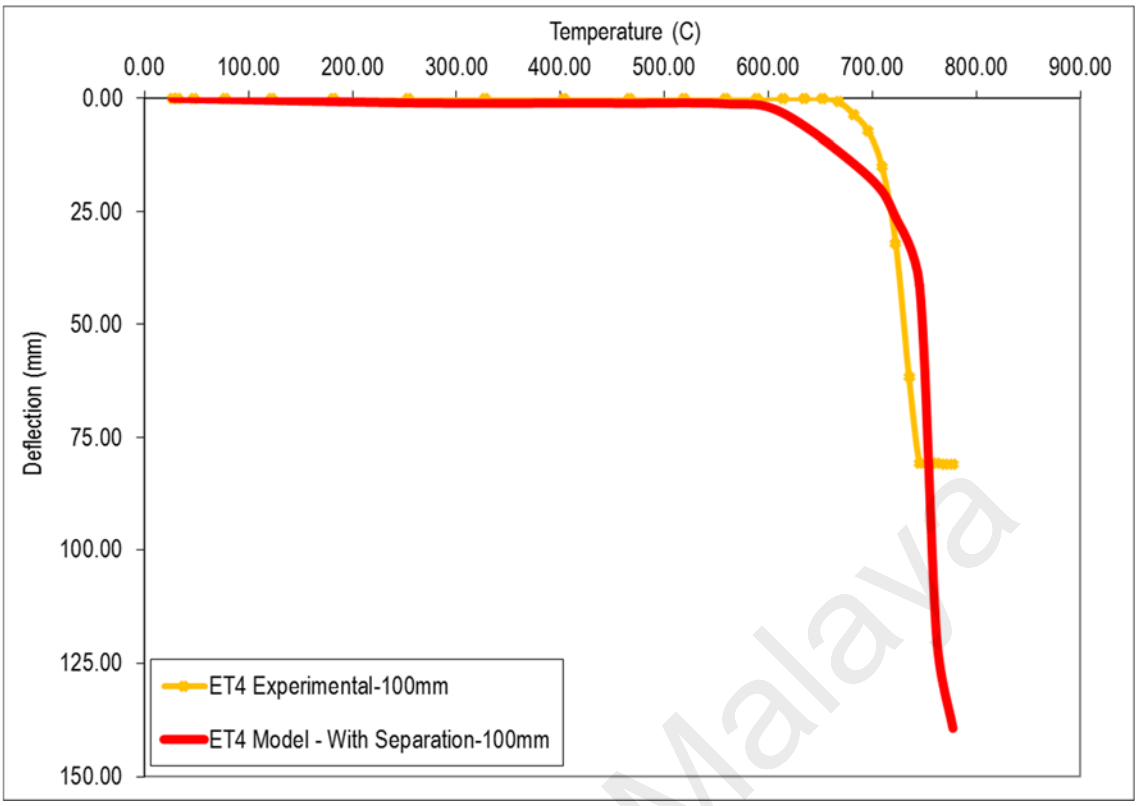

Figure 4.57 Comparison of ET4 and model for beam deflection

4.3.3.4 Deformation of Model

Meanwhile, in terms of connection deformation, the results from model are similar to those shown as a result from the experimental tests. For ET1, the tension angle deforms to a state that the tension capacity of the section governs the behavior. In the compression zone, the angle displays bending deformation to the state that the angle folds into the column at the heel, causing the bolts to be in contact with the other leg of the compression angle, as seen in Figure 4.58. Behavior of the ET2 model is compared to the experimental test results shown in Figure 4.59. T-stub deformation is governing in specimen ET2 and this is evident in the model, as shown by the figure.

However, due to the column failure in ET3, other than the tension angle in bending, no major deformation is noticeable in the model as shown in Figure 4.60. Column deformation is evident in ET4 due to the increased concentration of forces acting on the column. The welding failure has reduced the length over which the angle is able to distribute the forces, thus putting greater stress on the column in small area, pulling out the column face, indicated in the comparison in Figure. 4.61.

In terms of plastic strain, the concentration location is dependent on the type of connection detail. Examination and comparison of each of the components in the connection provides a general idea on the behavior of the connection. The plastic strain is a response to the force transfer in the connection under the applied loads. For ET3 and ET4, the discussion is concentrated on the models with tearing as these models are closest to the actual experimental results and behavior. The different components for the reverse top-seat angle connections are the tension angle, compression angle, end plate, column and beam.

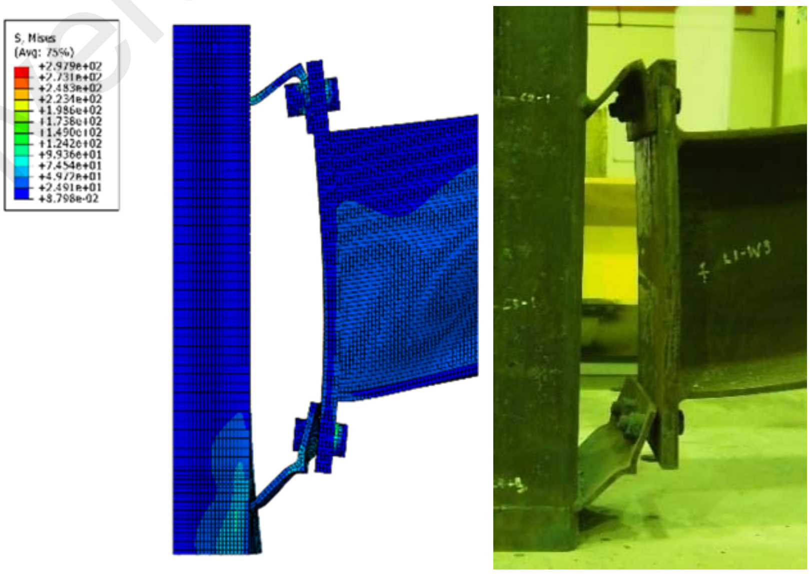

Figure 4.58 Model and Experimental Deformation Comparison for ET1

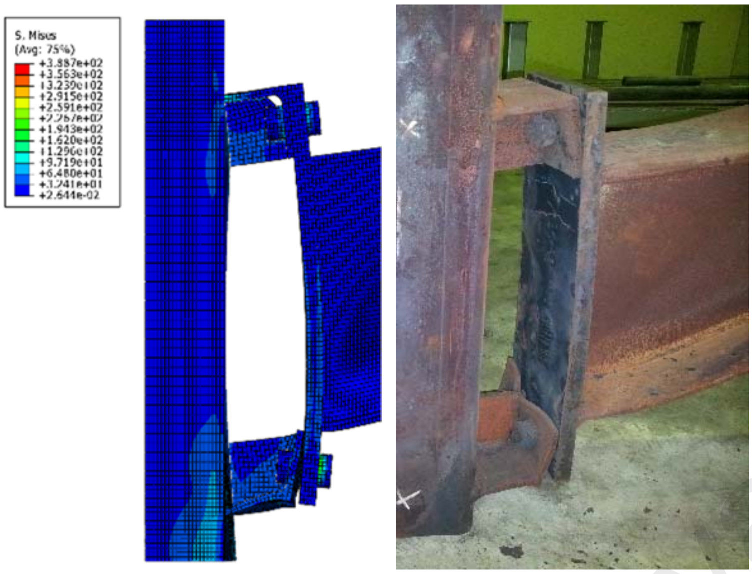

Figure 4.59 Model and Experimental Deformation Comparison for ET2

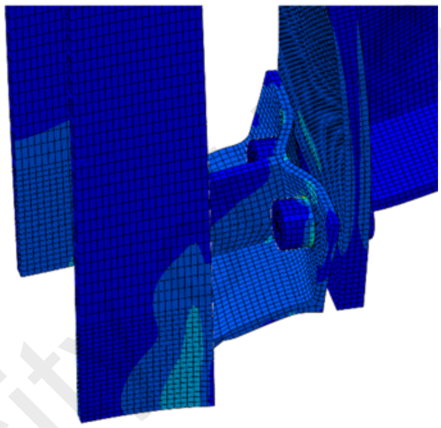

Figure 4.60 T-stub deformation of ET2 model

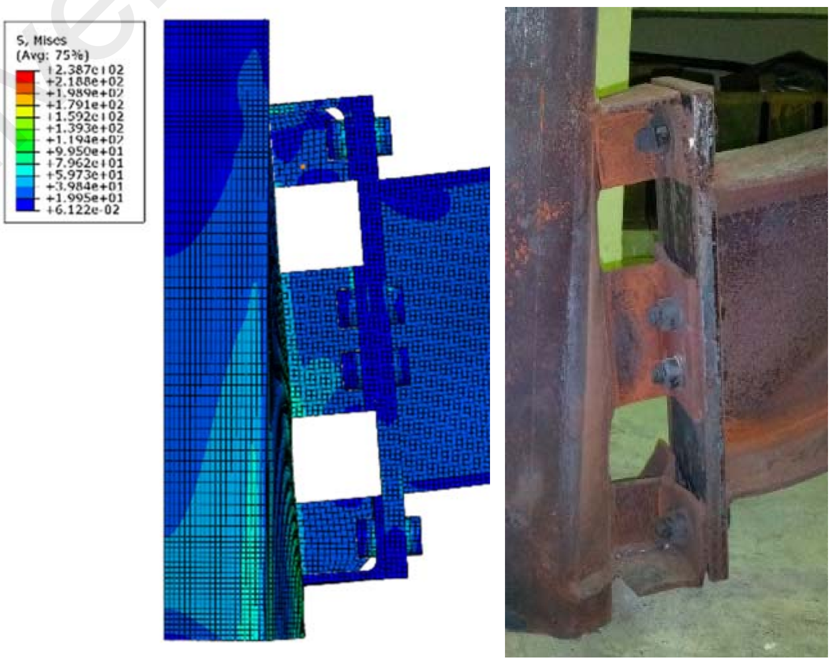

Figure 4.61 Model and Experimental Deformation Comparison for ET4

While ET1 and ET3 have similar configurations, with exception of the angle thickness of 8mm and 12mm, the plastic concentration for the tension angle for ET1 is focused on the heel of the angle and at the bolt hole area. Meanwhile for ET3 it is concentrated on the angle heel location and the edges of the welded edge, visible in Figure 4.62. Although this, the area is not concentrated on the whole thickness for ET3. Meanwhile, for ET2, the deformation is focused on the stiffener-connected area for the tension angle. As connection ET4 has load distribution to the mid-connection component, minimal deformation is shown for the tension angle. In addition to the mid-connection component, the weld tear reduces the force resistance of the tension angle, directing the forces towards the column by tension pullout from the column face. In which, both cases results in the plastic strain distribution at the angle component and focuses on the welded area for the tension angle of ET4.

Plastic concentration for the compression angle depends on the contribution of the tension angle as shown in Figure 4.63. In cases of ET3 and ET4, where the weld tear has been introduced, plastic concentrations are scattered and when compared to the tension angle, it is observed that the major plastic deformation occurs at the compression angle. For ET1, two bending hinges are observed, first at the welded length of the angle section and next adjacent to the bolt hole. While ET3 displays a similar pattern of deformation, the pattern is a result of compressive crushing as no visible bending is observed for the angle. Similarly, for ET4, the stiffener and angle are under crushing, producing the pattern shown in the model.

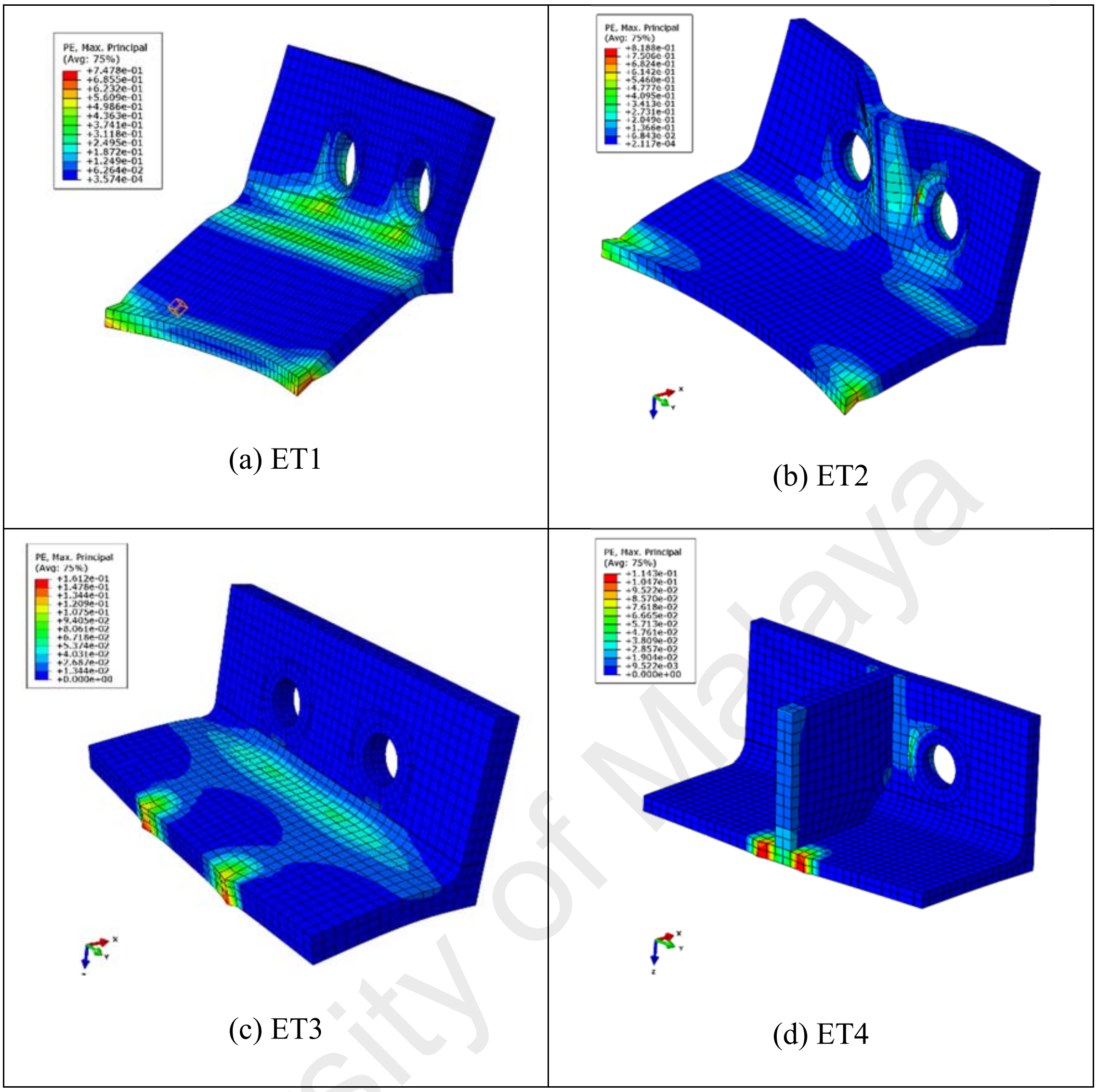

Figure 4.62 Plastic strain concentration of the tension angle for ET1-ET4 models

In terms of column plastic deformation, for ET3 and ET4 without the weld failure, it is expected to be similar to the pattern displayed for ET1 and ET2 in the tension zone. Both for ET3 and ET4 plastic deformation are concentrated at the center of column face due to the concentrated tension force exerted from the column tearing and weld failure, shown in Figure 4.64. In ET1 and ET2, tension distribution from the angle produces plastic strain on the sides of the column face, followed by pure tension from center of the angle, inducing the column face to result in a pullout behavior, thus showing the combination of both side and central plastic behavior. Meanwhile, in all models, no plastic strain formed on the bolts, resulting in possible reduction in bolt sizes.

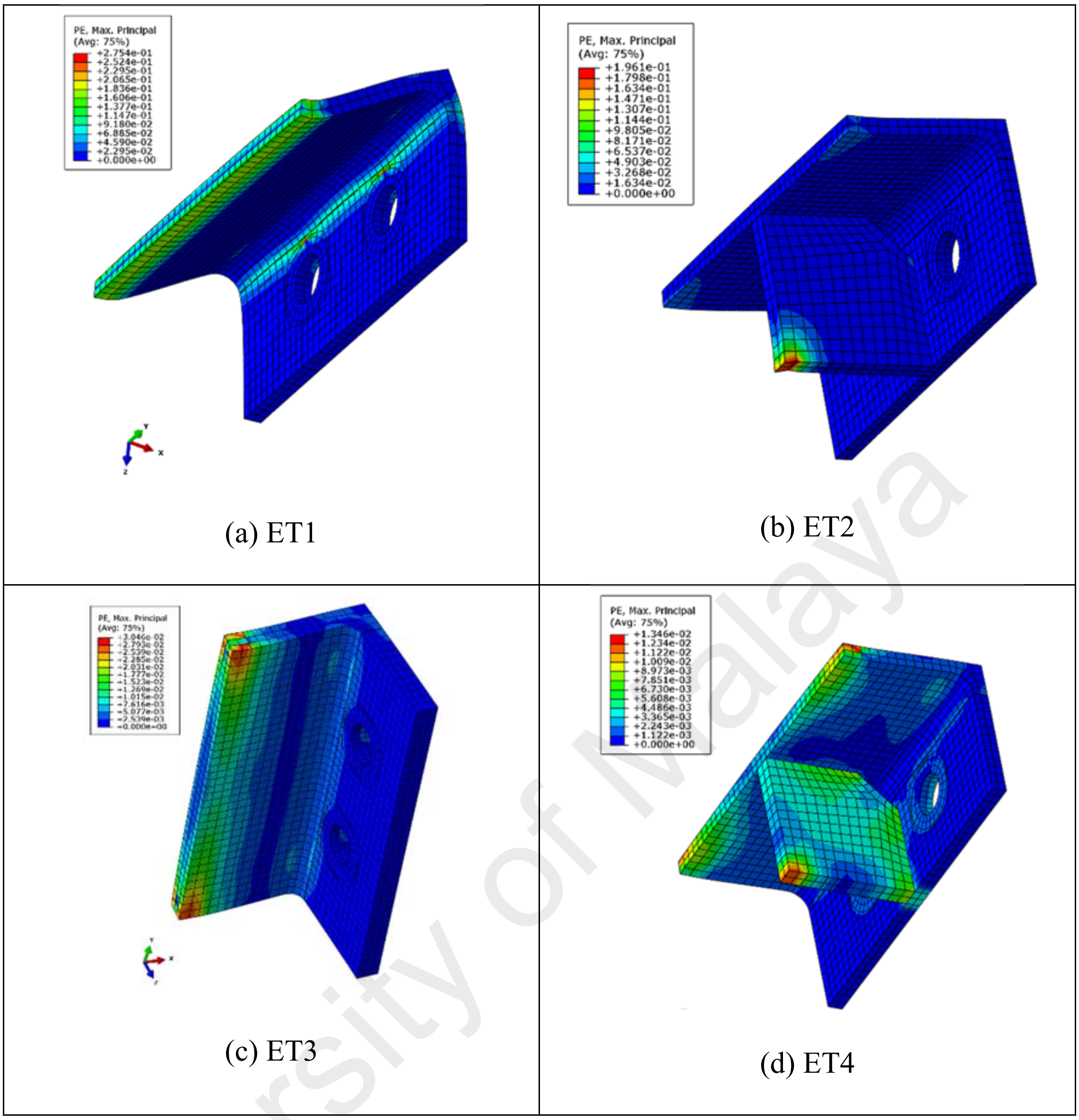

Figure 4.63 Plastic strain concentration of the compression angle for ET1-ET4 models

4.3.4 Expected Connection Failure Mechanism under Elevated Temperature

From the results and deformation seen in the test specimens of this study, the failure mechanism for reverse top-seat angle connection under elevated temperatures can be described as shear-tension. The applied first load at ambient temperature is only sufficient to cause minor displacements, enough to bend any components without restraint in the vertical direction as shear loads.

These loads will be resisted by the bolts and any floating components. This is evident in the comparison between ET1 of this study and AT1 of the study at ambient temperature where the end plate of AT1 is in bending while ET1 does not display this behavior.

Then as the temperature increases and the load is maintained, the beam begins to bend in reaction to the loads and increasingly weak material. This occurs approximately right before the yielding, which is about 500°C and the major force to be resisted by the connection is now tension. Up to the point where plastic onset begins, at about 600°C, the deformation of the column or the angle component, depending on the compared strength occurs. The deformation of the column will depend on either the angle thickness or the addition of stiffeners and mid-connection configuration. Finally, the beam buckles under combination of shear and catenary action acting on the beam.

4.3.5 Parametric Studies under Elevated Temperatures

Because ET3 and ET4 are governed by column tearing and welding failure respectively, only ET1 and ET2 are being considered for parametric studies in this work. Further experimental tests are necessary to study the effect of parametric variation on the reverse top-seat angle connection with higher angle thickness and with the mid-connection as existed in specimen ET4. The parametric variation includes the effect of uniform temperature on connection behavior, boundary conditions, and the effect of axial loading on the connection due to the existence of other structural members in proximity of the connection.

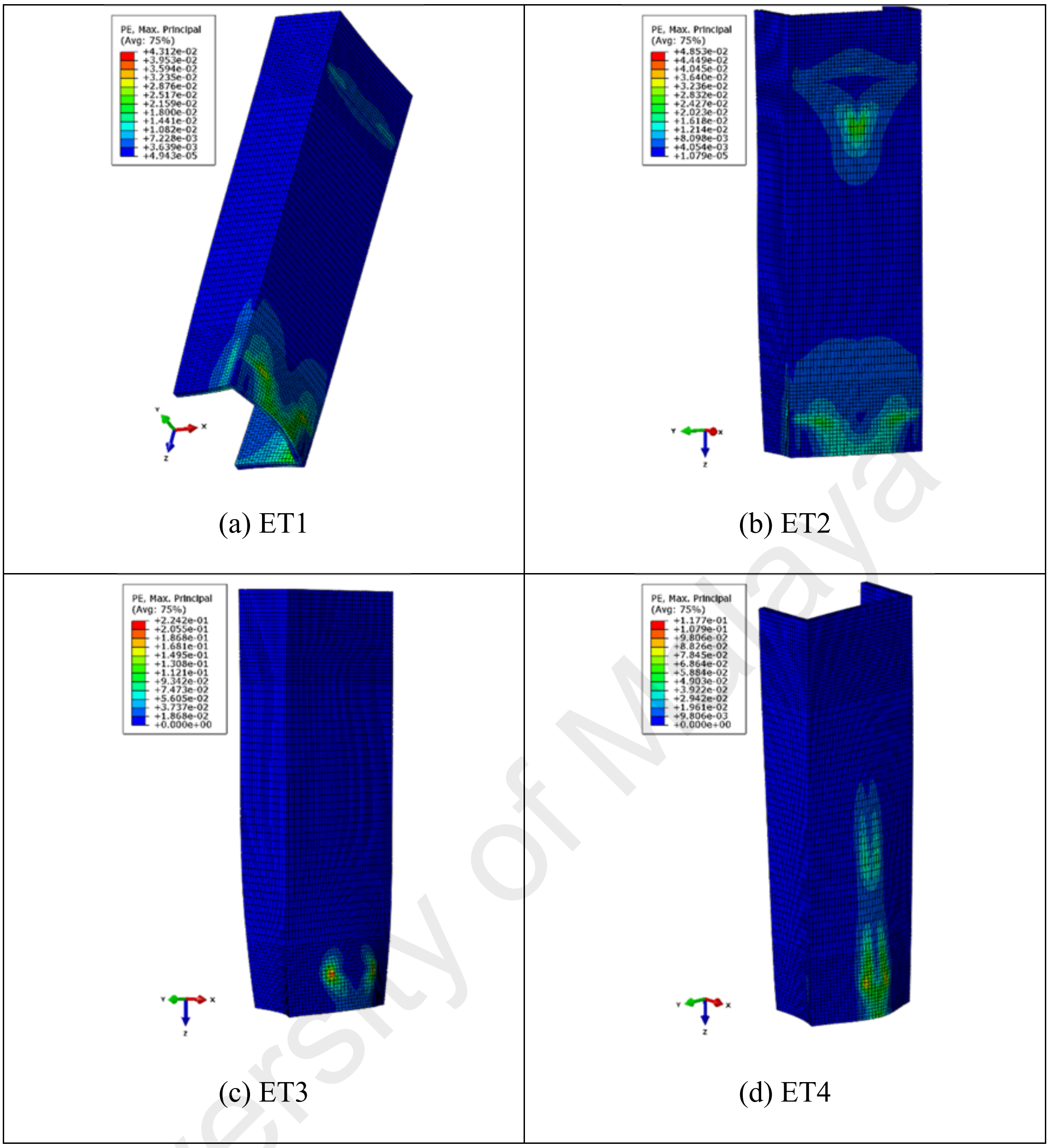

(a) ET1 (b) ET2

(c) ET3 (d) ET4

Figure 4.64 Plastic strain concentration of the column for ET1-ET4 models

4.3.5.1 Connection Behavior at Isothermal Conditions

In industrial structural design applications, machinery including broilers emit heat at a steady state and therefore, the surrounding connections are affected by the temperature at a steady rate, in which the isothermal condition design is applicable. While investigations in anisothermal conditions focus on the failure temperature for a connection given the fixed applied loading, studies in isothermal conditions is regarding the maximum moment for the connection for any particular temperature levels.

Determination of the failure in anisothermal conditions involves the intersection of the straight lines for both the plastic and elastic region, giving the temperature at which the connection yields. Meanwhile for isothermal condition, similar to ambient analysis, involves the intersection between the plastic and elastic region, resulting in the yield moment. In terms of material models, although the material models proposed by Outinen and Malakien (2002) is applicable for anisothermal heating conditions, as the material models have been applied for anisothermal models, the comparison is generally easier without using a different material model.

The selected temperatures for analysis of isothermal conditions are 100°C, 400°C, 500°C and 700°C. As shown in earlier sections, the degradation factor between 400°C and 500°C is a reduction of yield strength from 14% reduction to 40% reduction, in which the effect is shown by the results of the analysis. Meanwhile, at 700°C, on average the connection begins to yield, as shown by the results of the experimental tests. Material properties between 100°C and at room temperature is a minor difference of 3%, therefore, behavior with ambient temperature is expected to be minor with separate analysis at ambient temperature necessary. At other temperature levels, the connection behavior is between the selected extremes.

Under isothermal condition, the column deflection is used as the loading condition for the models and the reaction force measured as a result to produce the moment-rotation curve. Calculation of the moment is with the reaction force and distance of column face to the support. Meanwhile the rotation is calculated using the same distance with the respective deflection. Due to the same deflection values being applied on each of the isothermal models, the deformation pattern is similar and the difference between models are the forces required to achieve the deflection values and the concentration of plastic strain on the models.

4.3.5.1a Reverse Top-Seat Angle without Stiffener, ET1

The maximum column deflection for the model is set as 150 mm to coincide with the recorded result from experimental test under an-isothermal condition. Response of the connection in isothermal conditions for ET1 is as shown in Figure 4.65. When comparing to the behavior in 100°C, the stiffness for 400°C and 500°C is reduced by 28.2% and 38.3% respectively, while for 700°C, the stiffness is reduced by 90%. Reduction of stiffness is consistent with the reduction of the Young's Modulus value to 0.13 at 700°C, 0.7 at 400°C and 0.6 at 500°C when compared to the base reference at 100°C.

Meanwhile the yield moment is reduced by 24.2%, 48.5% and 87.9% for 400°C, 500°C and 700°C respectively when compared to the connection behavior at 100°C. The reduction factors for yield as shown in a previous section are 0.857, 0.619 and 0.105 respectively for 400°C, 500°C and 700°C, which are lower than the reduction in yield moment values. In terms of connection deformation, lower beam deflection at 150 mm column displacement is observed as the temperature increases. A clear distinction between the ambient temperature portion of the beam and the elevated temperature section in terms of beam bending between 700°C and 500°C models, where minimal beam deflection is detected for the ambient temperature section.

With the increase in temperatures, the angle components are increasingly making a critical contribution towards the behavior of the connection. As shown in Figure 4.68, deformation comparison for 100°C and 500°C shows minor differences in the beam deformation pattern but it is clear that the angle sections are relatively weaker, resulting in higher deflections. The compression angle is also similarly weaker under 500°C temperature when compared to the 100°C model. Under these isothermal conditions, the beams are the weaker component and therefore deforming first and contributing to the early stiffness, followed by the deformation of the angle sections, contributing to the difference in the plastic region. However, at 700°C, the angle sections control the earlier behavior and in the plastic region by the beam shear buckling.

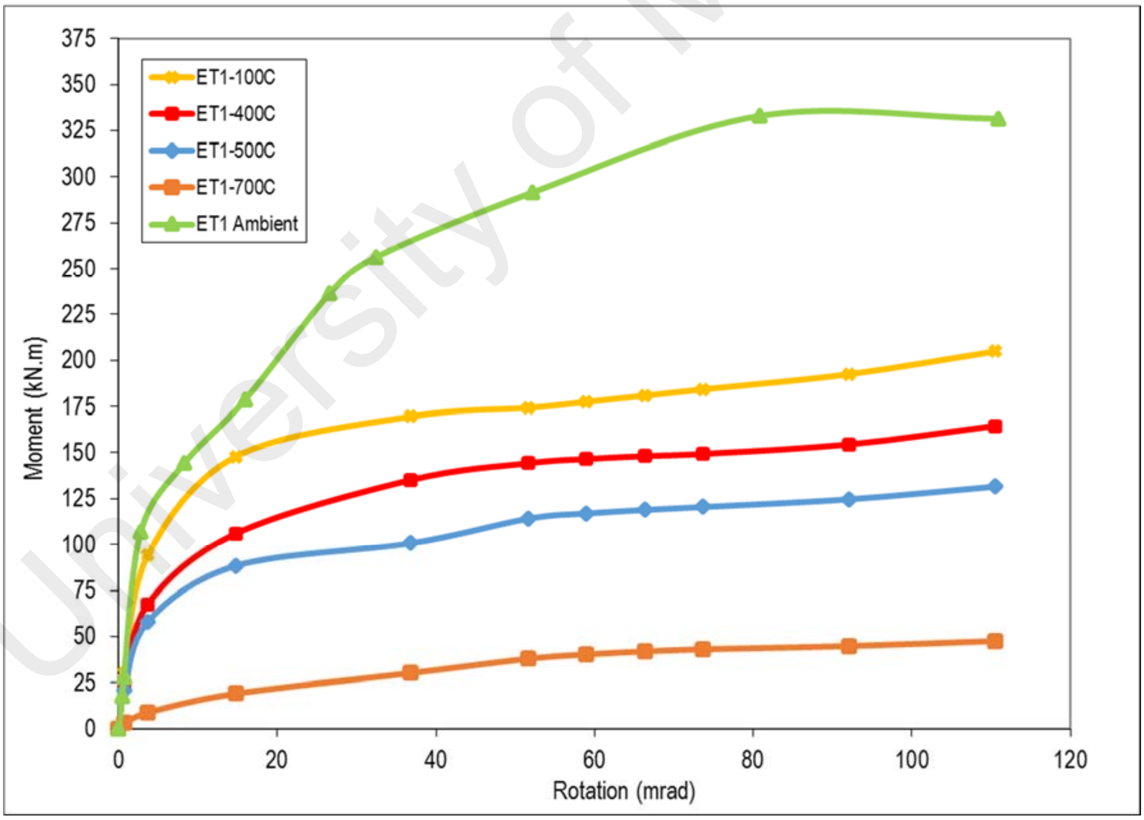

Figure 4.65 Isothermal response of connection ET1

4.3.5.1b Reverse Top-Seat Angle with Stiffener, ET2

Similar to the studies for ET1 in isothermal condition, 150 mm maximum column deflection is used for ET2 under isothermal conditions. Response of the connection when exposed to various levels of temperature are as indicated in Figure 4.66. As expected, from Figure 4.67, both stiffness and yield moment are reduced, at rates of 33%, 45% and 85% for 400°C, 500°C and 700°C respectively. In comparison the reduction of the Young's Modulus value is 0.13 at 700°C, 0.7 at 400°C and 0.6 at 500°C when compared to the base reference at 100°C, the reduction is slightly higher for ET2 under isothermal loads.

Meanwhile, yield moment values are reduced by 38% for 400°C, 44% for 500°C and 78.5% for 700°C. The reduction is inconsistent with the reduction factors for yield as highlighted in a previous section. Similar to ET1, the deformation difference between 100°C and 700°C is noticeable, with the ambient section beam deflection having minor results showing clear separation between the ambient and high temperature section of the beam.

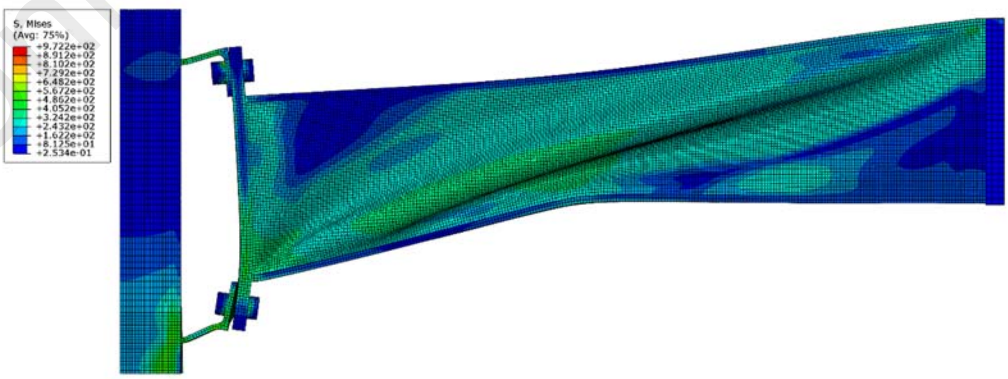

(a) Isothermal 100°C

Figure 4.66 (a-c) RTSA Connection deformation under

100°C, 500°C and 700°C uniform temperatures

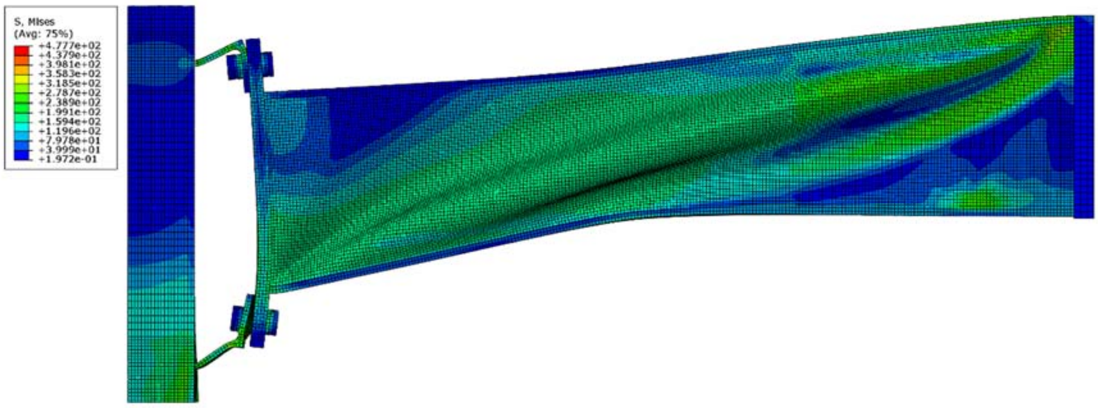

(b) Isothermal 500°C

(c) Isothermal 700°C

Figure 4.66 (a-c) RTSA Connection deformation under

100°C, 500°C and 700°C uniform temperatures

It is clear from the analysis results of the connection under isothermal conditions, that stiffness of the connection under any elevated temperature condition can be predicted with the reduction factors provided. Reduction in yield moment however, is inconsistent with the reduction ratio for material yield. Various factors are involved in the determination of the yield, as the resulting yield involves more than the material reduction considerations and more towards the stiffness contribution of each component. In addition, under similar loading applied to the anisothermal and isothermal models, the resulting deflection does not have the same value, showing that results of isothermal condition are not representative of the reactions under fire conditions and vice-versa.

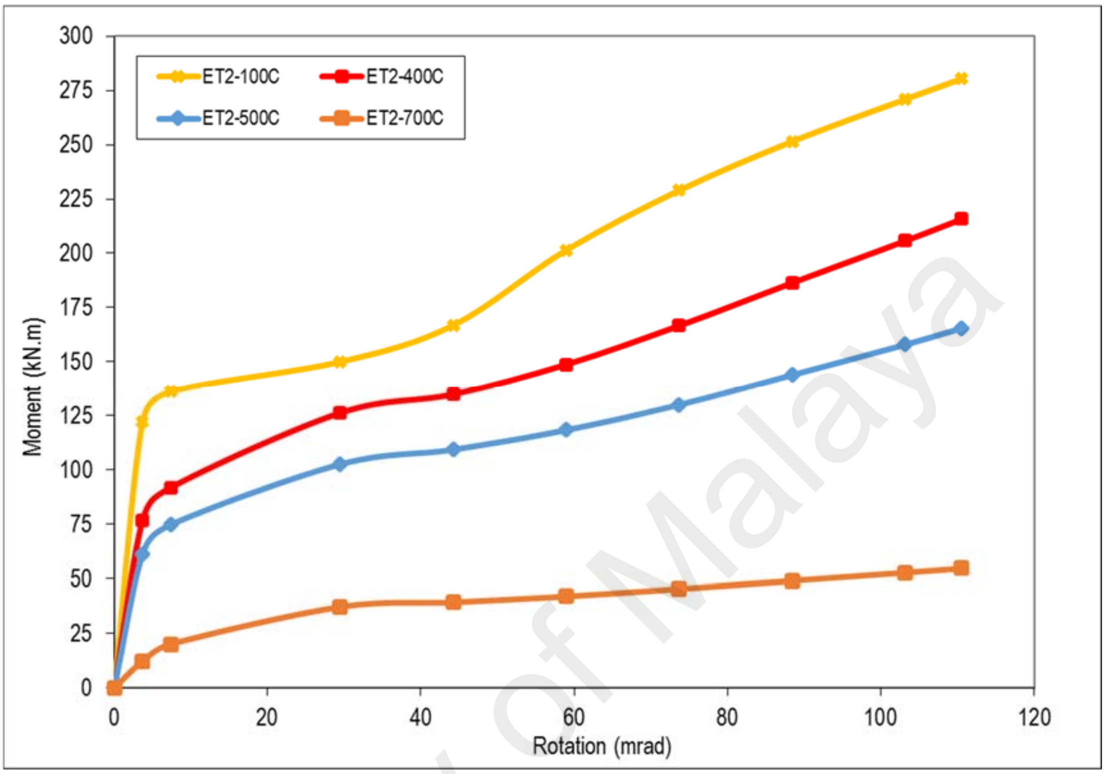

Figure 4.67 Isothermal response of connection ET2

4.3.5.2 Effect of Boundary Conditions

In the current experimental tests, the specimen is supported by the 'A' frames on both ends of the cruciform specimen. With the support frames, the specimen is horizontally restrained which prevents any horizontal movement of the specimen. Hogging moment acting on the beam combined with the catenary action of the beam results in the shear buckling in the beam web. The condition is simply supported located at 250 mm from the plate on the tension beam side, other boundaries and loading remain similar to the experimental test.

Response of connection ET1 with simple supports is as shown in Figure 4.68. In comparison with the experimental results of ET1, under similar loads, the direct effect of the boundary condition is the decreased stiffness and recorded column deflection at the plastic zone with 831% increase. In addition, maximum column deflection occurs at 742°C instead of at 805°C with ET1. In terms of deformation, from the moment loads applied by the simple support that is distributed into the compression and tension forces, the compressive axial forces induce the plate bending. In addition, the combination of the shear and moments induces localized crushing on the compression flange as shown in Figure 4.69. Angle bending governs the tension zone.

Similar to ET1, the response of connection ET2 under simple support shows an increase in column deflection when compared to the experimental test results, with an increase of 539% in deflection at 764°C furnace temperature as shown in Figure 4.70. However, due to the increased stiffness of the connection from the addition of the stiffener plate, instead of deformation at the connection components, beam resistance governs the connection behavior under simple supports. As indicated by Figure 4.71, localized buckling of the beam web occurs at an approximate distance of half of the beam length. The beam web buckling and bending occurrence is an extension from the shear buckling failure of the beam.

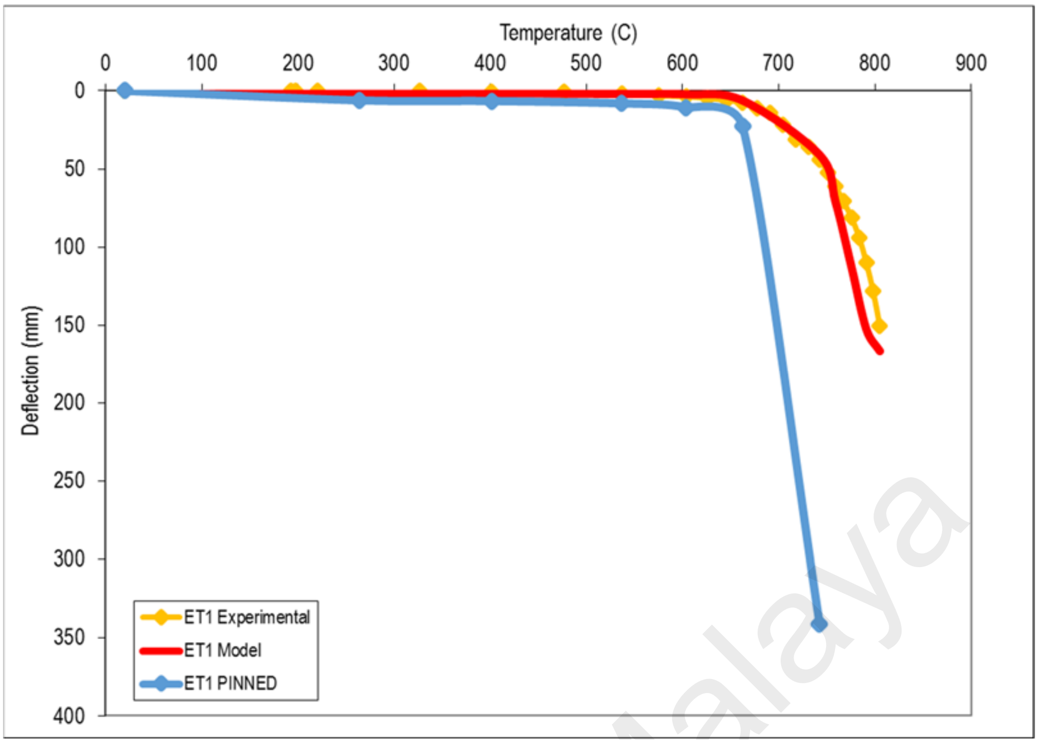

Figure 4.68 Response of connection ET1 in simply supported condition

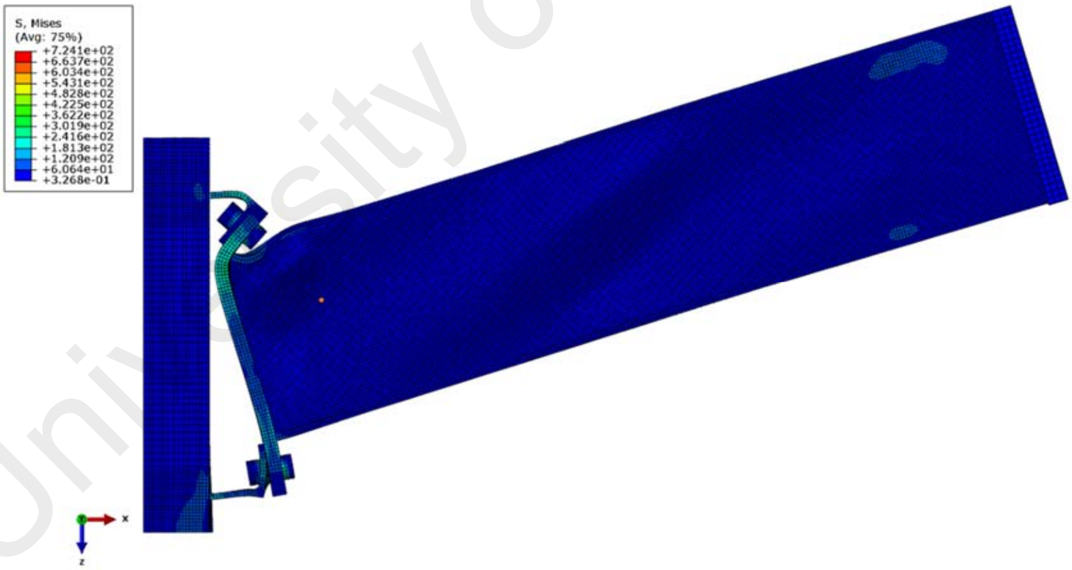

Figure 4.69 Deformation of RTSA ET1 connection under pin boundary conditions

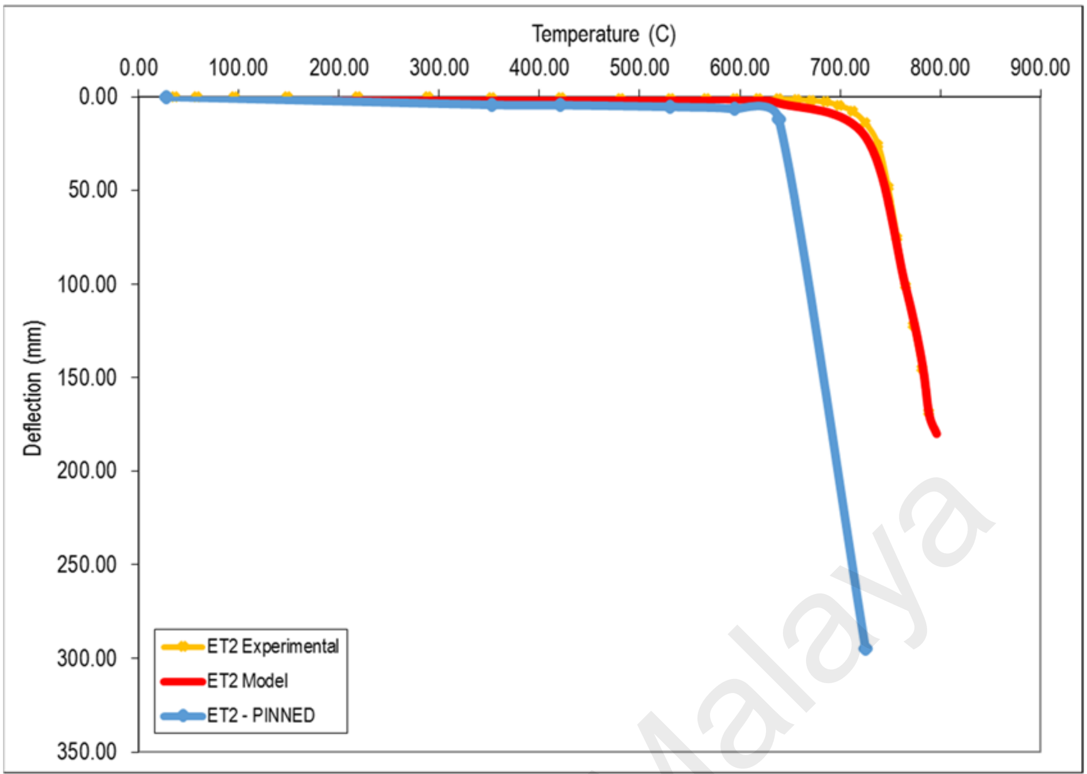

Figure 4.70 Response of connection ET2 in simply supported condition

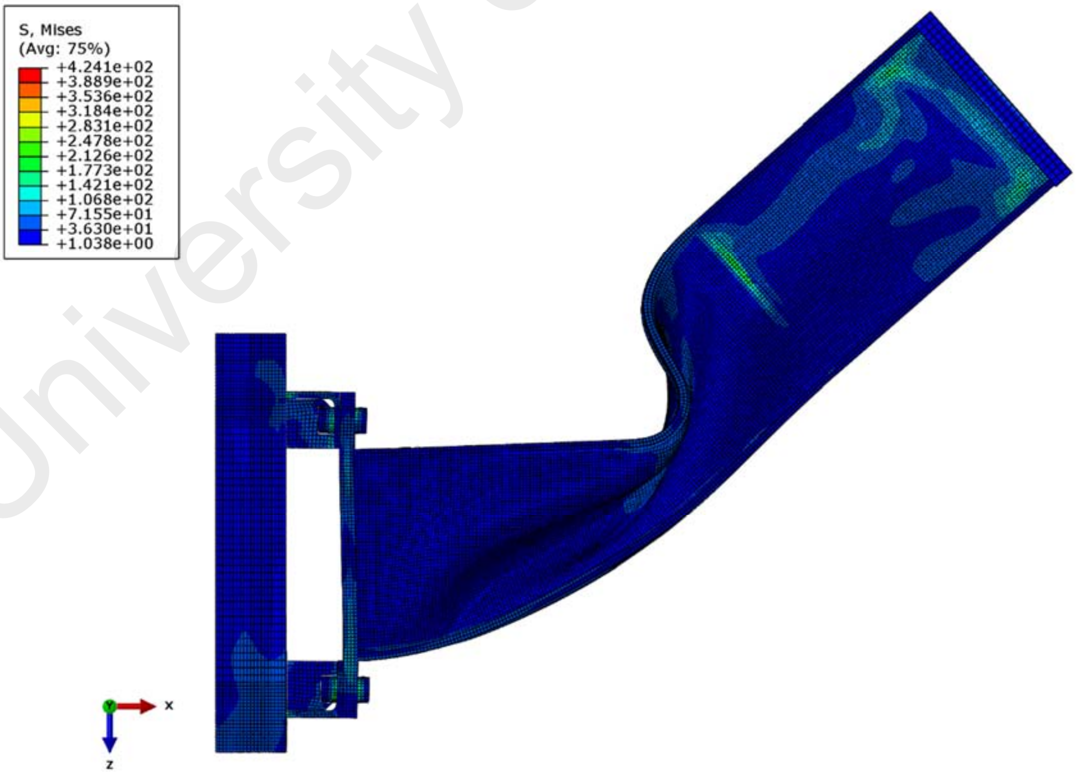

Figure 4.71 Deformation of RTSA ET2 connection under pin boundary conditions

4.3.5.3 Effect of Axial Loadings

Consideration at the effect of axial loadings is raised from the need to consider the thermal expansion of adjacent members. As temperatures of the steel material are raised, with expansion rates and length ratios described in an earlier section, the expansion results in additional stress and forces on other members. Axial loadings can also be further divided into compression and tension axial loading to cater for self-expansion under temperature and expansion due to other members in the vicinity respectively. The axial loading is derived from the reaction due to these expansions. In the study, model ET1 is utilized, with the modifications on the beam plate boundary conditions. Horizontal x-axis support on the beam end is released to allow for horizontal deformation of the model.

The numerical value of the applied axial loading is calculated as a proportion of the axial resistance of the beam cross-section. With section area for UB 305x165x40 kg/m of 5130 mm^2 and yield strength of 235 N/ mm^2 as defined in the material model, the resulting value is 1205.5 kN. EC3: Part 1-8 (2005) specifies that the moment resistance calculations for the design of bending moment capacity of the joint are only valid if the axial loadings do not exceed 5% of the beam cross-sectional capacity, therefore axial loading levels of 1%, 5% and 10% are selected, giving a value of 120.55 kN, 62.75kN and 12.55 kN respectively.

4.3.5.3a Compression Axial Loading

With the combined applied compression axial loading, tension forces from the distributed moment loads are reduced due to the counter direction forces. However, the compression zone effect is amplified from the additional compression forces acting. Comparing to ET1 model shows that the increase in compressive axial loading results in an increase in connection flexibility, with 10% compressive axial loading having the highest flexibility behavior as shown in Figure 4.72. It is observed that the 1% compression axial loading provides minor effect on the behavior of the connection, other than in the plastic area, which has reduced flexibility and deflection reduction of up to 22.17% at same levels of temperature. The end reduction is a result from the increased due to the shift from bending to shear of the angle cross-section.

With compressive forces preventing the development of angle prying in the tension zone, the deformation of the connection is reliant on the section bending of the angle component, resulting in the bolt in contact with the angle leg as shown in Figure 4.73. Continuous loading of the column results in the external face of the compression section being in contact with the column face, being crushed under load and the local buckling of the beam where the hinge is located near the intersection between the ambient and elevated temperature sections of the beam.

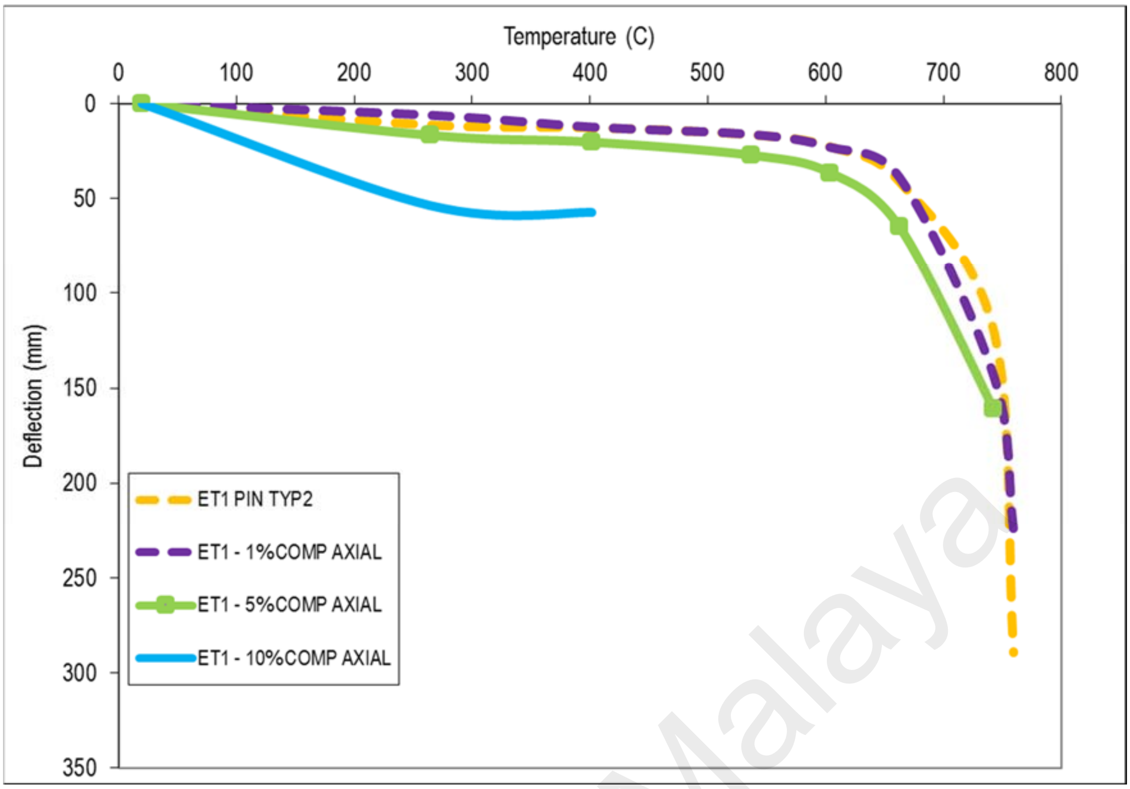

Figure 4.72 Effect of compressive axial loading on RTSA behavior

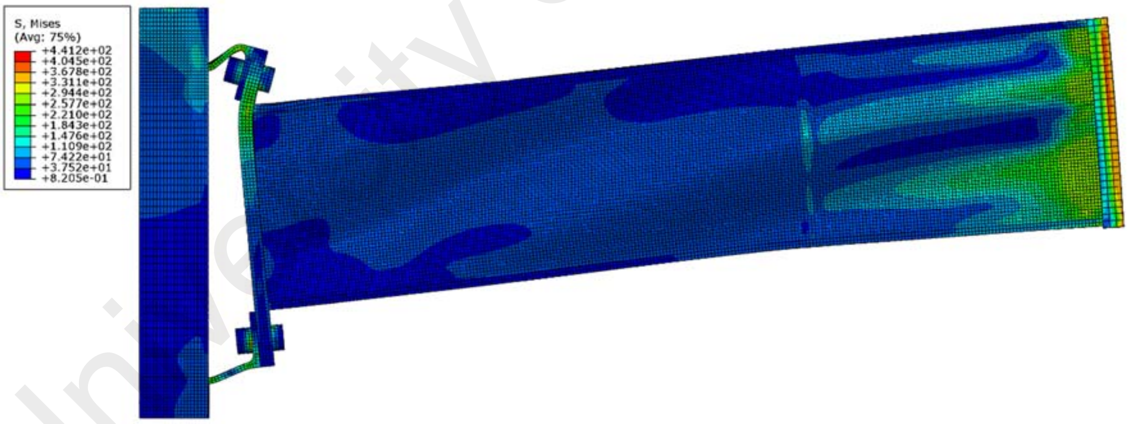

Figure 4.73 Deformation of RTSA under 5% compression axial load

in an-isothermal conditions

4.3.5.3b Tension Axial Loading

Under tension axial loading, the response of the connection ET1 is as shown in Figure 4.74 and Figure 4.75. Similar to the effect of compressive axial loading, the increase in tension axial loading reduces connection flexibility. However, 1% tension axial loading has minimal effect on the connection, with exception to the post-yield behavior, having reduced deflection under 10% tension axial loading. Under tension axial loading, contribution from the compression angle towards the connection behavior is reduced from the reduction of compressive forces acting on the angle, preventing the compression angle to display any major deformation until post-yield. Reduced deflection at the end of the connection is a result of the column face tension pullout, resulting in a shift in deformation pattern.

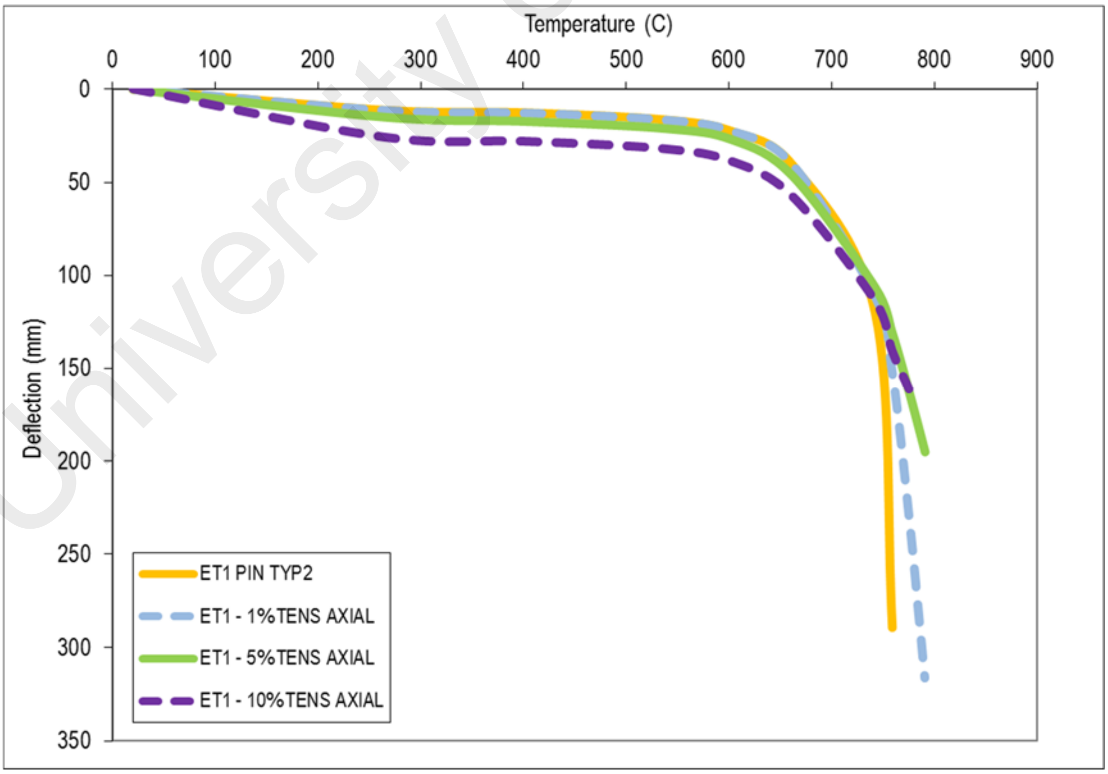

Figure 4.74 Effect of tension axial loading on RTSA behavior

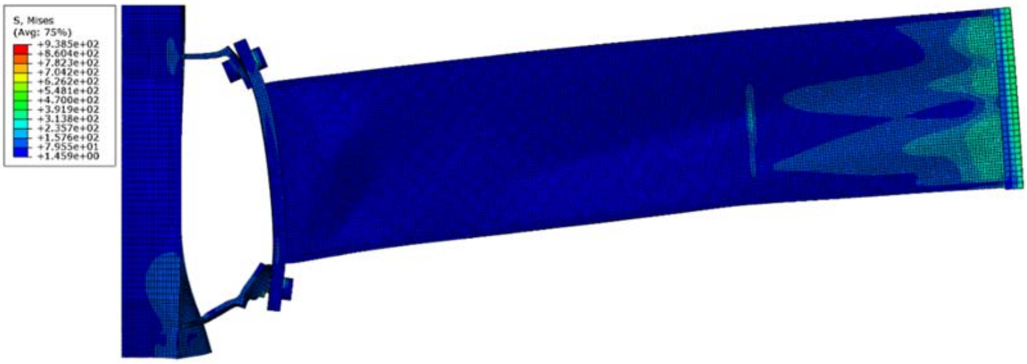

Figure 4.75 Deformation of RTSA under 10% tension axial load in an-isothermal conditions

At 1% axial loading, for either tension or compressive, the effect on the connection behavior is visibly beneficial post-yield as it reduces the deformation displayed. Between 5-10% however, the connection degrades with increase in flexibility and reduction in stiffness. Results from the model show that the RTSA connections does not adhere to the guidelines provided by EC3: Part 1-8 (2005) by showing that at axial loading of more than 1% beam section, the connection behavior diverges with increased flexibility. Guidelines provided by EC3: Part 1-8 (2005) on the axial loading are concluded to be insufficient to cater, and the percentage value of axial loading should be decreased.

4.3.5.4 Reverse Loading Condition

In the current research work, the angle section has a critical contribution to the behavior of the reverse top-seat angle connection. Under elevated temperature conditions, the experimental test shows that the temperatures for the top angle and bottom angle with difference of up to 6% and the bottom angle having the higher temperature. Current loading scheme results in the bottom angle behaving as the tension member while the top angle acts as the compression resistance component.

In actual loading conditions, the top angle with the lower temperature acts as the tension component and higher temperature bottom angle as the compression angle. By reversing the loading scheme, it is expected that the behavior has lower stiffness and higher deformation under similar loads. To study this effect, ET1 is chosen as the basis as it develops a distinctive deformation with angle bending in the tension zone and folded angle in the compression zone. Instead of loading on the top of the column, the pressure loads are applied from the bottom of the column facing -z axis, changing the direction of the load.

With ET1 as the basis, the response of the connection with the actual loading scheme is as shown in Figure 4.76, with lower deflection for the post-yield behavior when compared to the experimental ET1, with reduction of 14.8%. Lower deflection results from the increased stiffness from the lower temperatures for the tension zone. While in the compression zone, the increased temperature when compared to ET1, was not a major contributor to the connection behavior. Deformation of the reverse loading connection shows little to minor difference with ET1, which was using the experimental test-loading scheme as shown in Figure 4.77.

It is observed that while the deformation pattern is similar, the deformation severity is reduced under the reverse loading, especially for the tension angles. With the stiffer tension angle, the shear buckling in the beam occurs at two different locations, closer to the connection compared to the ET1 model as shown in Figure 4.78. It is also shown that at 759°C, the tension angle shows lower deformation on the column leg for the reverse loading. Due to the stiffer tension angle, the excess forces are concentrated on to the beam, causing earlier plastic deformation of the beam web.

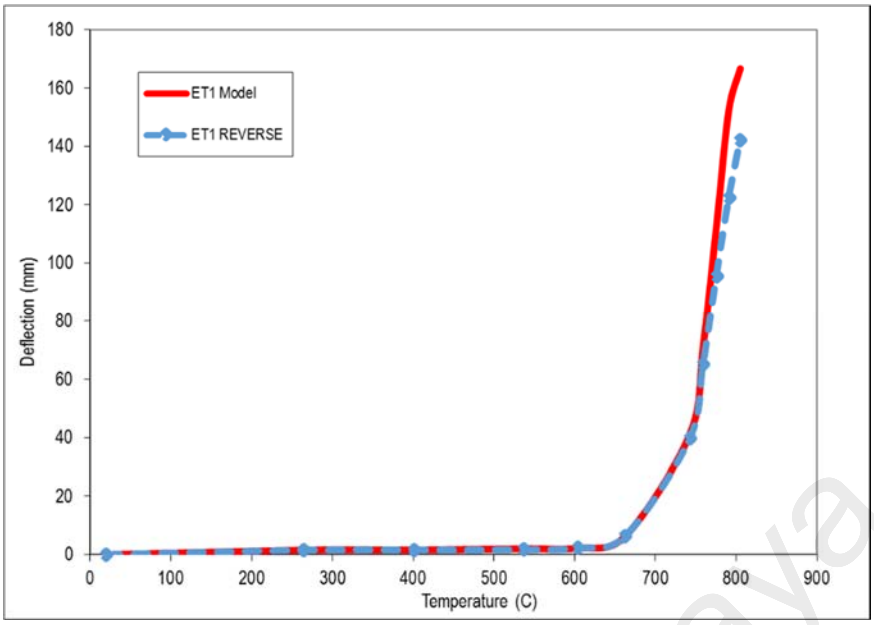

Figure 4.76 Behavior of ET1 under reverse loading in elevated temperature condition

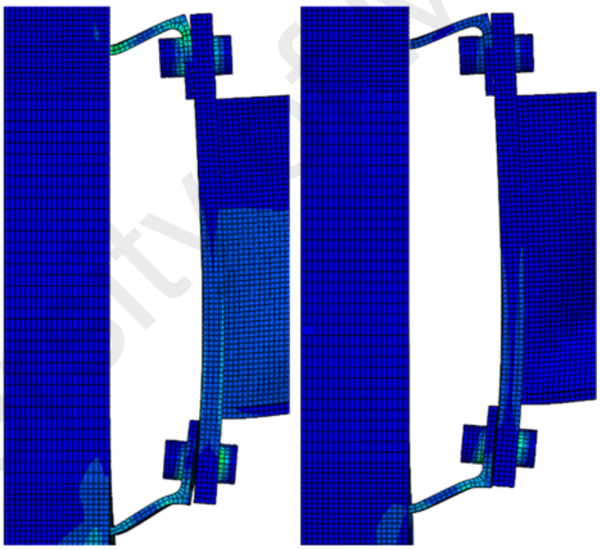

Figure 4.77 Deformation comparison between experimental

Loading (Left) and reverse loading scheme (Right)

(a) Reverse Loading

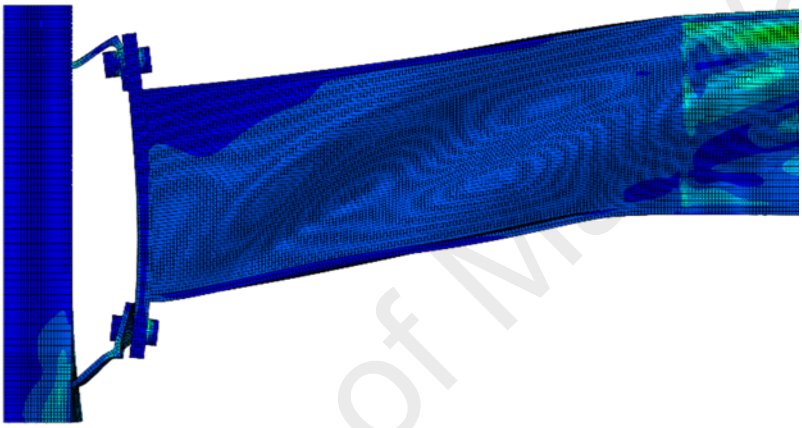

(b) Experimental Test Reference Loading

Figure 4.78 Beam shear buckling comparison

4.3.5.5 Connection Behavior with Average Temperature Ratio.

In practical steel joint design, the design for resistance in the elevated temperature condition focuses on the degradation of the material of each component due to temperature. Standard procedure includes thermal distribution analysis to determine the temperature of each component. For simplicity, the average uniform temperature is applied throughout the joint components. The difference from the isothermal analysis in the previous section is the effect from anisothermal conditions where the loading levels are fixed while the temperature increases. A possible scenario for this situation is a slow and steady heating of steel under constant loading.

In a previous section on the temperature ratio of the specimen as compared to the furnace temperature is highlighted. It is shown that the ratios are dependent on the current temperature levels. As the temperature levels increase, the average ratio between the specimen and furnace temperatures increases to a recorded ratio of 0.9 at 789.25°C. However, when the average ratio is used across all the connection components, the condition is similar to isothermal loadings. The difference is that the temperatures are different for each step, resulting in a *semi-anisothermal condition* as the loading remains the same. Models ET1 and ET2 are used to check the behavior of the connection under the semi-anisothermal condition. The average ratio as per Table 4.14, is calculated from the ratios detailed in the previous section.

As shown in Figure 4.79 for ET1, the average temperature ratio is less than the actual specimen temperature between 200°Cto 500°C. However, the average ratio is of average values between 600°C to 790°C. Meanwhile, Figure 4.80 shows that the average temperature is higher than the majority of components for ET2. From the temperature comparison graph, it can be deduced that the behavior for ET1 with average temperature has lower deformation at temperatures below 500°Cand higher deformation from 500°C to 790°Cdue to the higher than actual temperatures for the critical components which includes the compression angle, tension angle and end-plate. Instead for ET2 with average temperature, the deformation is expected to exceed the model due to the average temperature is consistently higher than the majority of components in the connection.

Table 4.14 Average temperature ratio for reverse top-seat angle connection

Furnace Temperature	Column	Top Angle	Bottom Angle	End-Plate	Beam Top	Beam Web	Beam Bottom	Average Ratio
Ambient	1.01	1.01	1.00	1.01	1.02	1.02	1.02	1.01
100	0.47	0.41	0.44	0.40	0.49	0.65	0.49	0.48
200	0.36	0.27	0.32	0.26	0.39	0.62	0.40	0.38
300	0.43	0.33	0.39	0.32	0.47	0.68	0.47	0.44
400	0.45	0.33	0.40	0.32	0.49	0.73	0.51	0.46
500	0.49	0.35	0.42	0.34	0.54	0.78	0.55	0.50
600	0.62	0.44	0.53	0.43	0.69	0.90	0.70	0.61
700	0.81	0.64	0.73	0.63	0.87	0.97	0.88	0.79
740	0.88	0.74	0.81	0.73	0.92	0.97	0.92	0.85
770	0.90	0.80	0.85	0.79	0.93	0.97	0.93	0.88
790	0.92	0.84	0.88	0.83	0.94	0.97	0.94	0.90
Average Component	0.66	0.55	0.61	0.54	0.70	0.84	0.70	

The comparisons between the average temperature models for ET1 and ET2 are shown in Figure 4.81 and 4.82 respectively. Under average temperature, the connections are comparatively more flexible for both ET1 and ET2 comparisons. For the ET1 comparison, the divergence begins at 275°Cand re-converges at 725°C. Meanwhile for ET2, behavior of the model with average temperature diverges from the 100°Cpoint and 750°C. The use of average temperature ratio, which defers from the actual experimental test results, assists in understanding the behavior of the connection and the contribution of the components.

For ET1 with average temperature, the increase in column deflection between 300°Cand 400°Cis justified with the closer temperature ratio at 400°Ccompared to the actual experimental ratio for the compression angle and end plate. This is then followed by a slightly higher average temperature ratio at 500°C. Subsequently, at 600°Cand

700°C, the average ratio is higher that for the tension angle. At a furnace temperature of 750°C, although the average temperature ratio continues to be relatively higher than the actual temperatures of the compression angle, end plate and tension angles, the beam web shear buckling dominates the connection deformations thus providing minor difference in column deflection when compared to experimental test connection behavior.

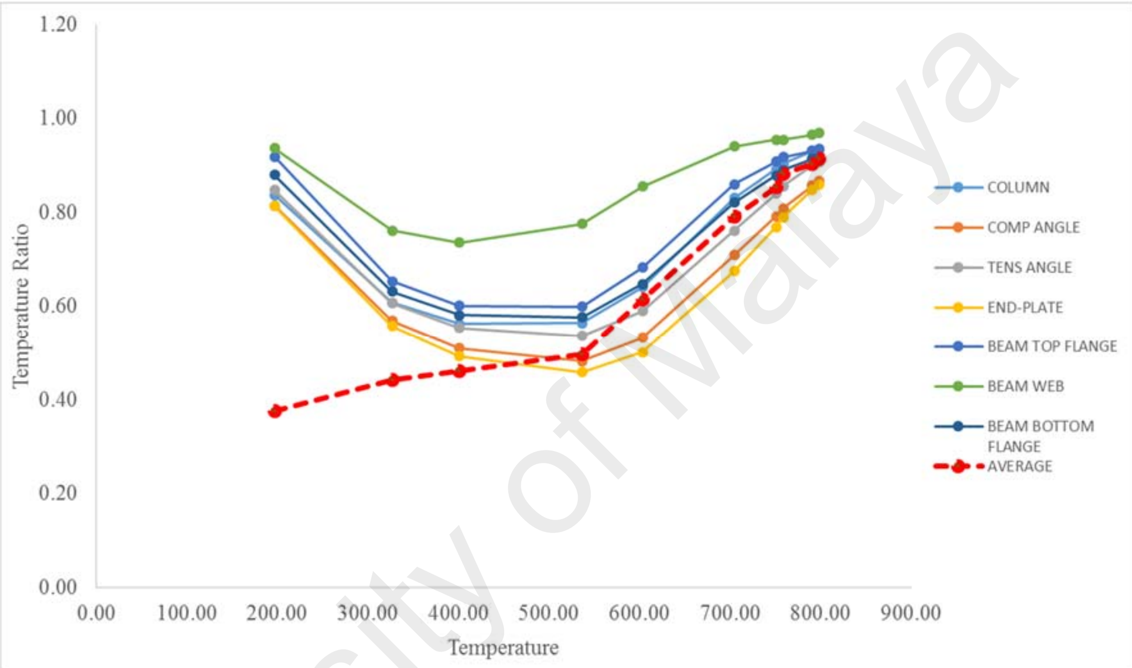

Figure 4.79 Comparison of average temperature ratio and component temperature ratio for ET1

Meanwhile, the behavior of ET2 with average temperature shows that the contribution of the beam towards the connection behavior begins at 740°C. The average temperature ratio at this stage is higher than the majority of components including the tension angle, end plate, and compression angle, but the column deflection is lower than the actual data recorded. Due to the actual temperature being lower than the average ratio, the column deflection of the model is lower, showing the effect from the beam. For temperatures lower than 700°C, the increased column deflection is justified with the average ratio higher than the actual temperature, causing the components to have decreased stiffness and strength.

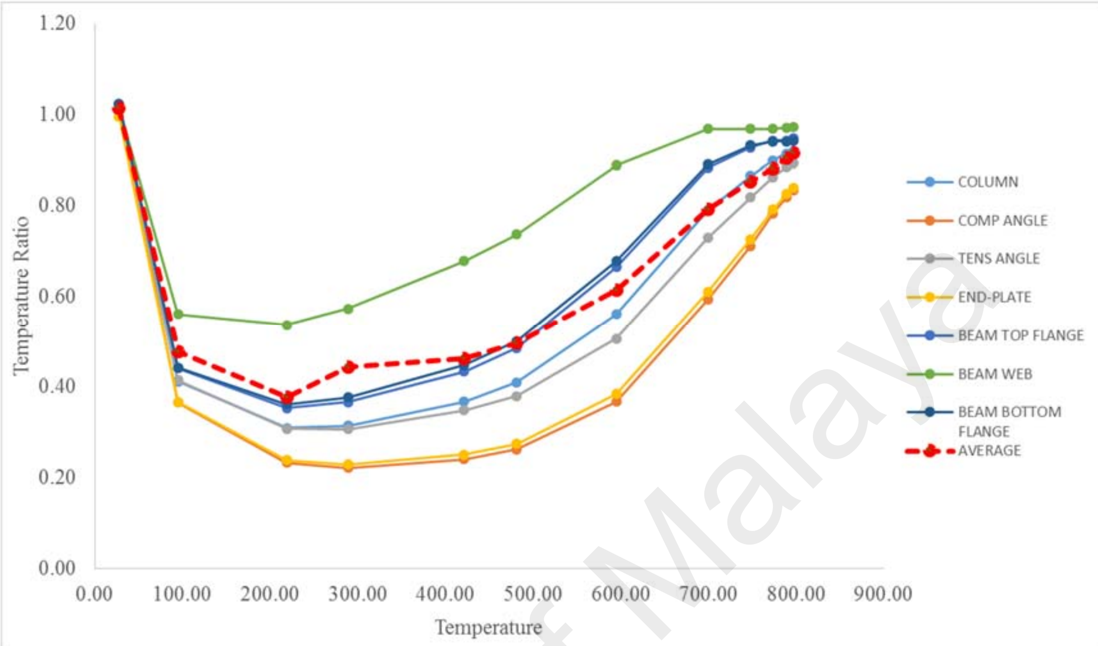

Figure 4.80 Comparison of average temperature ratio and component temperature ratio for ET2

From these results, it is clear that the shear buckling of the beam contributes to the deformation of the connection towards the end of the connection behavior post-yield, at approximately 740°C. Meanwhile the other components affect the earlier behavior of the connection, at temperatures below 740°C. With lower average ratio, at temperatures below 300°C, the effect is less critical on the connection behavior. Even at lower average ratio, the effect is minimal and there is little difference with the actual experimental behavior. While between 400°Cto 740°C, the difference between the average temperature ratio and is critical to determine the behavior especially when the temperature of the components such as the tension angle, compression angle and end plate differs from the average temperature ratio.

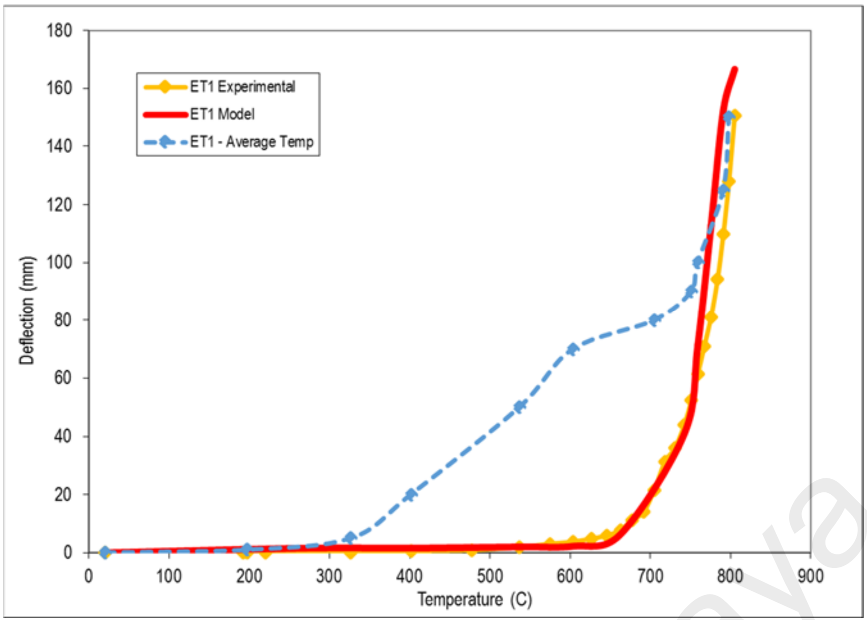

Figure 4.81 Behavior of ET1 with average temperature ratio

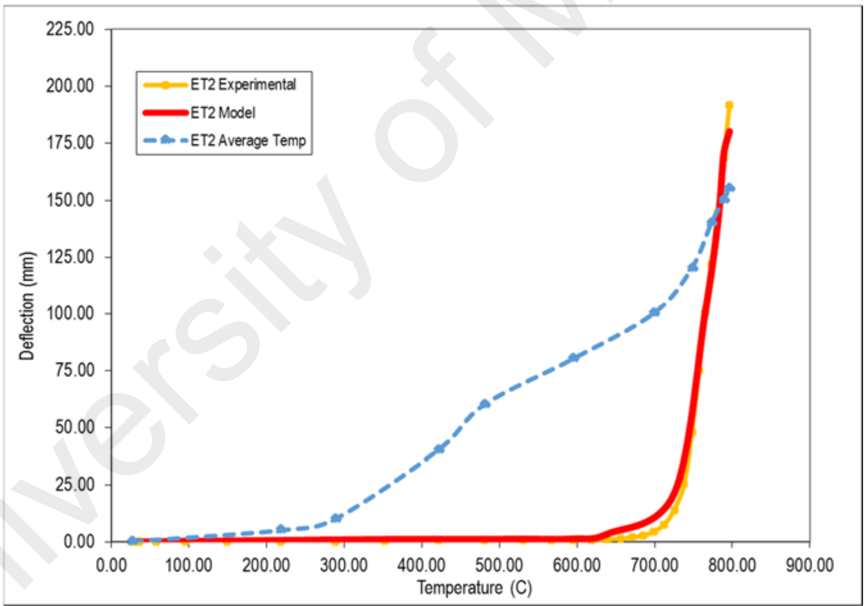

Figure 4.82 Behavior of ET2 with average temperature ratio

4.3.5.6 Behavior Relation between Ambient & Elevated Temperature

Due to the complexity in terms of temperature distribution for a connection, the design process is severely complicated. Previous studies have shown to be using the curve-fitting methods and the component method to accommodate temperature effect in the design of connections. In the component method, design for elevated temperature has basis on the application of relevant degradation factors and with assumption that the components and the connection in whole are of uniform temperature. However, it is shown in previous sections that using isothermal condition for the comparison basis does not provide the accurate representation of the behavior of the connection under elevated temperatures.

To simplify the design consideration, a design concept is proposed in this section with the use of elevated temperature design ratio of the ambient design results, which accommodates the resistance design for an-isothermal conditions. In the same method that connection design concerns often begins with ambient temperature analysis followed by the inclusion of temperature considerations. With the application of the ratio, the loads are multiplied by the ratio for consideration on the effect of fire conditions to achieve the same level of deformation exhibited at elevated temperatures.

To determine the ratio, model ET1 is subjected to ambient temperatures and displacement-loaded while other parameters including the boundary conditions remaining similar. For the elevated temperature condition model, it is known that the load remains constant throughout the various temperature levels. With the understanding, the required loads to achieve the displacement values at any particular temperature for the ambient temperature model, is compared to achieve the corresponding displacement values in order to obtain the ratio between ambient and elevated temperature condition design.

Results from the model analysis in ambient conditions are compared in Figure 4.83 while the ratio as indicated in Table 4.15. It should be noted that, similar to a previous study at ambient temperature the beam displays no visible shear buckling which is prominent in elevated temperature models. As the ratio table has indicated, the increase in temperatures has expectedly increased the load ratio required to accommodate the effect from elevated temperatures. It is expected that if the loads are increased to the level as indicated by the ratio, the beam shear buckling will be observed.

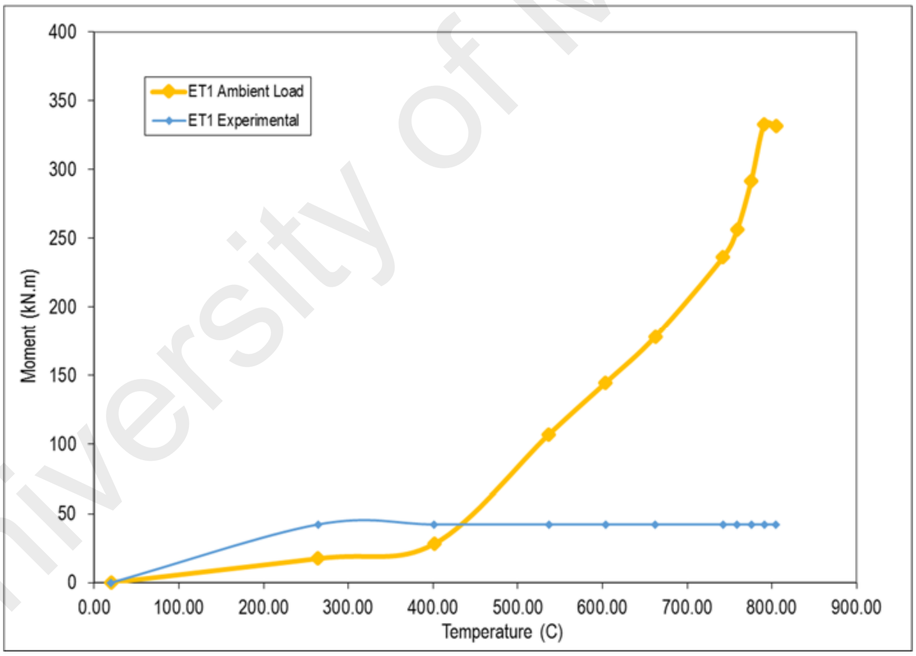

Figure 4.83 Moment Rotation Comparison for ET1 in Ambient and Elevated Temperature conditions

Table 4.15 Proposed Load Increment Factor for

Elevated Temperature condition design

Temperature	Load Increment Factor
264.33	0.41
401.40	0.67
536.57	2.53
603.50	3.42
662.43	4.22
742.43	5.59
759.07	6.06
775.60	6.90
790.93	7.87
805.07	7.83

4.3.5.7 Effect from Insulation of Angle Section

As discussed in the previous sections, the angle section has a critical role to the contribution of the capacity of the connection in general, therefore with the concept, by maintaining the capacity of the angle sections, resulting in a connection with greater capacity. By having the angle sections insulated, or having ambient temperature properties, the resulting performance of the connection is as shown in Figure 4.84.

Analysis results shows the critical contribution of the angle section post-yield and that the resistance of the connection at higher temperatures would be dependent on the angle sections. In addition, the results show that the early deformation of the connection is largely due to shear or the lack of shear capacity of the connection.

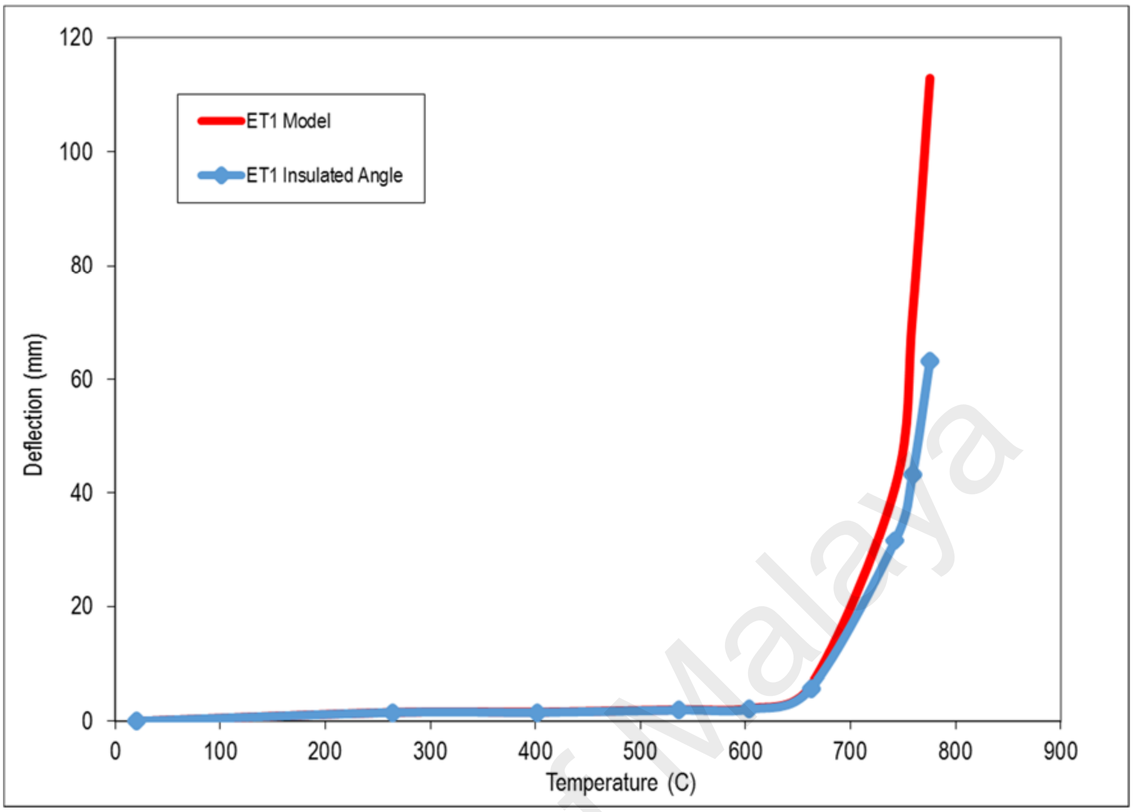

Figure 4.84 Behavior of ET1 with insulated angle sections

4.4 Discussion of Results

Under ambient temperature conditions, the behavior of top-seat angle connection is generally dependent on the end supports considered. With similar end conditions such as the experimental tests, moment loads are critical, while for pinned end support conditions, shear loads controls the connection behavior as seen in Section 4.2.3.8. Pinned end conditions are the standard considerations in actual designs, which limits the horizontal displacement of the beam flange. Similarly, deformation due to shear loading has been observed for elevated temperature tests, especially for specimen ET1 and is attributed to the support conditions of the experimental tests.

For moment controlling connections, the angle sections are critical in the tension zone while the end-plate thickness contributes to the compression zone capacity. Supporting the compression area at the beam flange location of the end-plate results in having to consider both end-plate and angle section thickness in the tension zone. By shifting the rotational point to a lower moment arm, a higher rotational force is required to achieve similar deformations, thus resulting in the deformation of the end-plate in the tension zone. As the angle section thickness decreases, the effect from shear forces are critical due to reduced flexural capacity of the angle sections as seen in the section on studies of connection behavior due to angle thickness of less than 8 mm. The effect is less visible for angle thickness of up to 12 mm. However, the effect from shear can be reduced by decreasing leg length for the angle connected to the column face (dimension 'B' in Figure 3.2) reducing the moment loads on the angle section.

For conditions where shear being the basic design loading, the angle section thickness controls the flexural capacity and thus connection capacity. To reduce the effect from the contribution of the angle section thickness, the simple solution is to introduce stiffeners welded in between the angle legs, thus effectively providing a higher rotational capacity with the high section modulus of the plate in the major axis. The result is the dependency on bolt prying action, similar to the connection to open section column. Although both cases are dependent on the angle thickness, however, the prying capacity has higher value than the flexural capacity in the minor axis of the horizontal leg of the angle section connected to the column face. Distribution of the forces to the column face must be checked in design then, assuming the stiffener plate as a point load and column face as a beam with the column width as unsupported length.

In comparison to similar basis connections (top-seat angle with reverse channel connection), RTSA manages to increase the stiffness and yield moment with relatively less number of bolts and components, even without the use of mid-section angle sections. While for end-plate and reverse channel connections, performance of RTSA in comparison are reduced stiffness and yield moment, which can be deduced to be from the lack of shear stiffness which the reverse channel had. As described in the previous paragraph and from FE analysis results, the performance of RTSA can be improved over by adding stiffener plates in between the angle section legs. In addition, the strength-weight ratio is relatively higher with RTSA and stiffeners compared to the two connections with reverse channels. While further studies are required, it is expected that the RTSA connection can be further stiffened with fin plates that may increase the rotational stiffness, increase yield moment values and reduce shear behavior tendency.

Under elevated temperature conditions, it is observed in this study that the deformation pattern for the connection components does not vary with ambient temperature conditions; however, comparisons should be made towards the respective support conditions defined. On the other hand, the beam under elevated temperature conditions deforms under web shear buckling. Designing for loads under ambient temperature with yielding of the components / material being the limitation, the connection shall be able to withstand up to 700°C, which is approximately 30 minutes according to the ISO 834 fire curve. Undoubtedly, the build-up of an actual fire is slower than the expected temperature of the ISO 834 curve, prolonging the onset of yielding under elevated temperature conditions. Temperature of 700°Crefers to the external furnace temperature recorded.

As discussed in the literature review, under elevated temperature conditions, a common indication of ductility shows the beam having high deflection values while maintaining connection integrity. High deflection values is also indicative of catenary action developing in the beam and connections. As the results of the experimental tests and deformation from FE analysis show, with the high beam deflection recorded in ET1 and ET2, the RTSA concept has a high beam deflection recorded under load and develop the necessary catenary action to resist the additional forces. With this, RTSA is able to reduce the eventuality of the progressive collapse of the structure, which is provided by the tension capacity of the angle section as after it has deformed under shear loads. Ductility under tension is considered sufficient ductility to resist additional tension loads from the cooling period after loading under elevated temperature conditions.

To design for connections under temperature loads, the standard method is to first conduct a temperature distribution study followed by the application of the relevant degradation factors for the materials. Often for simplicity, the temperature distribution is assumed uniform throughout the connection and the design is based on a uniform degradation factor throughout the connection components. However, FE analysis shows that isothermal temperature analysis does not reflect the forces developing in the connection under anisothermal conditions or fire case. In addition, the deflection values under isothermal conditions do not reflect the values for anisothermal conditions even under similar loading values as the result has indicated in the previous sections. To reduce the work for elevated temperature analysis, it is proposed that the analysis to be done for a few specimens and to simplify the difference between ambient and elevated temperature with ratios. The proposed ratio for RTSA is as shown in Table 4.15 earlier and indicated that loadings are as high as 7.8 multiples of the considered ambient temperature loadings.

Subsequently, after the high temperature phase, following is the cooling phase. As Sun et al. (2015) has discussed, the cooling phase of the connection after elevated temperature action involves in additional tensional forces developing in the connection as the material reduces the temperature to the original state from the expansion in steel at elevated temperature. Studies on the effect tension loads of up to 10% indicate that minor changes in the connection performance for up to 5% and at 10% of the cross-section tension loads result in a 20% in decrease in performance. While the axial loads has not been recorded in the test, considering that the cooling phase will reduce the temperature and therefore higher degradation factor value of the material, it is expected that the effect of tension axial loads on the connection would be less critical.

4.5 Results Conclusion

Results from both ambient and experimental tests are detailed in this chapter. Under ambient temperature, the addition of stiffener plates clearly increases the performance of the connection while thicker angle sections provided stiffener connections. Meanwhile, tests under elevated temperature shows that 700°C is the critical temperature where the majority of the connection begins to yield regardless of the ambient temperature capacity comparison. Validation of the experimental results shows close accuracy of the FE Models in both ambient and elevated temperature tests. Models under elevated temperature conditions is also able to replicate the failures, due to welding, however must be identified beforehand as the implicit method used by Abaqus cannot reproduce ultimate failure under the standard circumstances. A number of parameters has been studied including the effect of angle thickness, angle gauge length and angle leg lengths. In addition, by comparison with existing connections to tubular columns, RTSA connection has shown a good potential with higher performance capcity.

CHAPTER 5

CONCLUSION AND RECOMMENDATIONS

5.1 Conclusion

Literature review has shown that tubular columns are gaining increased usage in the construction industry due to its versatility and possibility of steel usage reduction due to the various advantages over the common open section columns. However, connection of these open-section beams are an issue due the cross-section limitations of the column. Welding and blind-bolts as the major structural component for a connection are both acceptable solutions but several disadvantages have been found with the use of both options and thus requiring a different approach.

In this study, a connection for open section beams to tubular columns is proposed. The connection consists of welding two angle sections on to a tubular column, while a beam welded to an end plate is bolted to the angle sections to complete the connection. This connection uses less welding and does not require blind bolts as the connector components. In addition, there are still plenty of space for additional components that may increase the connection capacity or for specific purpose such as increasing the ductility of the connection. The connection configuration is studied under both ambient and elevated temperatures consisting of experimental tests and finite-element based simulations. From the results and findings shown in this work, the following conclusions can be made with reference to the objective:-

1) The reverse top-seat angle connection (RTSA) has been developed as a new connection configuration to be explored and investigated with the combination of both welding and standard bolting. Development of the connection is based on the concept of material reduction, using minimal steel components, and flexibility due to the empty area at the mid area of the beam, which provides space for additional components to enhance the connection detail, depending on the required characteristics. Justifications for the member sizes tested in this current study are as indicated in Chapter 3.

Although other configurations are available, the other connections, such as the RCE and RCTSA connections, display a relatively lower ductility behavior when compared to the RTSA connection. The new connection was tested with static loading under both ambient and elevated temperature conditions. Three specimens are tested in ambient temperature while varying the angle thickness and stiffener plate. Under these boundary conditions, the connections display a angle bending and plate bending critical behavior. It was observed that from both experimental and FE results that the major deformation is dependent on the support conditions used. Meanwhile at elevated temperature conditions, four specimens are tested, varying in angle thickness, stiffener plate and mid-connection component. The elevated temperature specimens are tested with fixed load values with the temperature condition provided by a large-scale industry furnace.

2) Finite-element models are developed in ABAQUS with validation of procedure from test of other connections while the general model and parametric assumptions, including material, boundary conditions and the loading condition with the experimental results. Difference between the validation model and

experimental results are at an approximate 5-10%, showing acceptable accuracy of the model. In terms of elevated temperature models, the reduction factor proposed by Outinen and Makelainen (2002) is used and the result from the validation analysis shows that the factors provide a good accuracy with the experimental tests. On the other hand, the analysis models also show that static loading can be utilized to model the behavior under fire conditions and it is not necessary to conduct thermal distribution analysis due to the uniformity of material.

3) Under both ambient and elevated temperatures, parametric studies have been conducted and the resulting analysis shows that the end-plate thickness, angle thickness, and addition of stiffener affects not only the performance of the connection but also deformation pattern, leading to the difference in the component contribution. Besides the geometrical parameters involved, other structural considerations have also been studied, showing that boundary conditions and loading method determines the deformation pattern of the connection and loading resistance. Reducing the degrees of freedom by changing the boundary from pinned/roller to bolted pinned supports increases the load resistance of the connection. Other major study results includes:-

   a. Studies were made on the effect of various parameters and geometric details and it was found that the plate thickness, angle thickness, gauge length, angle length and the addition of stiffener has a significant effect over the behavior that was presented in a moment-rotation form. The effect from these parameters, other than from stiffeners, are justified through the distribution of moment loads into tension and compression forces acting on the connection. With simple support condition, no constraint for beam in terms of horizontal displacement and thus, flexural major behavior. With study based on the various geometrical modifications, it can be clearly seen increasing plate and angle thickness, reducing gauge and angle length results in an increased connection capacity performance.

b. While the semi-flush plate configuration is shown to reduce the yield design moment by 10%, the post-yield moment increases, thus increasing the ductility of connection. Flush plate configuration on the hand reduces the yield design by 25%, but continues to provide post-yield resistance. Ductility of the connection is related to stiffness and yield of the connection where a lower value is usually associated with high ductility due to the higher end moment values. As ductility involves in the failure moment of the connection, a higher failure moment results in higher ductility.

c. Isothermal condition analysis is shown to be unable to represent the behavior of the connection under fire conditions. Results from isothermal condition indicates that the temperatures could possibly be higher than the actual temperature of several components and thus affect the order of load transfer and deformation.

d. Comparison of ambient and elevated temperature shows that at higher temperature levels, a factor is to be included into the design to cater for the degradation effect from elevated temperature conditions. For the reverse top-seat angle connection under anisothermal elevated temperature condition, the ratio value exceeds 7.0. Minor difference in the deformation pattern of the connection under ambient and elevated temperature is observed, therefore implying that the use of the load increment factor is a feasible and simple method without considering the thermal distribution analysis.

e. The reverse top-seat angle connection is sensitive to the effects of axial loading as both compression and tension axial loads decreases the flexibility of connection, between the 5-10% cross-section capacities were studied in this research. Inclusion of the axial loading increases the effect from the relevant angle and plate component. The effect of the cooling phase can be attributed to the results of the FE analysis with tension axial. It is shown that tension forces up to 5% of the cross-section values has minimal effect on the connection. Additional compression axial forces is similarly, minor effect up to 5%. It should be noted that internal compression forces are also developing due to the degrees of freedom. No thermal expansion has been specified for the FE analysis as previous research has shown that

f. Shear deformation is the major deformation in the RTSA connection under actual construction support conditions. This is increasingly evident in elevated temperature conditions where the angles Reduction of shear deformation is done through the application of stiffener plates where the contribution of the shear resistance is from the flexural capacity of the stiffener plate.

4) Performance of the proposed connection is compared under ambient temperature conditions due to the complexity associated with elevated temperature conditions including the variation in temperature, geometrical issues and material differences. Under ambient temperature conditions, the RTSA as compared to the reverse channel and angle connection has higher performance in terms of yield and stiffness of at least 44% and 14.6% respectively for both performance parameters. Meanwhile, compared the reverse channel end-plate connection

(RCE), the reverse angle top-seat angle connection is comparatively lower in terms of stiffness by 50%. Strength to weight ratio is also evidently greater in RTSA, showing higher potential and flexibility, further supporting that the connection concept of having minimal components and fabrication.

However, the addition of a stiffener in RTSA increases the resistance of the connection, resulting an increased yield moment of the connection and results in 57.6% higher than RCE connection. In addition to the connection type and beam size, material properties must also be taken into consideration for connection performance comparison due to the various configurations possible. In comparison to RCE, which has stiffer resistance to vertical shear, due to the orientation of the reverse channel, the standard RTSA has minimal resistance due to vertical shear. This however is advantageous in elevated temperature condition due to the increased ductility and the ability to develop catenary action, which are critical in resisting the additional loads and forces from the distribution of loads because of adjacent localized failure in a structure. Effect of shear deformation allows the connection to modify the tension resistance from angle bending and bolt dependency to angle tension for catenary action.

While the shear deformation is a cause for concern for the RTSA connection, this can be mitigated with the addition of stiffener plates. Combined with the high strength to weight ratio, this connection type can be applied in actual construction even under elevated temperature conditions. As evident from the study results, the connection has good ductility and the ability to develop catenary action while also able to maintain capacity even with high deflection of the beam in the event of a fire. As the fire recedes, or under the cooling phase, the additional tension loads applies but the connection is still able to maintain the applied loads without failure, making the connection ideal for both ambient and elevated temperature. In addition, the connection capacity is expected to be improved with additional components such as fin-plates or end-plates at the beam-mid area, making the connection highly customizable to demand.

5.2 Recommendations

For future studies, the following recommendations can be made:-

1. Reverse top-seat angle connection can be studied in earthquake / dynamic loadings to determine the ductility performance under these loads.
2. Due to the gap at the beam central area from the focus of the connection components at the top and bottom of the column, additional components can be added that may increase the connection performance.
3. With the addition of the stiffener plate, the connection works similar to a column flange. Therefore, other connection types may be able to connect to the top-bottom reverse angles and the performance of the connection studied.
4. The component method is increasingly gaining attention due to the simplicity in application. The method can be applied to simplify the top-seat reverse angle connection for easier design in practical construction work.
5. Reinforcement of the beam with stiffener plates is necessary to avoid the shear buckling of the beam while under the effects of elevated temperature. The stiffener is expected to reduce the deformation through the shear buckling and therefore, transfer the forces to the connection components instead.
6. In ambient temperature conditions and simply supported boundary, minimal bolt deformation has been observed and therefore the effect from the reduction of bolt sizes can be investigated.

7. Design of connections under elevated temperature is proposed to be reduced to a single ratio for future designs without having to determine the temperature of each component by thermal distribution analysis. Isothermal conditions do not reflect the behavior in anisothermal conditions as the compressive components may have earlier failure under isothermal conditions.

8. Full analysis of the connection with thermal distribution analysis and addition of thermal expansion of steel under elevated temperature condition. This is to determine the effect of compression from the thermal expansion.

REFERENCES

Adam, S. M., & Hamburger, R. O. (2010). Steel Special Moment Frames - Connection Seismic Requirements. *STRUCTURE, November*.

Al-Jabri, K. S. (1999). *The Behaviour of steel and composite Beam-Column Connections in fire.* (PhD), University of Sheffield.

Al-Jabri, K. S., Burgess, I. W., & Plank, R. J. (2004). Prediction of the degradation of connection characteristics at elevated temperature. *Journal of Constructional Steel Research, 60*(3–5), 771-781. doi: http://dx.doi.org/10.1016/S0143-974X(03)00142-1

Al-Rodan, A.-K. (2004). T-cleat connections to Concrete-Filled Tubular Internal Columns. *Journal of Structural Engineering, 130*, 6.

AlHendi, H., & Celikag, M. (2015a). Behavior of reverse-channel and double-reverse-channel connections to tubular columns with HSS. *Journal of Constructional Steel Research, 112*, 271-281. doi: http://dx.doi.org/10.1016/j.jcsr.2015.05.017

AlHendi, H., & Celikag, M. (2015b). Parametric study on moment–rotation characteristics of reverse channel connections to tubular columns. *Journal of Constructional Steel Research, 104*(0), 261-273. doi: http://dx.doi.org/10.1016/j.jcsr.2014.10.009

Alostaz, Y. M., & Schneider, S. P. (1996). Analytical behavior of connections to concrete-filled steel tubes. *Journal of Constructional Steel Research, 40*(2), 95-127. doi: http://dx.doi.org/10.1016/S0143-974X(96)00047-8

Ang, K. M., & Morris, G. A. (1984). Analysis of Three-Dimensional Frames with Flexible Beam-Column Connections. *Canadian Journal of Civil Engineering, 11*, 245-254.

Bagheri Sabbagh, A., Chan, T. M., & Mottram, J. T. (2013). Detailing of I-beam-to-CHS column joints with external diaphragm plates for seismic actions. *Journal of Constructional Steel Research, 88*(0), 21-33. doi: http://dx.doi.org/10.1016/j.jcsr.2013.05.006

Barnett, T. C., Tizani, W., & Nethercot, D. A. (2000, 11-13 September). *Development of a Blind-Bolting System.* Paper presented at the International Conference on Steel Structures of the 2000's, Istanbul, Turkey.

Barnett, T. C., Tizani, W., & Nethercot, D. A. (2001). The practice of blind bolting connections to structural hollow sections: A review. *Steel and Composite Structures, 1*, 1-16. doi: 10.1296/SCS2001.01.01.01

Beutel, J., Thambiratnam, D., & Perera, N. (2001). Monotonic behaviour of composite column to beam connections. *Engineering Structures, 23*(9), 1152-1161. doi: http://dx.doi.org/10.1016/S0141-0296(01)00002-5

Burgess, I., Davison, J. B., Dong, G., & Huang, S.-S. (2012). The role of connections in the response of steel frames to fire. *Structural Engineering International, 22*(4), 449 - 461.

Cafer, H. U. (2009). *3-D Finite Element Analysis of Semi-Rigid Steel Conenctions.* (Masters), Middle East Technical University, Turkey.

Chen, L., & Wang, Y. C. (2012). Efficient modelling of large deflection behaviour of restrained steel structures with realistic endplate beam/column connections in fire. *Engineering Structures, 43*, 194-209. doi: http://dx.doi.org/10.1016/j.engstruct.2012.05.030

Cheng, C.-T., & Chung, L.-L. (2003). Seismic performance of steel beams to concrete-filled steel tubular column connections. *Journal of Constructional Steel Research, 59*(3), 405-426. doi: http://dx.doi.org/10.1016/S0143-974X(02)00033-0

Dai, X. H., Wang, Y. C., & Bailey, C. G. (2010). Numerical modelling of structural fire behaviour of restrained steel beam–column assemblies using typical joint types. *Engineering Structures, 32*(8), 2337-2351. doi: http://dx.doi.org/10.1016/j.engstruct.2010.04.009

Davison, J. B., Kirby, P. A., & Nethercot, D. A. (1987). Rotational stiffness characteristics of steel beam-to-column connections. *Journal of Constructional Steel Research, 8*, 17-54. doi: http://dx.doi.org/10.1016/0143-974X(87)90052-6

Díaz, C., Victoria, M., Martí, P., & Querin, O. M. (2011). FE model of beam-to-column extended end-plate joints. *Journal of Constructional Steel Research, 67*(10), 1578-1590. doi: http://dx.doi.org/10.1016/j.jcsr.2011.04.002

Ding, J., & Wang, Y. C. (2007). Experimental study of structural fire behaviour of steel beam to concrete filled tubular column assemblies with different types of joints. *Engineering Structures, 29*(12), 3485-3502. doi: http://dx.doi.org/10.1016/j.engstruct.2007.08.018

Ding, J., & Wang, Y. C. (2009). Temperatures in unprotected joints between steel beams and concrete-filled tubular columns in fire. *Fire Safety Journal, 44*(1), 16-32. doi: http://dx.doi.org/10.1016/j.firesaf.2008.02.004

Elghazouli, A. Y., Málaga-Chuquitaype, C., Castro, J. M., & Orton, A. H. (2009). Experimental monotonic and cyclic behaviour of blind-bolted angle connections. *Engineering Structures, 31*(11), 2540-2553. doi: http://dx.doi.org/10.1016/j.engstruct.2009.05.021

Elremaily, A., & Azizinamini, A. (2001). Experimental behavior of steel beam to CFT column connections. *Journal of Constructional Steel Research, 57*(10), 1099-1119. doi: http://dx.doi.org/10.1016/S0143-974X(01)00025-6

Elsawaf, S., & Wang, Y. C. (2012). Methods of improving the survival temperature in fire of steel beam connected to CFT column using reverse channel connection. *Engineering Structures, 34*(0), 132-146. doi: http://dx.doi.org/10.1016/j.engstruct.2011.09.004

Elsawaf, S., & Wang, Y. C. (2013). Behaviour of restrained structural subassemblies of steel beam to CFT column in fire during cooling stage. *Engineering Structures, 46*(0), 471-492. doi: http://dx.doi.org/10.1016/j.engstruct.2012.08.023

Elsawaf, S., Wang, Y. C., & Mandal, P. (2011). Numerical modelling of restrained structural subassemblies of steel beam and CFT columns connected using reverse channels in fire. *Engineering Structures, 33*(4), 1217-1231. doi: http://dx.doi.org/10.1016/j.engstruct.2010.12.043

. Eurocode 3 : Design of Steel Structures. (2005) *Part 1-2*. United Kingdom: British Standards Institution.

. Eurocode 3: Design of steel structures. (2005) *Part 1-8*. United Kingdom: British Standards Institution.

. Eurocode 4 - Design of Composite Steel and Concrete Structures Part 1-1. (2004) *Part 1-1*. United Kingdom: British Standards Institution.

Faella, C., Piluso, V., & Rizzano, V. (2000). *Structural steel semi-rigid connections: Theory, design and software*. Florida, USA: CRC Press LLC.

Flowdrill. from http://www.flowdrill.com/.

France, J. E., Buick Davison, J., & A. Kirby, P. (1999a). Moment-capacity and rotational stiffness of endplate connections to concrete-filled tubular columns with flowdrilled connectors. *Journal of Constructional Steel Research, 50*(1), 35-48. doi: http://dx.doi.org/10.1016/S0143-974X(98)00237-5

France, J. E., Buick Davison, J., & A. Kirby, P. (1999b). Strength and rotational response of moment connections to tubular columns using flowdrill connectors. *Journal of Constructional Steel Research, 50*(1), 1-14. doi: http://dx.doi.org/10.1016/S0143-974X(98)00235-1

France, J. E., Buick Davison, J., & Kirby, P. A. (1999). Strength and rotational stiffness of simple connections to tubular columns using flowdrill connectors. *Journal of Constructional Steel Research, 50*(1), 15-34. doi: http://dx.doi.org/10.1016/S0143-974X(98)00236-3

Frye, M. J., & Morris, G. A. (1975). Analysis of flexibly connected steel frames. *Canadian Journal of Civil Engineering, 2*(3), 280-291.

Galambos, T. (1988). *Guide to Stability Design Criteria for Metal Structures* (4th ed.). New York: John Wiley & Sons.

Ghobarah, A., Mourad, S., & Korol, R. M. (1996). Moment-rotation relationship of blind bolted connections for HSS columns. *Journal of Constructional Steel Research, 40*(1), 63-91. doi: http://dx.doi.org/10.1016/S0143-974X(96)00044-2

Heidarpour, A., & Bradford, M. A. (2008). Behaviour of a T-stub assembly in steel beam-to-column connections at elevated temperatures. *Engineering Structures, 30*(10), 2893-2899. doi: http://dx.doi.org/10.1016/j.engstruct.2008.04.007

Heidarpour, A., & Bradford, M. A. (2009). Generic nonlinear modelling of restrained steel beams at elevated temperatures. *Engineering Structures, 31*(11), 2787-2796. doi: http://dx.doi.org/10.1016/j.engstruct.2009.07.006

Heistermann, T. (2013). *Stiffness of Reverse Channel Connections at room and elevated temperatures.* (PhD), Luleå University of Technology., Sweden.

Hong, K., Yang, J. G., & Lee, S. K. (2002). Moment–rotation behavior of double angle connections subjected to shear load. *Engineering Structures, 24*(1), 125-132. doi: http://dx.doi.org/10.1016/S0141-0296(01)00014-1

Huang, S.-S., Davison, B., & Burgess, I. W. (2013). Experiments on reverse-channel connections at elevated temperatures. *Engineering Structures, 49*(0), 973-982. doi: http://dx.doi.org/10.1016/j.engstruct.2012.12.025

Huang, Z. (2011). A connection element for modelling end-plate connections in fire. *Journal of Constructional Steel Research, 67*(5), 841-853. doi: http://dx.doi.org/10.1016/j.jcsr.2010.12.009

Izzudin, B. A. (1991). *Nonlinear Dynamic Analysis of Framed Structures.* Imperial College of Science, Technology and Medicine, London.

Jafarian, M., & Wang, Y. C. (2014). An experimental study of the behaviour of reverse channel connection components to concrete filled steel tubes under tension at elevated temperature. *Journal of Constructional Steel Research, 101*(0), 96-113. doi: http://dx.doi.org/10.1016/j.jcsr.2014.05.006

Jafarian, M., & Wang, Y. C. (2015). Force–deflection relationship of reverse channel connection web component subjected to transverse load. *Journal of Constructional Steel Research, 104*(0), 206-226. doi: http://dx.doi.org/10.1016/j.jcsr.2014.10.002

Jaspart, J., Piertraposa, C., Weynand, K., & Klinkhammer, R. (2004). Development of a full consistent design approach for bolted and welded joints in building frames and trusses between steel members made of hollow and/or open sections - application of the component method *CIDECT Report 5BP-4/04*: Universite de Liege.

Jones, M. H., & Wang, Y. C. (2010). Tying behaviour of fin-plate connection to concrete-filled rectangular steel tubular column — Development of a simplified calculation method. *Journal of Constructional Steel Research, 66*(1), 1-10. doi: http://dx.doi.org/10.1016/j.jcsr.2009.07.011

Jones, M. H., & Wang, Y. C. (2011). Shear and bending behaviour of fin plate connection to concrete filled rectangular steel tubular column — Development of a simplified calculation method. *Journal of Constructional Steel Research, 67*(3), 348-359. doi: http://dx.doi.org/10.1016/j.jcsr.2010.10.006

Kang, C.-H., Shin, K.-J., Oh, Y.-S., & Moon, T.-S. (2001). Hysteresis behavior of CFT column to H-beam connections with external T-stiffeners and penetrated elements. *Engineering Structures, 23*(9), 1194-1201. doi: http://dx.doi.org/10.1016/S0141-0296(00)00119-X

Kishi, N., Ahned, A., & Yabuki, N. (2001). Nonlinear finite-element analysis of top-and seat angle with double web angle connections. *Structural Engineering and Mechanics, 12*, 201-214.

Korol, R. M., Ghobarah, A., & Mourad, S. (1993). Blind Bolting W-Shape Beams to HSS Columns. *Journal of Structural Engineering, 119*(12), 18.

Lee, C.-H., Chiou, Y.-J., Chung, H.-Y., & Chen, C.-J. (2011). Numerical modeling of the fire–structure behavior of steel beam-to-column connections. *Journal of Constructional Steel Research, 67*(9), 1386-1400. doi: http://dx.doi.org/10.1016/j.jcsr.2011.02.014

Lee, J., Goldsworthy, H. M., & Gad, E. F. (2010a). *Blind bolted collar plate connections to unfilled hollow section columns.* Paper presented at the Steel & Composite Structures - Proceedings of the 4th Conference.

Lee, J., Goldsworthy, H. M., & Gad, E. F. (2010b). *Blind bolted side connection for unfilled hollow section columns*. Paper presented at the Australian Conference on the Mechanics of Atructures and Materials (ACMSM21), Melbourne: Australia.

Lee, J., Goldsworthy, H. M., & Gad, E. F. (2010c). Blind bolted T-stub connections to unfilled hollow section columns in low rise structures. *Journal of Constructional Steel Research, 66*(8–9), 981-992. doi: http://dx.doi.org/10.1016/j.jcsr.2010.03.016

Lee, J., Goldsworthy, H. M., & Gad, E. F. (2011a). Blind bolted moment connection to sides of hollow section columns. *Journal of Constructional Steel Research, 67*(12), 1900-1911. doi: http://dx.doi.org/10.1016/j.jcsr.2011.06.007

Lee, J., Goldsworthy, H. M., & Gad, E. F. (2011b). Blind bolted moment connection to unfilled hollow section columns using extended T-stub with back face support. *Engineering Structures, 33*(5), 1710-1722. doi: http://dx.doi.org/10.1016/j.engstruct.2011.02.008

Lee, S.-S., & Moon, T.-S. (2002). Moment–rotation model of semi-rigid connections with angles. *Engineering Structures, 24*(2), 227-237. doi: http://dx.doi.org/10.1016/S0141-0296(01)00066-9

Leong, S. H., Ramli Sulong, N. H., & Jameel, M. (2016). Effect of axial restraints on top-seat angle connections at elevated temperatures. *KSCE Journal of Civil Engineering, 20*(6), 2375-2383. doi: 10.1007/s12205-015-1129-y

Leston-Jones, L. C., Burgess, I. W., Lennon, T., & R.J., P. (1997). Elevated-temperature moment-rotation tests on steelwork connections. Proceedings of the Institution of Civil Engineers. *Structures and Buildings, 122*, 410-419.

Li, G.-Q., Chen, L.-Z., Li, J.-T., & Lou, G.-B. (2012). Modeling of end-plate bolted composite connection in fire considering axial force effects. *Journal of Constructional Steel Research, 76*, 133-143. doi: http://dx.doi.org/10.1016/j.jcsr.2012.03.021

Lin, X., & Sugimoto, H. (2004). *Experimental study on inelastic behaviour and ultimate strength of steel beam-to-column connections with bolts and angles*. Paper presented at the 13th World Conference on Earthquake Engineering.

Liu, T. C. H. (1996). Finite element modelling of behaviours of steel beams and connections in fire. *Journal of Constructional Steel Research, 36*(3), 181-199. doi: http://dx.doi.org/10.1016/0143-974X(95)00016-O

Liu, T. C. H., Fahad, M. K., & Davies, J. M. (2002). Experimental investigation of behaviour of axially restrained steel beams in fire. *Journal of Constructional Steel Research, 58*(9), 1211-1230. doi: http://dx.doi.org/10.1016/S0143-974X(01)00062-1

Liu, Y., Málaga-Chuquitaype, C., & Elghazouli, A. Y. (2012a). Behaviour of beam-to-tubular column angle connections under shear loads. *Engineering Structures, 42*(0), 434-456. doi: http://dx.doi.org/10.1016/j.engstruct.2012.04.027

Liu, Y., Málaga-Chuquitaype, C., & Elghazouli, A. Y. (2012b). Response and component characterisation of semi-rigid connections to tubular columns under axial loads. *Engineering Structures, 41*(0), 510-532. doi: http://dx.doi.org/10.1016/j.engstruct.2012.03.061

Lopes, F., Santiago, A., Silva, L. S., Heistermann, T., Veljkovic, M., & Silva, J. G. (2013). Experimental Behavior of the Reverse Channel Joint Component at Elevated and Ambient Temperatures. *International Journal of Steel Structures, 13*(2), 459-472.

López-Colina, C., Serrano-López, M. A., Gayarre, F. L., & del Coz-Díaz, J. J. (2011). Stiffness of the component 'lateral faces of RHS' at high temperature. *Journal of Constructional Steel Research, 67*(12), 1835-1842. doi: http://dx.doi.org/10.1016/j.jcsr.2011.05.006

López-Colina, C., Serrano-López, M. A., Gayarre, F. L., & Suárez, F. J. (2010). Resistance of the component 'lateral faces of RHS' at high temperature. *Engineering Structures, 32*(4), 1133-1139. doi: http://dx.doi.org/10.1016/j.engstruct.2009.12.039

López-Colina, C., Serrano, M. A., Gayarre, F. L., & González, J. (2014). The component 'lateral faces of RHS' under compression at ambient and high temperature. *International Journal of Steel Structures, 14*(1), 13-22. doi: 10.1007/s13296-014-1002-8

Madas, P. J. (1993). *Advanced modeling of composite frames subjected to earthquake loading.* (PhD.), Imperial College, London: United Kingdom.

Málaga-Chuquitaype, C., & Elghazouli, A. Y. (2010a). Behaviour of combined channel/angle connections to tubular columns under monotonic and cyclic loading. *Engineering Structures, 32*(6), 1600-1616. doi: http://dx.doi.org/10.1016/j.engstruct.2010.02.008

Málaga-Chuquitaype, C., & Elghazouli, A. Y. (2010b). Component-based mechanical models for blind-bolted angle connections. *Engineering Structures, 32*(10), 3048-3067. doi: http://dx.doi.org/10.1016/j.engstruct.2010.05.024

Mao, C. J., Chiou, Y. J., Hsiao, P. A., & Ho, M. C. (2009). Fire response of steel semi-rigid beam–column moment connections. *Journal of Constructional Steel Research, 65*(6), 1290-1303. doi: http://dx.doi.org/10.1016/j.jcsr.2008.12.009

Maquoi, R., Naveau, X., & Rondal, J. (1984). Beam-column welded stud connections. *Journal of Constructional Steel Research, 4*(1), 3-26. doi: http://dx.doi.org/10.1016/0143-974X(84)90032-4

Marwan, S. (2007). *The behavior of steel fin plate connections in fire.* (PhD), University of Sheffield.

Outinen, J., & Mäkeläinen, P. (2002). *High-temperature strength of structural steel and residual strength after cooling down.* Paper presented at the nternational Colloquium on Stability and Ductility of Steel Structures, Budapest University of Technology and Economics, Budapest, Hungary.

Pakala, P., Kodur, V., & Dwaikat, M. (2012). Critical factors influencing the fire performance of bolted double angle connections. *Engineering Structures, 42*, 106-114. doi: http://dx.doi.org/10.1016/j.engstruct.2012.04.011

Park, A. Y., & Wang, Y. C. (2012). Development of component stiffness equations for bolted connections to RHS columns. *Journal of Constructional Steel Research, 70*(0), 137-152. doi: http://dx.doi.org/10.1016/j.jcsr.2011.08.004

Pipes, B. S. T. (1997). *SHS Jointing - Flowdrill & Hollo-bolt*. British Steel Plc.

Pirmoz, A., Danesh, F., & Farajkhah, V. (2011). The effect of axial beam force on moment–rotation curve of top and seat angels connections. *The Structural Design of Tall and Special Buildings, 20*(7), 767-783. doi: 10.1002/tal.551

Pirmoz, A., Daryan, A. S., Mazaheri, A., & Darbandi, H. E. (2008). Behavior of bolted angle connections subjected to combined shear force and moment. *Journal of Constructional Steel Research, 64*(4), 436-446. doi: http://dx.doi.org/10.1016/j.jcsr.2007.09.006

Pirmoz, A., Khoei, A. S., Mohammadrezapour, E., & Daryan, A. S. (2009). Moment–rotation behavior of bolted top–seat angle connections. *Journal of Constructional Steel Research, 65*(4), 973-984. doi: http://dx.doi.org/10.1016/j.jcsr.2008.08.011

Pitrakkos, T., & Tizani, W. (2013). Experimental behaviour of a novel anchored blind-bolt in tension. *Engineering Structures, 49*(0), 905-919. doi: http://dx.doi.org/10.1016/j.engstruct.2012.12.023

Qian, Z.-H., Tan, K.-H., & Burgess, I. W. (2009). Numerical and analytical investigations of steel beam-to-column joints at elevated temperatures. *Journal of Constructional Steel Research, 65*(5), 1043-1054. doi: http://dx.doi.org/10.1016/j.jcsr.2008.11.010

Qian, Z., Tan, K., & Burgess, I. (2008). Behavior of Steel Beam-to-Column Joints at Elevated Temperature: Experimental Investigation. *Journal of Structural Engineering, 134*(5), 713-726. doi: 10.1061/(ASCE)0733-9445(2008)134:5(713)

Qin, Y., Chen, Z., Yang, Q., & Shang, K. (2014). Experimental seismic behavior of through-diaphragm connections to concrete-filled rectangular steel tubular columns. *Journal of Constructional Steel Research, 93*(0), 32-43. doi: http://dx.doi.org/10.1016/j.jcsr.2013.10.020

Ramli-Sulong, N. H. (2005). *Behaviour of steel connections under fire conditions.* (PhD), Imperial College London, London.

Rathburn, J. (1936). Elastic Properties of Riveted Connections. *ASCE*, 524-563.

Saedi Daryan, A., & Yahyai, M. (2009a). Behavior of bolted top-seat angle connections in fire. *Journal of Constructional Steel Research, 65*(3), 531-541. doi: http://dx.doi.org/10.1016/j.jcsr.2008.07.021

Saedi Daryan, A., & Yahyai, M. (2009b). Modeling of bolted angle connections in fire. *Fire Safety Journal, 44*(7), 976-988. doi: http://dx.doi.org/10.1016/j.firesaf.2009.06.005

Satish Kumar, S. R., & Prasada Rao, D. V. (2006). RHS beam-to-column connection with web opening—experimental study and finite element modelling. *Journal of Constructional Steel Research, 62*(8), 739-746. doi: http://dx.doi.org/10.1016/j.jcsr.2005.11.016

Selamet, S., & Garlock, M. E. (2010). Robust fire design of single plate shear connections. *Engineering Structures, 32*(8), 2367-2378. doi: http://dx.doi.org/10.1016/j.engstruct.2010.04.011

Sheet, I. S., Gunasekaran, U., & MacRae, G. A. (2013). Experimental investigation of CFT column to steel beam connections under cyclic loading. *Journal of Constructional Steel Research, 86*(0), 167-182. doi: http://dx.doi.org/10.1016/j.jcsr.2013.03.021

Shen, J., & Astaneh-Asl, A. (1999). Hysteretic behavior of bolted-angle connections. *Journal of Constructional Steel Research, 51*(3), 201-218. doi: http://dx.doi.org/10.1016/S0143-974X(99)00030-9

Shin, K.-J., Kim, Y.-J., Oh, Y.-S., & Moon, T.-S. (2004). Behavior of welded CFT column to H-beam connections with external stiffeners. *Engineering Structures, 26*(13), 1877-1887. doi: http://dx.doi.org/10.1016/j.engstruct.2004.06.016

Simões da Silva, L., Santiago, A., & Vila Real, P. (2001). A component model for the behaviour of steel joints at elevated temperatures. *Journal of Constructional Steel Research, 57*(11), 1169-1195. doi: http://dx.doi.org/10.1016/S0143-974X(01)00039-6

Song, T.-Y., & Han, L.-H. (2014). Post-fire behaviour of concrete-filled steel tubular column to axially and rotationally restrained steel beam joint. *Fire Safety Journal, 69*(0), 147-163. doi: http://dx.doi.org/10.1016/j.firesaf.2014.05.023

Spyrou, S., Davison, J. B., Burgess, I. W., & Plank, R. J. (2004a). Experimental and analytical investigation of the 'compression zone' component within a steel joint at elevated temperatures. *Journal of Constructional Steel Research, 60*(6), 841-865. doi: http://dx.doi.org/10.1016/j.jcsr.2003.10.005

Spyrou, S., Davison, J. B., Burgess, I. W., & Plank, R. J. (2004b). Experimental and analytical investigation of the 'tension zone' components within a steel joint at elevated temperatures. *Journal of Constructional Steel Research, 60*(6), 867-896. doi: http://dx.doi.org/10.1016/j.jcsr.2003.10.006

Strejček, M., Řezníček, J., Tan, K.-H., & Wald, F. (2011). Behaviour of column web component of steel beam-to-column joints at elevated temperatures. *Journal of Constructional Steel Research, 67*(12), 1890-1899. doi: http://dx.doi.org/10.1016/j.jcsr.2011.06.004

Sun, R., Burgess, I. W., Huang, Z., & Dong, G. (2015). Progressive failure modelling and ductility demand of steel beam-to-column connections in fire. *Engineering Structures, 89*, 66-78. doi: http://dx.doi.org/10.1016/j.engstruct.2015.01.053

Tabsh, S. W., & Mourad, S. (1997). Resistance factors for blind bolts in direct tension. *Engineering Structures, 19*(12), 995-1000. doi: http://dx.doi.org/10.1016/S0141-0296(97)00011-4

Tizani, W., Al-Mughairi, A., Owen, J. S., & Pitrakkos, T. (2013). Rotational stiffness of a blind-bolted connection to concrete-filled tubes using modified Hollo-bolt. *Journal of Constructional Steel Research, 80*(0), 317-331. doi: http://dx.doi.org/10.1016/j.jcsr.2012.09.024

Tizani, W., & Ridley-Ellis, D. J. (2003). *The performance of new blind bolt for moment resisting connections.* Paper presented at the 10th International Symposium on Tubular Structures, Madrid, Spain.

Tizani, W., Wang, Z. Y., & Hajirasouliha, I. (2013). Hysteretic performance of a new blind bolted connection to concrete filled columns under cyclic loading: An experimental investigation. *Engineering Structures, 46*(0), 535-546. doi: http://dx.doi.org/10.1016/j.engstruct.2012.08.020

Torabian, S., Mirghaderi, S. R., & Keshavarzi, F. (2012). Moment-connection between I-beam and built-up square column by a diagonal through plate. *Journal of Constructional Steel Research, 70*(0), 385-401. doi: http://dx.doi.org/10.1016/j.jcsr.2011.10.017

Tschemmernegg, F., & Humer, C. (1988). The design of structural steel frames under consideration of the nonlinear behaviour of joints. *Journal of Constructional Steel Research, 11*(2), 73-103. doi: http://dx.doi.org/10.1016/0143-974X(88)90045-4

Vandegans, D., & Janss, J. (1995). *Connection Between Steel Beams and Concrete Filled R.H.S. Based on the Stud Technique (Threaded Stud).* Paper presented at the Connections in Steel Structures III - Behavior, Strength and Design, , Trento, Italy.

Wang, J., & Chen, L. (2012). Experimental investigation of extended end plate joints to concrete-filled steel tubular columns. *Journal of Constructional Steel Research, 79*(0), 56-70. doi: http://dx.doi.org/10.1016/j.jcsr.2012.07.016

Wang, J., & Guo, S. (2012). Structural performance of blind bolted end plate joints to concrete-filled thin-walled steel tubular columns. *Thin-Walled Structures, 60*(0), 54-68. doi: http://dx.doi.org/10.1016/j.tws.2012.07.006

Wang, J., & Spencer Jr, B. F. (2013). Experimental and analytical behavior of blind bolted moment connections. *Journal of Constructional Steel Research, 82*(0), 33-47. doi: http://dx.doi.org/10.1016/j.jcsr.2012.12.002

Wang, J., Zhang, L., & Spencer Jr, B. F. (2013). Seismic response of extended end plate joints to concrete-filled steel tubular columns. *Engineering Structures, 49*(0), 876-892. doi: http://dx.doi.org/10.1016/j.engstruct.2013.01.001

Wang, M., & Wang, P. (2013). Strategies to increase the robustness of endplate beam–column connections in fire. *Journal of Constructional Steel Research, 80*, 109-120. doi: http://dx.doi.org/10.1016/j.jcsr.2012.09.017

Wang, W.-Y., Li, G.-Q., & Dong, Y.-L. (2007). Experimental study and spring-component modelling of extended end-plate joints in fire. *Journal of Constructional Steel Research, 63*(8), 1127-1137. doi: http://dx.doi.org/10.1016/j.jcsr.2006.10.006

Wang, Y. C., & Davies, J. M. (2003). An experimental study of the fire performance of non-sway loaded concrete-filled steel tubular column assemblies with extended end plate connections. *Journal of Constructional Steel Research, 59*(7), 819-838. doi: http://dx.doi.org/10.1016/S0143-974X(02)00092-5

Wang, Y. C., & Xue, L. (2013). Experimental study of moment–rotation characteristics of reverse channel connections to tubular columns. *Journal of Constructional Steel Research, 85*(0), 92-104. doi: http://dx.doi.org/10.1016/j.jcsr.2013.03.006

Wang, Z. Y., Tizani, W., & Wang, Q. Y. (2010). Strength and initial stiffness of a blind-bolt connection based on the T-stub model. *Engineering Structures, 32*(9), 2505-2517. doi: http://dx.doi.org/10.1016/j.engstruct.2010.04.005

Wu, L.-Y., Chung, L.-L., Tsai, S.-F., Shen, T.-J., & Huang, G.-L. (2005). Seismic behavior of bolted beam-to-column connections for concrete filled steel tube. *Journal of Constructional Steel Research, 61*(10), 1387-1410. doi: http://dx.doi.org/10.1016/j.jcsr.2005.03.007

Yang, J.-G., & Jeon, S.-S. (2009). Analytical models for the initial stiffness and plastic moment capacity of an unstiffened top and seat angle connection under a shear load. *International Journal of Steel Structures, 9*(3), 195-205. doi: 10.1007/BF03249494

Yang, J. G., & Lee, G. Y. (2007). Analytical models for the initial stiffness and ultimate moment of a double angle connection. *Engineering Structures, 29*(4), 542-551. doi: http://dx.doi.org/10.1016/j.engstruct.2006.06.001

Yang, J. G., Murray, T. M., & Plaut, R. H. (2000). Three-dimensional finite element analysis of double angle connections under tension and shear. *Journal of Constructional Steel Research, 54*(2), 227-244. doi: http://dx.doi.org/10.1016/S0143-974X(99)00048-6

Yao, H., Goldsworthy, H. M., & Gad, E. F. (2008). Experimental and Numerical Investigation of the Tensile Behavior of T-stub Connections to Concrete-Filled Circular Columns. *Journal of Structural Engineering, 134*, 20.

Yu, H., Burgess, I. W., Davison, J. B., & Plank, R. J. (2008, May 28-30). *Experimental Investigation of the Behavior of Flush End Plate in Fire.* Paper presented at the Structures in Fire 2008 Conference, Singapore.

Yu, H., Burgess, I. W., Davison, J. B., & Plank, R. J. (2009). Experimental investigation of the behaviour of fin plate connections in fire. *Journal of Constructional Steel Research, 65*(3), 723-736. doi: http://dx.doi.org/10.1016/j.jcsr.2008.02.015

Zoetemeijer, P. (1974). A design method for the tension side of statically loaded bolted beam-to-column connections. *Heron, 20*(1), 1-59.

CONFERRENCES & PAPER

Conferences

1. Leong S-H, N.H. Ramli (2015) “Seat angle Parameter Effect on Bolted Top-Seat Angle Moment Rotation” 7th Asia Pacific Young Researchers and Graduates Symposium: University of Malaya.

Paper

1. Leong S-H, N.H. Ramli, Mohammed Jameel (2015) “Effect of axial restraints top-seat angle connections at elevated temperatures”. Korean Society of Civil Engineers. –*Published*

2. Leong S-H, N.H. Ramli, Mohammed Jameel (2016) “Bolted Connections to Tubular Columns at Ambient and Elevated Temperatures – A Review”. Steel and Composite Structures. -*Accepted*

3. Leong S-H, N.H. Ramli, Mohammed Jameel (201x) “New Reverse Top-Seat Angle Connections to Steel Tubular Columns” -*In Progress*

4. Leong S-H, N.H. Ramli, Mohammed Jameel (201x) “Behavior of Reverse Top-Seat Angle Connection to Unfilled Steel Tubular Columns in Elevated Temperature” -*In Progress*